

FACILITY FORM 802	N66 81552	
	(ACCESSION NUMBER)	(THRU)
	219	7/6/66
	(PAGES)	(CODE)
	CR-70141	
	(NASA CR OR TMX OR AD NUMBER)	(CATEGORY)

JET PROPULSION LABORATORY
 CALIFORNIA INSTITUTE OF TECHNOLOGY
 PASADENA, CALIFORNIA

Reproduced by
 NATIONAL TECHNICAL
 INFORMATION SERVICE
 Springfield, Va. 22151

FEORDER NO. 61-13

This report has been
approved for release
to ASTIA by Technical
Reports Section
April 1961

ARMOUR RESEARCH FOUNDATION
of
ILLINOIS INSTITUTE OF TECHNOLOGY
Technology Center
Chicago 16, Illinois

ARMOUR RESEARCH FOUNDATION

FINAL REPORT

ON

LUNAR DRILL STUDY PROGRAM

by

A. V. Dunzila and J. A. Campbell

issued in
January 1961

for
Jet Propulsion Laboratory
Pasadena, California

under

Contract No. N-33554
(ARF Project No. K208)
A Subcontract under NASA Contract No. NASw-6

218

FOREWORD

This is the Final Report, ARF No. 8208-6, on the "Lunar Drill Study Program," covering work performed from August 15, 1960, to December 15, 1960, by Armour Research Foundation (ARF) for the Jet Propulsion Laboratory (JPL), Pasadena, California, under Contract No. N-33554, ARF Project No. K208.

The following ARF personnel made contributions to this program:
W. H. Baier, J. A. Campbell, N. W. Carey, C. J. Costantino, A. V. Dundzila, F. M. Freis, D. P. Grover, G. W. Kalal, N. A. Weil, and R. S. Weiner.

Respectfully submitted,

ARMOUR RESEARCH FOUNDATION OF
ILLINOIS INSTITUTE OF TECHNOLOGY

W. H. Baier

W. H. Baier, Project Engineer

APPROVED:

N. W. Carey

N. W. Carey, Supervisor
Space Systems

W. D. Bobco

W. D. Bobco, Assistant Director
Mechanics Research

AVD/JAC/WHB:pah/mjw

ABSTRACT

The purpose of this project was the generation of quantitative engineering information needed for technical definition of feasible devices to perform various types of remotely controlled drilling operations from a spacecraft placed on the moon.

The study was intended to use existing applicable geological drilling performance data, with major efforts concentrated on problems posed by lunar environment, lunar vehicle capacity, and the very drill unit concept development. Unfortunately, the existing literature contributed negligible amounts of specific drilling data; thus, the project was reoriented into two major phases: experimental data gathering phase and lunar drill concept selection study.

The experimental drilling phase contributed room environmental drill data for the parametric systems analysis and dimensional analysis and played a major part in the drill unit concept selection. A number of drill unit concepts and relating mechanisms were studied: the rotary-impact method was determined to be the most suitable for the lunar drill application.

It is recommended that several of the areas studied be further investigated in the immediate future in order to give a more complete understanding of the problems involved.

TABLE OF CONTENTS

<u>Section</u>	<u>Page</u>
I INTRODUCTION.	1
A. Lunar Drill Requirements	1
B. Drilling Survey	2
1. Introduction.	2
2. Drilling Methods	3
3. Physical Properties of Rocks.	6
4. Drilling Mechanics	12
5. The Drill Bit	17
6. Chip and Core Recovery	21
II EXPERIMENTAL DRILLING AND PARAMETRIC STUDIES.	23
A. Drilling Phase	23
1. Introduction.	23
2. Equipment	23
3. Instrumentation	25
4. Drills	26
5. Materials.	27
B. Analysis Phase	33
1. Introduction.	33
2. Evaluation of Experiments	34
3. Bit and Rock Particle Temperature	65
4. Parametric Systems Analysis.	68
5. Dimensional Analysis	74
C. Discussion and Conclusions.	82
1. Recommended Drill	82
2. Recommended Reliability Study	82
III CONCEPT STUDIES	88
A. Drilling Studies	88
1. Rotary-Impact Drill Systems	88
2. Rotary Drilling Systems	118
3. Chip Removal.	127
4. Casing the Hole	144
5. Instrumentation (Rotary-Impact Drill)	146
6. Dynamic Environment	147
7. Friction and Lubrication	148
8. Evaporation of Materials.	150
9. Fatigue Life	152
10. Motor Operation.	153
11. Pressurization	154
12. Day Versus Night Drilling	156
13. Heat Dissipation.	157

TABLE OF CONTENTS (Continued)

<u>Section</u>	<u>Page</u>
IV PRIME MOVER CLASSIFICATION STUDY.	158
A. Survey	158
1. Electric Motors	158
2. Pneumatic Motors	160
3. Hydraulic Motors.	160
4. Gas Generators	160
B. Comparisons of Systems	165
1. Electric Motor.	165
2. Pneumatic Systems.	170
3. Hydraulic Systems	171
4. Conclusions	171
V RECOMMENDATIONS FOR FUTURE RESEARCH	172
REFERENCES.	174
APPENDIX A DIMENSIONAL ANALYSIS.	A-1
APPENDIX B PARAMETRIC SYSTEMS ANALYSIS DATA	B-1
APPENDIX C PRIME MOVER CLASSIFICATION DATA.	C-1
APPENDIX D CORING DRILL PERFORMANCE ANALYSIS	D-1
APPENDIX E GAS FLOW THROUGH A NARROW ANNULUS.	E-1

I. INTRODUCTION

A. Lunar Drill Requirements

This program was designed to generate quantitative engineering information needed for the technical definition of feasible devices for performing various types of automated drilling operations from a spacecraft placed on the moon and to provide a limited number of preliminary design studies of such devices.

The salient aspects of the environment in which lunar equipment is to operate are: the essentially complete absence of an atmosphere, the high surface temperature during the lunar day, the low surface temperature during the lunar night, the long time periods during which these temperature extremes exist, the low gravitational potential (approximately 1/6 g).

Since the properties of the lunar subsurface materials are uncertain, the drilling system must be capable of drilling through materials with properties similar to those of solid hard silicates, as well as finely divided materials with various degrees of compaction.

The equipment is to withstand a landing deceleration of as much as 100 g's, as well as the lower level, but longer duration accelerations and vibrations imposed during launch and retrorocket operation and is to be integrated into the space vehicle.

Primary emphasis in the design of the lunar exploration equipment is in maximizing reliability while minimizing weight and size.

The following nominal drill system capacity is to be considered:

1. Drill unit weight is not to exceed 60-lb for the immediate application.
2. The operation is to be performed with a 50-lb maximum load for immediate application and to have a growth capacity up to 200-lb load.
3. The unit is to drill a 1.5-in. -diam. hole up to 60-in. deep and to have definite growth potential.
4. The unit is to operate at minimum power levels and feature low total energy requirement.
5. The drill is to penetrate rocks ranging from sandstone to granite.

B. Drilling Survey

1. Introduction

The comparison of various drilling methods for the lunar drill application, in which materials ranging from Berea Sandstone to Gabbro Granite may be encountered, requires that many engineering variables be considered. Size and depth of the hole, lunar environment, contamination of the hole, and range of materials to be drilled, all influence the choice of drilling methods and hence the drill unit itself. Drill unit weight, available downward thrust, requirement for a low vibration environment, need for semi-automatic or remotely controlled operation, reliability, simplicity, capability of power sources, and sequencing requirements, are dictated by the lunar vehicle capacity. The mission of the lunar drill requires that material samples from known depths be delivered to a location where they can subsequently be pulverized (if necessary) and delivered to various scientific analyzers. In addition, the drilled hole must accept a scientific probe.

Many drilling techniques are available for geological and masonry work today. Nonmechanical methods, such as flame, arc and chemical drills are receiving considerable engineering attention. Mechanical techniques - rotary, impact, and rotary-impact are widely used and offer possibilities for the lunar application. These will be considered in detail.

Analysis and evaluation of drilling mechanics involves the consideration of a number of parameters. These are: drill loading (thrust), depth and diameter of the hole, penetration rate, torque, power, rock strength, and, in the case of rotary-impact devices, impulse and frequency. Relatively recent developments, discussed below, have provided additional data concerning the factors of drillability and the universal indexing function.

This qualitative review of rock mechanics is, of course, based largely on the results attained for the geological drilling industry. Manual operation, economy, dimensions, power and structural facilities, as well as other factors, influenced investigative aims and approaches in the problems

studied therein. Lunar drilling considerations place emphasis on factors that were either completely ignored or considered outside of practical range in the past. As a result, this study concerns a new area in the field of drilling.

2. Drilling Methods

The basic principles of rotary and impact penetration have been known for centuries. However, the availability of applicable prime movers and advances in metallurgy were required to initiate modern drilling technology. Surprisingly enough, many drilling concepts are old. Stimulated and financed by metal working and geological exploration industry, some of the concepts were proposed more than 100 years ago as shown in the list below. (Ref. 81, 86).

- Flame drill, 1853
- Bottom-hole rotary hydraulic motor, 1873
- Electric arc (British patent), 1874
- Conventional rotary, 1884
- Chemicals to soften rock, 1887
- Bottom-hole electric percussor, 1890
- Bottom-hole electric motor, 1891
- Bottom-hole hydraulic percussor, 1900
- Retractable bit and bottom hole motor, 1902
- Rotary-impact drill, 1922
- Reelable drill pipe, 1935
- Abrasive laden jets, 1941
- Shaped explosive charge, 1954
- Pellet impact drill, 1955.

Many authorities agree that development of more efficient drilling methods is retarded because of a lack of understanding of the basic earth-boring process. Despite this lack of information, a variety of systems are in use or under promising development today. Generally, these systems are classified by their "rock-attack" means and are so reviewed in the brief descriptions in the paragraphs that follow.

a. Rotary Impact Drills

Drilling rate can be increased by adding vibratory energy to already available rotary power. Electro-magnetic conversion, eccentric weights, and pneumatics are used to produce this vibratory motion. Existing development efforts are aimed toward geological drilling where relatively large holes (3-to-8-in. -diam.) and, as far as the lunar drill system is concerned, unacceptable power demands (10 to 20 hp) are contemplated.

b. Pellet Impact Drill

The pellet impact device utilizes high velocity pellets to impinge on the rock and cause rock failure. Energy is supplied to the pellets by means of a fluid, which makes the method unacceptable for lunar drilling. The calyx drill, for example, is basically a miniaturized pellet system. In these drills, small steel shot provides a constantly renewed cutting edge for the tool. Shot is pumped down with drilling fluid and is circulated at bottom of the hole until consumed.

c. Shock Wave Drill

The basic concept of the shock wave drill involves shock waves traveling through liquid to deliver crushing loads to the rock.

d. Explosive Drills

Explosive methods employ a shaped charge to disintegrate the rock.

e. Down Hole Prime Mover Types

Down hole prime mover drills are of two types; turbo- and electro-drills. Turbo drills transmit large amounts of power to the bit through the drilling fluid. In electro drill designs, the prime mover, an electric motor, is integrated into the top of the drill bit. Both designs are aimed at eliminating the rotating drill pipe.

f. Nonmechanical Drill Means

Chemical flame drills use high temperatures to spall rock. The electric arc is being developed as a replacement for chemically supported combustion. Abrasion-erosion principles and chemical rock softeners, such as sodium carbonate or sodium hydroxide, have been utilized for hole formation.

g. Rotary Drilling

For relatively shallow hole geological drilling, masonry work, metal working industry, solid or coring type rotating drills are used. Fluids and flutes of various auger designs suffice for chip removal and transportation. A variety of materials are employed for cutting edges, including hardened steel, carbide tips, and diamond bits.

h. Summary and Recommendations

This evaluation will be focused on the pure rotary, and the combined rotary-impact drills because none of the other drilling methods meet all of the lunar drilling requirements as stated below.

1. The drill unit is to be of low weight.
2. The power demands are to be maintained at low level, approximately one horsepower or less, during the drilling cycle.
3. The unit is to drill the hole in the lunar vacuum.
4. The unit is to operate in subzero temperature range and to drill at -244°F .
5. The unit is not to deposit appreciable amounts of foreign material in the hole nor is it to contaminate material samples.
6. The operation is not to change the chemical composition of material samples.
7. The operation is not to change physical characteristics of the pulverized samples or the hole walls.
8. The operation is to be performed with a 50-to-200-lb external load.
9. The unit is to deliver samples from specified depths.
10. The operations are to be reliable and simple.

11. The unit is to survive the flight and landing environments.
12. The unit is to penetrate material ranging in composition from sandstone to granite.
13. The operations are to be monitored so that either preliminary information or substantiating data are available to indicate the type of material drilled.
14. The unit is to drill a 1.5- to 2-in. diam. hole, up to 60-in. deep and to have definite growth potential.

These considerations serve to map out a lunar drill unit. With either a pure rotary or a rotary-impact means of drilling, the device will feature a feeding-retracting and power conversion mechanism (e. g., electric motor) located above lunar surface. Power will be transmitted to the drill bit by means of hollow shafting. In case of a pure rotary drill, a coring carbide tip or coring diamond drill will be employed. Core and/or pulverized material transportation methods will be used to clean the hole of debris and to deliver material samples to the spacecraft. No cooling would be required for a rotary-impact device; intermittent drilling would provide sufficient heat control for the carbide tip coring drill. Diamond drills would require an accurate bit temperature control. Spare bits may be required for pure rotary techniques.

3. Physical Properties of Rocks

Drill performance is a function of the type of material drilled. In geological (ref. 93) drilling, continuous efforts are being exerted to classify rocks according to hardness, toughness, and abrasiveness and to use these classifications as a criterion of the ease or difficulty with which they may be drilled. On a large scale, these attempts have met with little success. Drilling perpendicular or parallel to the strata of the same rock produces different results; fine grained rocks of granular texture are far more difficult to drill than equivalent rocks of coarse texture; silicified rocks are very hard but shatter very easily.

Thus, for a hand-held impact drill ref. 93 has proposed the following definition of "drillability":

"The drillability of a rock shall be that penetration speed expressed in inches per minute obtained when drilling a typical rock specimen using a 2-1/2 inch bore rock-drill of 44-50 lb weight with a 1.375 inch diameter cross-bit on a 2 ft 0 inch length of 7/8 inch hexagon collared drill rod; the working air pressure at the inlet air nozzle of the drill to be 70 lb per square inch gauge."

In the above definition, physical properties are ignored, and data for cost estimation is of primary concern.

In lunar drilling, the physical properties of rocks must be taken into account. R. Simon (ref. 84) defines a so-called drilling strength parameter, a measure of that rock property strength directly related to the process of drilling rock. It is defined as the ratio of the kinetic energy contained in a unit length of a cutting chisel edge to the average cross-sectional area of crater formed by the edge for a wedge with a 90° included angle. The value of this parameter is found by means of a drop test, in which the ratio of total impact energy of a cutting drill to the volume of the crater formed by it for a long wedge is found. End effects are neglected.

Drilling strength is believed to be related to other material properties such as tensile, compressive, and shear strengths. Unfortunately, this relationship is not as yet known. However, typical values for the drilling strength are: Indiana limestone (11,000 psi) and Columbus limestone (40,000 psi).

Work by various researchers is continuing to derive some indication of performance from the "classical" material properties such as compression strength, hardness, abrasiveness. With the above in mind, the Physical Properties of Typical American Rocks are presented in Table 1.

Abrasiveness of a given rock is a function of rock composition, especially silicon content and grain size. A rigorous classification is difficult to establish, but general rules have been found: metamorphic rocks are considered more abrasive than igneous, igneous rocks more abrasive than sedimentary.

Table 1

PHYSICAL PROPERTIES OF TYPICAL AMERICAN ROCKS (Ref. 82)

No. Name of Rock Specimen	Location Found	Hard- ness, Shore Number	Coeffi- cient of Thermal Expansion, Room T. to 212° F	Maximum Compress- ive Stress, lb/sq. in.	True Specific Gravity	Apparent Specific Gravity	Weight, lb/cu. ft.	Absorp- tion, Percent	Pores, Percent	Solids, Percent
IGNEOUS ROCKS										
Rhyolite-Granite Series										
1 Felsitic Rhyolite	Mojave, Calif.	86.0	41×10^{-7}	17,250	2.59	2.49	155.2	1.67	4.13	95.9
2 Rhyolite Breccia	Animas Forks, Colo.	101.4	45	42,500	2.55	2.62	163.8	0.41	1.02	98.9
3 Granite Porphyry	Winchester, Mass.	78.7	34	17,700	2.67	2.65	165.2	0.27	0.70	99.3
4 Binary Granite	Concord, N.H.	94.4	49	25,800	2.68	2.57	168.6	1.55	3.98	96.0
5 Biotite Granite	Picton Island, N.Y.	103.7	36	34,500	2.64	2.61	163.0	0.36	0.94	99.1
6 Biotite Granite	Cripple Creek, Colo.	97.0	19	25,900	2.60	2.57	160.7	0.48	1.19	98.9
7 Biotite Granite	Westerly, R.I.	91.8	47	20,650	2.63	2.60	162.4	0.39	1.00	99.0
8 Biotite Granite	Westerly, R.I.	99.1	*	19,930	2.65	2.63	164.2	0.34	0.88	99.1
9 Biotite Granite	Barre, Vt.	95.2	52	28,500	2.65	2.63	164.2	0.34	0.88	99.1
10 Biotite Granite	Llano County, Tex.	91.1	39	23,500	2.66	2.64	165.0	0.20	0.44	99.5
11 Biotite Granite	Spring Creek, Colo.	84.6	*	8,830	2.61	2.53	158.2	1.13	2.87	97.1
12 Biotite Granite (Granitite)	Woodbury, Vt.	98.9	38	25,380	2.65	2.63	164.0	0.38	0.97	99.0
13 Biotite Muscovite Granite	Georgetown, Colo.	97.4	66	27,500	2.68	2.67	166.6	0.21	0.53	99.4
14 Biotite Muscovite Granite	Peekskill, N.Y.	85.1	41	18,000	2.60	2.58	161.2	0.25	0.64	99.3
15 Biotite Muscovite Granite	Mount Airy, N.C.	96.9	45	24,700	2.62	2.60	162.1	0.38	0.98	99.0
16 Alkali Granite	Quincy, Mass.	75.4	29	19,200	2.67	2.64	164.8	0.36	1.01	99.0
17 Alkali Granite	Quincy, Mass.	100.5	58	22,600	2.64	2.62	163.6	0.33	0.86	99.1
18 Aplite	Boulder County, Colo.	71.3	50	20,750	2.61	2.50	156.1	1.67	4.11	95.8
19 Flourite Granite	Clinton County, N.Y.	50.9	56	13,250	3.04	2.99	186.6	0.58	1.67	98.3
20 Spring Creek Granite	Cripple Creek, Colo.	85.6	37	22,200	2.60	2.54	158.5	0.92	2.23	97.7
21 Hornblende Granite	Fredericksburg, Tex.	83.1	37	25,800	2.63	2.61	162.8	0.36	0.89	99.1
22 Amphibole Granite	Hurricane Island, Me.	100.5	60	23,700	2.64	2.62	163.5	0.32	0.79	99.2
Trachyte-Syenite Series										
23 Quartz Syenite	Tianderoga, N.Y.	70.1	37	21,600	2.67	2.63	164.1	0.62	1.54	98.4
Dacite-Quartz-Diorite Series										
24 Granodiorite	St. Cloud, Minn.	98.8	42	29,500	2.78	2.70	168.5	0.19	0.50	99.5
25 Dacite	San Luis Obispo Co., Cal.	99.6	28×10^{-7}	23,970	2.55	2.46	153.6	1.44	3.50	96.4
Andesite-Diorite Series										
26 Hornblende Andesite	Mount Shasta, Calif.	73.7	23×10^{-7}	13,610	2.49	2.22	138.8	4.86	10.77	89.2
27 Andesite Porphyry	Newton, Mass.	69.4	25	22,400	2.81	2.79	174.3	0.29	0.74	99.2
28 Andesite Porphyry	Boulder County, Colo.	92.7	39	32,700	2.71	2.69	167.8	0.27	0.70	99.3
29 Andesite	San Juan County, Colo.	90.2	57	28,750	2.72	2.71	169.3	0.05	0.10	99.9
30 Obicular Gabbro Diorite	Davis County, N.C.	66.1	*	25,000	3.02	2.97	185.3	0.57	1.67	98.3

PHYSICAL PROPERTIES OF TYPICAL AMERICAN ROCKS (Cont.)

No. Name of Rock Specimen	Location Found	Hard- ness, Shore Number	Coeffi- cient of Thermal Expansion, Room T. to 212° F	Maximum Compressive Stress, lb/sq. in.	True Specific Gravity	Apparent Specific Gravity	Weight, lb/cu. ft.	Absorp- tion, Percent	Pores, Percent	Solids, Percent
Basalt-Gabbro Series										
31 Hornblende Basalt	Chaffee County, Colo.	89.0	26	30,300	2.78	2.77	172.9	0.17	0.44	99.5
32 Olivine Basalt	Jefferson County, Colo.	77.2	22	23,950	2.75	2.74	171.0	0.10	0.22	99.8
33 Olivine Basalt	Mt. St. Helens, Wash.	75.7	33	6,540	2.84	2.81	138.2	9.97	22.06	77.9
34 Basalt Porphyry	Lake County, Ore.	75.2	26	18,750	2.81	2.76	172.2	0.66	1.76	98.2
35 Dolerite Porphyry	Cape Ann, Mass.	87.5	35	23,600	2.87	2.84	177.5	0.37	1.03	98.9
36 Fine-Grained Diabase	Somerset County, N.J.	96.4	35	38,000	2.96	2.95	184.4	0.06	0.17	99.8
37 Diabase	Somerville, Mass.	71.6	31	23,250	2.85	2.82	176.0	0.38	1.00	99.0
38 Greenstone	Winton, Minn.	53.8	50	*	2.70	2.69	167.7	0.19	0.46	99.5
39 Bytownite Gabbro	Duluth, Minn.	80.2	30	*	3.00	3.00	187.3	0.00	0.00	100.0
40 Orthoclase Gabbro Quarts	Wichita Mts., Okla.	88.8	20x10 ⁻⁷	18,600	2.73	2.72	169.6	0.25	0.62	99.5
41 Orthoclase Gabbro	Duluth, Minn.	76.5	*	26,400	2.87	2.86	178.4	0.13	0.29	99.7

SEDIMENTARY ROCKS

Breccias and Conglomerates										
42 Syenite Breccia	Boulder County, Colo.	83.6	30x10 ⁻⁷	27,550	3.12	3.10	193.3	0.27	0.78	99.2
43 Chert Breccia	Cherokee County, Kans.	104.5	67	*	2.60	2.56	159.8	0.66	1.65	98.3
44 Limestone Breccia	Boulder County, Colo.	27.3	52	5,960	2.80	2.28	142.1	8.26	18.73	81.2
Sandstones										
45 Argillaceous Sandstone	Portageville, N.Y.	57.2	47	13,900	2.65	2.48	155.1	2.48	6.10	93.8
46 Red (Ferruginous) Sandstone	Potsdam, N.Y.	61.3	57	18,350	2.63	2.49	155.6	2.12	5.26	94.7
47 Gray Sandstone (Berea Grit)	Berea, Ohio	42.0	51	5,840	2.66	2.13	132.7	9.36	19.84	80.1
48 Gray Sandstone	Keeseville, N.Y.	86.5	37x10 ⁻⁷	33,350	2.62	2.58	160.9	0.66	1.62	98.3
49 Sandstone	Jordan, Minn.	22.0	56x10 ⁻⁷	4,920	2.60	1.91	119.5	13.80	26.40	73.6
50 Sandstone	Medina, N.Y.	72.7	63	18,270	2.60	2.46	153.7	2.09	5.15	94.8
51 Brownstone	Somerset County, N.J.	51.3	55	14,100	2.52	2.35	146.8	2.92	6.75	93.2
52 Calcareous Sandstone	Sorocco, N.M.	60.3	65	18,810	2.62	2.31	144.5	5.14	11.85	88.1
Limestones and Dolomites										
53 Coquina	St. Augustine, Fla.	*	*	220	2.73	1.19	74.0	47.80	56.70	43.3
54 Limestone	Boulder County, Colo.	56.5	40	19,780	2.78	2.67	166.6	1.56	4.10	95.8
55 Limestone	Onondaga County, N.Y.	64.2	24	26,900	2.73	2.72	169.7	0.12	0.27	99.7
56 Coral Limestone	LeRoy, N.Y.	58.5	28	16,780	2.70	2.67	166.4	0.52	1.38	98.6
57 Coral Limestone	Jeffersonville, Ind.	57.9	49	14,220	2.68	2.66	166.1	0.31	0.75	99.2

PHYSICAL PROPERTIES OF TYPICAL AMERICAN ROCKS (Cont.)

No. Name of Rock Specimen	Location Found	Hard- ness, Shore Number	Coeffi- cient of Thermal Expansion, Room T. to 212° F.	Maximum Compressive Stress, lb/sq. in.	True Specific Gravity	Apparent Specific Gravity	Weight, lb/cu.ft.	Absorp- tion, Percent	Pores, Percent	Solids, Percent
58 Gray Limestone	Valcour Island, N. Y.	58.1	17	19,980	2.71	2.69	167.8	0.25	0.63	99.3
59 Gray Limestone	Ruth, Nev.	43.0	48	8,470	2.70	2.68	167.4	0.26	0.64	99.3
60 Enderinal Limestone	Lockport, N. Y.	36.8	68	12,280	2.71	2.66	166.1	0.70	1.85	98.1
61 Enderinal Limestone	Trenton Falls, N. Y.	44.1	56	10,400	2.70	2.67	166.4	0.49	1.27	98.7
62 Argillaceous Limestone	Rochester, N. Y.	66.4	51	23,350	2.80	2.74	170.9	0.80	2.19	97.8
63 Pale Gray Limestone	Concrete, Colo.	45.4	24	18,500	2.66	2.54	158.9	1.73	4.36	95.6
64 Cherty Limestone	Buffalo, N. Y.	96.2	*	*	2.65	2.65	163.4	0.08	0.15	99.8
65 Obolitic Limestone	Batesville, Ark.	48.0	31	14,520	2.66	2.61	163.2	0.70	1.82	98.2
66 Obolitic Limestone	Bedford, Ind.	27.9	43	8,210	2.66	2.29	143.2	5.97	13.66	86.3
67 Black Oolite (Fossiliferous)	Milton, Pa.	59.3	30	20,900	2.72	2.71	169.4	0.14	0.30	99.7
68 Dolomitic Limestone	Gouverneur, N. Y.	46.6	58	9,230	2.74	2.73	170.3	0.12	0.28	99.7
69 Dolomitic Limestone	Rochester, N. Y.	59.8	58	20,100	2.76	2.65	165.4	1.49	3.89	96.0
70 Birdseye Limestone	Watertown, N. Y.	64.1	37	18,670	2.72	2.70	168.4	0.27	0.71	99.3
71 Chocolate "Tenn. Marble"	near Knoxville, Tenn.	45.7	53	14,590	2.69	2.68	167.6	0.09	0.19	99.8
72 Siliceous Rocks										
73 Diatomaceous Silica	Santa Barbara, Calif.	17.5	15	477	1.93	0.48	30.3	154.60	74.90	25.1
73 Chert	Joplin, Mo.	97.9	64	86,300	2.59	2.48	155.1	1.69	4.10	95.8
74 Chemical Precipitates										
74 Travertine (onyx marble)	Suisun, Calif.	41.1	62	14,220	2.68	2.63	164.3	0.75	1.94	98.0
75 Travertine (onyx marble)	Great Salt Lake, Utah	42.1	44x10 ⁻⁷	16,200	2.65	2.64	165.2	0.09	0.21	99.7

METAMORPHIC ROCKS

Gneisses and Crystalline Schists

76 Biotite Gneiss	Uxbridge, Mass.	79.6	34x10 ⁻⁷	12,950	2.74	2.68	167.1	0.84	2.23	97.7
77 Biotite Gneiss	Baltimore, Md.	87.2	44	15,640	2.66	2.65	165.8	0.12	0.30	99.7
78 Biotite Gneiss	Cripple Creek, Colo.	95.7	13	14,950	2.68	2.65	165.6	0.47	1.16	98.8
79 Granitoid Gneiss	Salisbury, N.C.	99.4	42	29,400	2.62	2.62	162.9	0.12	0.32	99.7
80 Gabbro Gneiss	Ablemarle County, Va.	71.4	43	27,200	3.15	3.12	195.0	0.30	0.86	99.1
Quartzites and Slat										
81 Baraboo Quartzite	Ableman, Wis.	93.5	61	33,800	2.65	2.64	164.8	0.12	0.34	99.7
82 Quartzite	Dell Rapids, S. D.	97.2	60	23,440	2.63	2.61	162.8	0.25	0.65	99.4
83 Quartzite	Sioux Falls, S. D.	77.8	*	43,800	2.68	2.67	166.6	0.13	0.40	99.6
84 Red Slate	Granville, N. Y.	75.3	49	19,100	2.79	2.78	173.6	0.13	0.29	99.6
85 Gray Slate	Bangor, Pa.	59.1	45	*	2.76	2.71	169.3	0.67	1.84	98.2
86 Green Slate	Pawlet, Vt.	58.8	49	17,700	2.77	2.77	173.0	0.00	0.00	100.0
87 Catlinite	Pipestone County, Minn.	30.2	35	18,300	2.88	2.78	173.7	1.30	3.62	96.4

PHYSICAL PROPERTIES OF TYPICAL AMERICAN ROCKS (Cont.)

No.	Name of Rock Specimen	Location Found	Hard- ness, Shore Number	Coeffi- cient of Thermal Expansion, Room T. to 212° F	Maximum Compressive Stress, lb/sq. in.	True Specific Gravity	Apparent Specific Gravity	Weight, lb/cu.ft.	Absorp- tion, Percent	Poros- ity, Percent	Solids, Percent
Crystalline Limestone and Dolomites											
88	Crystalline Limestone	Rutland, Vt.	35.7	27	6,540	2.71	2.68	167.3	0.40	1.14	98.8
89	Napoleon Gray Marble	Phenix, Mo.	42.5	51	13,180	2.71	2.66	165.8	0.77	2.02	98.0
90	White (Yule) Marble	Marble, Colo.	38.3	38	24,900	2.72	2.70	168.7	0.19	0.45	99.5
91	Dolomitic Marble	Lee, Mass.	46.0	50	15,420	2.88	2.86	178.7	0.29	0.81	99.2
92	Pink and Gray Banded Marble	Hewitts, N. C.	55.0	38	15,420	2.74	2.73	170.2	0.14	0.38	99.6
93	French Gray Marble	Plattsburg, N. Y.	52.5	48	14,400	2.52	2.51	156.5	0.26	0.65	99.4
94	St. Lawrence Marble	Gouverneur, N. Y.	41.1	45	14,400	2.53	2.52	157.5	0.13	0.31	99.7
95	Pittsford Valley Marble	Florence, Vt.	42.8	45	32,450	2.50	2.49	155.5	0.19	0.45	99.5
96	Variegated Dolomitic Marble	Swanton, Vt.	66.1	44	13,500	2.83	2.82	175.7	0.13	0.40	99.6
97	Verd Antique	Pyrenees Mts., France	71.4	34x10 ⁻⁷	13,500	2.75	2.73	170.1	0.29	0.76	99.2

* Data not obtained because of lost or defective specimen.

Because of possible heat transfer control requirements, especially in diamond core drilling, thermal constants that might influence the drill section are shown for representative classes of materials below (ref. 89).

THERMAL PROPERTIES OF ROCKS

	<u>Sandstones</u>	<u>Granites</u>
Thermal conductivity, Btu/hr/ft/°F	1.5	1.6
Specific heat, Btu/lb/°F	0.21	0.19
Thermal diffusivity, ft ² /hr	0.044	0.050
Coefficient of thermal expansion, in./in./°F	5.3×10^{-6}	4.6×10^{-6}

4. Drilling Mechanics

The successful combination of pure rotary and pure impact (often called "percussive") drilling techniques has led to what is known today as the rotary-impact drilling technique. The mechanics of rock breakdown in rotary drilling, and those of fragmentation in impact drilling, form the basis of present-day knowledge on the topic of rock penetration.

a. Rotary Drilling

The rotary bit bores into the rock along a helical path under the combined action of an axial force on the drill and a rotary torque applied to it. This action results in planing off the rock in front of the cutting edge. Actual rock breakdown occurs in the following manner:

1. A buildup of forces and deflection of the bit takes place until a sudden fracture of the rock occurs.
2. A rapid release of stored energy in the deflected bit takes place, causing the bit to impact upon the rock.
3. A buildup of forces again occurs, with some failure of the rock along the irregular lines of the fracture rock and new contact

plane. This action continues till the next fracture occurs, completing the cycle.

Studies indicate that reaction of the rock to the bit load is influenced by friction between the rock and the face of the cutting tool and by the compression strength of the rock. Generally, two theoretical conclusions are supported by experimental evidence:

1. The axial load for a given penetration rate varies directly with the area of the wear flat.
2. The torsional moments required are the sum of the torque required for cutting pressure and that of frictional drag.

Unfortunately, the frictional drag varies through an appreciable range. In addition, high axial loads, hence high frictional loads, are unavoidable. If these axial loads are not maintained the drill cannot maintain contact with the rock.

Drill wear characteristics appear to be strong functions of axial loading (ref. 87). At low loading levels, cutting edges appear to be bouncing over the surface of the rock, resulting in predominantly abrasive action. At high rates of penetrations (per revolution of the drill), the bit deteriorates because of overloading of the cutting edges. Chipping of the tool occurs, and the bit suffers an impact fracture. This tool chipping phenomenon is apparently evident in hard rocks even at "ideal loadings." Thus, for a given axial load, two parameters are evident: rock hardness and rotational speed.

The cutting mechanics of diamond drills differ from those of carbide tools. Here, dependent upon the rock being drilled, the drill either breaks the bond holding the rock particles together or cause conchoidal fracture of the material itself. That the loosened rock particles be removed before a succeeding rock fragment is formed is vitally important. Thus, a proper flow of flushing medium is imperative for successful drilling. Sufficient cooling is required, primarily to protect bit matrix material. Efficient diamond drilling is a very strong function of the pressure on the bit, rate of rotation, sludge clearance, and drill vibration. Generally, diamond drilling is performed at lower rotational-speed-to-axial-feed ratios (100 to 400 rpm/in.) to avoid polishing. Although the demands associated with

ARMOUR RESEARCH FOUNDATION OF ILLINOIS INSTITUTE OF TECHNOLOGY

diamond drilling are exacting, the technique is very effective in hard rocks. However, performance drops in softer materials.

b. Impact Drilling

Impact drilling is the result of successive penetrations of a symmetrical wedge-like tool into the rock. An all-metal tool is given an impulsive blow to drive it into the rock, and, then, after contact with the rock is made, the tool is free to rebound. The mechanics of fragmentation can be visualized in stages:

1. Crushing of rock surface as the bit makes initial contact.
2. Elastic deformation of the rock.
3. Pulverization of rock beneath the point of contact. Concurrent with the pulverization phenomenon, a stress wave is propagated along the path of least resistance, which results in a rock fracture.
4. Chip production. Fracture relieves the stress and the force between the rock and bit is reduced. Dependent on the energy stored in the tool, the bit may continue down through the pulverized region causing a second fracture to occur or the rock may go through elastic deformation only, causing the bit to rebound.

Actual penetration time during a given cycle is a small percentage of the cycling period. The remaining time is occupied in rebounding and in positioning the bit for the next cycle. Experimental results have been given for low overall penetration rates in pure impact drilling.

Wedge geometry plays an important role in the successful impact drill design. Theoretically, acute wedge angles are desirable, however, the usual wedge employs a compromise angle that considers both fracturing potential and bit wear characteristics. The bit is under compressive loads throughout its working phase of the cycle.

61-13

The cutting tool must be indexed or positioned from cycle-to-cycle to avoid impacting continuously at the same point; (ref. 84) has developed an indexing function to determine the optimum angle of rotation between blows. Axial loading influences the rate of penetration. Low loading produces "chatter" (overall contact time between the cutting wedge and the rock face is too short). Correct loadings lead to maximum penetration rates and maximum benefit from each blow. Excessive loads limit rotation and reduce penetration rates.

In summary, impact drilling is applicable for hard rocks, though fragmentation mechanics are not efficient. This statement is confirmed by the presence of a large percentage of very fine rock particles, which indicates a waste of energy. Penetration times occupy only a small part of the total cycle period, as was mentioned earlier.

c. Rotary-Impact Drilling

The rotary-impact drilling technique contains elements of both of the two above systems. No fundamental analysis of the mechanics of the system has been proposed as yet, but the following model is visualized.

First, the tool bit is assumed to be rotated against the rock face with insufficient load to cause failure. Then, an impact is delivered in the direction of the resultant vector of the tool bit force field, increasing the stress in the rock. The rock then fractures at a lower value of the rotary mode force field than that required in pure rotary drilling. The stressed rock below the bit tip is pulverized or fragmented, as in impact drilling. Following impact the bit rebounds and is then rotated forward to a new impact as in rotary drilling.

Impulse and frequency of the blow must be correlated with rotational speed and axial load. Thus, the bit must withstand imposed loads, and the impact must be such so as not to exceed optimum penetration depths, which would result in rotary stalling. Frequency of the blows, axial loading, and rotational speeds can be optimized for maximum efficiency. If one drill parameter assumes an unfavorable value, performance drops.

d. Comparison of Drilling Methods

Fairhurst and W. D. Lacabanne summarize the characteristics of pure rotary and pure impact drilling in the following statements and then argue that rotary-impact drilling tends to eliminate the major disadvantages of each, while retaining the main advantages:

1. Impact Drilling

- a. Can be used in most rocks.
- b. Does not require heavy axial loads.
- c. Utilizes a mechanically robust.
- d. Has a limited penetration rate.
- e. Is an inefficient method of breaking rock.

2. Rotary Drilling

- a. Is limited to use in soft and medium-hard rock.
- b. Requires heavy axial loads.
- c. Utilizes a structurally weaker drill bit than that for pure impact.
- d. Under suitable conditions, is capable of high penetration rates.
- e. Approaches a continuous cutting cycle.
- f. Is more efficient than impact drilling.
- g. Cannot be used in abrasive rocks.

Penetration rate is compared in ref. 87 for rotary, impact and rotary-impact drilling methods. The results of the reference are shown below:

Rock Type	Drilling System	Penetration Rate, in. /min.
Sandshale	Impact	11.0
	Rotary	60.0
	Rotary-Impact	----
Sandstone	Impact	6.1
	Rotary	----
	Rotary-Impact	57.0
Very Hard Sandstone	Impact	----
	Rotary	20.6
	Rotary-Impact	46.1

Penetration rate vs. applied load is presented qualitatively for the three methods discussed. The successful design compromise resulting from the use of rotary-impact drilling is evident (Fig. 1).

Rate of bit wear has been considered by some investigators and will influence the lunar drill design. The results of an investigation by Lacabanne are shown in Fig. 2.

5. The Drill Bit

Two major bit types may be considered for lunar drill application: (a) solid and (b) coring bits. For this application, the test program completed as a part of this study showed a rotary-impact drill utilizing a solid carbide bit to be most suitable. There was an indication however, that a carbide coring bit may also prove satisfactory. If pure rotary drilling is to be used, only the coring bit is acceptable and then only if cooling is provided. From a theoretical point of view, these choices are dictated by the factors of rock hardness and fragmentation, structural strength of the bit, allowable axial load, and power considerations. In the ARF testing program, the above were the only bits that would penetrate the hardest material available, namely, Gabbro granite.

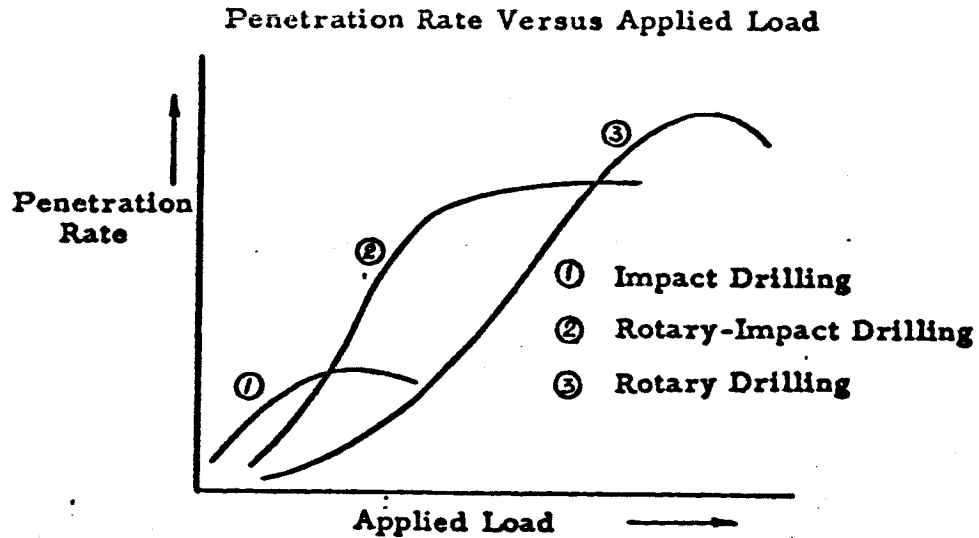


Fig. 1 Ref. 87

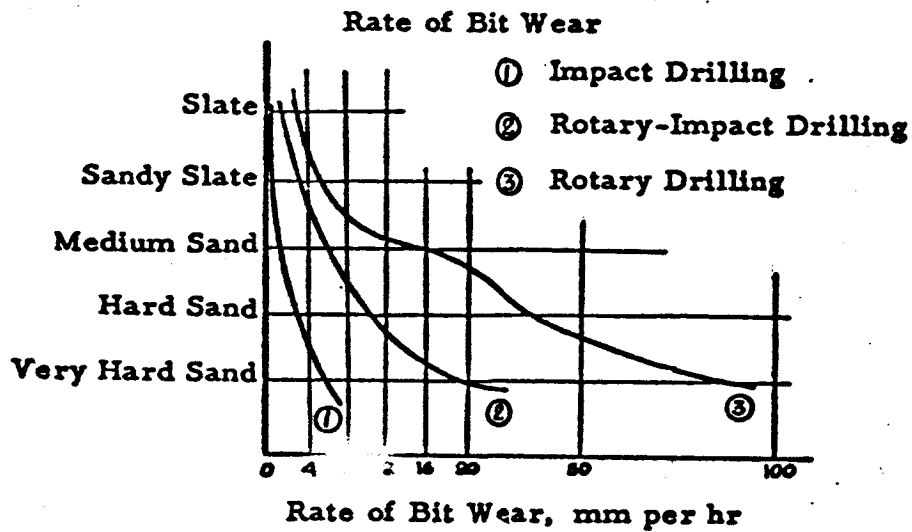


Fig. 2, Ref. 83

a. Solid Bits

The bit (also designated as insert) may be positioned in the tool shank in one of several possible ways. The simplest is that in which the bit is placed diametrically across, and perpendicular to, the cross-section of the shank. Another symmetrical design features four bits, placed radially at 90° from each other ("crossbits"). Their inner edges are separated to provide a small radial clearance at the shank centerline. Bits of unsymmetrical patterns are also available. In all designs, the effective radial width of the bit exceeds the diameter of the tool shank. On the average, the wedge angle of the bit is approximately 90°, the axis of which is not necessarily perpendicular to the rock surface. The flat face of a noncoring bit is ground to an approximate included angle of 150°, where 180° would represent a plane perpendicular to the shank axis.

Most inserts are made of tungsten carbide alloy, featuring high compressive strength and resistance to abrasive wear. However, tensile strength requirements must also be considered since the tensile strength of tungsten carbide is only 1/4 its compressive strength. Since rotary-impact loading stresses the bit in tension and compression, overdesign and conservatism must be resorted to, in the interests of reliability. Specific properties of the recommended alloy are largely influenced by its cobalt content.

Judging from ARF test results in Concrete, Sandstone and Gabbro granite, cooling presents no problems.

b. Coring Bits

As the name implies, coring bits produce holes of annular cross section. This statement holds true only for very shallow holes: the very process of drilling, with its associated vibration, friction and - sometimes - heat phenomena, results in circular holes, when the drill and the core are retrieved. Basically, the drill consists of a hollow cylindrical steel shank, with cutting bits that protrude beyond the outer and the inner radius of the tube inserted in the lower edge.

When compared to pure rotary solid drills, energy is conserved when coring methods are utilized. For identical hole diameters, energy is used up to chop and pulverize the rock of a smaller net cross-sectional area. Coring drills penetrate hard rocks much more rapidly: for a given rotational speed, no center portion of the tool has an effective radius equal to zero and thus zero velocity.

Coring drills are made with both tungsten carbide and diamond bits.

(1) Tungsten Carbide Coring Bits

From a metallurgical viewpoint, tungsten carbide bits used for rotary drills are designed by employing similar considerations to those in the design of rotary-impact drills. The geometry of the bit is different, however, due to an emphasis on purely rotary motion, the higher tangential velocities required, and larger tensile loading characteristics encountered. Efficient drilling requires incorporation of a moderate cooling capability as a result of the smaller overall heat capacity and conduction area afforded with the hollow shank as compared to a solid shank. Three to eight cutting inserts, spaced at either regular or irregular intervals, are used on drills of moderate diameter.

(2) Diamond Coring

Up to 500 small diamonds (ref. 88) (8 to 90 pieces per carat) are set into a cast metal or a powder metal matrix to form the diamond coring bit. Setting pattern is of importance, as is the matrix material. The diamonds are set to project beyond the outer and the inner radii of the cylinder and to face the bottom of the hole. The diamonds and matrix metal both wear during drilling, the latter at a slightly higher rate, which exposes additional diamond cutting area. Proper amounts of flushant are imperative to remove pulverized rock and to cool the bit matrix material. Generally, diamond drilling is performed at higher rotational speeds than carbide tip rotary drilling. This technique is very effective in hard rocks.

6. Chip and Core Recovery

a. General

All drilling systems feature provisions for removal of pulverized and fragmented rock from the bottom of the hole. Chip transportation is needed to expose new layers of rock to the bit face, in order that axial thrust can load the bit in the designed manner and to ensure that no energy is lost in damping-cushioning or further pulverization mechanics. In diamond bits, where actual protrusions of the cutting edge are small, chip transportation is of utmost importance because of possible dulling effects. Rotary bit tools often suffer from clogging (ref. 93), which can be traced to inadequate chip and pulverized rock removal from the cutting area. In addition, the lunar drilling experiments require pulverized rock for scientific examination.

Generally, core recovery is dependent upon composition of rock formation. In hard, uniform rocks, core recovery may reach 100%. In soft, cleavable strata, unless the drill bit is raised every few inches, recovery can be as low as 10%. For good recovery in hard rock, the drill should be run at low speed and heavy axial loading, while, in soft rock, the reverse is true. Core recovery concern is of major importance for the lunar drill application for several reasons: to permit utilization of available energy for actual drilling rather than pulverization of the coring rock volume; to ensure raising solid core pieces for additional experiments, such as vidicon inspection; and to produce clean holes for subsequent scientific probing and logging techniques.

b. Chip Recovery

Fluting and flushing methods are used in the drilling industry for chip recovery. The rotation of fluted helical shanks or auger mechanisms is sufficient to raise chips from moderate depths of a few feet. This method is suitable for rotary drilling and is difficult to surpass for its inherent simplicity. Rotary-impact devices employ fluting designs in the same manner; however, the effective depth of the hole over which flutes can be used for chip recovery has not yet been determined.

c. Core Recovery

Cores are recovered either by flushing methods or mechanical means. Flushing techniques employ liquids only. As an example of the mechanical means, the drilling industry employs the wire-line core barrel method, which features core removal without raising of the drill bit. During drilling, the core barrel is held in place within the bit. A wire-line lowered through the center of the drill shank is hooked onto the core barrel and the core raised.

Mechanical (camming) techniques that cause a pair of arms incorporated in the drill shank to grip the core appear, in ARF studies, to show promise for the lunar drill application.

d. Lunar Environment Effects on Chip and Core Recovery

Certain aspects of lunar environment, such as low temperature, vacuum, lower gravitational acceleration, possible cavities or high porosity of the rock, place special demands on the drill unit. Liquid flushing techniques are unacceptable because of the low temperatures encountered; gas fluidization implies a sealed, closed loop system with probable continuous losses of the fluidizing medium in the lunar atmosphere; auger or helical fluting methods would have to work with degassed and pulverized material against a lower gravity field. The effects of increased friction coefficient as well as other considerations, influence the chip and core recovery problem toward a solution featuring simple mechanical means.

II. EXPERIMENTAL DRILLING AND PARAMETRIC STUDIES

The experimental drilling program conducted by ARF to obtain quantitative data regarding the drilling of rock formation is described in this section of this report. The results of this program are summarized and discussed at the end of this section.

A. Drilling Phase

1. Introduction

The object of the experimental drilling program was to obtain data for determining the determination of (a) the most suitable lunar drilling method, (b) the most suitable drill bits, and (c) input data for the subsequent parametric and dimensional analysis of the results.

The program was arranged to permit the study of (a) rotary and rotary-impact drilling methods, and (b) solid and coring bit performance in a variety of geological materials.

2. Equipment

Two rotary drill presses and four portable rotary-impact drills were used during the program. These are discussed below:

Rotary Drill Presses:

(a) An ARF-modified vertical drill press, powered by a 3/4-hp, 1750-rpm, 220-v, 3-phase motor (later by a 2-hp, 24-v d-c, 4000-rpm motor), capable of 36-in. -deep holes, up to 200-lb axial load and a variety of speeds (Fig. 3).

(b) Model 120 VE, Diamond Core and Saw, Inc., diamond core drilling machine, powered by a 2-1/4-hp, 900-rpm, 110-v, a-c - d-c motor.

Rotary-Impact Drills:

(c) Model No. 736 Roto-Hammer, Skil Corp., 325 rpm; 2200 blows per min; weight: 24-3/4 lb, principle of operation: pneumatic spring.

(d) Model No. 726 Roto-Hammer, Skil Corp. This drill is scaled-down version of Model No. 736, described above. 500 rpm; 2400 blows per min; weight: 13 lb.

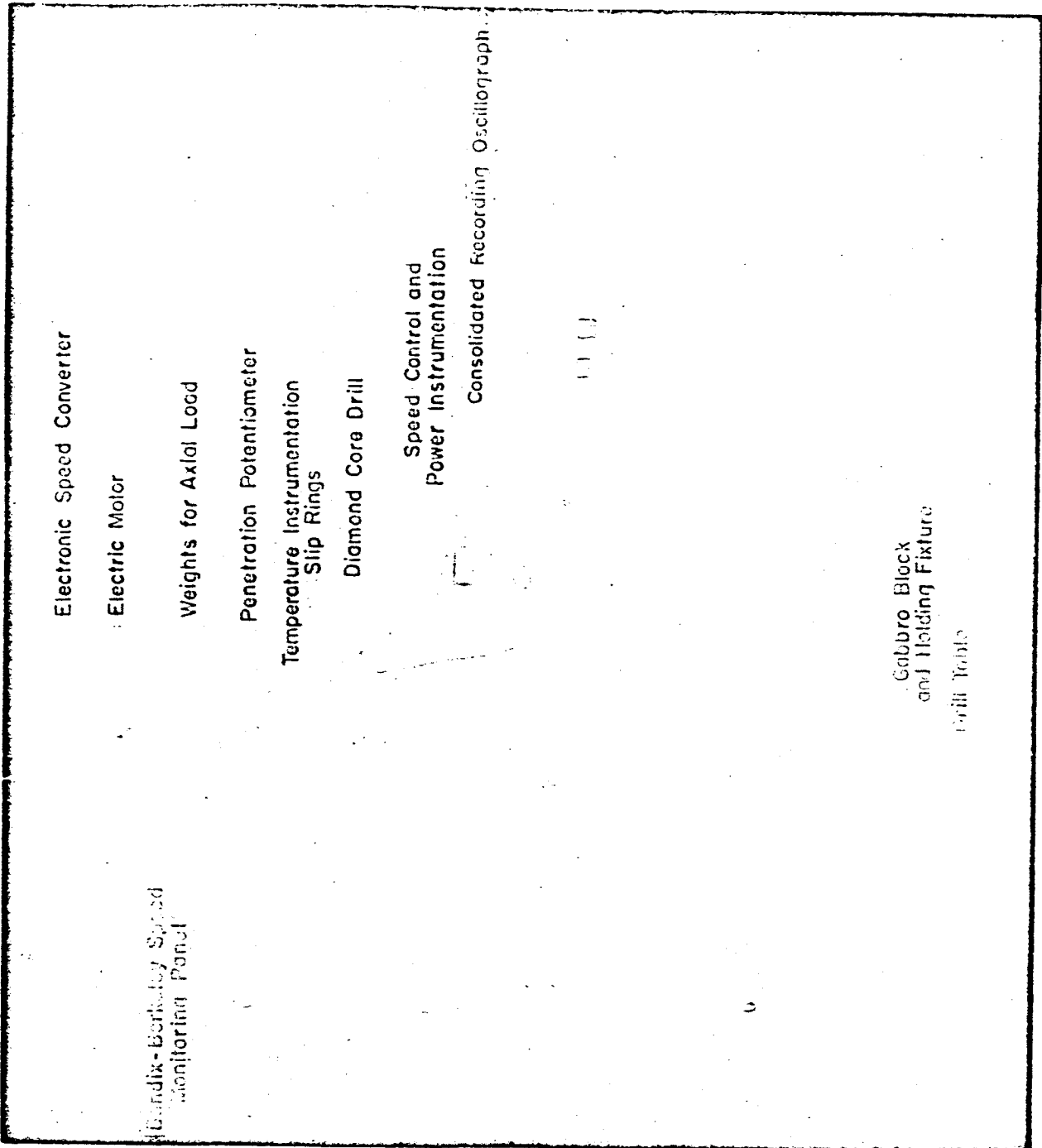


Fig. 3 EXPERIMENTAL DRILLING SET-UP

(e) Model No. 4E-100, Universal Electric Hammer, Thor Power Tool Co., based on a mechanical scotch-yoke principle. This is a non-rotating unit.

(f) Model No. 404, Heavy Duty Impact Drill, Stanley Electric Tools, producing 16,000 to 21,500 mechanically actuated impacts per min; drill rotated at high speed; weight: 22-1/2 lb.

(g) Model No. 38-RO Electric Hammer Drill, Syntron Co., produces 3600 blows per min, plus constant, automatic rotation, weight: 38-3/4 lb. Principle of operation, electromagnetic.

All tested rotary-impact drills were hand-operated in vertical position and loaded with a steel plate when necessary. No variation in rotational rate, frequency, or momentum was possible.

3. Instrumentation

At a given axial load, drilling experiments were instrumented to obtain the following data:

a. Rotary Drilling

1. Power input into the drill shank. The electric driving motor was properly calibrated. Its voltage and current input were either visually or continuously recorded.
2. Drill speed was measured on the motor output shaft with an electronic converter and visually recorded from a Bendix-Berkely monitoring panel.
3. Penetration was measured continuously with a 14-in. -stroke precision potentiometer.
4. Automatic continuous data recording was made on a Consolidated Electrodynamics recording oscillograph. The following data were recorded: armature current, armature voltage, penetration, time.

b. Rotary-Impact Drilling

Rotary-impact drilling involved power, penetration, and time measurements. All recordings were made visually.

4. Drills

Approximately 450 drill bit and mining equipment manufacturing companies were contacted, their replies and literature studied. Applicable drills were bought and tested. A list of drills used in the experimental program follows.

(a) Rotary carbide tip drills:

- ARF-designated C-1: New England Carbide Tool Co., cyclo-twist carbide tip masonry drill, 1-in. diam., with 2 flutes.
- C-2: U. S. Expansion Bolt Co., carbi-twist masonry drill, No. 9416, 1-in. diam., with 2 flutes.
- C-3: North American Viking Co., carboloy tip masonry drill EVN 444, 1-in. diam., with 2 flutes.
- C-4: North American Viking Co., carbide tip masonry drill SM 390, 1-in. diam., with 2 flutes.
- C-5: Coffey-Cummins Manufacturing Co., Du-Drill, 1-in. diam. with ARF-cut flute.
- C-6: Arro Expansion Bolt Co., carbide tip masonry drill FDM-16, 1-in. diam., with 1 flute.
- C-7: New England Carbide Tool Co., Inc., cyclo-core, 3 insert-tooth drill, 1-in. diam., fluted.
- C-8: Relton Corp., Core Style coring masonry drills, fluted: No. 16-TD, 1-in. diam., with 5 inserts; No. 24-TD, 1-1/2-in. diam., with 6 inserts; No. 32-TD, 2 in. diam., with 8 inserts.
- C-9: U. S. Expansion Bolt Co., Core-Vent masonry drill No. 9916, 1-in. diam., with 6 inserts.
- C-10: Vascolony-Ramet Corp., auger drill bit, No. DB 1-3/8-8 1-3/8 in. diam.

(b) Diamond coring drills:

- ARF-designated D-1: Diamond Core and Saw, Inc., Di-Cor drill, 1-in. diam.
- D-2: Diamond Core and Saw, Inc., diamond drill, 2-in. diam.
- D-3: E. J. Longyear Co., diamond drill, 1-in. diam.
- D-4: Felker Manufacturing Co., diamond drill, 1-in. diam.
- D-5: Fish-Schurman Corp., 1/16-in. -wall diamond drill, 1-in. diam.

(c) Rotary-impact bits were recommended and supplied by the rotary-impact drill manufacturers with their drill unit. No separate bit identification was available. Physical drill descriptions are therefore

limited to fluted, solid, carbide tip bits. Rotary impact drilling was performed with 18-in.-long drills and/or 42-in.-long drill shanks.

5. Materials

The materials listed in Table 2 were drilled during the experimental program.

Table 2

MATERIALS DRILLED

Material	Experimentally determined compressive strength, lb/in ²
Concrete No. 1	not measured
Marble	not measured
Limestone	not measured
Hornblend Schist	not measured
Steel Mill Slag	not measured
ARF-mixed Materialite	4,500 - 5,000
Average density, solid: 95.4 lb/ft ³	
Water to cement ratio: 0.86	
Slump: 2-1/2 in.	
Cement content: 5.3 bags/yd ³ (94 lb/bag)	
Aggregate composition, lb/yd ³ :	
3/4 in. - 3/8 in.: 46.3	
3/8 in. - No. 4 : 45.0	
No. 4 - No. 16 : 47.0	
No. 16 - No. 50 : 37.0	
No. 50 - No. 100: 14.0	
No. 100 - No. 700: 2.0	
ARF-mixed Concrete No. 2	5,300 - 6,000
Universal Type III Cement: 46 lb/batch	
No. 2 Torpedo Sand: 98 lb/batch	
1-1/2 in. - No. 4 gravel: 166 lb/batch	
Water: 24 lb/batch	
Wet density: 153.2 lb/ft ³	
Slump: 2-1/2 in.	
Water-to-concrete ratio: 0.53	
Yield: 2.183 ft ³	
JPL-procured Gabbro Granite	40,000 perpendicular to strata 27,000 parallel to strata

Table 2 (Continued)
MATERIALS DRILLED

Material	Experimentally ₂ determined compressive strength, lb/in ²
Berea Sandstone	7,300
Wood, Structural, 2 in. x 4 in.	not measured

An analysis of the rock particle size resulting from drilling was performed on materialite, ARF-mixed concrete No. 2, Gabbro granite and Berea sandstone. Materialite and concrete No. 2 were drilled with an ARF-designated C-4 drill; Gabbro granite and Berea sandstone samples were obtained with Model No. 736, Skil Corp. Roto-Hammer. The resulting data, in the form of cumulative weight percent vs. particle diameter, are presented in Fig. 4.

6. Drilling Experiments

The program resulted in approximately 120 individual meaningful drilling runs. A number of these are tabulated and presented graphically. Some served merely to determine that the bit being tested was unsatisfactory and therefore produced no drilling data suitable for plotting. The outline below serves to provide detailed information on experimental conditions, parameters, and the list of graphical presentations.

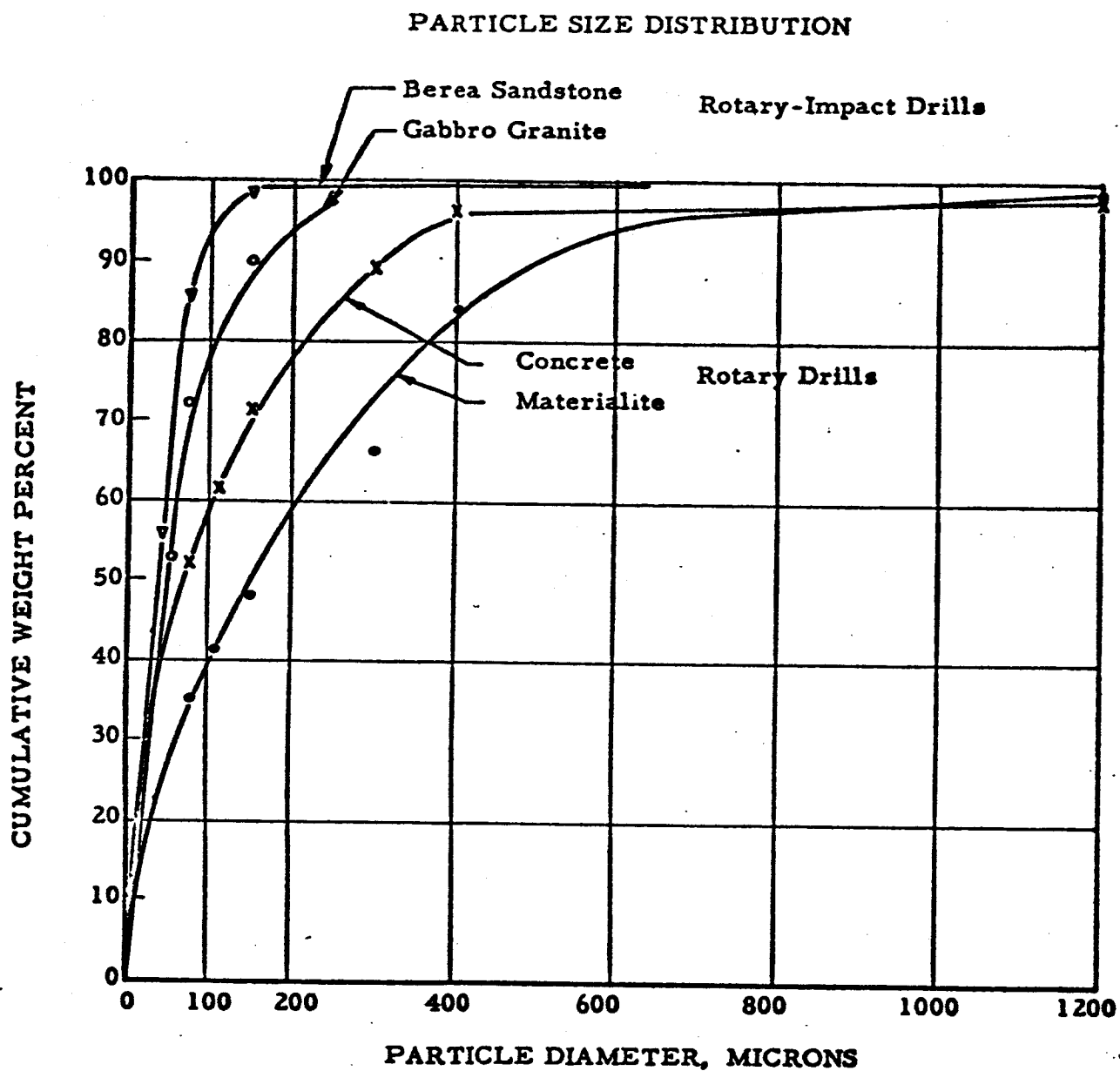



Fig. 4

ROTARY AND IMPACT DRILLING EXPERIMENTS

Drill Designation	Material	Load, lb.	Speed, rpm	Comments	Fig. No.
D-1	Concrete No.1	25, 35, 45,	900	 Ample cooling and flushing medium, special diamond drill press.	5
D-1	Limestone	25, 35, 45,	900		6
D-1	Hornblend Schist	25, 35, 45,	900		7
D-1	Marble	25, 35, 45,	900		8
D-2	Marble	25, 35, 45,	900		8
D-2	Hornblend Schist	25, 35, 45,	900		9
D-2	Limestone	25, 35, 45,	900		10
D-2	Concrete No.1	25, 35, 45,	900		11
D-1	Granite	50	735	No coolant, no penetration.	
D-3	Granite	50	1190	No coolant, no penetration.	
D-4	Granite	80	500, 800	Specially temperature instrumented drill, no penetration.	
	Sandstone	80	500, 800		
D-5	Granite	50	735	No coolant, no penetration.	
C-1	Materialite	24, 45, 62	328		12
C-2	Materialite	24, 45, 62	328		13
C-3	Materialite	24, 45, 62	328		14
C-4	Materialite	24, 45, 62	328		15
C-4	Materialite	24, 45, 62	328		16
C-2	Concrete No.2	40	500		
		80	250, 735		17
		160	750		
C-4	Concrete No.2	40	500		
		80	252		18
C-4	Sandstone	50	300, 735		
		80	500, 1000		19
		160	500, 735		

ROTARY AND IMPACT DRILLING EXPERIMENTS (Continued)

Drill Designation	Material	Load, lb.	Speed, rpm	Comments	Fig. No.
C-4	Sandstone	50	300, 735		20
		80	500, 735		
		160	500, 735		
C-6	Concrete No.2	80	500		21
C-7	Granite	50	350		22
		50	500		
		50	732		
C-8, 1 in. diam.	Sandstone	50	350, 500, 735		23
		80	390, 740, 1030		
		160	250, 500, 735		
C-8 1 in.	Sandstone	50	350, 500, 735		24
		80	390, 740, 1030		
		160	250, 500, 735		
C-8 2 in.	Sandstone	50	250, 500, 735		25
		80	210, 350, 500		
	Sandstone	50	250, 300, 735		26
		80	210, 350, 500		
C-8 1 in.	Granite	50	250, 500, 735		27
		80	735		
		160	250, 500		
C-8 1-1/2 in.	Granite	160	250, 500		28
C-8 2 in.	Granite	160	500		
C-9	Granite	50	310, 500	No penetration.	
C-10	Granite	160	530	No penetration.	

ROTARY-IMPACT DRILLING EXPERIMENTS (Continued)

Make	Bit Diam., in.	Drill Length, in.	Material	Load, lb.	Fig. No.
Skil Corp. 736	1-1/2	60	Granite	51	30
	1-1/2	18	Granite	51	29
	1	18	Granite	50	29
	1-1/2	60	Sandstone	51	30
	1	18	Wood	35	
Skil Corp. 726	1-1/2	60	Granite	48	30
	1	18	Granite	48	29
	1	18	Sandstone	48	29
	1-1/2	60	Sandstone	48	30
	3/4	18	Granite	48	29
Stanley Electric Tools	1	12	Granite	80	No penetration.

B. Analysis Phase**1. Introduction**

The objectives of these analyses were: (a) to evaluate the experimental drilling data, (b) to determine the most suitable drilling methods and drill bits, (c) to obtain system energy parameters, and (d) to present drill performance in both dimensionless and graphical form.

Experimental results were analyzed with several problem areas in mind. First, drill types that would penetrate the specified materials - soft wood, sandstone, to granite were determined. Drills and drilling methods which performed satisfactorily were further explored through a range of operating conditions to determine the optimum values. Additional tests were made to study special problems, such as temperature in diamond drills or internal energy losses in 60-in. -long drills on rotary-

impact units. Other problem areas studied included dulling of cutting edges and drill unit structural rigidity requirements.

2. Evaluation of Experiments

a. Discussion

Geological drilling is evaluated in terms of drilling parameters discussed below. Rocks, in general, are described by the physical properties that vary from rock to rock and are of paramount importance to a given drilling task. "Classical" drilling parameters consist of penetration rate, drill loading, drill rotation, drill size, impact frequency, power, and torque. The following rock properties are of importance: ultimate strength, hardness, abrasiveness, elastic modulus, coefficient of friction, and brittleness. A portion of qualitative functional dependence is presented in Sec. I-B of this report; more data deduced from the ARF experimental drilling investigation for lunar drill systems as follows:

(a) With regard to penetration, a general rule can be stated: For the bits tested, the type of bit that penetrates hard rocks (granite) will penetrate soft ones (sandstone, materialite, concrete). Speed and load optimization problems are different. The reverse may not be true. Solid rotary bits were found to be ineffective in hard rocks; thus, only diamond and carbide tip coring drills (in the rotary category) and solid carbide tip rotary-impact bits were found to satisfy the requirement that such rocks be penetrable.

(b) High penetration rates at lower power level are desired from a system economics viewpoint. Torque and rotation speed provide a limited control of these basic variables. High rotary speeds are undesirable because of inherent shank balancing (whipping) requirements, while torque is limited by lunar vehicle parameters. Generally, diamond drills require higher speeds than carbide tips in the rotary category; higher penetration per revolution produces higher torques with carbide tips. Rotary impact devices combine high penetration rates with lower speeds and very low torque values.

(c) Power and energy considerations indicate that, in rotary drilling, a greater percentage of work is expended in the rock fracturing process. This conclusion points out large technical optimization possibilities for the rotary impact devices.

(d) Diamond drilling can be considered on par with carbide core drilling from a penetration point of view. However, diamond bits require additional system support that complicate its application to the lunar drill problem. These are: temperature control (matrix softening), higher loadings, flushing of pulverized rock, very rigid drill support and dynamic stability; and more severe drilling parameter values of load and speed. On the other hand, a diamond matrix offers at least one very desirable feature, the self-sharpening effect that results from different wear rates of diamond insert and matrix seating material.

(e) Bit wear is obvious in all drills, methods and materials. Diamond drills are more sensitive to wear when run at non-optimum speeds and loads; carbide tip coring drills exhibit higher wear rates in granite than in sandstone and would require sharpening or changing to meet the lunar drilling specification; rotary impact drilling showed least wear, though the bit dulled more in a 60-in. hole in sandstone than in an 18-in hole in granite.

(f) The means by which chip removal is effected influences the performance of rotary drills. Power, penetration, and bit wear are affected.

(g) The use of a 50-lb axial load places severe limitations on the penetrating ability of the drill unit. With some rotary drills and materials, this load does not permit any penetration.

b. Graphical Presentation

The following paragraphs discuss individual drilling experiments, in an effort to analyze particular drill performance based on the data obtained. Part III of this report will utilize this analysis for the lunar drill unit formulation.

(1) Diamond Core Drills - Rotary Drilling

Figures 5 through 11 describe the performance of diamond core drills D-1 and D-2 in a variety of materials. The results indicate:

Drill penetration rate increases with drill loading.

Drill penetration rate, for a given loading, increases with decreasing drill size, i.e., "load per unit area" proportionality exists to some extent.

Of the materials tested, Hornblend Schist is the most difficult material to drill.

Power requirements, assuming a power factor of 0.8, were in the range of 0.58 hp (Schist) to 0.69 hp (limestone). The drill bit takes a deeper cut in softer material, thus increasing the torque requirement. The influence of compressive and shear strength of the material was not determined in the tests performed.

For the 900-rpm speed, used throughout these tests, optimum loading is in excess of the maximum value of 45 lbs. available.

Higher loads tend to produce more nearly constant penetration rates.

Penetration rate is not constant at the beginning of drilling because the rock surface was intentionally left roughened.

Properly supported diamond drills start well on an uneven, rough surface and do not "wander". In this case, the drill press was specially designed for the application (Sec. II-A 2-b).

Drills showed definite wear. Inspection and subsequent discussion with the manufacturer resulted in the conclusion that the burnishing was caused by insufficient drill loading.

D-1 DRILL IN CONCRETE NO. 1

900 RPM

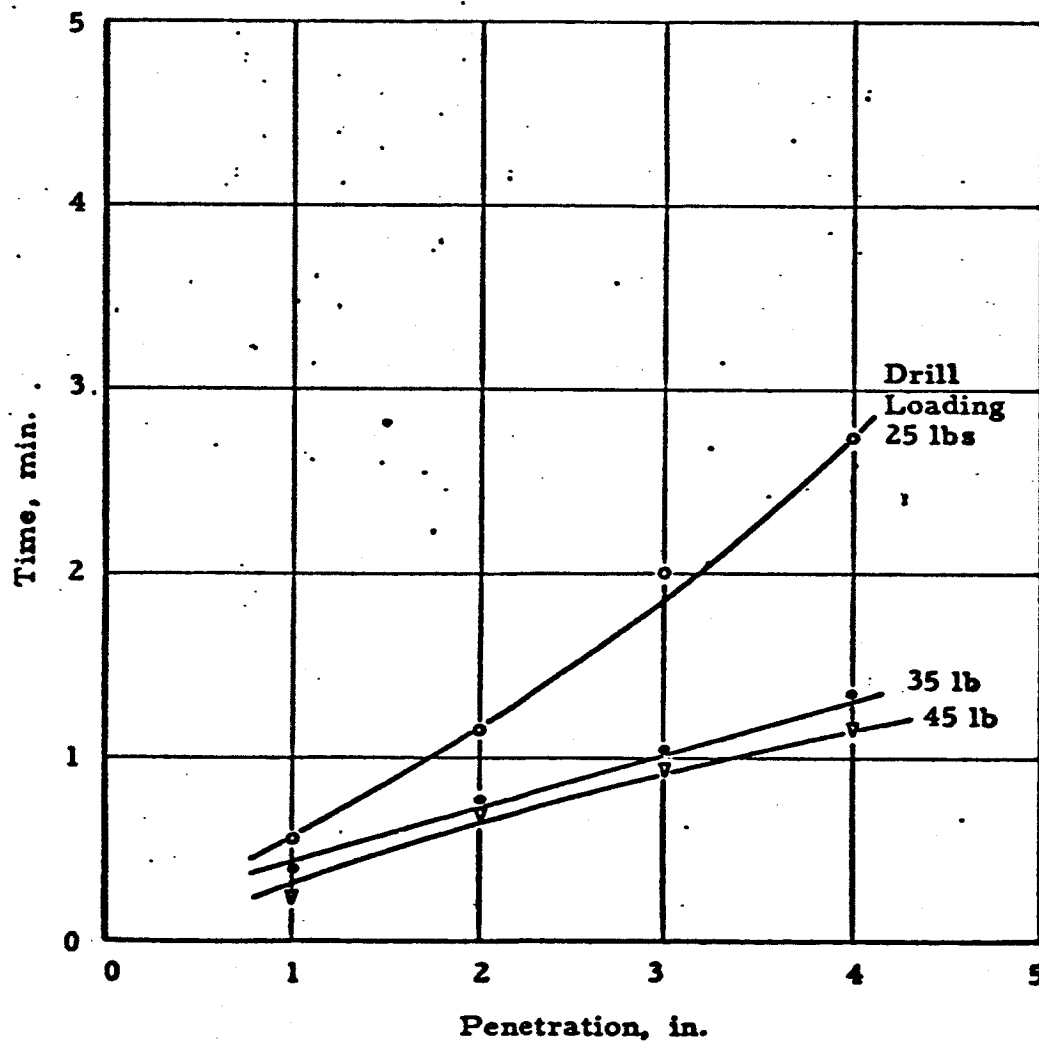


Fig. 5

D-1 DRILL IN LIMESTONE
900 RPM

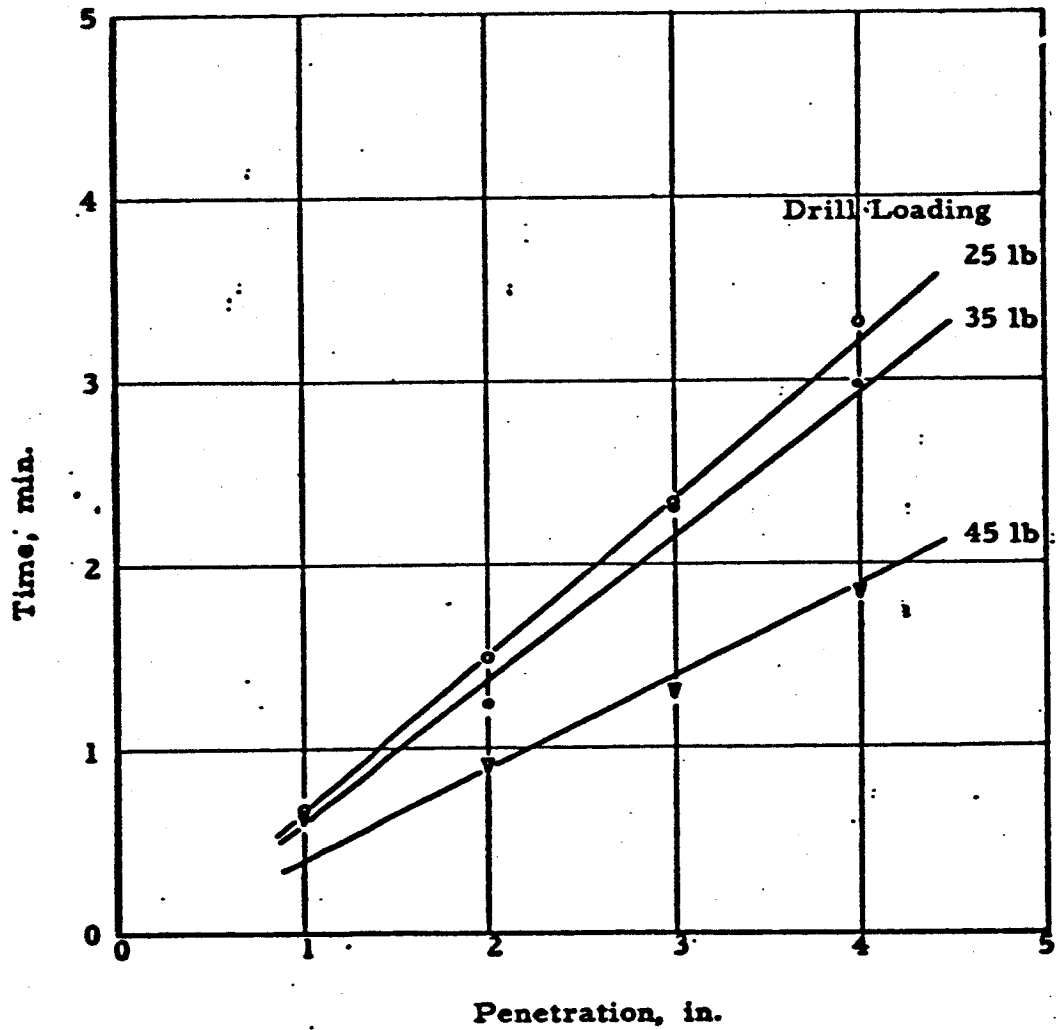


Fig. 6

D-1 DRILL IN HORNBLEND SCHIST
900 RPM

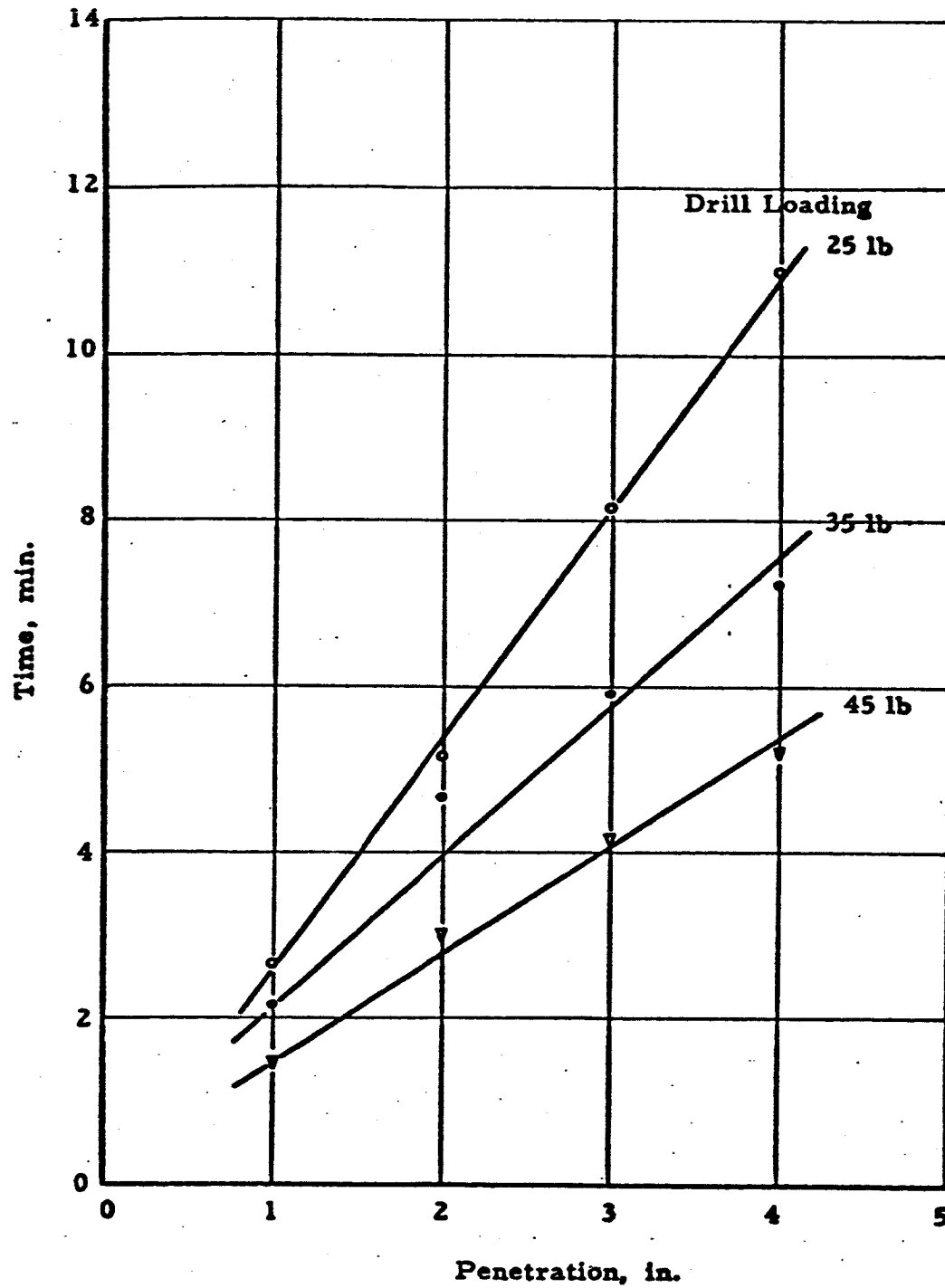


Fig. 7

D-1 AND D-2 DRILLS IN MARBLE 900 RPM

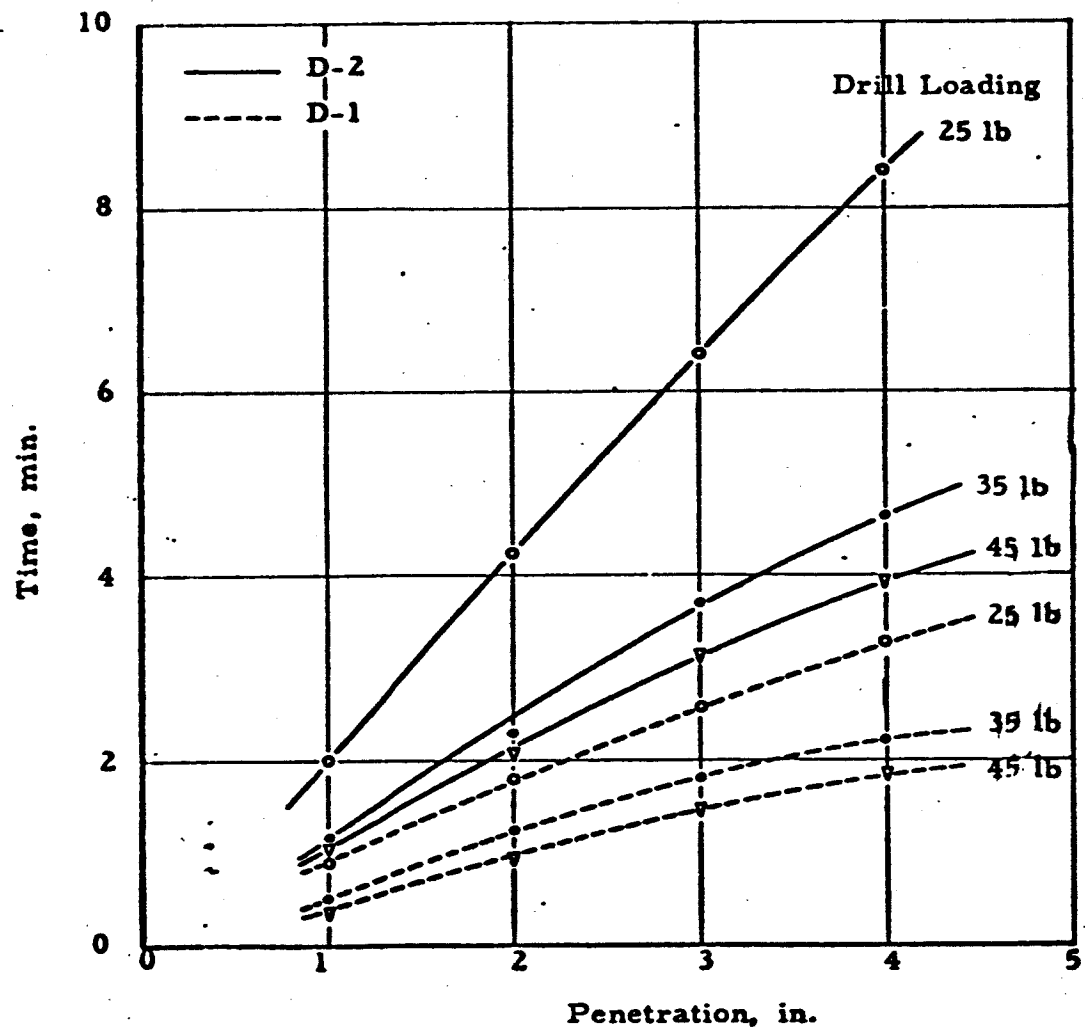


Fig. 8

D-2 DRILL IN HORNBLEND SCHIST
900 RPM

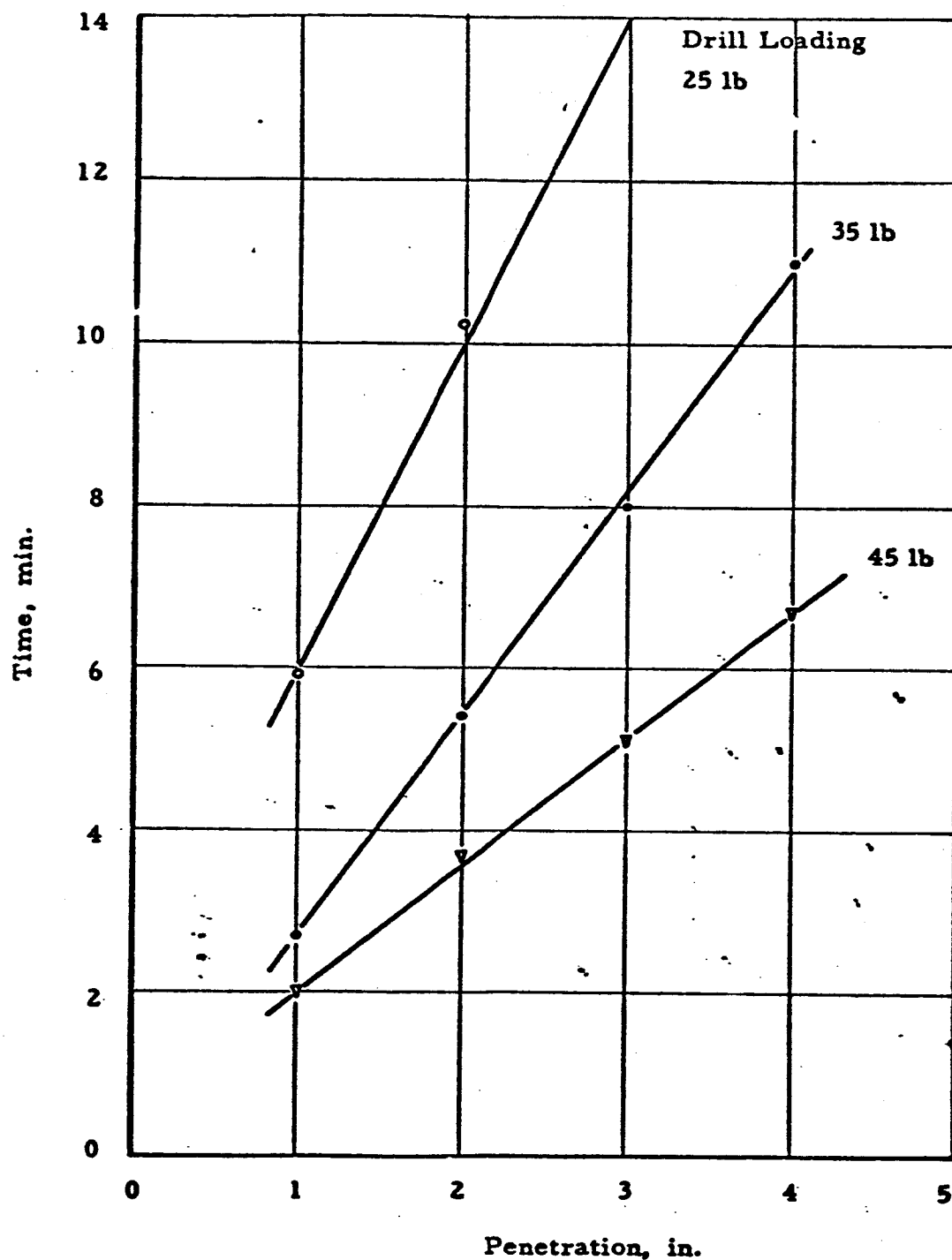


Fig. 9

ARMOUR RESEARCH FOUNDATION OF ILLINOIS INSTITUTE OF TECHNOLOGY

D-2 DRILL IN LIMESTONE
900 RPM

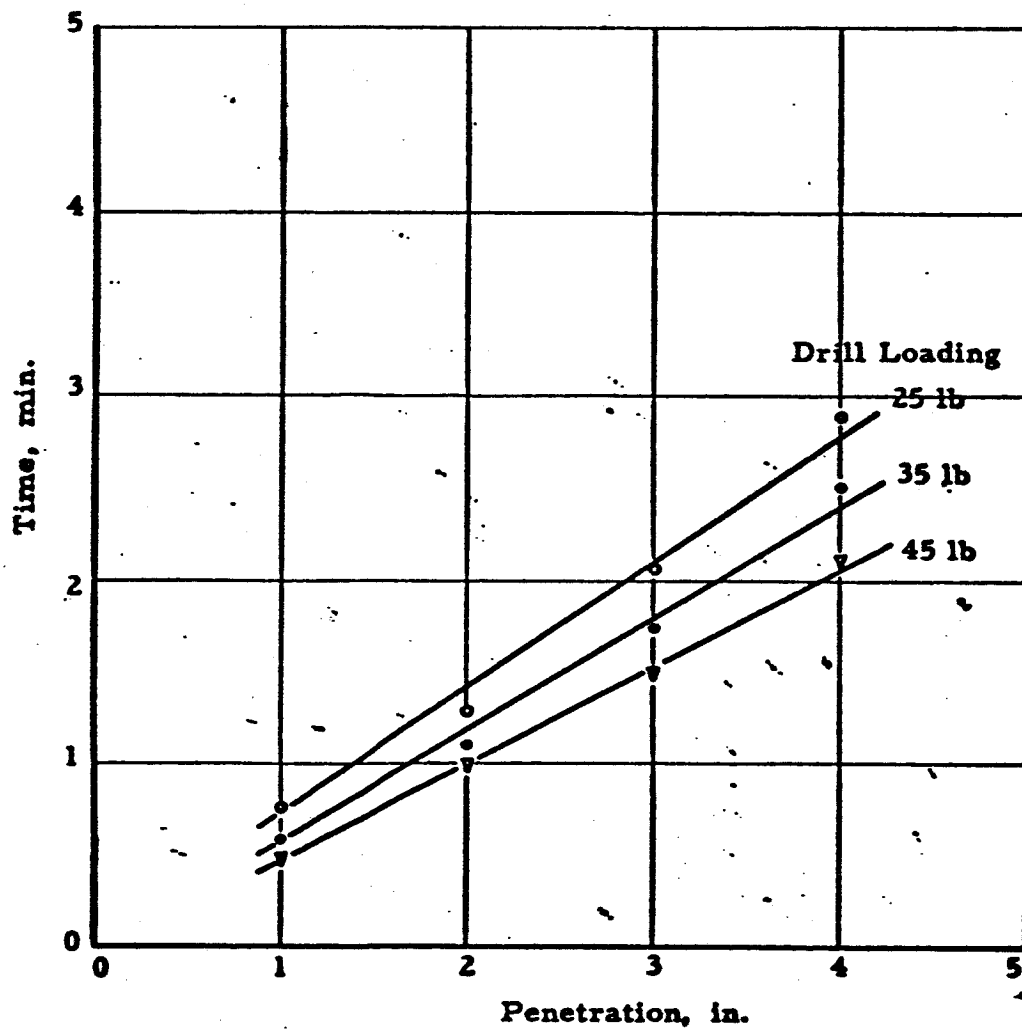


Fig. 10

D-2 DRILL IN CONCRETE NO. 1

900 RPM

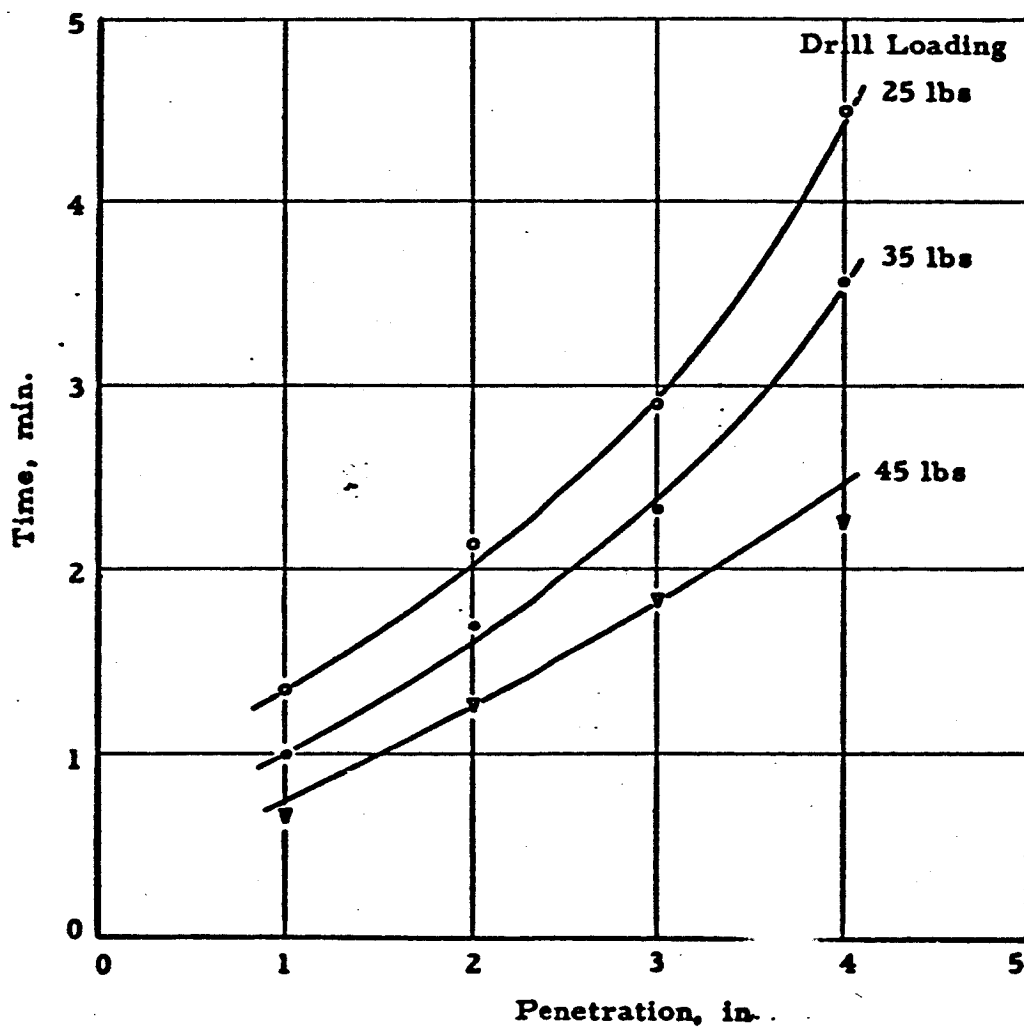


Fig. 11

One diamond drill (D-4) was instrumented for temperature and tried in granite and sandstone. The results of these tests are discussed in Sec. II-B-3, "The Bit and Rock Particle Temperature."

The D-1 drill was checked in granite on the ARF-modified drill press at 50-lb load and 735 rpm, without any cooling. No significant penetration was recorded. Drill press vibration made starting the hole difficult, and even a pre-drilled starting hole did not improve performance. The D-3 and D-5 drills were tested with 50-lb load and 1190 rpm and 735 rpm respectively, other conditions being the same as in the D-1 drill test. The same problems were encountered, and no penetration was recorded. (No plots are presented for this sequence of tests.)

(2) Carbide - Rotary Drilling

The C-1, C-2, C-3, and C-4 drill performances in materialite, concrete No. 2, granite and sandstone are presented in Fig. 12, 13, 14, 15, 16, 18, 19, 20.

Drilling in materialite demonstrated the importance of adequate chip transportation. Figs. 12, 13, 14, 15 present the power, penetration, time relationships for three loading conditions (24, 45, 62 lb) at 328 rpm and for the as - delivered flute length of each drill. Unless the drill shank is fluted to permit chip transportation to the surface, power requirements increase. In one case (Fig. 13) the 24-lb drill load was not sufficient to maintain constant penetration rate.

Power consumption for all of the drills ranged between 130 to 250 w., and the maximum penetration rate recorded was 1.42 in. /min. Optimum drill loading, at 328 rpm, was greater than 62 lb, the highest loading utilized. Power requirement increased with penetration rate and drill loading. Cutting surfaces showed wear after 40 to 50 in. of penetration. There were no hole starting problems: all drills, being of conical shape, showed no tendencies to wander. The surfaces of drilled hole walls were coated with fine dust particles, highly polished and hard; this was the result of the clogging effect.

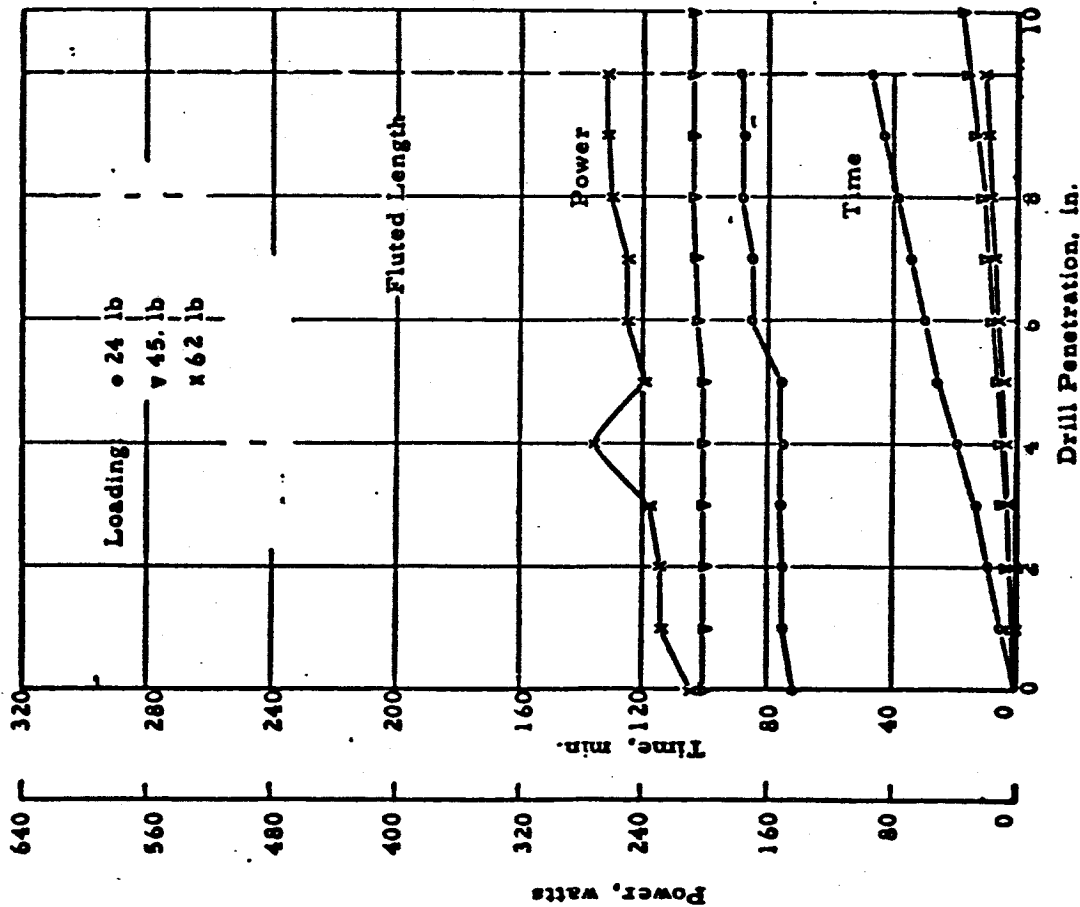


Fig. 12

C - 1 DRILL IN MATERIALITE
328 RPM

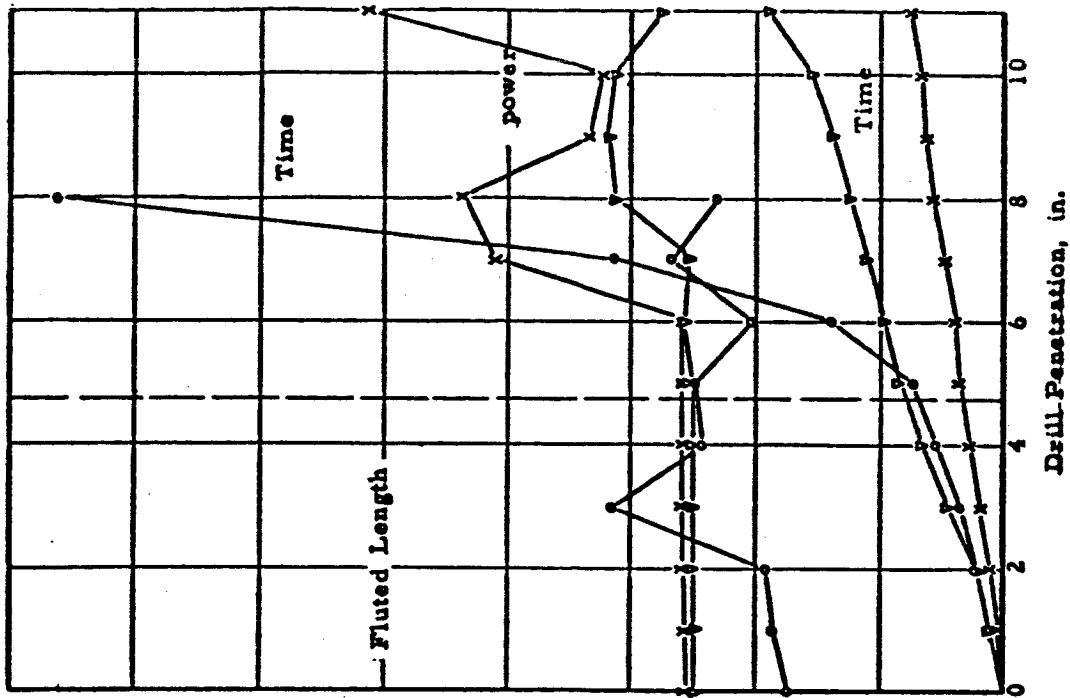
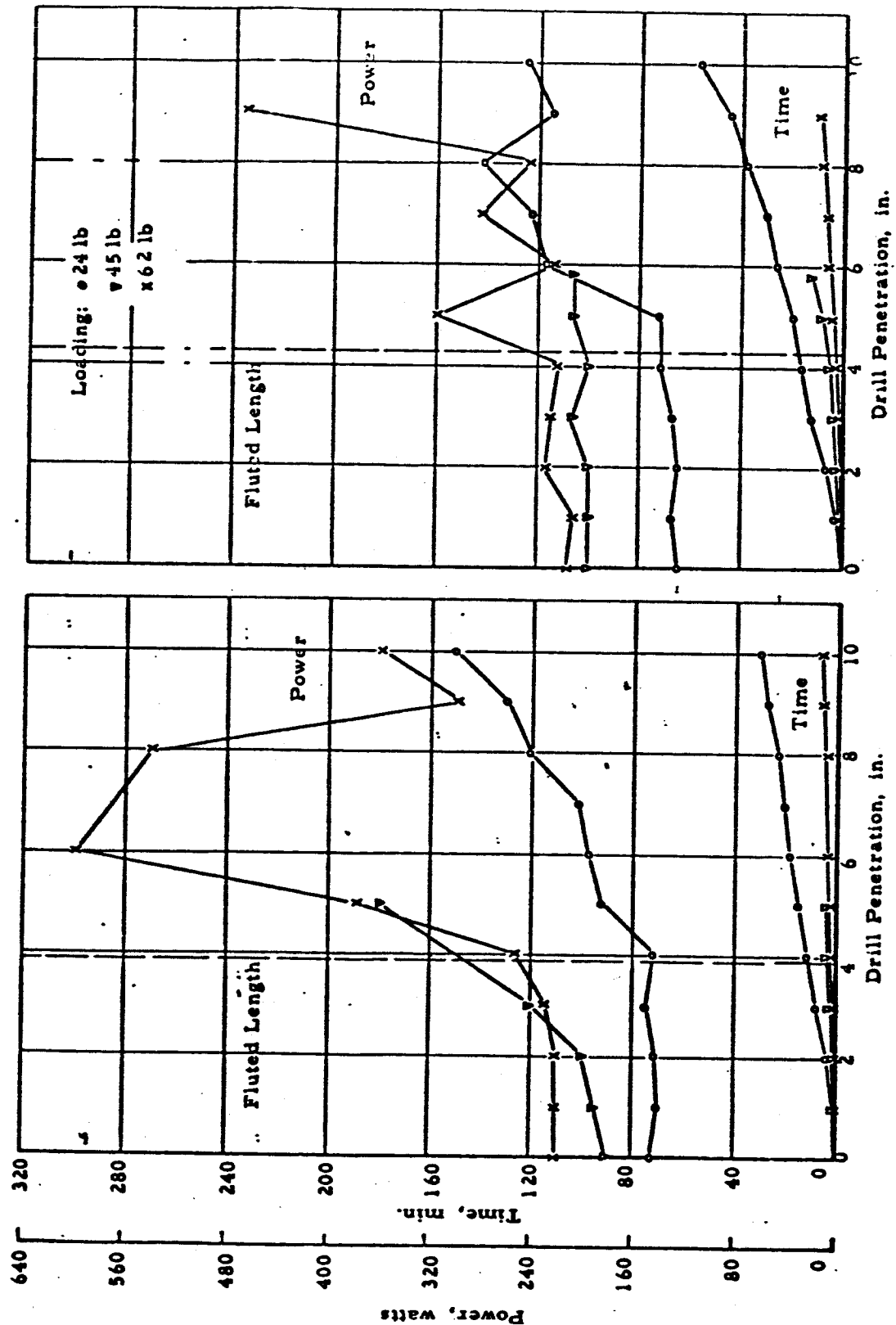


Fig. 13

C - 2 DRILL IN MATERIALITE
328 RPM



ARMOUR RESEARCH FOUNDATION OF ILLINOIS INSTITUTE OF TECHNOLOGY

C-4 DILL IN MATERIALITE; 328 RPM

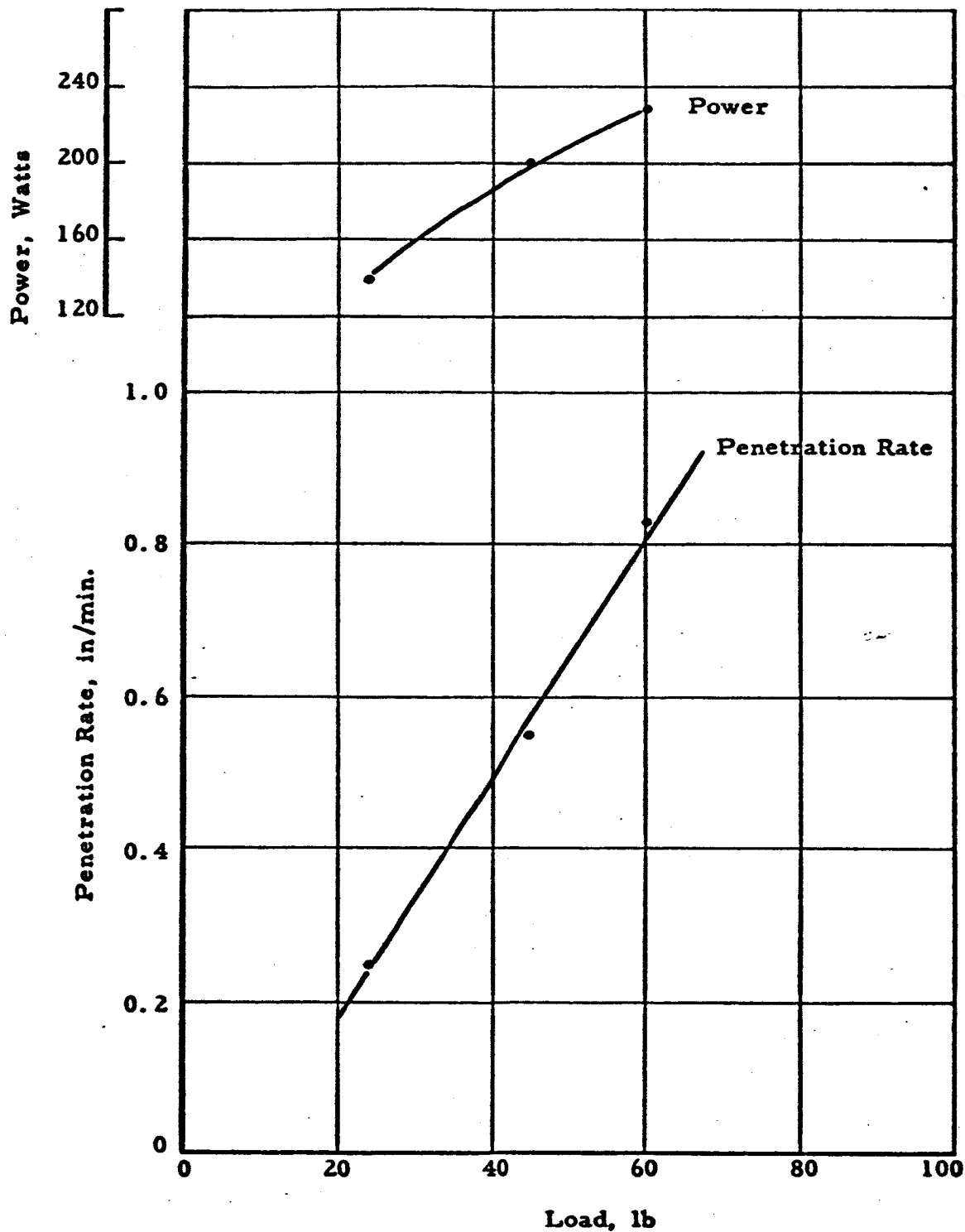


Fig. 16

ARMOUR RESEARCH FOUNDATION OF ILLINOIS INSTITUTE OF TECHNOLOGY

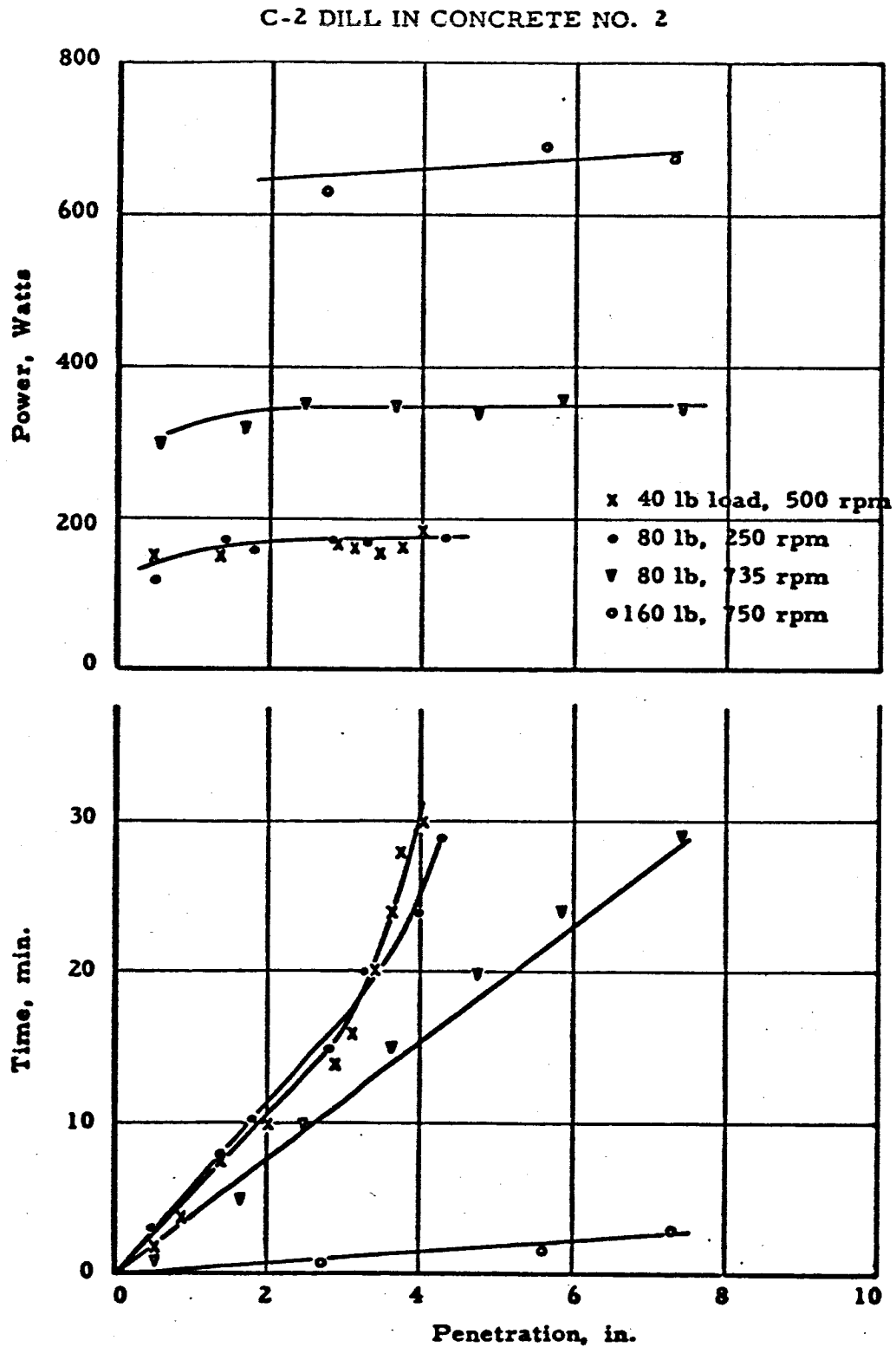


Fig. 17

ARMOUR RESEARCH FOUNDATION OF ILLINOIS INSTITUTE OF TECHNOLOGY

C-4 DRILL IN CONCRETE NO. 2

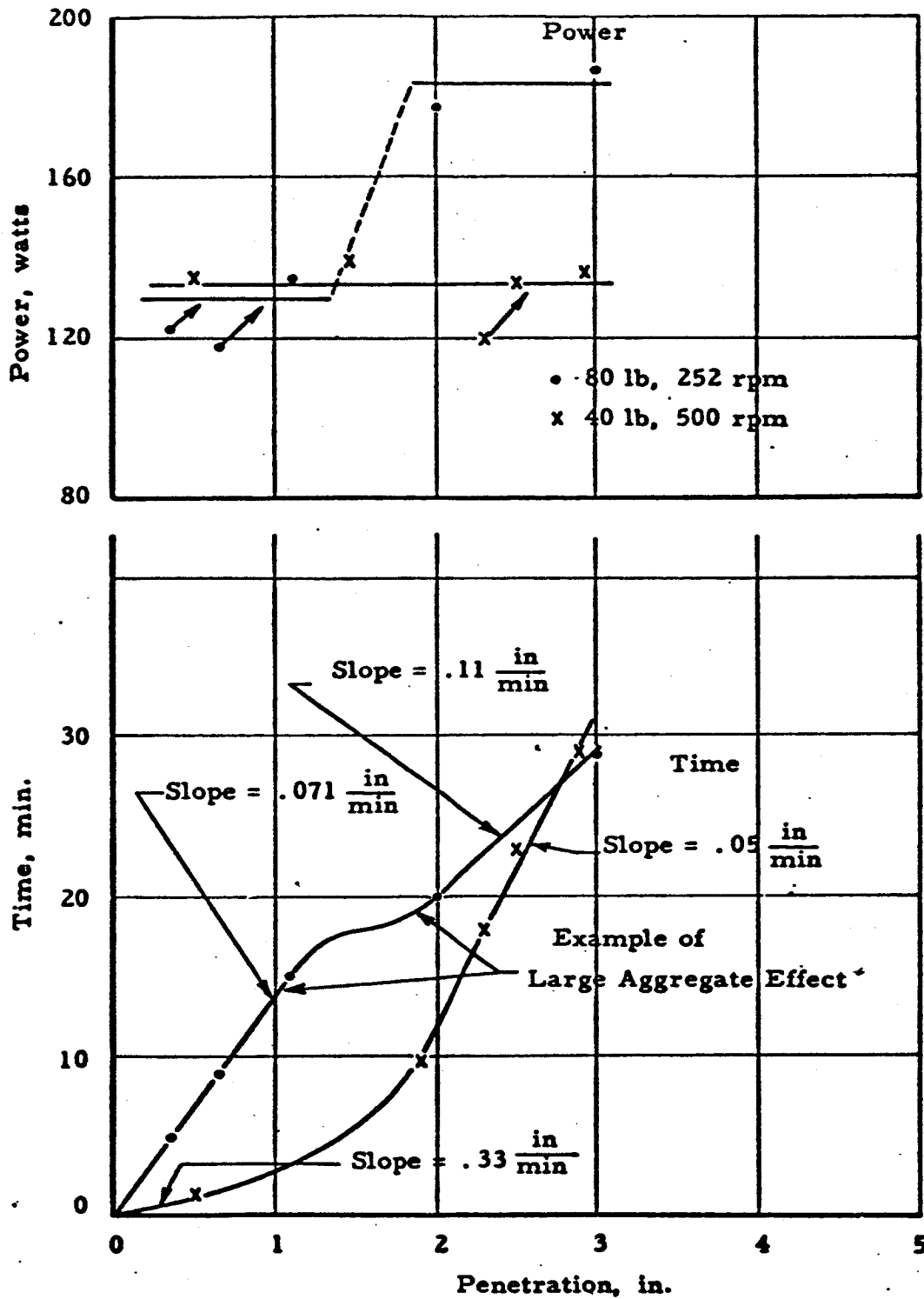


Fig. 18

C-4 DRILL IN BEREA SANDSTONE

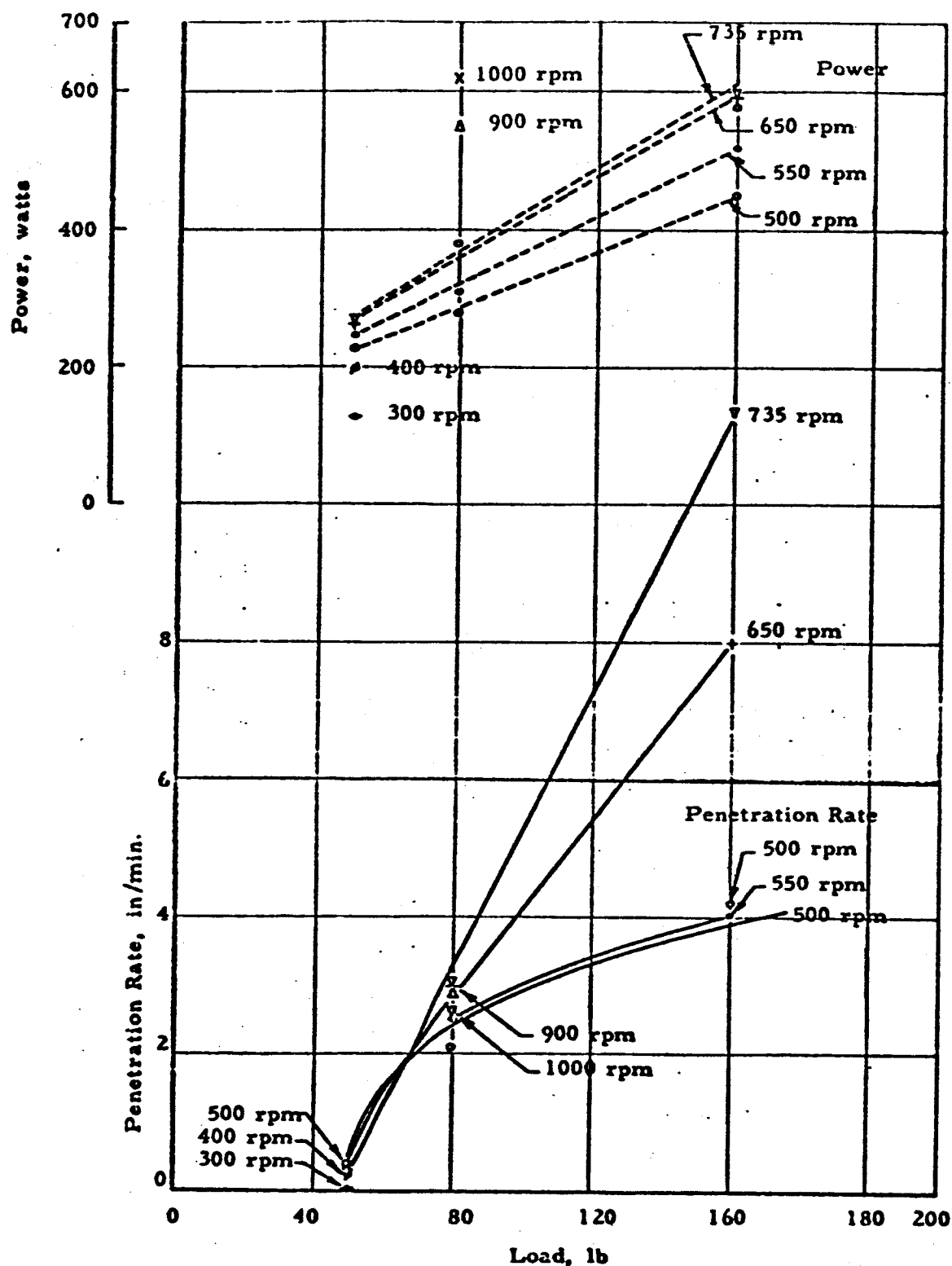


Fig. 19

ARMOUR RESEARCH FOUNDATION OF ILLINOIS INSTITUTE OF TECHNOLOGY

C-4 DRILL IN BEREA SANDSTONE

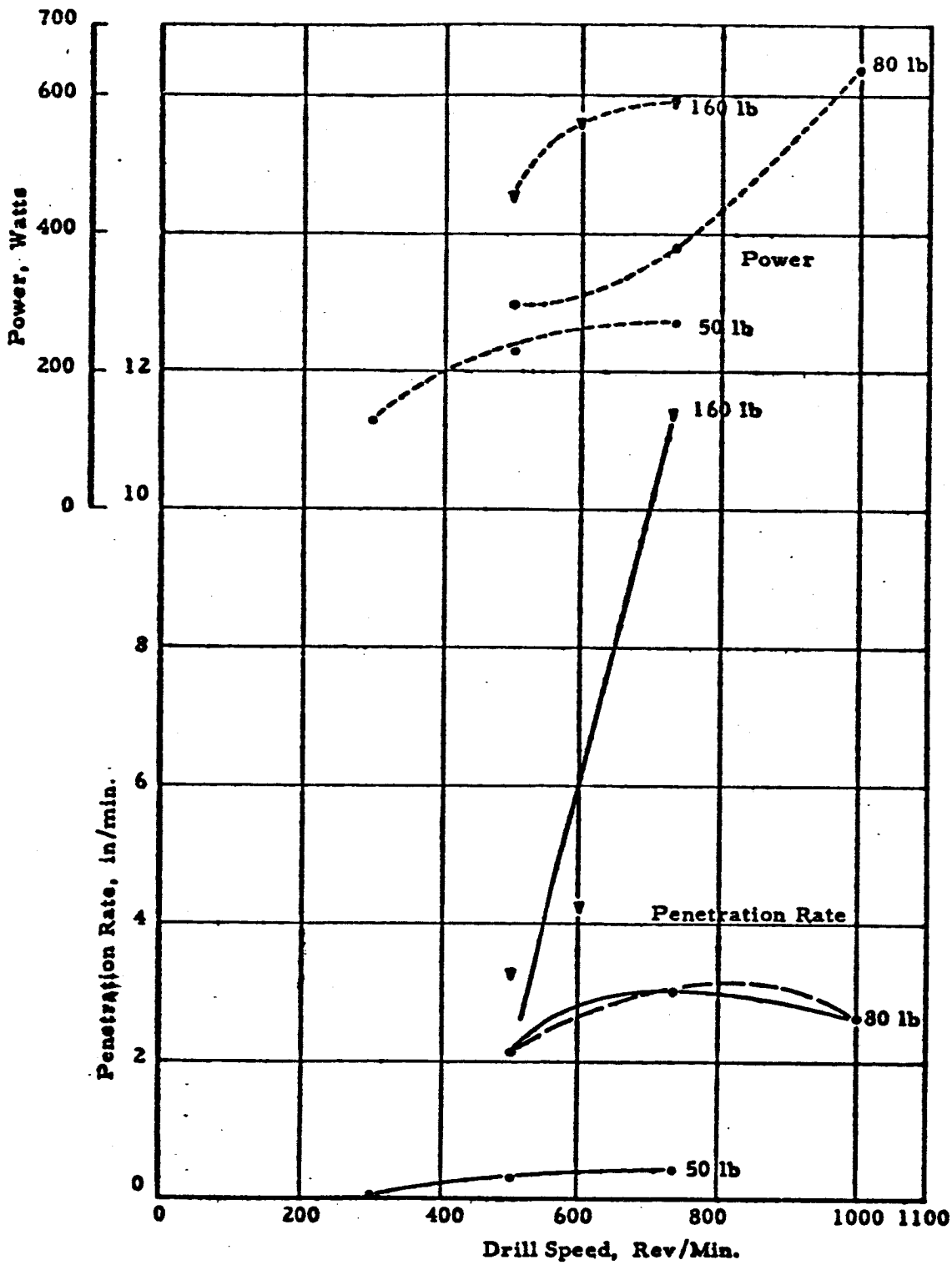


Fig. 20

ARMOUR RESEARCH FOUNDATION OF ILLINOIS INSTITUTE OF TECHNOLOGY

Drills C-3 and C-4 were further tested in concrete No. 2 (Fig. 17, 18). Concrete No. 2 (Sec. II-A-5) features an appreciable amount of large aggregate and thus can not be considered as a "uniform" rock. Tests in concrete No. 2 illustrate well non-uniform rock drilling effects and possible lunar drill data interpretational pitfalls. As shown in Fig. 17, the penetration rate of the C-4 drill at 80 lb and 252 rpm changes from 0.071 in. /min at the start of the test to 0.11 in. /min at a point during the test with a comparable power increase from 130 to 184 w. At 40 lb and 500 rpm the same drill produces an initial penetration rate of 0.33 in. /min and a final rate of 0.05-in/min. A constant power input level is maintained throughout the run. Starting and initial wear phenomena might be theorized in the latter case, but this is refuted by the results of the first test. Fig. 18 illustrates the desirability of higher loading. For a 160-lb load, a 3-in. depth is attained in 1.25 min, utilizing $(1.25 \text{ min})(650 \text{ w}) = 812 \text{ w-min}$ of energy. No dulling effects were apparent. For a 40- or 80-lb load, 3 in. is drilled in 17 min, utilizing $(17) \times (170) = 2890 \text{ w-min}$ of energy. Definite dulling effects were encountered.

C-2 and C-4 drills were tried in granite. No significant penetration was recorded.

Sandstone was drilled with the C-4 drill and these data are plotted in Fig. 19, 20. Constant penetration rates were obtained throughout these tests. The results indicate that a 50-lb load and 300 rpm combination defines the lower penetration limit: lower load and speed settings result in zero penetration. Optimum speed for this drill at the 50-lb load lies in the 700-rpm range, at a 270-w power level. Further experimental data is required to explain the slope of the power curve in Fig. 20. This bit showed wear after 15 in. of drilling, especially at low speeds.

Of the four carbide rotary drills tested, the C-4 drill provided the highest performance. Data regarding the remainder is summarized below.

The C-5 drill was found to be ineffective in granite.

The C-6 drill (Fig. 21) was tried in concrete No. 2 at an 80-lb load, 500 rpm. The highest penetration rate was 0.1 in. /min at 230- to 260-w level. Dulling of the bit was evident.

ARMOUR RESEARCH FOUNDATION OF ILLINOIS INSTITUTE OF TECHNOLOGY

C-6 DRILL IN CONCRETE NO. 2
80 lb., 500 RPM

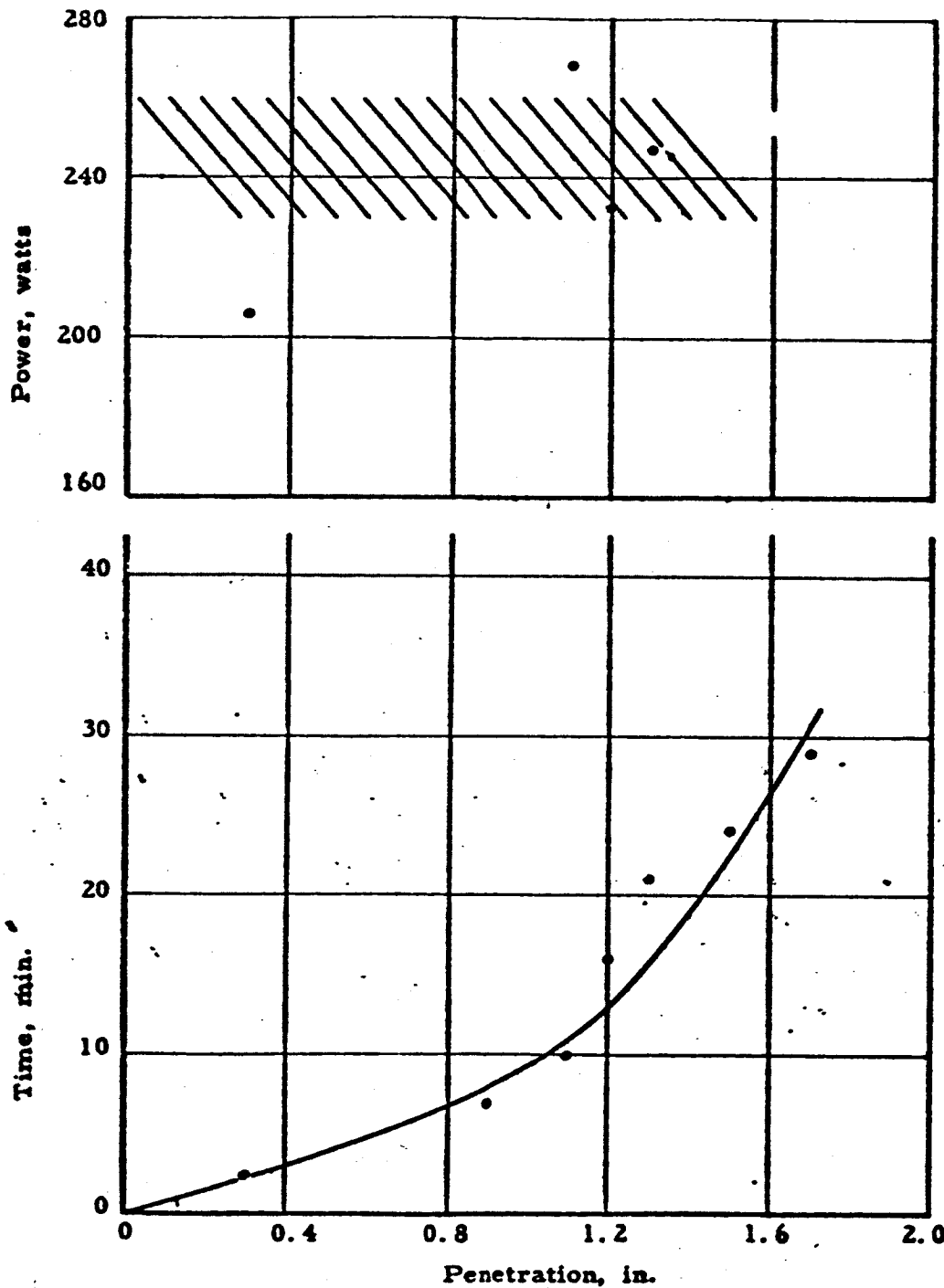


Fig. 21

The C-7 1-in. -diam. drill was tested in granite at a 50-lb load and 350, 500, 732 rpm. Optimum speed is at approximately 500-rpm as reflected in the parameters of penetration rate, energy requirement, and bit wear. Test results are presented in Fig. 22.

Three sizes (1-in., 1-1/2-in., 2-in. diam.) of the C-8 type drill were tested in sandstone and in granite.

Sandstone drilling (Fig. 23, 24, 25, 26) produced constant penetration rates and consistent data. The results indicate that maximum penetration rate at a 50-lb load can be achieved with speeds greater than 800 rpm, but possibly at prohibitive power and energy levels. (See Fig. 24):

A drill loading of 50 lb and a speed of 350 rpm results in a penetration rate of 1 in. /min and a total energy requirement of 180 w-min/in. Similarly values of 50 lb and 800 rpm result in a penetration rate of 3.2 in. /min and an energy input of 2180 w-min/in. Slightly higher loading, 80 lb, results in improved performance, however, a 160-lb load is greater than optimum. At a load of 50 lb, drill speeds as high as 500 rpm were found ineffective in varying the penetration rate of the 2-in. -diam. drill (Fig. 26). At speeds above 400 rpm, noticeable starting problems were encountered and holes had to be predrilled. Wear was evident after 15 to 20 in. of penetration.

Drilling in granite (Fig. 27, 22, 28, 13, 23) produces a drop in power with a decrease of penetration rate as the drill begins to penetrate. This results because dulling prevents the drill from taking as large a cut. Higher loads produced higher penetration rates with lower total energy requirements. A penetration rate of 0.146 in. /min with 1-in. drill (Fig. 27) at 50-lb load, 500 rpm, resulted in an energy requirement of $205/0.146 = 1400$ w-min. /in. Similarly the rate was 0.384 in. /min at 50-lb load, 500 rpm, and the energy $345/0.384 = 900$ w-min/in. (Fig. 28). It is of significance to note that at high loads and high speed combinations (160 lb, 500 rpm, 760 rpm) the 1-in. -diam. drill produced no penetration. This finding not substantiated by tests at larger drill diameters, requires additional experimental study.

Immediate bit dulling was evident during the tests. The drill would "grind itself" to a constant penetration rate configuration (Fig. 28, 1-1/2-in. and 2-in. diam., 160 lb, 500 rpm) and maintain this rate till destruction by dulling. Wear was found with all drills.

ARMOUR RESEARCH FOUNDATION OF ILLINOIS INSTITUTE OF TECHNOLOGY

C-7 DRILL IN GABBRO GRANITE

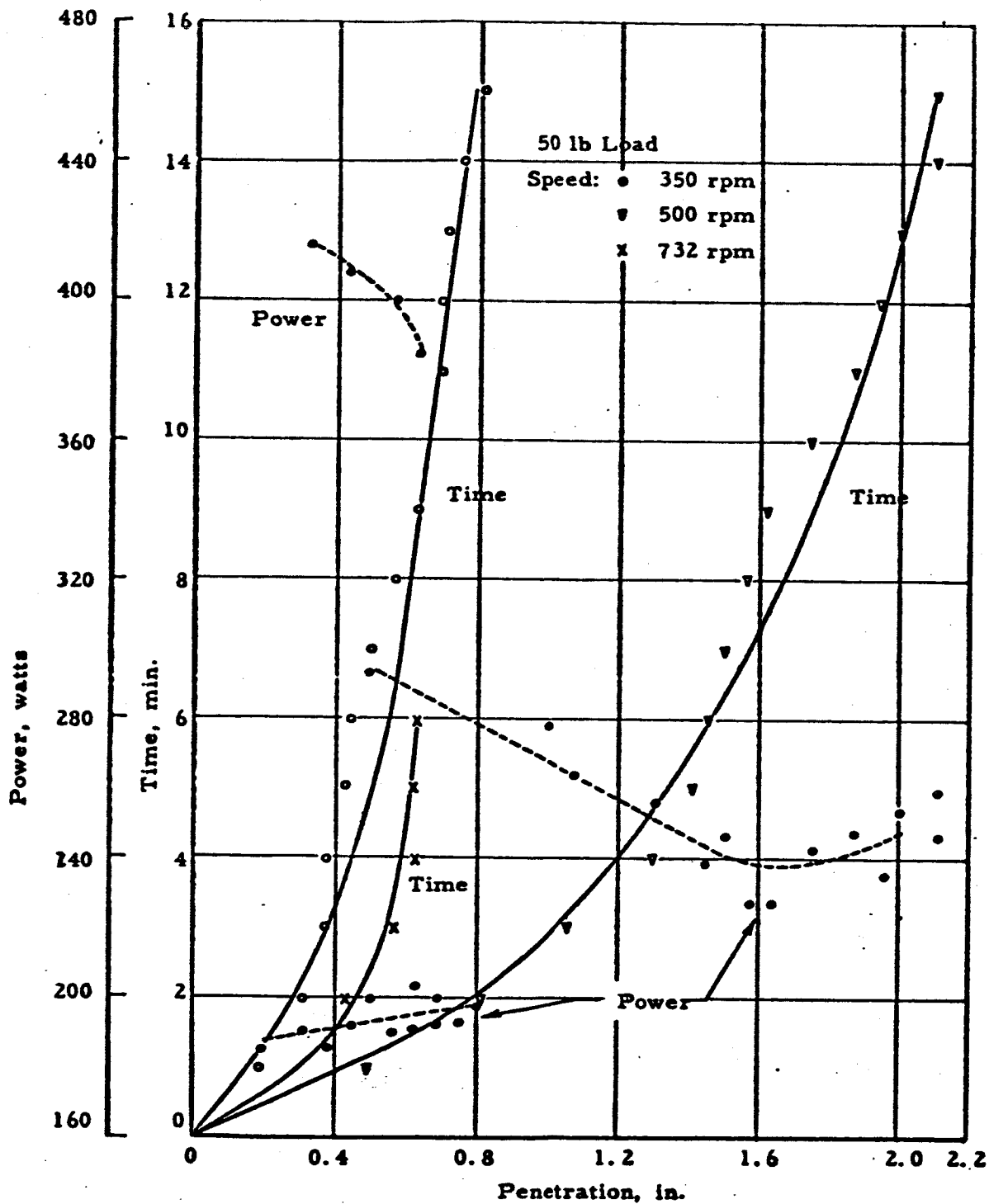


Fig. 22

C-8 1 INCH DIAMETER DRILL IN
BEREA SANDSTONE

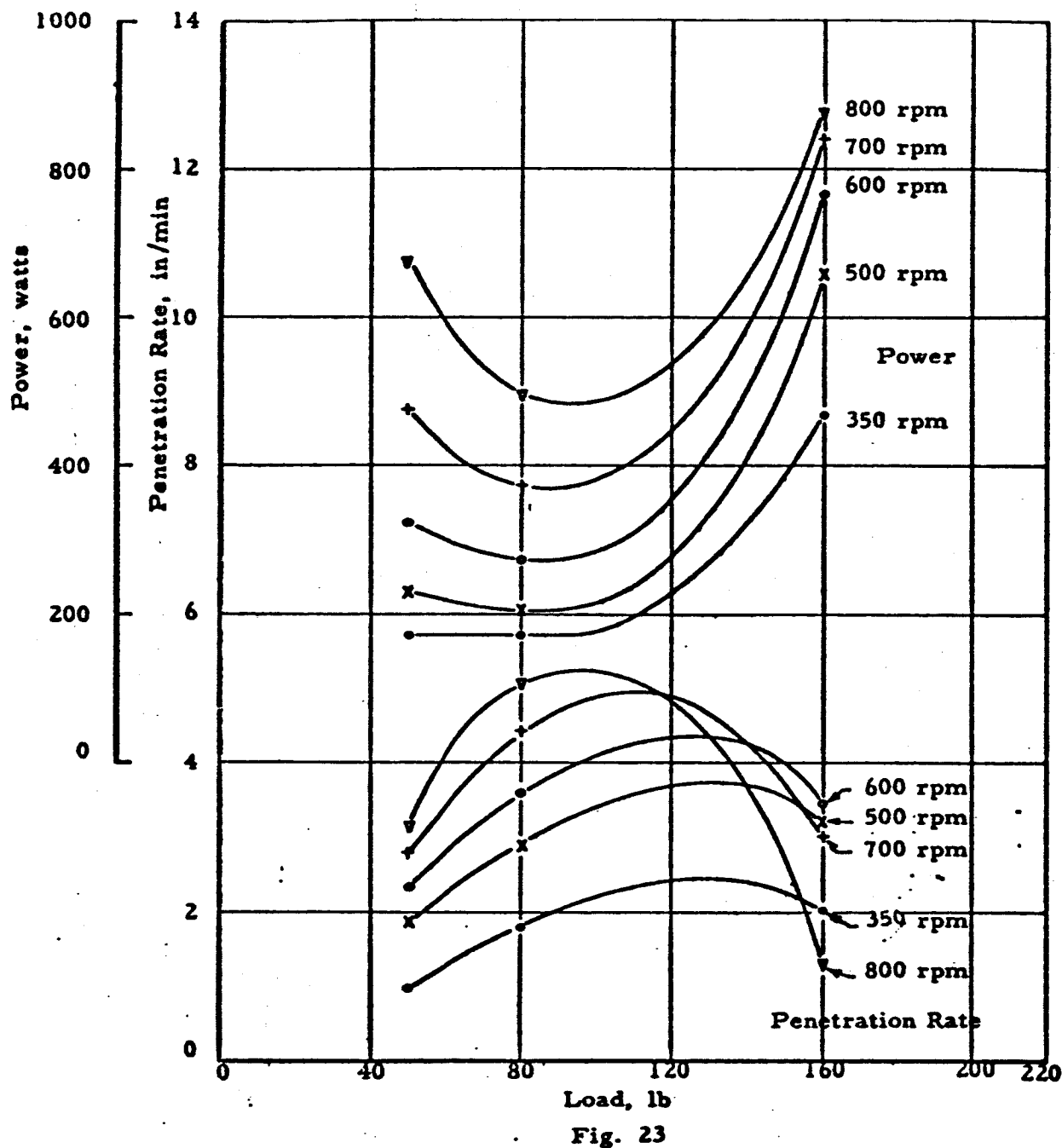


Fig. 23

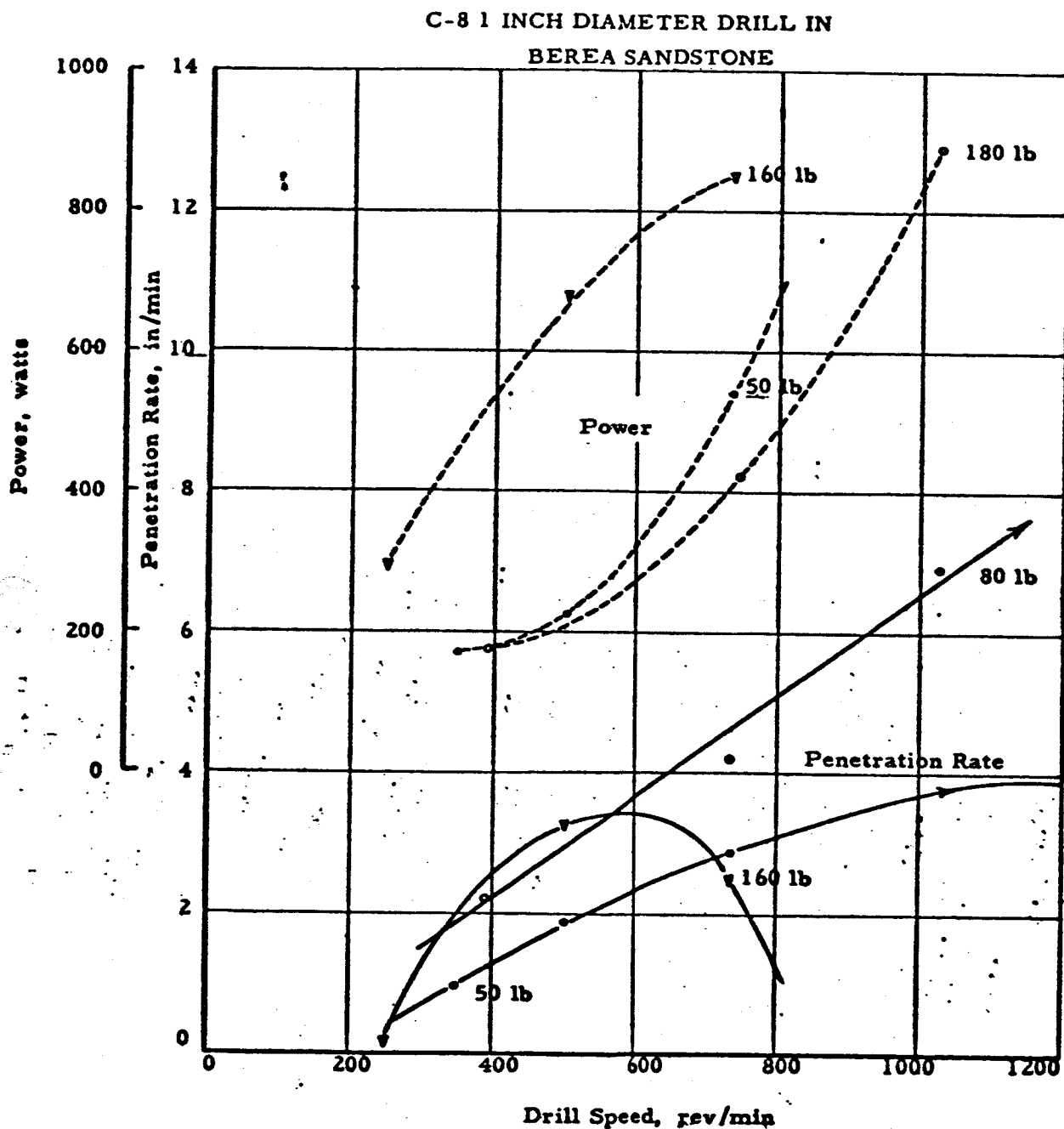


Fig. 24

C-8 2 INCH DIAMETER DRILL IN BEREA SANDSTONE

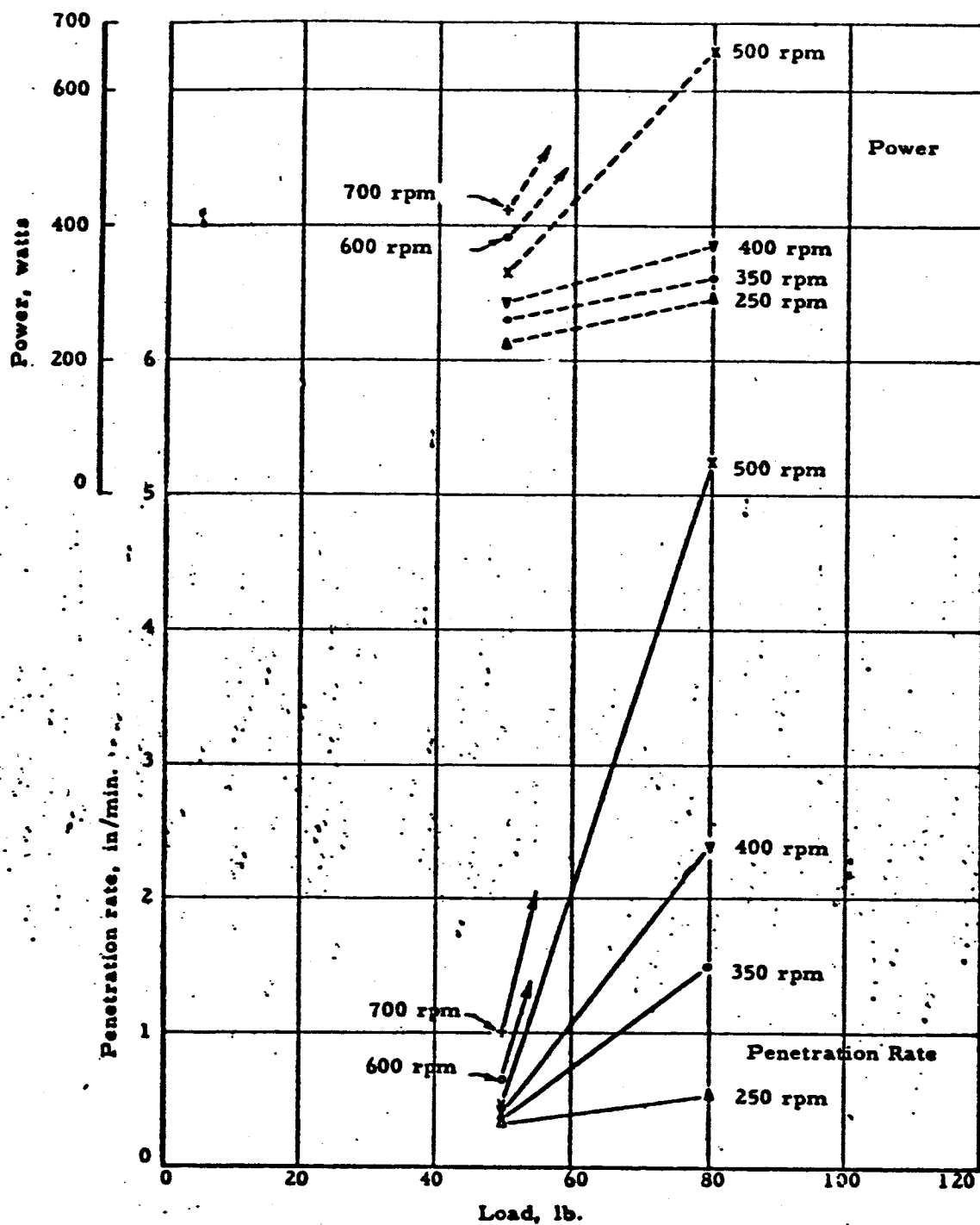


Fig. 25

C-8, 2 INCH DIAMETER DRILL IN
BEREA SANDSTONE

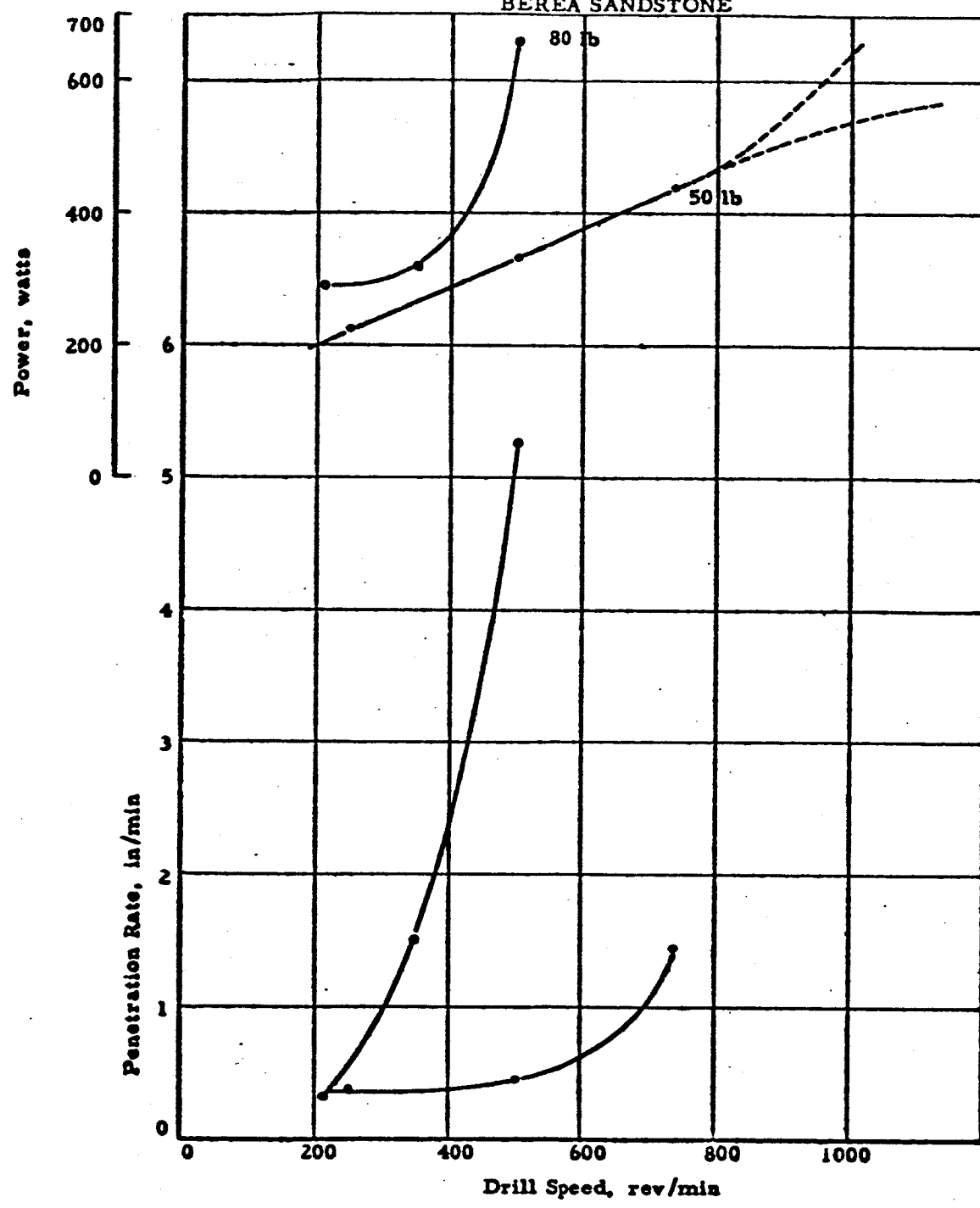


Fig. 26

C-8, 1 INCH DIAMETER DRILL IN
GABBRO GRANITE

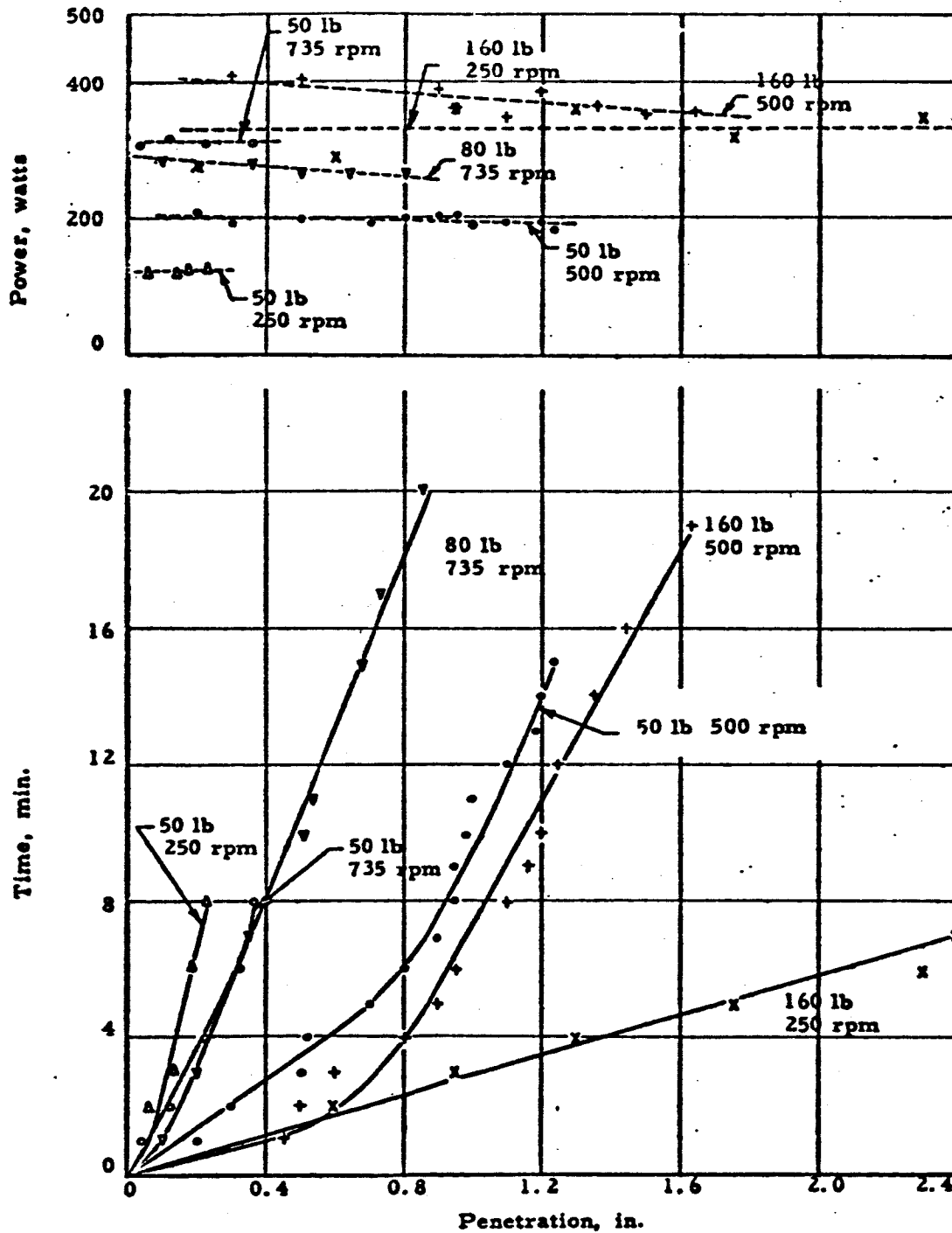


Fig. 27

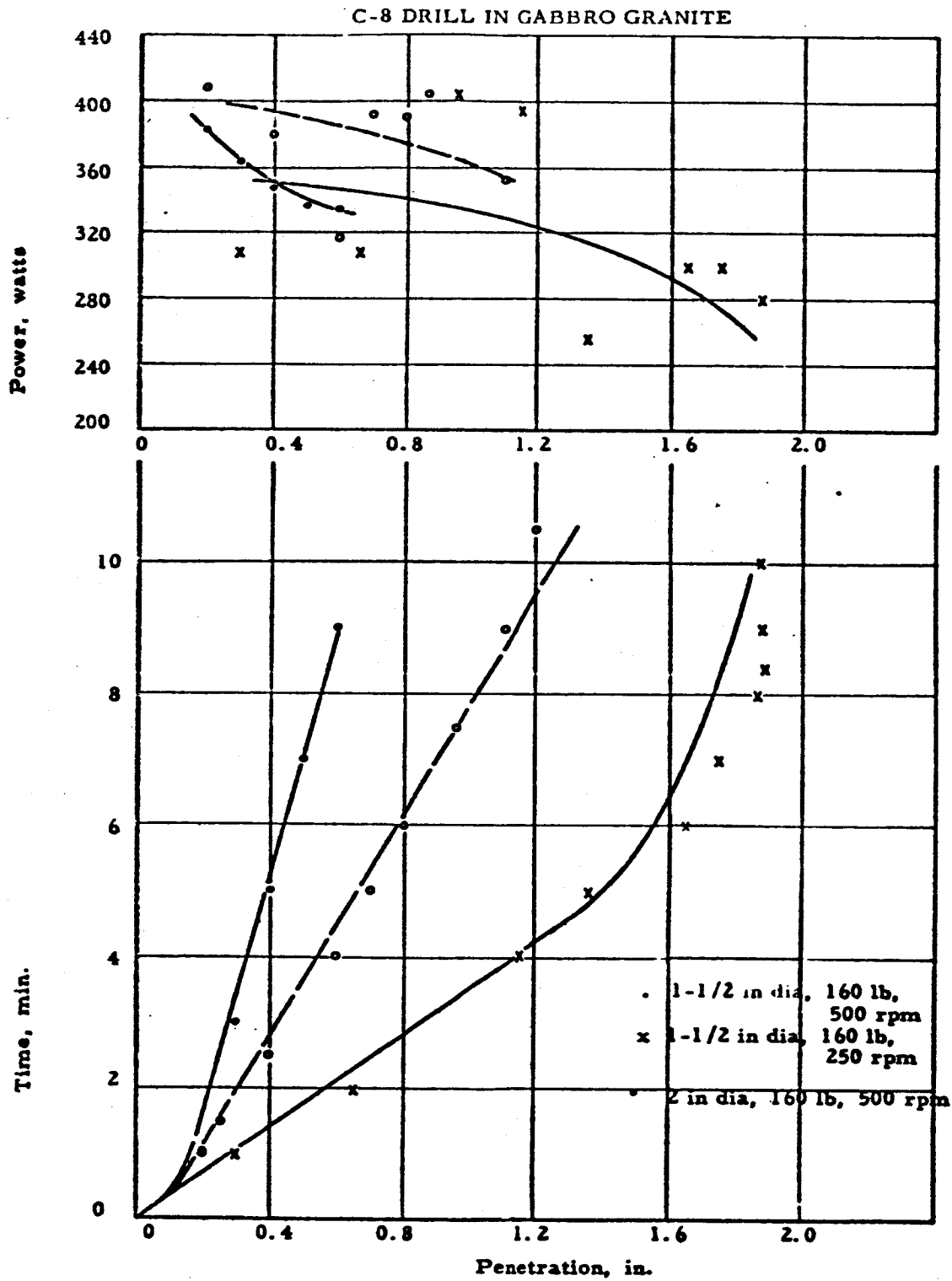


Fig. 28

C-9 and C-10 drills were tested out in granite and were found to produce insignificant penetrations.

In general, carbide tip coring drills tend to dull rapidly in granite. The result is reduced power consumption because of lighter cut being taken. This drop in power consumption towards a limiting value is a symptom of carbide bit dulling.

(3) Rotary Impact Drilling

Skil Corp. Roto Hammers, Model No. 736 and No. 726, were tested in granite and sandstone. All tests were made with a 50-lb load. The performance is summarized in Fig. 29 and 30.

Model No. 736 drilled 1-in. and 1-1/2-in.-diam. holes in sandstone, granite, and wood at a constant 940-w power level. The drill idled at a no load power consumption of 900 w.

Model No. 726 drilled sandstone and granite at 550 w. Figure 29 presents a summary of results for 18-in.-long bits; Fig. 30 summarizes the performance for an 18-in. bit with a 42-in.-long extension shank.

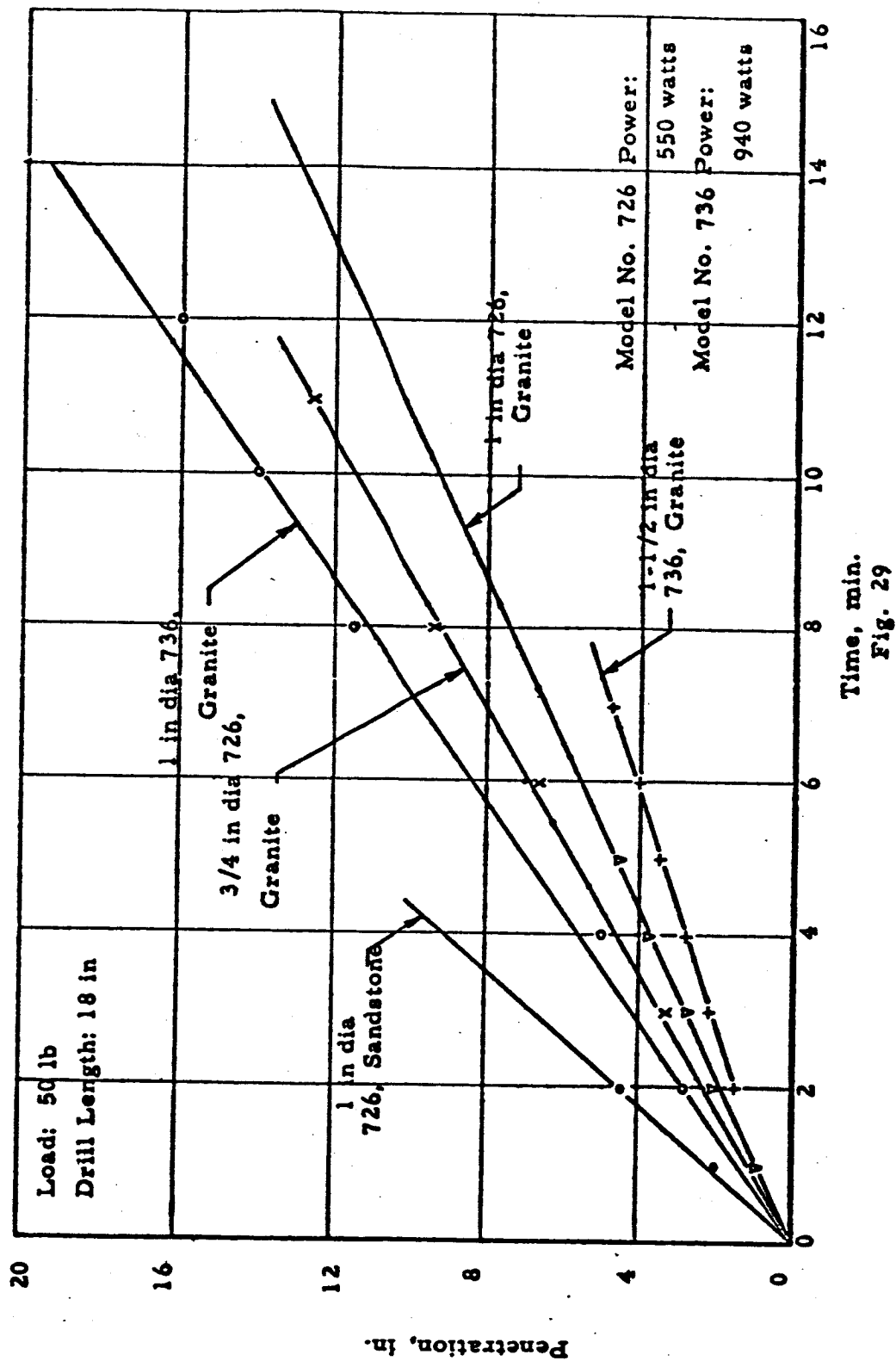
The tests demonstrated appreciable energy loss in the longer drill shank. As an illustration, consider the 1-1/2-in.-diam. bit in granite, powered with the Model 736 Roto-Hammer:

Drill Length	Penetration Rate	Energy
18 in.	0.666 in. /min	$(940 \text{ w}) \left(\frac{1}{0.666 \text{ in. /min}} \right) = 1410 \frac{\text{w-min}}{\text{in.}}$
18 + 42 in.	0.51 in. /min	$(940) \left(\frac{1}{0.51} \right) = 1845 \frac{\text{w-min}}{\text{in.}}$

The energy lost in 42 inches of drill shank is $435 \frac{\text{w-min}}{\text{in.}}$. The time required to penetrate 1 in. of granite with the 42-in.-long shank is 1.96 min/in.

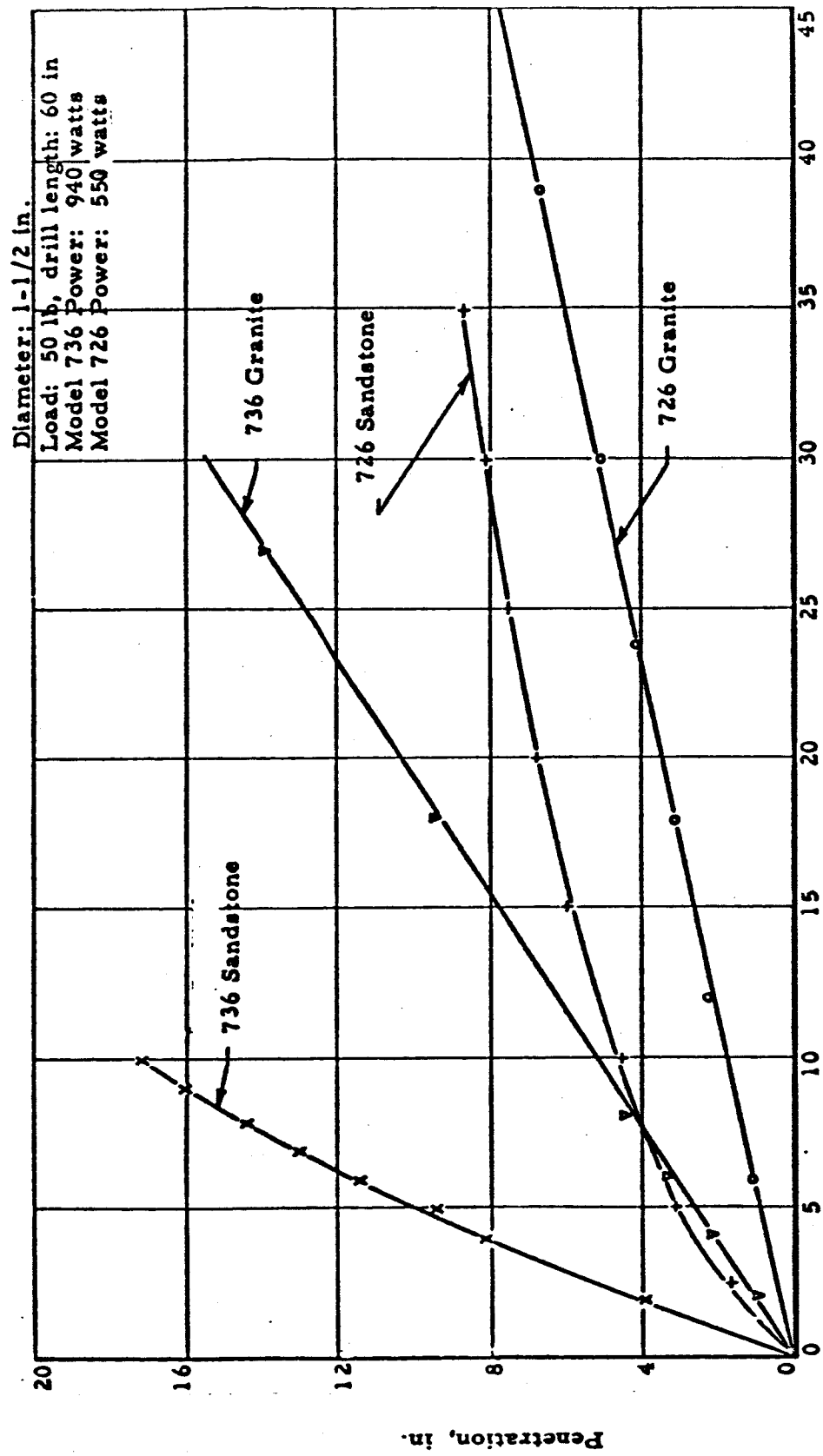
The drill operates at 2200 blows/min, therefore, the energy lost per blow is $435 \times \frac{1}{1.96} \times \frac{1}{2200} = 0.101 \frac{\text{w-min}}{\text{blow}}$.

SKIL CORP. ROTARY IMPACT DRILLS IN GABBRO GRANITE AND BEREA SANDSTONE



ARMOUR RESEARCH FOUNDATION OF ILLINOIS INSTITUTE OF TECHNOLOGY

SKIL CORP. - ROTARY IMPACT DRILLS IN GABBRO GRANITE AND BEREA SANDSTONE



Time, min.
Fig. 30

Bit wear was greater when drilling in sandstone than in granite. The statement is illustrated in Fig. 30, which shows a non-constant rate of penetration in sandstone. Five 12-in.-deep holes were drilled in granite with a 1-in.-diam. drill on Model 736. Penetration rate and power remained constant, though the examination of the bit revealed a definite dulling of cutting edges. The following penetration rates were obtained during the tests:

Model	Drill diam. in.	Drill length, in.	Material	Penetration rate, in. /min
736	1-1/2	18 + 42	granite	0.51
	1-1/2	18	granite	0.66
	1	18	granite	1.38
	1-1/2	18 + 42	sandstone	2.8, average
726	1-1/2	18 + 42	granite	0.172
	1-1/2	18 + 42	sandstone	0.137 minimum
	1	18	granite	0.924
	1	18	sandstone	2.22
	3/4	18	granite	1.14

These units exert a negligible torque on the rock, but are noisy and vibrate. Wood was drilled to check if the hammer would be at all effective. No measurements were taken, but Model No. 736 with a 1-in. drill did penetrate wood.

The Stanley Impact Drill (Sec. II-A-2-f) was tested in granite. At 900 w and an 80-lb load, a 1-in. drill penetrated 2-1/2 in. in 3.67 min for a penetration rate: 0.68 in. /min. No further tests were made.

3. Bit and Rock Particle Temperature

Interest in temperature is due to two reasons: (a) drill wear and (b) possible change in physical properties of the rock samples.

Diamond drills heat up very quickly, thus a large amount of coolant is required in diamond drilling. Coolant is used as the particle flushing medium at the same time. The state of the art in the diamond drilling industry is such that no data is available for heat transfer requirements as separate from mass transfer demands. Initial diamond drilling tests, Fig. 5 through 11, were made with the recommended water flow rate: 1/2-in. water pipe, fully opened at regular in-house water pressure and connected to the water swivel of the drill (See Section II-B-2-i). Later in the program, D-1, D-3, and D-5 drills were checked in granite, without any cooling or flushing medium. Every drill was completely dulled in less than 1 min, and no appreciable penetration was produced.

The D-4 drill was instrumented for temperature measurements and was tested at an 80-lb load in granite. The flushant medium was air. Results are summarized below:

Material	Duration of Test, min	Speed, rpm	Penetration, in.	Cooling-Flushing Medium	Temp. °F
Sandstone	0.8	712	0.04	high air flow	160
Sandstone	1	650	0.02	very low air flow	405
Granite	1	820	0.03	no air flow	315

The carbide tip drills were also tested. Although not instrumented for temperature, the onset of blue oxide coloration was recorded. This coloration is related to the metallurgical blue brittleness phenomenon (ref. 44).

Blue brittleness is encountered in the steel tempering process and is accompanied by a decrease in impact toughness (from 12 to 7 ft-lb of Charpy impact). The oxide is formed in the 450° to 650°F range and the upper value is used in calculating the approximate cutting edge temperature, as follows.

The drill is assumed to be made of uniform steel of constant cross section. Carbide tip inserts are neglected. An one-dimensional heat transfer equation is applied to the semi-infinite solid, initially at temperature T_o ; for time $t = 0$, one surface is maintained at constant temperature T_s . The model implies that the cutting edge temperature remains at a constant T_s value throughout the test. Mathematically, this is expressed as

$$\frac{\partial T}{\partial t} = \frac{\partial^2 T}{\partial x^2}$$

$$\text{At } (t, x) = (0, x), T = T_o$$

$$(t, x) = (t, 0), T = T_s$$

The solution to this equation is, (ref. 89) is of the form

$$\frac{T - T_s}{T_o - T_s} = \Phi(x\eta),$$

where

$$\eta = \frac{1}{2\sqrt{\alpha t}}$$

T = temperature, °F

t = time, hr

x = distance, ft

α = thermal diffusivity, $\frac{\text{ft}^2}{\text{hr}}$

$$\Phi(x\eta) = \text{error function, } \Phi(z) = \frac{2}{\sqrt{\pi}} \int_0^z e^{-\beta^2} d\beta.$$

The C-4 and C-2 drills exhibited blue brittleness at the very bottom end of the fluted steel shank when tested in concrete. Neglecting the carbide tip insert and weld material temperature distributions, the above equations indicate that the tip temperature did not exceed 650°F.

The C-8 1-in. -diam. drill in granite attained blue brittleness discoloration 1-in. away from the cutting plane, after 5 min of drilling. A calculation of the upper temperature range follows.

The given assumed or experimental data includes:

Thermal diffusivity, $\alpha = 0.48 \text{ ft}^2/\text{hr}$

Time to observation, $t = 0.0834 \text{ hr}$

Distance to discoloration, $x = 0.0834$.

The value of the function η is

$$\eta = \frac{1}{2\sqrt{\alpha t}} = 2.5$$

That of

$$\eta x = 2.5 \times 0.0834 = 0.208$$

while the error function Φ , is

$$\Phi(\eta x) = 0.233$$

The resulting temperature at the cutting edge is

$$T_s = \frac{T - T_o \Phi(x\eta)}{1 - \Phi(x\eta)} = \frac{650 - 80 (.233)}{1 - .233} = 825^\circ F.$$

This temperature is based on an assumed blue brittleness temperature of $650^\circ F$.

The determination of rock particle temperature at the instant of fracture and during contact with the cutting edge, whether higher or lower than the cutting edge, requires more elaborate instrumentation than could be justified on this program.

Elastic energy released during fracture, the surface formation energy consumed (surface energy is relatively higher in brittle materials), the heat exchange between drill and rock, all influence the relative temperature. It appears however, that the temperature of the rock in contact with the cutting bit will be approximately the same as that of the cutting bit.

No blue brittleness discoloration was encountered with any of the rotary-impact drills. However, midsections of the 42-in. -long extension shanks heated up until they were too hot to touch with bare hands indicating high energy losses once again. (Sec. II-B-3-p).

4. Parametric Systems Analysis

a. General

The experimental drilling results were used to formulate parametric systems data a summary of pertinent drilling parameters, intended for preliminary design estimates, in order that power, energy, and hole size

functions could be formulated. Unit weight is another parametric function to be considered in the in extraterrestrial drilling task. However, the complexity of drilling methods, the great number of prime mover and drill actuator mechanism combinations, the systems considerations, and the constantly changing state of the art in component design preclude a realistic system parametric analysis based on system weight. The present study is confined to an analysis of the energy, power, penetration rate, and size of drill considerations for a given material.

Parametric systems data are presented in Fig. 31, 32, 33. Energy per inch of drill penetration is plotted as a function of drill load. The above energy value was obtained by dividing power by penetration rate. Drill speed is the parameter of the plot.

The above analysis presents no clues as to penetration rates or the power levels involved. Therefore each of Fig. 31, 32, 33 should be viewed in relation to Fig. 24, 27, 19, which given penetration rates and power levels. The two corresponding plots give a complete parametric optimization picture: energy, power, and penetration rates as functions of the drill type, drill size, load, speed, and the material drilled.

The parametric analysis is made for rotary drills only. Rotary-impact drill experiments indicated no detectable variation in input power. The variable of most importance to the drill performance in this case was the length of the drill shank which provides no useful data. At a given load for a given rotary impact drill, energy values and penetration rates remain constant as seen in Fig. 29, 30. They are summarized in the table below.

ENERGY VS LOAD C-8 1 INCH DRILL IN SANDSTONE

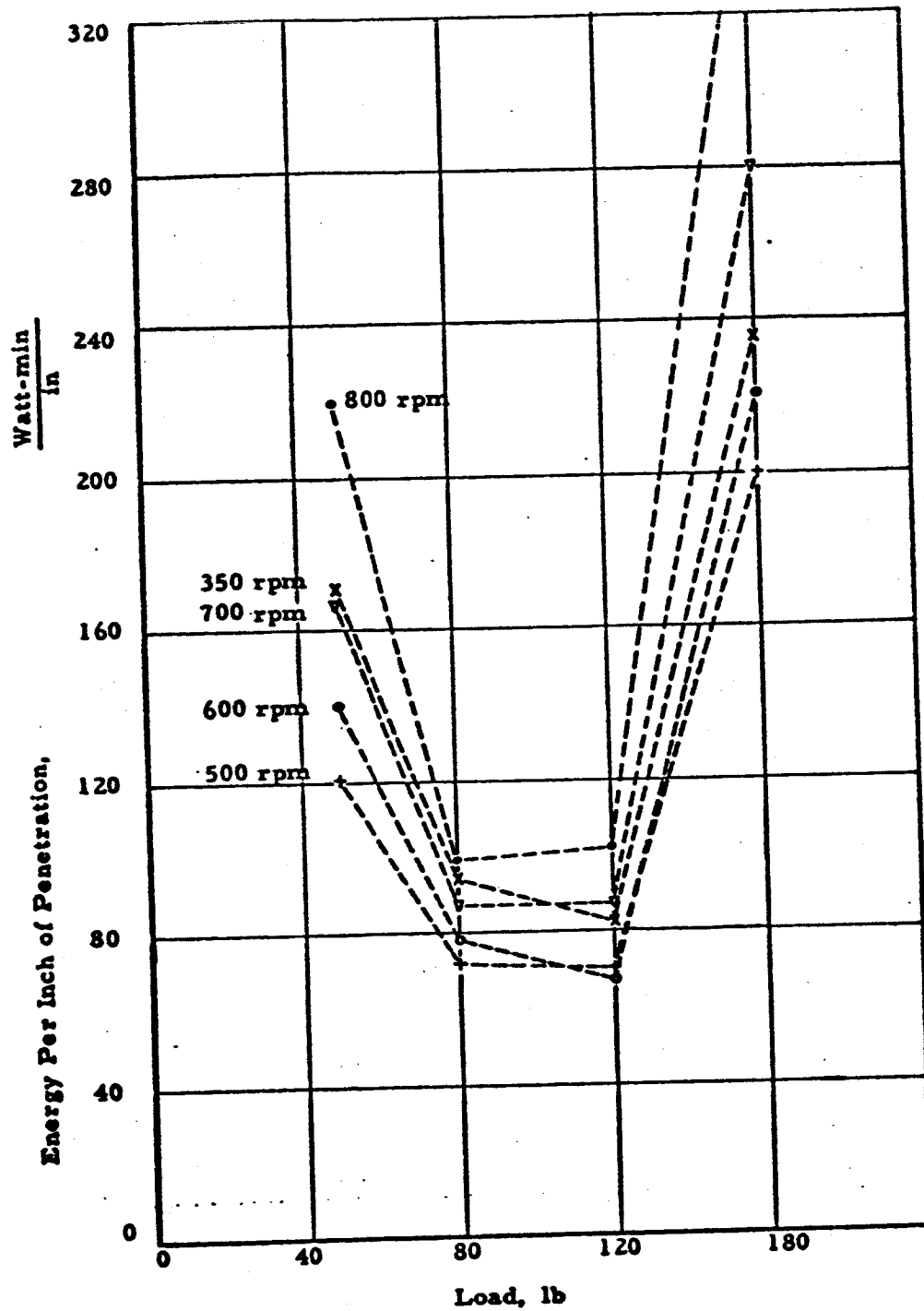


Fig. 31

ENERGY VS LOAD C-8 2 INCH DRILL IN SANDSTONE

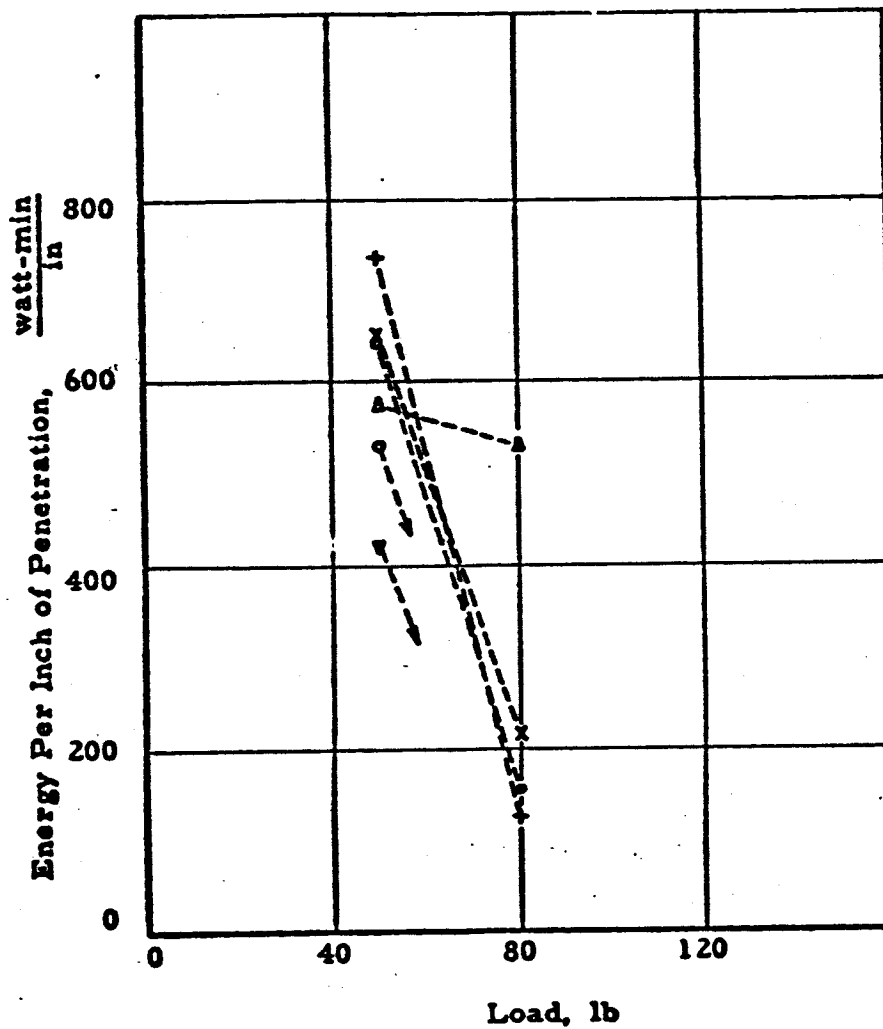


Fig. 32

ENERGY VS LOAD C-4 DRILL IN SANDSTONE

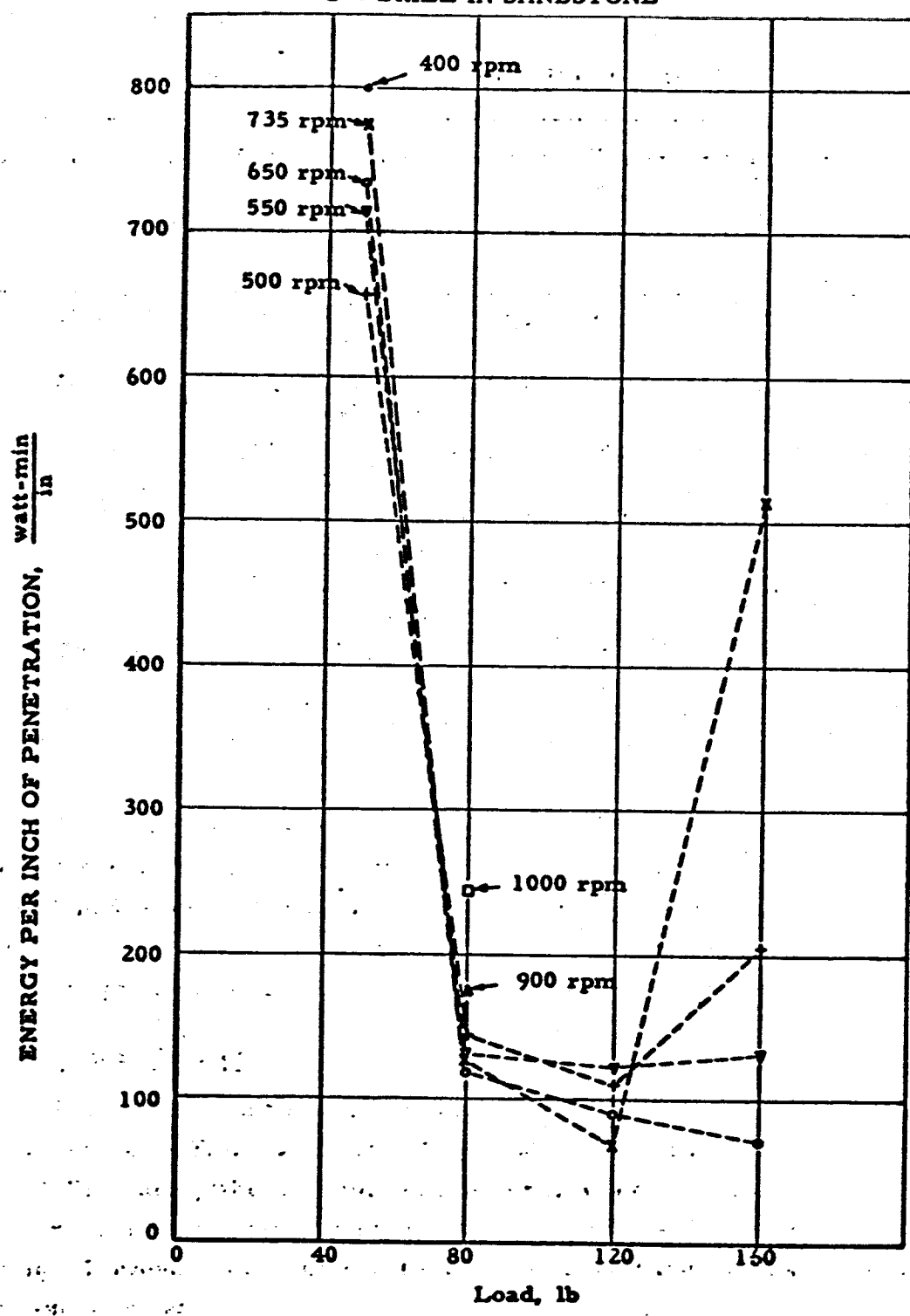


Fig. 33

ROTARY-IMPACT DRILLING RESULTS

Test No.	Material	Model	Drill Size	Load lb	Power watts	Penetration Rate in. /min	Energy, Penetration Rate watt-min in.
1	Granite	736	1" diam., 18" long	50	940	1.4	670
2	Granite	736	1-1/2" diam., 18" long	50	940	.666	1410
3		736	1-1/2" diam., 60" long	50	940	.532	1770
4	Sandstone	736	1-1/2" diam., 60" long	50	940	1.87	502
5	Sandstone	726	1" diam., 18" long	50	550	2.28	241
6	Granite	726	1" diam., 18" long	50	550	.92	600
7	Granite	726	1-1/2" diam., 60" long	50	550	.172	3200

In comparing Test 1 and 6 it is seen that Model 726 is more economical of both power and energy than Model 736, when both are fitted with a 1 inch drill. When fitted with a 1-1/2 in. drill, the reverse is true. These results show that a careful match between drill capacity and drill bit size must be made for optimum results.

b. Rotary Impact

The energy parameter and performance of the C-4 drill in sandstone are presented in Fig. 33 and 19. Attention is directed at the inefficient 50-lb drill loading which results in a minimum energy consumption of 650 w-min/in. This value is to be compared with 74 w-min/in. at a 120 lb loading. However, this optimization is obtained at the expense of a relatively high (490 w) power.

The C-8 1-in. drill in sandstone is hardly more efficient at its optimum load and speed (Fig. 31, 24) though it operates at a low power level, 280 to 300 w. A comparison with the C-4 drill only indicates the effectiveness of the coring geometry.

Two loading conditions were available for the C-8, 2-in. diam. drill analysis in sandstone: 50 lb and 80 lb (Fig. 32, 27). Higher loads to obtain optimum results is again indicated.

Granite was drilled with the C-8 type of drill: 1 in., 1-1/2, 2 in. in diam., Fig. 23, 26. A limited number of data points were available for the energy plot, (Fig. 34) however several interesting conclusions can be drawn as shown below: (1) At a 50-lb load, 500 rpm is the optimum speed. Power level is 202 w. At a 160-lb load, 250 rpm is the optimum speed. (2) At 500 rpm and a 160-lb load, a 2-in. -diam. drill requires the least amount of energy, while at 250 rpm, the 1-in. -diam drill requires least. (3) The energy required to penetrate granite is approximately 10 times that required for sandstone.

c. Rotary Vs. Rotary Impact Performance

At 50-lb drill loadings and at optimum speeds, rotary coring drills provide either inferior or at best, equivalent performance in sandstone. Performance in granite is definitely inferior. Solid rotary drills do not penetrate granite at loads to 160 lb.

In addition rotary drills suffer high rates of wear.

Accordingly, the rotary impact drill promises superior performance in the lunar drill unit application.

5. Dimensional Analysis

A number of analytical approaches suitable for studying drill performance as related to the characteristics of the rock being drilled were examined. Dimensional analysis based on Buckingham's Pi Theorem supported with experimental data provided desired relationships.

ENERGY VS LOAD
C-8 DRILLS IN GRANITE

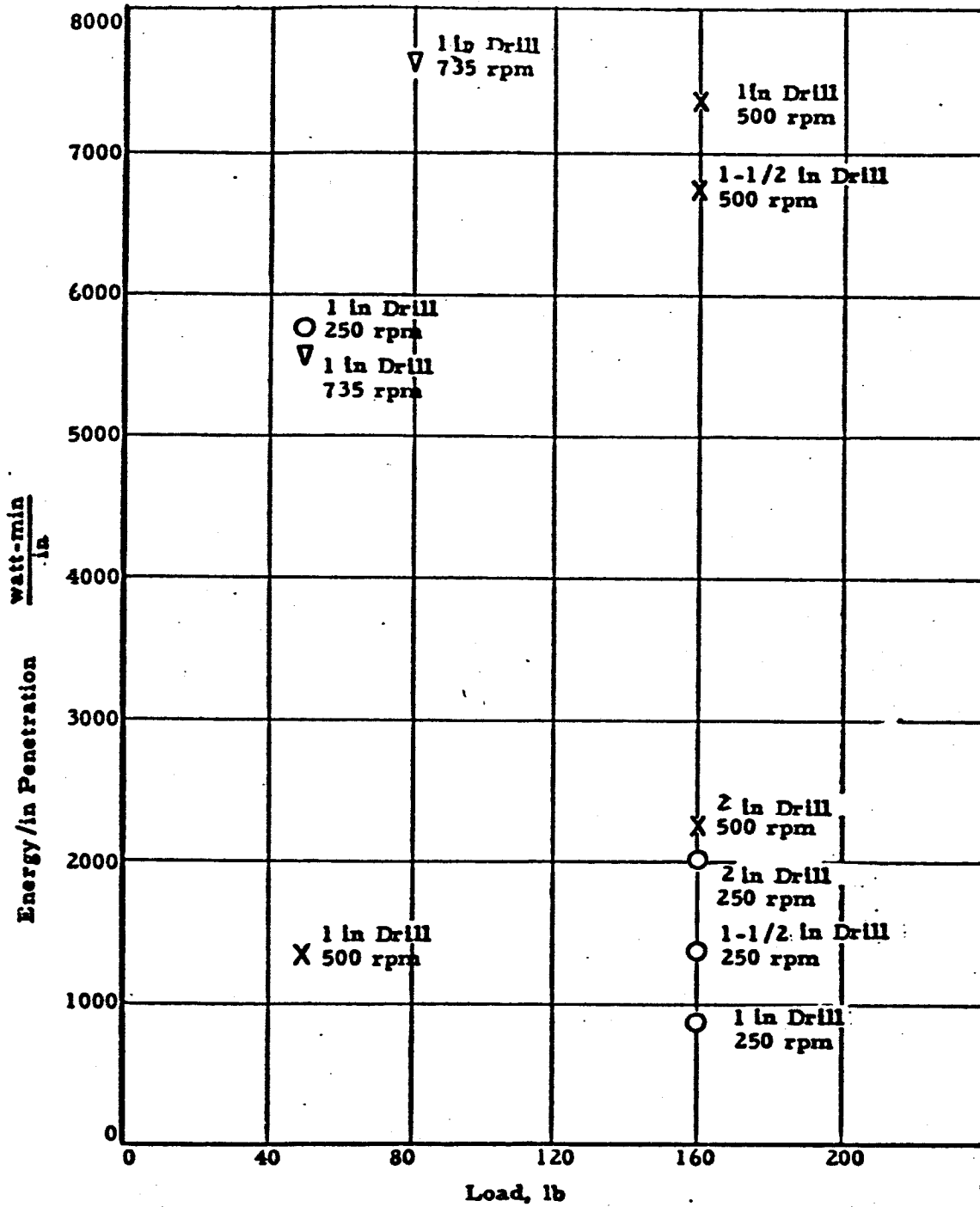


Fig. 34

The purpose of the parametric study is to correlate effects of the hole size, thrust, rotational speed, power, torque, penetration rate, with pertinent rock parameters such as strength, density, modulus, and perhaps some laboratory determined indices. The value of such parametric correlations would be in (a) telemetry channel economy, and (b) substantiating data availability.

Dimensional analysis as a tool is definitely limited by the type of drilling employed. Rotary drilling, with its relatively simple rock chipping mechanics, lends itself to greater parametric generalizations and results in more accurate estimates. Rotary-impact drilling requires more detailed description of the drilling model and introduces more variables for consideration. Here, individual types of machines introduce a number of parameters which must be considered, including proper rotational-indexing requirements, rebounding drill bit and impact transmission mechanics. It must also be borne in mind that since the state-of-the-art for rotary-impact drilling theory is less advanced than that for pure rotary drilling and since the results obtained by dimensional analysis are limited by completeness and correctness of the original assumptions, the expected accuracy of rotary-impact parametric studies is less than those for pure rotary.

The major source of difficulty in the establishment of a mathematical model lies in lack of a readily available analytical description of rock parameters. Considerations of rock compressive strength and moduli do not represent adequate models even at room temperatures. Adequate representations depend on precise test results, of a type which still remain to be obtained by the drilling industry, especially for the rotary impact drills.

a. Solid Rotary Drill Dimensionless Functions

A dimensional analysis for solid rotary drills is given below. The following parameters and drill characteristics were considered:

Characteristics	Symbol	Dimensions
Rock Strength	σ	lb/in. ²
Rock Modulus	E	lb/in. ²
Rock Density	ρ	slugs/in. ³
Hole Diameter	d	in.
Hole Depth	Z	in.
Applied Load	F	lb
Drill Speed	N	rad/sec
Penetration Rate	R	in./sec
Power Input	P	$\frac{\text{in.} \cdot \text{lb}}{\text{sec}}$
Developed Torque	T	in. - lb

A derivation of dimensionless functions appears in Appendix A, only the results of this analysis are presented below:

$$\begin{aligned}\pi_n &= \Phi_n[\pi_4, \pi_5] \\ R &= dN \Phi_5 \left[\frac{F}{\sigma d^2}, \frac{\rho d^2 N^2}{\sigma} \right] \\ P &= \sigma d^3 N \Phi_6 \left[\frac{F}{\sigma d^2}, \frac{\rho d^2 N^2}{\sigma} \right]\end{aligned}$$

b. Application to Drilling Sandstone with Drill C₄

One dimensionless relationship was determined for the C-4 drill in sandstone (Fig. 35 and 36): here a family of straight lines intersect at $(\pi_4, \pi_5) = (1.16 \times 10^{-2}, 0.73 \times 10^{-3})$, the slope of each line being a function of drill speed. The general equation for a given line can be written,

$$(\pi_5 - .73 \times 10^{-3}) = m (\pi_4 - 1.16 \times 10^{-2}), \quad (1)$$

where

$$\pi_5 = \frac{R}{dN}, \quad \pi_4 = \frac{F}{\sigma d^2},$$

here m , is the slope of the line, is a function of drill speed (Fig. 35) and can be expressed analytically as

$$m = 0.00595 N - 0.309. \quad (2)$$

DIMENSIONAL ANALYSIS:
C-4 DRILL IN SANDSTONE

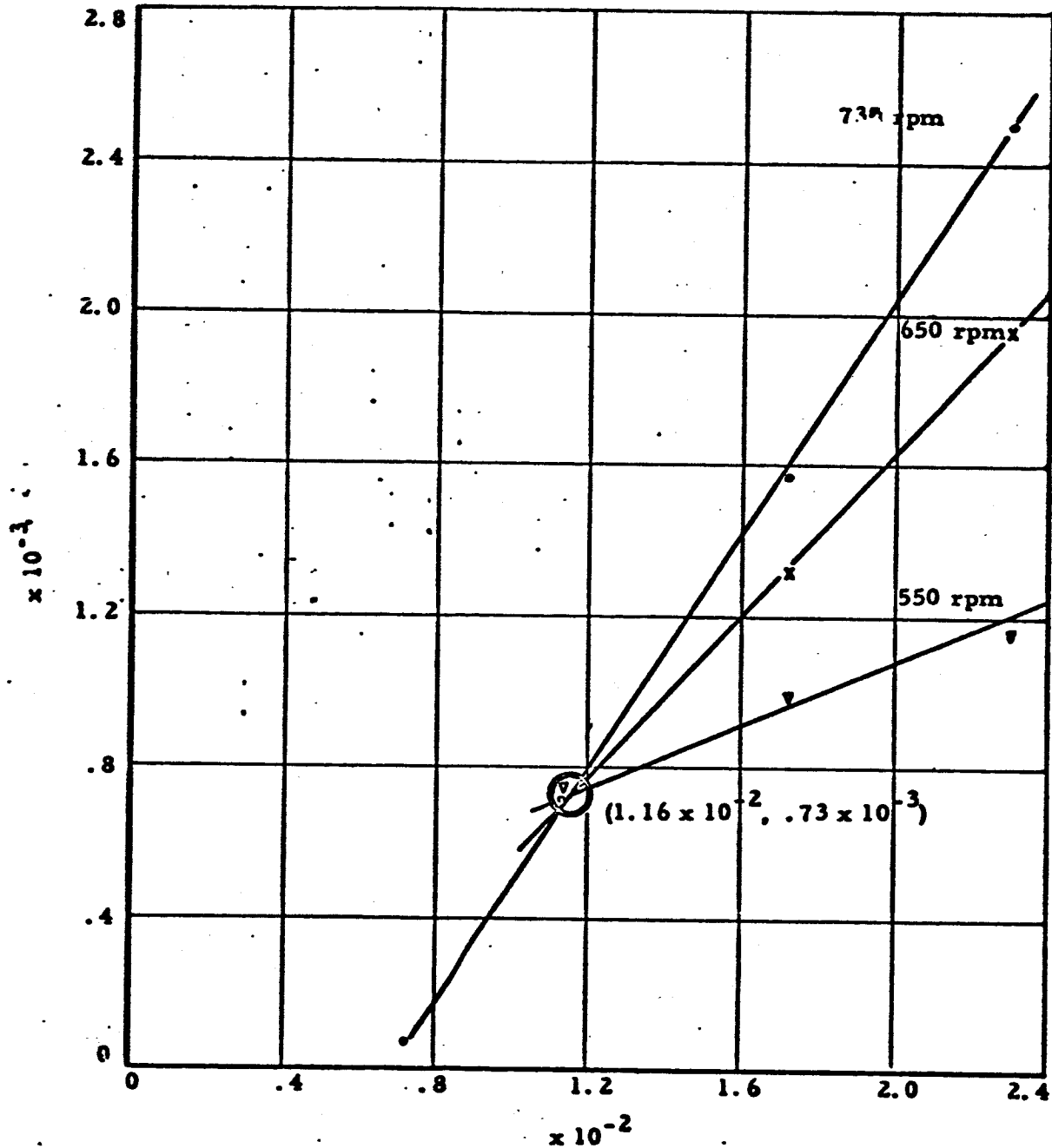


Fig. 35

ARMOUR RESEARCH FOUNDATION OF ILLINOIS INSTITUTE OF TECHNOLOGY

SLOPE VS DRILL SPEED RELATION FOR FIG. 35
C-4 DRILL IN SANDSTONE

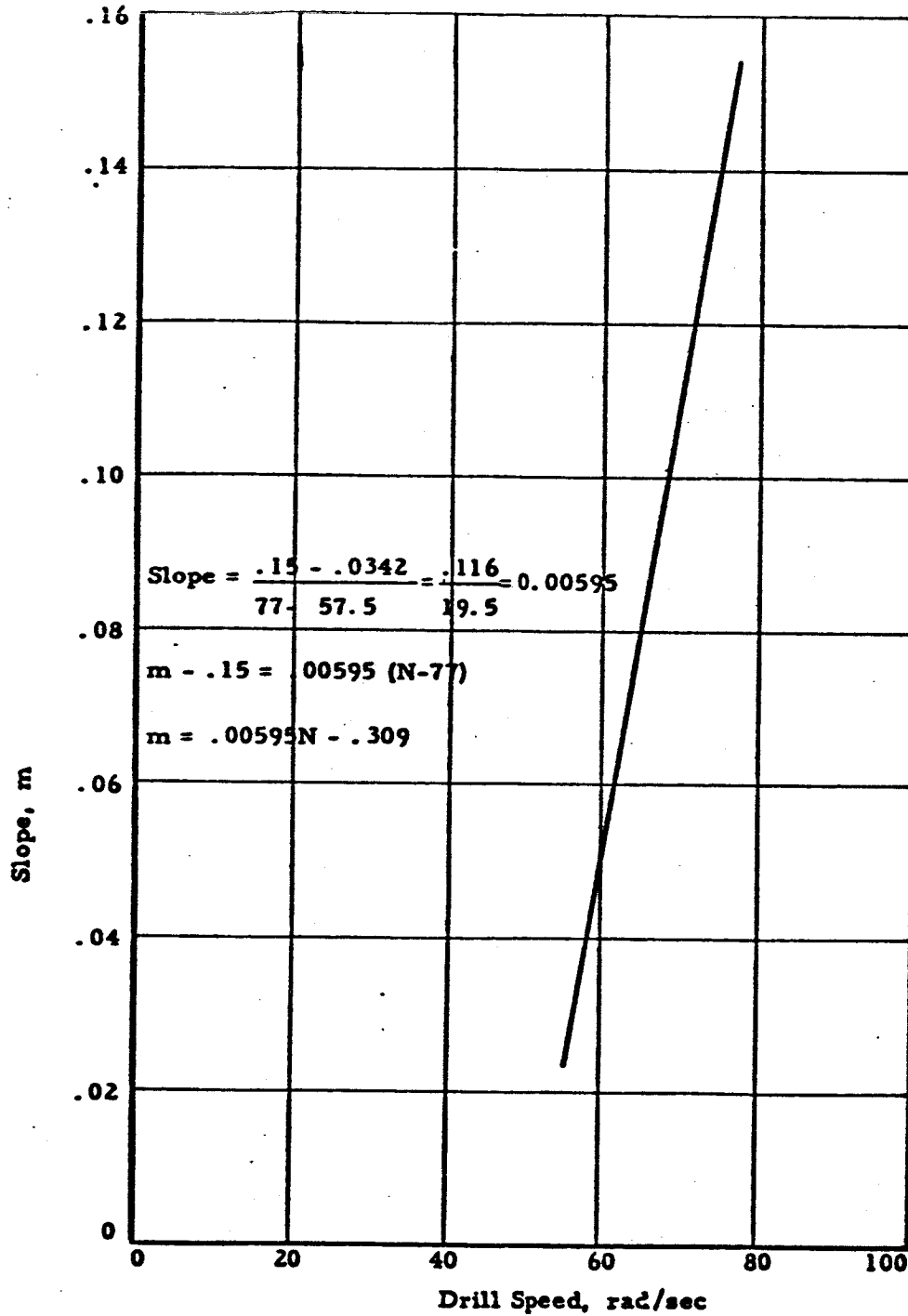


Fig. 36

A combination of Eq. 1 and 2 gives

$$\frac{R}{dN} - .73 \times 10^{-3} = (.00595 N - .309) \left(\frac{F}{\sigma d^2} - 1.16 \times 10^{-2} \right). \quad (3)$$

Equation 3 was derived on the basis of data plotted in Fig. 19 and 20 and is valid for the experimentally determined range only. This restriction is placed because of two reasons: (1) lack of experimental evidence with all the parameters and (2) surprisingly wide drill performance variation as computed in Appendix C, indicating shortages even for the simplest of models.

Attempts to derive analytical power relationships turned out to be unsuccessful.

c. Application to Drilling Granite with Drill Cg

As derived in Appendix A, dimensionless combinations were modified to take the coring effect into account, and several new Pi functions were used (Appendix A, Eq. 6, 7). Figure 37 presents a dimensionless functional relationship for the three different diameter drills (at 160-lb load and two speeds). It is again evident as was the case above, that some common point of intersection exists, the slope of the loci being functions of drill speed. The lack of experimental data precludes the derivation of a more general expression, thus only the dimensionless equations at each of the two speeds are given below.

That for 160-lb load and 250 rpm is

$$(\pi'_4) (\pi'_2) (\pi'_8) + 1.47 \times 10^{-4} (\pi'_5) = 1.47 \times 10^{-7},$$

where

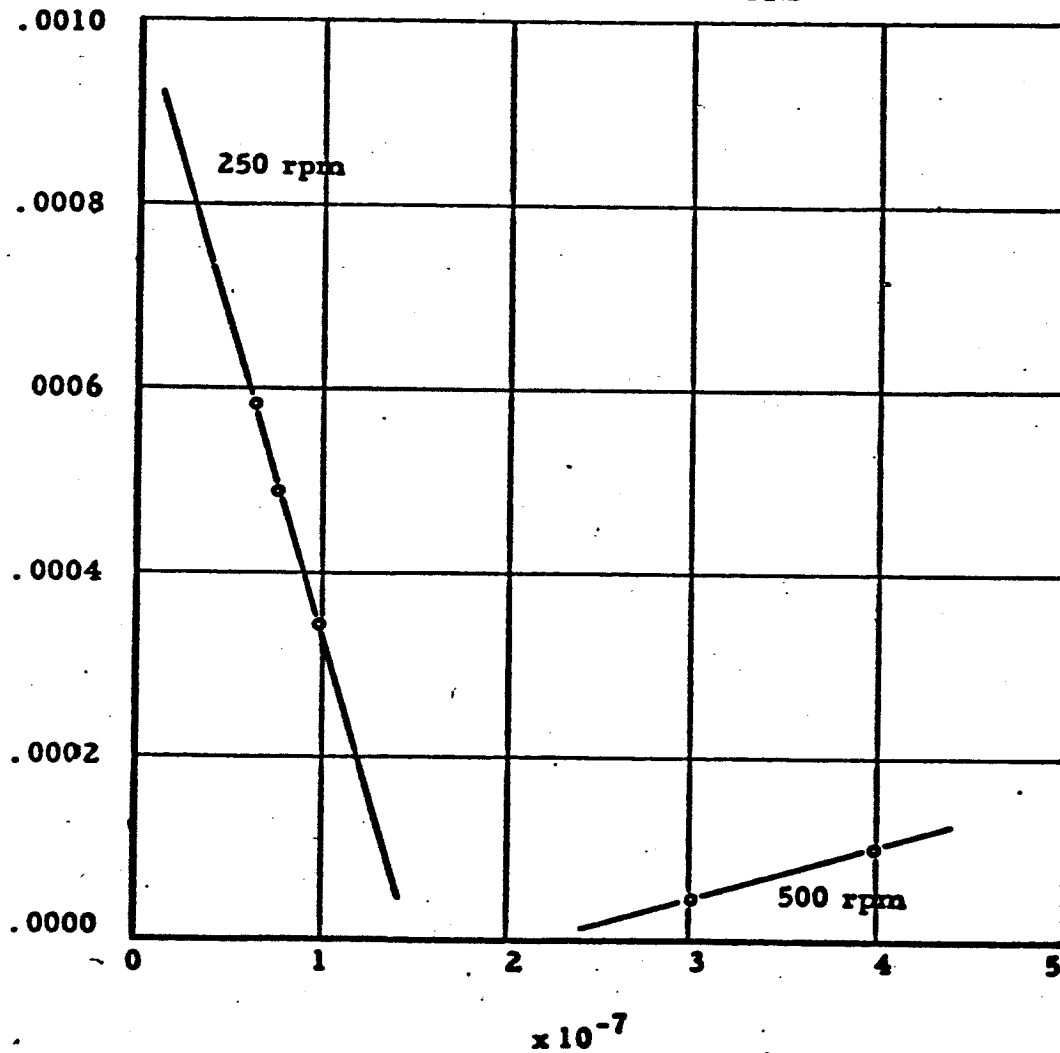
$$\pi'_5 = \frac{R}{(d_o - d_i) N}$$

$$\pi'_4 = \frac{F}{\sigma (d_o^2 - d_i^2)}$$

$$\pi'_2 = \frac{\rho (d_o^2 - d_i^2) N^2}{\sigma}$$

$$\pi'_8 = \frac{L}{d_o - d_i}.$$

DIMENSIONAL ANALYSIS C-8 DRILLS IN GRANITE



$\times 10^{-7}$
Fig. 37

Subscripts o and i designated the outer and inner diameter and ℓ is the total length of the cutting surfaces.

The equation for 160-lb load and 500 rpm is

$$(\pi'_5) = 598 (\pi'_4) (\pi'_2) (\pi_8) - .00134.$$

The numerous restrictive conditions which must be applied to these equations illustrates the difficulties inherent in the present-day application of dimensional analysis. However, with a better understanding of drilling mechanics and with specially designed experiments, this approach should prove a powerful tool in gaining an insight into an optimum design approach.

C. Discussion and Conclusions

1. Recommended Drill

Drill durability and rock penetration capacity of the rotary-impact drill recommend this concept for the lunar drill application. When compared with the other drilling methods (rotary coring drills), rotary-impact devices require comparable energy and power levels (Sec. II-B-4). The use of a pneumatic spring in the drive unit will introduce developmental problems to avoid excessive leakage, however these problems do not appear to be severe.

The rotary impact drill has a reasonable growth potential in its present form. Advanced units, employing an in-hole drive motor will reduce the vibrations transmitted to the spacecraft structure. The present unit will employ a simple spring-damper system to reduce transmitted vibrations.

2. Recommended Reliability Study

a. Introduction

The complexity, advanced design, and unusual requirements associated with this program require that the utmost effort be devoted to attaining the high reliability goals set. While in no way minimizing the difficulties associated with directing and accomplishing a sound reliability program for previous or existing satellite or spacecraft applications, it is

recognized that the reliability program required for the lunar drill project introduces many aspects for which only more limited studies have been performed. For example, the lunar drill package is required to survive the following sequences of differing environmental conditions prior to equipment operation: limited storage in earth environments, launch, flight, entry, land, and intermingled storage and operation in the atmosphere of the moon. In contrast, our space program to date requires equipment operation during a part or all of the launch, flight, and re-entry phases. Of major significance is the added requirement that the equipment be operational following the stresses incurred in entry and landing. Successful operation of the lunar drill package in the atmosphere of the moon is a difficult undertaking, because of the severity of the environments which will be encountered. For example, the motor operation in a high vacuum poses the problems of heat dissipation, loss of bearing lubricant and more severe limits on corona discharge and voltage breakdown. The wide temperature range to which the motor will be subjected creates severe problems in providing electrical insulation and bearing lubricants that will withstand these extremes.

The problems imposed by the environmental conditions are discussed in detail elsewhere in this report. Of significance, however, is the recognition that these problems exist and must be solved.

b. Differences between Electronic and Non-Electronic Components

The state of the art of reliability activities is far more advanced with respect to electronic parts, components, and equipments than it is with respect to their mechanical equivalents. Historically, this has resulted from electronic equipments causing the major portion of the difficulties in maintaining proper operation. For this reason, the growth of reliability has centered about the elimination of problems in electronics to the exclusion of similar mechanical considerations.

Until recently, the major accomplishments in the field of reliability analysis and prediction centered about studies of "random" failures. Here, randomness of failures includes so-called catastrophic failures, e. g.,

resistor shorts and opens, as well as gradual change of characteristics resulting from prolonged application of environmental and electrical stress levels. The significant point is that the level of effort for "wear out" phenomena, or change in properties through such processes as material deletion, has been low. Until recently, this emphasis was proper, in the sense that the tactical life of electronic components and equipments was generally far shorter than the time at which significant material depletion effects would begin to take place.

Mechanical components are generally conceded to exhibit pronounced wear-out, which appears relatively early in operational life (ref. 91). Stated in different terms, a failure of an electronic component carries the implication of a reliability problem; whereas failure of a non-electronic component carries the connotation of a design problem (ref. 92). An excessive failure rate in the former case may well be misapplication of the component; on the other hand, it is a relatively simple matter to determine whether this is in fact the case. If not, reliability techniques can be applied effectively to improve reliability. In the case of non-electronic components, excessive failure invariably are treated as a problem in redesigning the component to extend the time at which significant wear-out commences.

c. Wear-Out Failures

The preceding discussion points out some of the major elements of difference between consideration of electronic and non-electronic components, from a reliability standpoint. However, the recent emphasis upon satellite applications of electronic components, and the implied long operational lives, had made necessary the reconsideration of the electronics problem from a point of view of wear-out phenomena actually occurring. Thus, significant contributions have been and are being made in the application of reliability techniques applicable to the unique problem of the lunar drill.

In short, the frequency distribution curve of wear-out failure characteristics often approximates a normal distribution, which can be defined in terms of mean time to failure and deviation about the mean. Knowing this wear-out distribution characteristic and the required operational

life of the component, one can accurately predict the reliability. Still more important, meaningful design and quality control data are available for product improvement work. For example, supposing tests show the failure rate to be higher than allowable over the operational life. One can estimate how much the mean time to failure must be increased (redesign - a more critical task than that discussed previously) or whether or not reduction in the deviation limits would be more practical. In applying either approach to product improvement, all possible information on the applicable mechanisms of failure should be obtained to guide subsequent effort.

d. Reliability in the Design

One of the important tasks to which the reliability personnel must be committed is that of support during the research, development, and design stages. That is, reliability personnel will be assigned the task of aiding in the selection and use of parts and components so as to orient effort toward the ultimate reliability objectives. For example, a technique for decreasing probability of component failure is the use of electronic components at a fraction of rated value. For deposited carbon resistors, exposed to high humidities, this technique does not apply, as the absence of I^2R heating does not allow the component to operate dry. This results in an excessive change in resistance. Considerations such as these suggest the type of support the reliability group can furnish.

e. Reliability Tests

Ultimately, it will be necessary to perform tests on the assembled drilling packages to verify conformance to reliability requirements. Determination of the tests to be performed, the quantities to be tested, and the time intervals over which the tests continue, are matters for the reliability activity. Establishment of test conditions require the talents of specification and environmental specialists. Design of test sequences and analysis of test results include the need for the services of operations research and statistics specialists.

Tests of complete packages should be made for the purpose of verifying predicted results. To perform reliability predications and analyses, suitable information is necessary regarding each of the elements of the package. In the case of, for example, portions of the electronics, it is more than likely that data are available either in the literature or from component manufacturers, in a form suitable for inclusion in the analysis. While some data on mechanical and electro-mechanical parts are available, the fact that much of this portion of the package will be special to the application, indicates that many of the reliability characteristics will be determinable only by test. As before, the reliability group will be responsible for conducting such a program.

Such test programs as those discussed above would furnish other necessary information. An analysis of the resulting failures is necessary to avoid their future occurrence and to effect improvements. Determination of the cause of failure, through the use of such analytical techniques as cross sectioning and photographs, together with a determination of the principle stress or stresses (and their values at failure), must be accomplished, if significant improvements are to be made as expeditiously and efficiently as possible.

f. Special Considerations in Reliability

The differing environments existing during each phase of the lunar drill "trip," e. g., launch, flight, etc., may well require totally separate reliability considerations. That is, electronic failures occurring during launch, such as a shorted component or a loose wire, clearly must be attributed either to a random catastrophic failure, poor workmanship, or poor design practices. In the realm of reliability analysis only, the first acquires major significance. The same considerations should reasonably hold for the non-electronic components. Once landing is successfully effected, however, the strong limits upon weight, and their effect upon structural safety factors, may indicate that the major reliability concern with certain of the non-electronic components is wear-out phenomena, as previously suggested. Thus, the separate phases of the flight will require separate reliability studies, and, in fact, that these studies will be concerned with different

modes of failures, (e. g., catastrophic and wear-out) and different principle stresses (e. g., acceleration at launch and extreme temperatures on the surface of the moon).

g. Radio-Frequency Interference

Various electrical and electronic devices, as well as mechanical operations involving the accumulation and discharge of electrical charges due to frictional forces, create sufficiently large electromagnetic fields to interfere with the operation of electronic equipment, including sensitive command receivers, electronic control apparatus and electronic analysis communications equipment of various kinds. In order to prevent malfunctioning of such equipments, the drill unit must not create excessive radio-frequency (RF) interference.

Certain types of electric motors are prolific sources of RF-interference. If such motors should be desirable in the lunar drill for their torque or other characteristics, means for the suppression of RF-interference must be provided in order to prevent interference to the drill's own automated control circuitry, as well as to other electronic operations which may have to be performed concurrently.

Interference-reduction measures must be applied in a manner involving as little weight and volume as necessary and yet permit a maximum level of reliability under conditions of high g-deceleration and other salient environmental conditions. The most severe of these environmental conditions is anticipated to be the large temperature variations to be encountered.

The drill concepts described in this report can utilize d-c motors and controls designed for aircraft and missile applications which meet the military specification on radio interference, MIL-26600. Therefore, none of the drill system designs will create a source of interference with electronic equipment.

III. CONCEPT STUDIES

A. Drilling Studies

Several design concepts applicable both to initial and to future lunar geological exploration systems were conceived and carried to the preliminary design stage as a part of the program. These concepts include both rotary and rotary-impact drill systems and also various methods of removing chips from the hole during drilling operations. A concept for the emplacement of a casing in a drilled hole is also presented. A particular drilling system used on a lunar vehicle might embody features of several of these concepts depending on the specific mission. Since the requirements are specified for the initial lunar drill systems to be used with the Surveyor vehicle, two concepts, directly applicable to that program have been extensively examined. The remaining drilling concepts are primarily suited for future drilling programs.

1. Rotary-Impact Drill Systems

ARF studies indicated that only a rotary-impact drill system would have the capability to perform as required for the drilling experiments proposed for the Surveyor soft-landing lunar vehicle and also future deep-hole drillings. Therefore, three concepts were developed for rotary-impact drill systems. Two of these concepts are suitable only for drilling shallow holes, while the third is suitable for drilling relatively deep holes.

a. Selection of Rotary-Impact Mechanism

For reliability and minimum development effort, the rotary-impact drill should be based on a commercially available device. Both rotary-impact and straight-impact electric hammers were investigated by ARF. (Rotation can be easily added to those hammers that do not have that feature). In these devices, impact force to the drill bit is supplied by accelerating a mass that strikes either the end of the drill shank or an anvil attached to the end of the drill shank. The prime mover that accelerates the impacting mass in these hammers is either based on electromagnetic or on electric motor principles. The electromagnetic type uses the magnetic field produced by current flowing through a coil to accelerate an impacting

mass. Its operating principle is similar to that of a solenoid. Electric motor-driven types translate motor rotation into linear motion of a spring-mass system that applies the impact to the drill. The spring serves to cushion the impact force from the rotor. Both mechanical and air springs are used. The advantages and disadvantages of each type of prime mover are shown in Table 3.

The electromagnetic type of drill has the advantages of containing only one moving part in the impact mechanism and also of not depending on the presence of an atmosphere inside the hammer case for its operation. However, the solenoid-type mechanism is relatively inefficient in the performance of work as compared to an electric motor. This means it will require more power, heat up more quickly, and tend to be heavier than an electric motor-powered device. The simplicity inherent in having only one moving part is offset to a considerable degree by the need for a motor and associated gearing to provide even a moderate amount of torque for rotation. Some pressurization will also be required for satisfactory bearing surface friction and operation of a d-c motor. To reduce impact and vibration caused by the accelerating mass after it has struck the drill shank and reversed its direction of motion, a mechanical spring must be used. The performance and fatigue life of this spring must be investigated under lunar environmental conditions. Another disadvantage of an electromagnetic-type hammer is the magnetic field produced during operation, as well as the residual magnetism that will remain. To prevent interference with instrumentation, recording, and telemetry, the hammer must be well shielded, which will increase the weight of the unit.

An electric motor-powered hammer with a mechanical spring is a relatively efficient device and, like the electromagnetic hammer, does not depend on any internal atmosphere inside the hammer case. Its main disadvantage is in the use of a mechanical spring. Even in normal usage, fatigue failure of springs is common. The adverse conditions of temperature and vacuum encountered may affect the properties of the spring material. Considerable development might be necessary to determine what spring material, if any, would perform satisfactorily, and give the high reliability necessary under the rapidly fluctuating stresses to which it is subject.

Table 3
ADVANTAGES AND DISADVANTAGES OF THE
BASIC TYPES OF ELECTRICALLY POWERED ROTARY IMPACT HAMMERS

Electromagnetic		Electric Motor	
		Mechanical Spring	Air Spring
<u>Advantages</u> Impact mechanism has one moving part Impact mechanism does not depend on presence of internal atmosphere	<u>Advantages</u> Relatively efficient mechanism Impact mechanism does not depend on presence of internal atmosphere Motors for aircraft and missile use are developed which are compatible with overall specifications	<u>Advantages</u> Relatively efficient mechanism Motors for aircraft and missile use are developed which are compatible with overall specifications	<u>Advantages</u> Relatively efficient mechanism Motors for aircraft and missile use are developed which are compatible with overall specifications
<u>Disadvantages</u> Relatively inefficient compared to a motor Motor must be added for rotation Motor case must be pressurized Magnetic field during operation and the residual magnetism may interfere with other instrumentation Mechanical spring required to reduce vibration	<u>Disadvantages</u> Motor case must be pressurized Fatigue failure of springs is common in normal usage Temperature and vacuum environment may effect the spring material	<u>Disadvantages</u> Impact mechanism depends upon internal atmosphere for functioning Motor case must be pressurized Loss of pressure is catastrophic	

There is a possibility that the lunar vacuum environment may actually improve the fatigue life of a mechanical spring (See Sec.IIIA-9). If experiments indicate that this will occur, a rotary impact drill using a mechanical spring would appear more favorable.

The electric motor-powered hammer using an air spring appears to offer good reliability and low weight. A disadvantage of this hammer is that the impact mechanism depends upon an atmosphere inside the hammer case. However, the motor operation and satisfactory bearing surface friction, any device would require some pressurization. Therefore, adequate seals must be used in any case. The higher pressure required in this type hammer complicates the sealing; however, by careful design and the use of multiple seals, the leakage can be held to a minimum. However, loss of pressurization on the hammer would end drilling, while if pressurization was lost on the other types of hammer, they might drill for a brief interval before the motor brushes wore away or the bearings siezed.

b. Rotary-Impact Drill - Commercial Type

(1) Introduction

This concept developed by ARF is based on a relatively simple, off-the-shelf, mechanism. By this means, the reliability already obtained by field use of the drill concept will be utilized to accelerate the attainment of the reliability goals imposed by the lunar drilling task. It is expected further, that the incorporation of a modified, lighter-weight version of a drill unit of proven performance will materially reduce the development period.

The proposed drilling unit consists of a rotary-impact type drill having a 1-5/8-in. -diam. carbide-tipped drill bit whose drill shank is 5 ft long. Because the shank is of sufficient length to drill the maximum hole depth desired, the complexities inherent in adding extensions to a rotary-impact drilling mechanism, are avoided. In addition, this system also has a provision for placing an instrumentation probe into the drilled hole.

(2) Method of Operation

The proposed concept, see Fig. 33, employs a drill bit, which, together with the rotary-impact unit, is free to move vertically along two guide columns. Thrust is applied to the drill by means of two constant-force springs mounted on the drill unit and connected to the bottom ends of the two guide columns. A winch mounted on the drilling unit, and attached to the spacecraft structure above the unit, is employed for retraction of the drill bit.

Chips from drilling are collected in the hollow-drill bit assembly. To remove the chips, the drill is raised from the hole and the chips are dumped into a sample collector or onto the lunar surface. The system design in itself keeps the drill chips away from the bearing areas. This prevents damage or jamming of the bearings by drill chips.

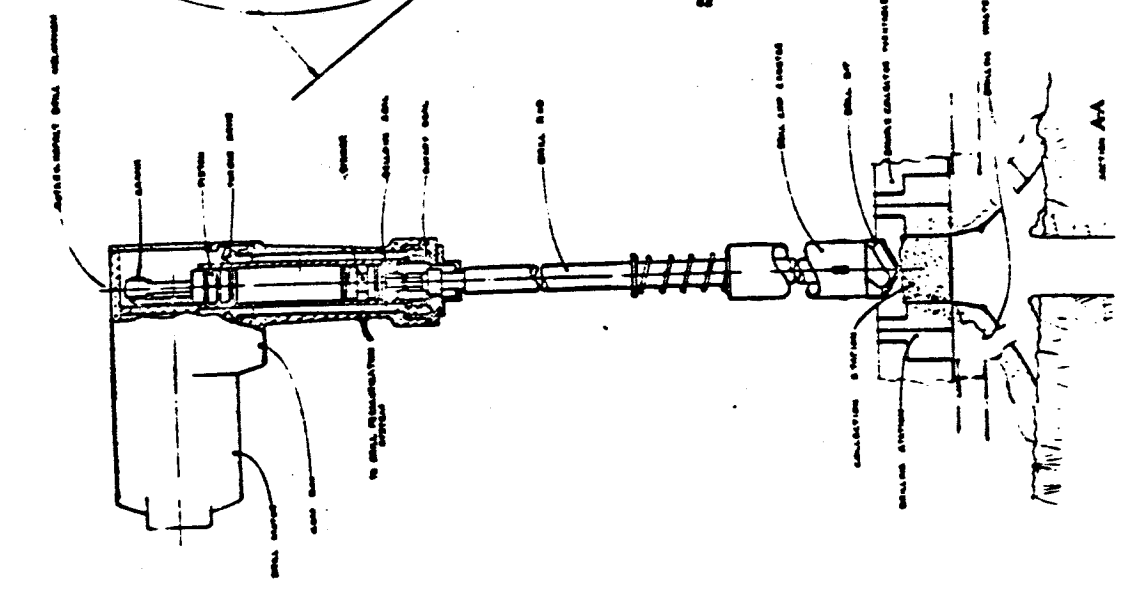
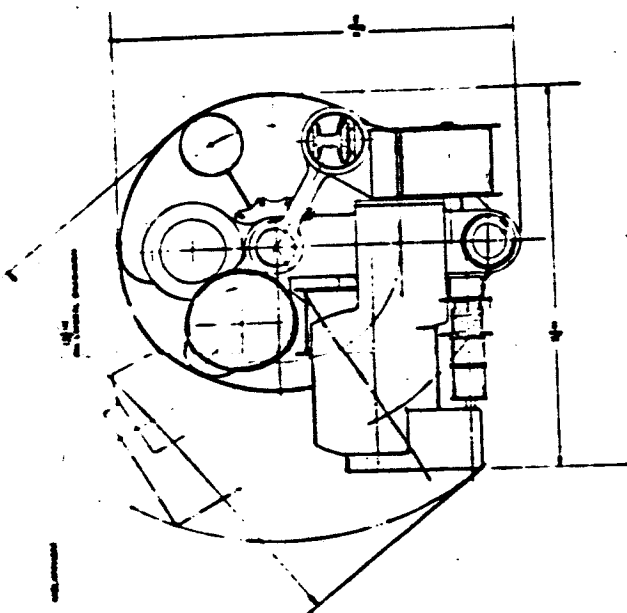
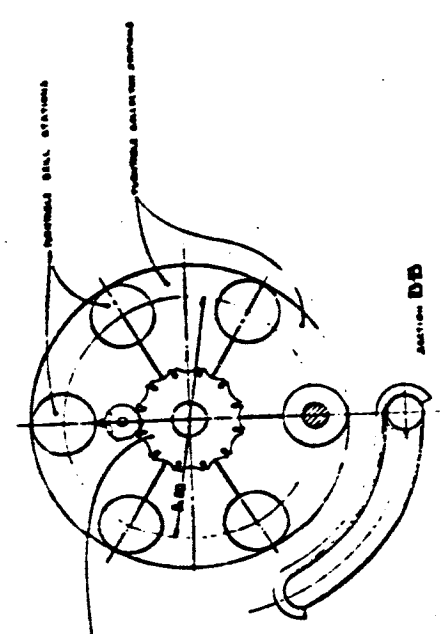
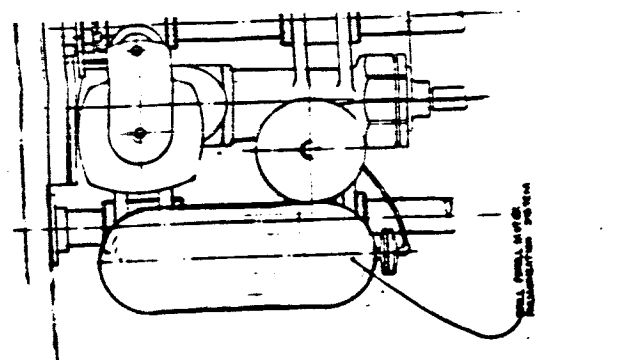
A minimum number of bearings will be exposed to low atmospheric pressures. However, all bearings that must be exposed to low pressures will be coated with a solid lubricant. The system is controlled through a hermetically sealed relay box, which can be operated by signals from a command controller or from an automatic programmer.

This assembly can be divided into items, which will be individually described in the following paragraphs.

(3) Rotary-Impact Producing Mechanism

The rotary-impact device is based on the Skil Corp. Model 726 Roto Hammer. A drawing of this drill is shown in Fig. 33. The rotation of the electric motor causes a piston to move upward. The gas pressure in the volume between piston and striker is thereby reduced. The difference in the pressures acting on the two faces of the striker causes the striker to move upwards. When the piston reaches the top of its stroke, further rotation of the electric motor causes it to move downward. The striker continues moving upward. The increase in pressure of the gas between the piston and the striker results in a deceleration in the upward motion of the striker. Deceleration continues until the striker reverses its direction of motion and begins to descend. The striker accelerates downward under the influence of the compressed gas, between it and the piston, until it delivers an impact

CONCEIVED & DRAWN BY
MURRAY FREEDMAN
DATE 10-10-68



SECTION DB

SECTION AA

blow to the drill shank. When the drill bit is not in contact with the rock surface, the shank moves downward following the impact, causing the striker to impact on a shoulder integral with the mechanism body. Therefore, when the prime mover is rotating the drill and the bit is not in contact with the rock surface, no impacts will be delivered to the drill bit.

The rotary impact device will be pressurized with a freon gas, probably either bromotrifluoromethane or dibromodifluoromethane. The pressure will depend upon the performance of the impact device using these gases. Multiple bellows and multiple sealing rings can be employed to minimize gas leakage from the case to the lunar atmosphere. A high-pressure gas-supply cylinder and a regulating valve will maintain the desired pressure inside the case.

Items such as drive motors and handles, present on the commercial unit, are eliminated in the modified unit. A 0.75-hp 24-v reversible motor, which has operated satisfactorily at an altitude of 150,000 ft, will provide drilling impacts and torques. The motor case will be pressurized to about 3 psf through controlled leakage through the drive from the rotary impact case.

The gear box design of the present unit will require some modification to provide the proper ratio between motor and drill speeds, when the proposed, higher-speed motor is incorporated in the design.

(4) Feed, Thrust, and Retracting Mechanism

Vertical motion of the drill unit is guided by linear ball bushings, which are free to slide on the two vertical guide columns. These bearings will be coated with molybdenum disulfide to reduce friction. The drill may move freely in a vertical direction, however lateral restraint is provided. The lack of rigid vertical restraints aids in isolating the vibrations arising at the drill bit from the spacecraft structure.

Two 25-lb constant force springs are mounted on the drill unit and connected to the spacecraft structure at the bottom of the guide columns. This insures a constant 50-lb force acting downward on the drill. The drill can be raised by a winch mounted on the drill and attached to the spacecraft

61-13

structure above the drill. The winch is driven through a power take-off from the rotary impact motor by means of a self-energizing clutch. A brake can lock the winch in any desired position.

The drill is moved downward by the force of the springs and its own weight. During downward motion, the winch is declutched from the motor and the locking brake released. The rate of descent, prior to contacting the lunar surface, is limited by an inertial friction brake.

(5) Drill Bit Assembly

The 5-ft-long drill bit assembly consists of a 1-5/8-in. -diam. carbide tipped cutting tool, a drill chip collector and a drill shank. A standard rotary impact drill bit was used in the preliminary design studies at ARF, however design modifications in existing bits were suggested by test results. The properties of the carbide to be used should be selected on the basis of the impact forces it receives in drilling and on the necessity for remaining a cutting edge as long as possible. The design of existing commercial drill bits must give consideration to the rough handling the bit receives prior to drilling.

The shank is inserted into a socket in the bottom portion of the drill unit. Three stainless steel bellows seal the unit above this socket, but allow axial motion in a vertical direction. No torque need be transmitted through the bellows. A retaining clip and shoulder on the drill that contacts a similar should on the inside of the drill case, limit the downward axial travel. The striker applies the impact blows onto the top of the shank.

The configuration and material chosen for the long drill shank must be carefully analyzed to obtain optimum performance. The loss of energy during impact must be minimized to obtain maximum penetration and drill bit life. In one experiment at ARF, a 5-ft shank, chosen with no regard for system optimization, absorbed nearly 50% of the total input energy.

The drill chips are collected in a cannister which forms an integral part of the drill bit assembly. During drilling the chips enter the cannister and are pushed upward into the chamber formed by the flat top of the bit and the cannister. When the cannister is full, the drill is retracted and emptied into a sample collector. A complete description of the operation of this device is found in chip removal cannister in this report in Section III-A-3 titled Chip Removal Cannister.

(6) Sample Collectors

Three potential designs were studied for use as the sample collector for this lunar drill. The choice of collector will depend on the amount of sample required. If a large sample is desired for analysis, the first system is preferred, while, if a small sample is desired, the second system would be chosen. The third system is adaptable to any sample size and can handle all of the drilling chips from the hole. Desirable features from all these systems may be readily combined into a modified system, which would be more suitable for other sampling requirements.

The first two systems are based on an indexing turntable operated by a motor using a Geneva type of drive. The motor will be a 28-v d-c motor already proved suitable for high-altitude operation. A pressurized case will be used, and the motor will be operated in an atmosphere of less than 3 psf. The first system is shown in Fig. 38. It consists of a turntable that has 12 indexing stations, consisting of six, 1-3/4-in. holes and six hoppers. The holes and hoppers are alternately spaced about the circumference of a 3-1/2-in. radius. To drill, the indexing mechanism is positioned so that the drill shaft may be lowered through one of the openings. When a sample is desired, the drill is retracted upward out of the opening and the indexing mechanism indexed so that a hopper is rotated under the drill. The sample is dumped into the hopper and the indexing unit again indexed so that an opening is located under the drill. The drill may then be lowered for further drilling. Chips in excess of the hopper 6-in.³ capacity will overflow and fall to the lunar surface through the adjacent holes. Two deflectors prevent the excess chips from falling into the drilled hole. For each operation, drilling or sampling, the turntable is indexed 1/12 of a

drilled and the condition of the drill bit. To ensure a uniform particle size, a pulverizer should be included in the overall spacecraft system.

The third sample collecting mechanism is shown in Fig. 39. The chips are dumped from the canister on the drill bit assembly into a hopper whose bottom is a cleated metal slat conveyor. The conveyor transports the drilling chips to a point about 15 in. above the bottom of the spacecraft where a wire brush removes the particles from the conveyor and drops them into a collection chute. One of the five conveyor idlers is spring-loaded and another held in position by a simple powered linkage (Fig. 39). During drilling, one idler and the conveyor pivot downward to permit the drill bit to pass through the sample hopper into the hole. The spring-loaded idler moves to maintain tension on the conveyor at all times.

(7) Mounting

To withstand the acceleration forces of boost and landing, the drill unit and shank can be rigidly attached to the spacecraft structure by means of a link and clamp. After the spacecraft has landed, an explosive charge would disengage these holddowns. This method provides both a positive restraining device and a simple and reliable release mechanism.

(8) Probe Emplacement

After drilling the hole is completed, it is desired that a mechanism be provided which will lower an 18-in. -long, 1.5-in. -diam. probe into the hole. In order to minimize weight, the probe mechanism was integrated with the drill mechanism in the manner shown in Fig. 38. The unit is currently designed to lower the probe only upon completion of drilling; and no provision is made for retracting the probe or for stopping it at other than the bottom of the hole. After completion of drilling, the drill is retracted and rotated (indexed) about one-sixth revolution relative to one of the stationary guide columns. This motion removes the drill from over the hole and simultaneously indexes the probe to a position above and in line with the hole from which it is subsequently lowered into the hole.

revolution, always in the same direction. This provides a total of six samples, one from the surface and five from equally spaced positions along the length of the hole.

The second system considered, while somewhat more complex than that discussed above, is also fairly simple. It does, however, provide a smaller sample from a more accurately determined point along the length of the drilled hole. The turntable has nine indexing stations as follows: six storage hoppers of 1-in.³ capacity, one opening for passage of the drill, one into which dumping of the waste chips occurs, and one for disposal of waste chips. In this concept, the hole is drilled to the depth at which a sample is required and then the drill is retracted. The turntable is indexed to the waste hopper station into which the chips are dumped. The drill is then raised and the turntable indexed 180° and the chips dumped. The turntable is indexed again to the drilling position, and sufficient material is drilled to provide a 1-in.³ sample. The drill is retracted and the turntable indexed to a sample hopper. The chips are then dumped into this hopper. This procedure is repeated at regular or programmed intervals for a total of six samples. Because of the increased amount of indexing, the second type of sample collector requires a more complex control circuit. The mechanical features of this system are quite similar to the first type of sample collector.

Since both of the above sample collectors dump chips onto the lunar surface the possibility of these falling back into the hole must be considered. Experimental studies are necessary to determine the angle of repose of outgassed rock drilling in a vacuum. This angle can then be analytically evaluated for the lower lunar gravity to determine the need of baffles to prevent the waste chips from falling into the drilled hole.

The hoppers in these collectors provide a convenient sample storage place until it is desired to analyze the material. The material can then be transferred to the analyzer by a system such as a vibratory conveyor. The conveyor design will depend on the location of the analyzer with respect to the drill unit.

The need for a pulverizer is dependent upon the particle size produced in drilling. Particle size varies with both the type of rock being

(9) Weight Estimate

The weight of this lunar drill system is estimated to be 40.9 lb with either the 9 or 12 station sample collector and 37.5 lb with a conveyor sample collector. This estimate does not include the weight of the batteries or solar cells used as a power source. The weights of the component parts are shown in Tables 4 and 5. This is a conservative weight estimate, and it is expected that a more detailed design, together with a thorough stress analysis, would reduce the total weight slightly.

Table 4

ESTIMATED WEIGHT OF LUNAR DRILLING MECHANISM
(TURNABLE SAMPLE COLLECTOR)

Item	Weight, lb.
Sliding Parts:	
Drill Housing and Motor	10.0
Winch and Clutches	1.0
Ball Bushings	1.0
Support Arms	1.0
Constant Force Springs and Reels	3.0
Pressure Tank and Control	2.25
Drill Bit Assembly	5.0
Sub-total	23.25
Mounted Parts:	
Mounting Brackets	1.50
Guide Columns	2.50
Geneva Drive Wheel and Gearing	2.20
Indexing Motor	3.00
Indexing Motor Pressurizing System	0.75
Sample Collector Turntable	1.15
Gear Sectors	3.00
Probe Station	1.05
Relay Box and Wire	2.50
Sub-total	17.65
Total <u>40.9</u>	
ARMOUR RESEARCH FOUNDATION OF ILLINOIS INSTITUTE OF TECHNOLOGY	

Table 5
WEIGHT ESTIMATE
Lunar Drill Mechanism
CONVEYOR SAMPLE COLLECTOR

Item	Weight, lb
Sliding Parts:	
Drill Housing and Motor	10.0
Winch and Clutches	1.0
Ball Bushings and Supports	1.5
Constant Force Springs and Reels	2.5
Pressure Tank and Control	2.25
Drill Bit Assembly	5.0
Sub-total	22.25
Mounted Parts:	
Mounting Bracket	0.50
Guide Columns	3.00
Conveyor Belt	1.00
Conveyor Drums	0.25
Conveyor Drive	1.00
Conveyor Motor	3.00
Conveyor Motor Pressurization	0.75
Conveyor Support Structure	1.50
Collection Hopper	0.25
Swing-Away Mechanism	1.50
Clean-Off Brush	0.25
Relay Box and Wire	2.50
Sub-total	15.50
Total	37.75

(10) Power and Control

Based on drilling experiments described in Section III-B-2, a minimum of 630 w-hr. will be required for drilling operations alone in penetrating 18 in. of Gabbro granite. If the requirements for other electrical equipment and the energy loss in the drill shank are added to this, about 1000 w-hr. would be required.

The power can be supplied through the spacecraft electrical system, by batteries, or by a combination of these. Because of the high power level, solar cells are not feasible as a direct power source. However, by using intermittent drilling and rechargeable batteries, energy from solar cells could be utilized.

Based on battery output of 50 w-hr. /lb, 20-lb of batteries would be required to provide the drill unit energy requirement.

Solar cells combined with batteries would provide the desired energy at less weight. The drill would operate on battery current until the battery voltage dropped below a designated value. The drilling would stop until the solar cells recharged the batteries, at which time drilling would be resumed. Based on a battery capacity of 190 w-hr. and a 12-hr. recharge period at 80% efficiency, 4.1 lb of batteries and connectors and 7 lb of solar cells would be required. This total power supply weight of 11.1 lb could be further reduced by allowing a longer battery recharge period.

The drill system can be controlled by either a command or programmed system through a relay control box. In this system, eleven relays control the performance of the complete drilling system. A block diagram of the system utilizing a conveyor for sample collection is shown in Fig. 40. The control system block diagram for the other two previously discussed types of sample collectors is shown in Fig. 41. Only the relays controlling the two motors remain energized for extended time periods, while the others are actuated for only a brief period. All electrical controls can be hermetically sealed. Wires must be insulated with suitable materials for the high-temperature, low-pressure environment. Power and control wires to the drill unit are a flexible coiled cable, similar to a telephone cord. No slip rings are used.

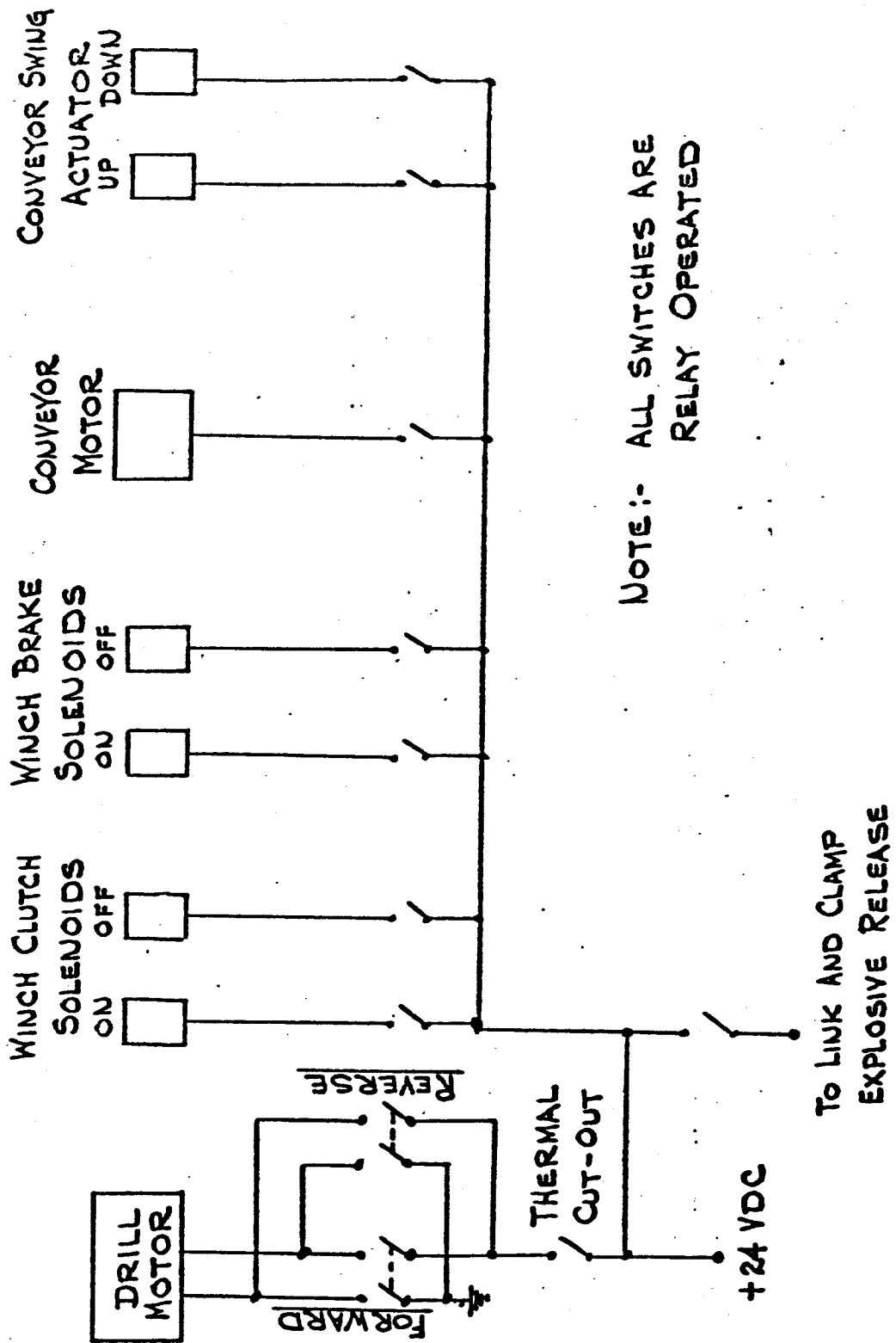


Fig. 40 - ELECTRICAL BLOCK DIAGRAM
DRILL SYSTEM - CONVEYOR SAMPLE COLLECTOR

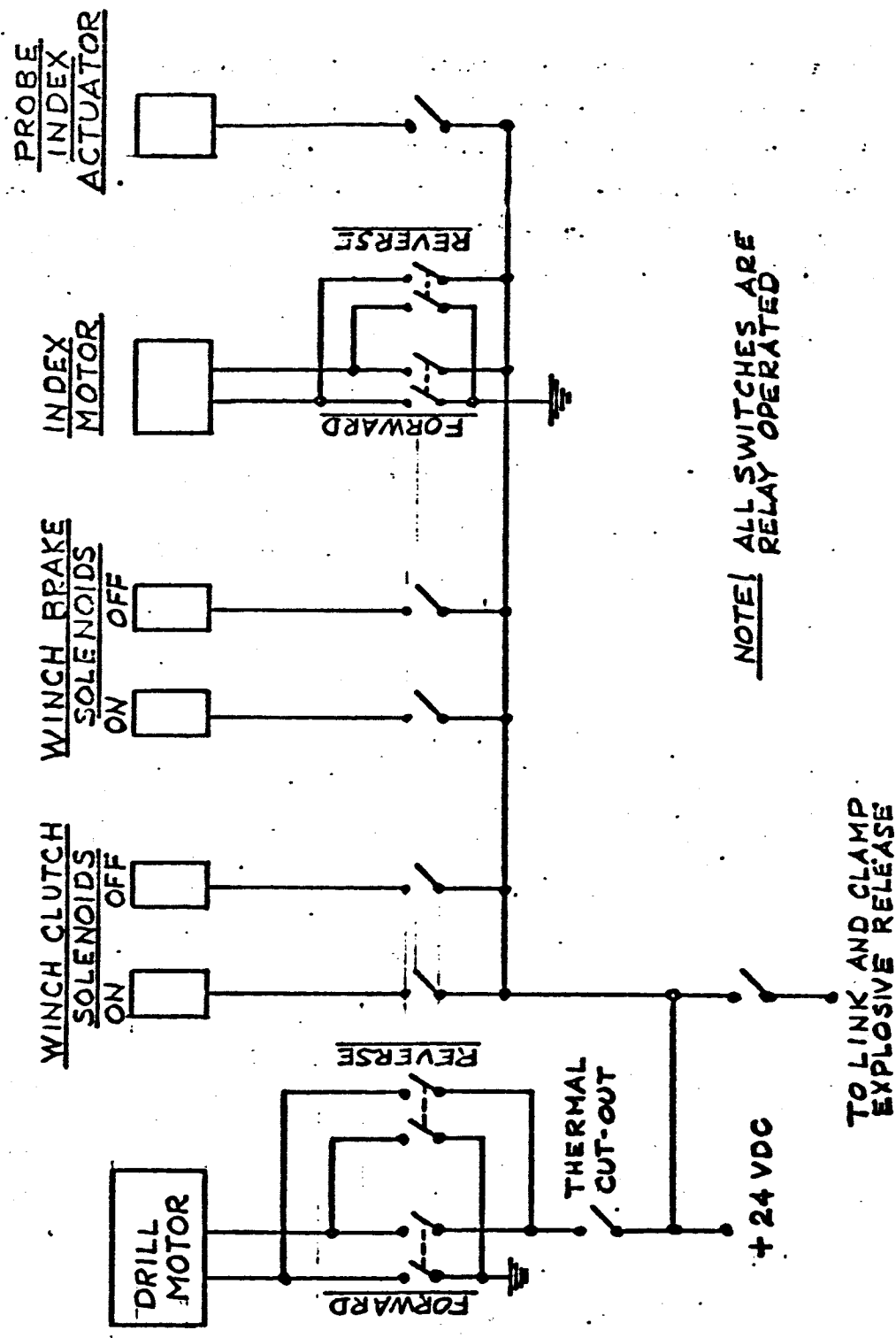


Fig. 41 - ELECTRICAL BLOCK DIAGRAM
DRILL SYSTEM - ROTARY SAMPLE COLLECTOR

Drilling must be intermittent to allow the drill motor to cool. A thermal cutout will stop the motor when its temperature rises above a predetermined level. The motor is then allowed to lose heat until its temperature drops below another predetermined limit. All relays may be operated by a nominal 24-v d-c. The operation of the drill motor relays will require about 2.5-w power, that of the index motor relays 1.0 w, and that of the solenoid relays, 0.15 w.

Table 6
OPERATION SEQUENCE
(9 Station Collector)

1. Simultaneously:
 - a. Start motor clockwise
 - b. Release winch brake
 - c. Release holddown links and clamps
 - d. Release waste chip baffles
2. Lower drill to lunar surface (rate of descent controlled by overspeed brake)
3. Drill for first sample
4. Retract drill by
 - a. Reversing motor
 - b. Engaging winch clutch
 - c. Energizing winch brake and releasing clutch when drill is at top
5. Index turntable to sample station No. 1
6. Release winch brake, lower drill 1-1/4 inches, apply brake
7. Dump sample into collector
8. Retract drill completely as in step 4
9. Index turntable to drill station
10. Energize drill motor clockwise.
11. Repeat step 2 except lower drill to bottom of hole
12. Drill for next sample
13. Retract drill by
 - a. Reversing motor
 - b. Engaging winch clutch
 - c. Energizing winch brake and releasing clutch when drill is at top
14. Index turntable to waste station
15. Release winch brake, lower drill 1-1/4 inches, apply brake
16. Dump chips into hopper
17. Same as step 8
18. Index turntable to dump position and dump waste
19. Repeat steps 9 through 18 for a total of 6 samples
20. Repeat steps 4 through 12 for a total of 6 samples

Table 7

SEQUENCE OF OPERATIONS

(12 Station Sample Collector)

(Battery Charging and Motor Cooling Sequence Operation Not Included)

1. Simultaneously:
 - a. Start motor clockwise
 - b. Release winch brake
 - c. Release holddown links and clamps
 - d. Release waste chip baffles
2. Lower drill to lunar surface (rate of descent controlled by overspeed brake)
3. Drill for first sample
4. Retract drill by
 - a. Reversing motor
 - b. Engaging winch clutch
 - c. Energizing winch brake and releasing clutch when drill is at top
5. Rotate collector turntable 1/12 revolution by energizing indexing motor in positive direction
6. Release winch brake, lower drill 1-1/4 inches, apply brake
7. Dump sample into collector hopper
8. Retract drill completely as in step 4
9. Index collector turntable 1/12 revolution (in positive direction)
10. Turn drill motor clockwise
11. Repeat step 2 except lower drill to bottom of hole
12. Drill for next sample
13. Repeat steps 4 through 12 for a total of 6 samples
14. After last sample has been dumped, under drill and probe clockwise 1/6 revolution about stationary guide pillars.

Table 8

SEQUENCE OF OPERATIONS
(Conveyor Sample Collector)

(Battery Charging and Motor Cooling Sequence Operation Not Included)

1. Simultaneously:
 - a. Start motor clockwise
 - b. Release winch brake
 - c. Release holddown links and clamps
 - d. Swing conveyor down
2. Lower drill to lunar surface (rate of descent controlled by overspeed brake)
3. Drill for first sample
4. Retract drill by:
 - a. Reversing motor
 - b. Engaging winch clutch
 - c. Energizing winch brake and releasing clutch when drill is at top.
5. Energize conveyor drive and swing conveyor up under hopper
6. Release winch brake, lower drill 1-1/4 inches, apply brake
7. Dump sample into hopper and transport by conveyor to chute
8. Retract drill completely as in step 4
9. Swing conveyor down and stop conveyor motor
10. Turn drill motor clockwise
11. Repeat step 2 except lower drill to bottom of hole
12. Drill for next sample
13. Repeat steps 4 through 12 until desired hole depth is reached
14. Repeat step 4.

c. Rotary-Impact Drill - Spring Mass System

The previously discussed modification of an "off-the-shelf" item for the lunar drill systems has many advantages. An alternate, more advanced system, designed specifically for this application may be contemplated. This alternate design incorporates efficiently the features most desirable in a lunar system. This concept would require a complete development program. However, the final product would be a mechanism designed specifically to drill a hole and recover samples under the conditions in which it will be used. Such a device is described below, and shown in Fig. 42.

After emplacement of the vehicle package on the lunar surface, the drill begins to operate. The package has several functions: (a) to drill the hole and dispose of the drillings, (b) to take samples for the lunar surface and from the subsurface at intervals of one foot, (c) to store the samples until called for by the analyzing apparatus, (d) to deliver the samples to the analyzing apparatus when ordered, and (e) to store a probe and to lower it into the hole after the full depth is reached and the final sample extracted.

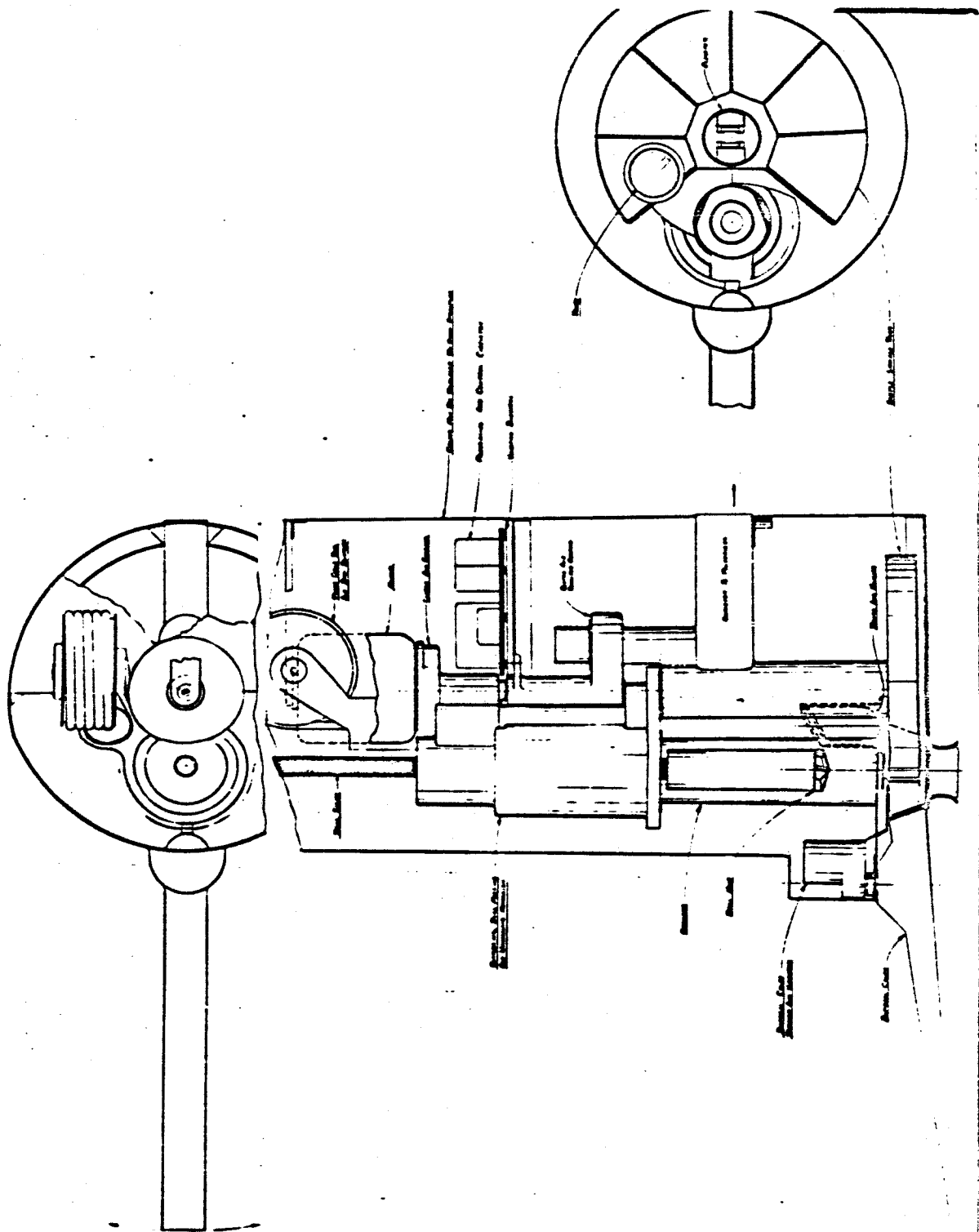
Each of these operations will be controlled from the programming circuitry in its proper sequence, subject to overriding signals from other parts of the vehicle, and to intelligence acquired from feedback circuitry.

In the simplest sequence, the drill operation will commence after emplacement and erection of the vehicle package on the lunar surface as follows:

1. The drill is fed to the lunar surface by rotating in a forward direction.
2. Upon contact of the drill point with the surface the depth control is actuated. This control will sense the depth of the drill and initiate depth-dependent activities, such as sampling.
3. First actuation of the depth control actuates the first sampling. After a few turns of the drill, the drill is reversed, thus retracting it above the sample trays.
4. Tray No. 1 rotates into position under the drill, and the drillings are discharged into the tray as described in connection with Fig. 49, showing the operation of the canister.

Conceived & Drawn By
Arthur Bernard Pennington Pennington
Drawn - Paul J. Pennington
Witness - John J. Pennington
Date - Nov. 11, 1916

24 42



5. The tray rotates to the storage position, upends, and dumps its contents into the elevator. The elevator conveys the sample to a higher level and discharges it onto a conveyor, which conveys it to the analyzer.
6. During operation 5, the drill is again advanced to the lunar surface and starts drilling. After penetration of a distance equal to approximately six cubic inches of displaced material, the canister should be full, and the drill is withdrawn.
7. This time, as the drill reaches its top position, the disposal tray rotates under it. The drillings are discharged into it, again as described in connection with Fig. 49, and the vibrating conveyor removes the drillings a distance sufficient to keep them from falling back into the hole.
8. Operations 6 and 7 are repeated until the depth control indicates that one foot of lunar surface has been penetrated, at which time operations 3 and 4 are repeated, except that tray No. 2 is filled. The material is not sent to the analyzer immediately, but is held until called for.
9. In like manner, operations 6, 7, and 8 are repeated until the sixth sample is in the tray. At this time a squib or other disconnect is operated and a spring rotates the drilling unit from over the hole, and the probe in line with the hole. Since the probe has been restrained merely by resting on a "shelf," when it clears the shelf lunar gravity causes it to drop out of the vehicle. Being now lined up with, and smaller than, the hole, it enters the hole and continues to fall until it reaches the bottom. The rate of fall of the probe under lunar gravity is controlled by a damping system contained within the probe cable reel.

In addition to the sample collector described here any of the sample collectors described in the first design concept can be adapted to this design concept.

All of the operations within the drill unit are powered by the single drive motor, with the exception of the disposal chute and conveyor, which operate by means of a rotary solenoid and two vibrators.

The impact drill mechanism described below performs the following functions:

1. Rotates the drill
2. Impacts the drill
3. Applies a constant load on the drill during drilling
4. Feeds the drill at a rate which is dependent upon the load
5. Retracts the drill without impact.

In Fig. 43 the motor is shown driving a shaft in the mechanism through a gear box clutch and a pair of spur gears. The lower end of the shaft drives the feed gears through a reduction spur gear. The upper end of the shaft drives a pair of bevel gears, which in turn drive a scotch yoke through a sprag clutch. The scotch yoke causes the hammer yoke to reciprocate vertically, riding on ball bushings, which in turn ride on the hardened sleeve surrounding the drill shank. Connected to the arms of the hammer yoke are two intertwined "clock springs," their inner ends connected to the "hammer" which in turn rides on ball bushings on the sleeve. As the hammer yoke reciprocates, the hammer follows out of phase and, at the lower end of its stroke, impacts the anvil, which is threaded onto the drill shank. Thus, the impact is transmitted to the drill shank and consequently to the drill point. The hammer is splined into the feed collar and rotates with it.

The large spur or "driver" gear at the bottom of the assembly is keyed to the drill shank by means of a key and a slot in the shank (not shown). The feed gears are carried by the driver gear and mesh with the threaded drill shank and with the internal threads in the feed collar. The load spring, backed up by the vehicle, loads the feed collar through an anti-friction thrust bearing.

When the driver gear is rotated in a forward direction, the ratchet, or sprag, rides freely, and the feed collar rotates with the driver gear until the dog engages the spur inside the framework. This stops the rotation of the feed collar so that the feed gears are rotating around the drill shank. In so doing they are rotated on their axes by the internal threads inside the feed collar, and thus feed the drill shank downward. When the drill point encounters resistance and will not longer feed downward, the feed collar is fed upward, compressing the load spring until the dog disengages from the spur, at which time friction allows the feed collar to again rotate with the assembly. The spring load is now applied to the drill shank through the feed gears. When the drill has drilled far enough for the dog to again engage the spur, the feed collar again compresses the spring.

When the direction of rotation of the driver gear is reversed the ratchet engages and the feed collar locks and does not rotate. Thus, when

the feed gears rotate around the drill shank axis inside of the feed collar, they also rotate around their own axes, feeding the drill shank upwards.

When the drill motor is reversed to raise the drill and canister from the hole it is desirable that the hammer does not operate. This is accomplished by means of the overrunning sprag clutch built into the large bevel gear that drives the scotch yoke.

It now becomes evident that to advance the drill and drill a hole, the driver gear must be rotated forward, and to retract the drill from the hole, the driver gear must be reversed. The reason for the complexity of the system is the requirement that the maximum drilling load of 50 lb must not be exceeded, which would be the case if the drill were advanced into a hard material by merely screwing it forward.

The clutch, which is integral with the motor reduction gear, disengages the entire drill mechanism when the motor power is being used for other requirements of the package, such as operating the elevator.

The canister performs the function of containing the drill chips or drillings, in order to extract them from the hole. The actual construction and operation of the canister are the same as that described in the previous concept.

Because of the additional research and development necessary on this concept the power requirements cannot be specified. However, because it is basically more efficient than the first concept, the total energy required should be less than the 1000 w-hr estimated for the first concept.

The weight of the complete lunar drilling unit package is estimated to be between 47 and 48 lb. The weight of the individual subassemblies in the package are shown in Table 9. These data are based on slightly conservative estimates (higher than actual) rather than an exact determination of the weight of the unit, which may be modified during the design and development programs. It is expected that the final design would weigh somewhat less than the unit analyzed herein.

Table 9
COMPONENT WEIGHT ESTIMATES
 (Alternate Design Concepts)

Item	Material	Weight, lb
Canister	Seamless Steel Tubing	0.2130
Drill Point	Steel and Carbide	0.188
Drill Shank	Steel	8.84
Canister Cam	Steel	0.235
Elevator Tube	Steel	0.84
Elevator	Steel	2.00
Conveyor	Steel	0.75
Feed Collar	Steel	0.72
Hammer	Steel	0.418
Driver Gear	Steel	0.21
Driver Gear	Steel	0.500
Feed Gears	Steel	0.128
Sleeve	Steel	0.315
Bottom Plate	Aluminum	
Hammer Housing	Aluminum	1.54
Motor		5.00
Addition to Hammer Housing		0.75
Other Gear Housings		1.00
Programming		5.00
Probe Reel and Escapement		0.75
Wiring and Switches		2.80
Outer Casing		3.00
Sample and Storage Box and Associated Equipment		2.75
Discharge Chute	Aluminum	0.17
Discharge Solenoid	Aluminum	1.75
Casing Supports		2.50
Casing Base		0.904
Probe Container Tube		0.50
Reel Supports		0.5
Connections and Miscellaneous		2.5
Total Weight		<u>47.26</u>

ARMOUR RESEARCH FOUNDATION OF ILLINOIS INSTITUTE OF TECHNOLOGY

d. Deep-Hole Drilling

A concept was developed for drilling holes of 40 ft or more in depth and 3 in. in diameter. ARF studies indicate that a down-the-hole rotary-impact drill will be required for this purpose. There are several problems involved in designing such a drill in addition to those encountered in the design of a conventional rotary-impact drill. For minimum weight, it is impractical to use a long shaft to apply a thrust to the drill through the weight of the spacecraft. Similarly, the drill torque cannot be reacted against the spacecraft. Unlike conventional down-the-hole drills, it does not appear feasible to use air to flow the chips up from the bottom of the hole, so a positive collection means must be provided. Another problem is packaging, that is, selecting components and designing the drill with a diameter of 3 in. or less. Although down-the-hole rotary-impact drills have been made with diameters as small as 2 in., their down-the-hole mechanism provides only the impact force. Rotational torque is transmitted from the surface generally at quite a low rotational speed. One such drill operates at 6000 blows/min at 60 rpm.

A block diagram of this deep-hole drilling concept is shown in Fig. 44. The drill is lowered from the spacecraft on a combination cable, umbilical cord. When the drill reaches the bottom of the hole (during down-the-hole operation) a friction ring and torque reacting rings are forced against the side of the hole. Connecting links between the drilling package and the bonnet are released, and the compressed load spring applies a thrust to the drill, the upward reaction being sustained by the friction rings. Power is applied through the umbilical cord to the rotary impact mover and drilling starts. Chips are collected in a canister located just above the drill bit. As the drill penetrates, the load spring extends, but the bonnet with the friction rings remains stationary. Maximum desired spring expansion occurs when the canister is filled. The friction and torque rings are then released, and the drill is raised into the spacecraft, where the canister is emptied. The load spring is recompressed and the drill package locked onto the bonnet. Then the drill is lowered into the hole and the cycle repeated.

The preliminary concept, not studied in detail, illustrates a feasible lightweight down-the-hole rotary impact drill.

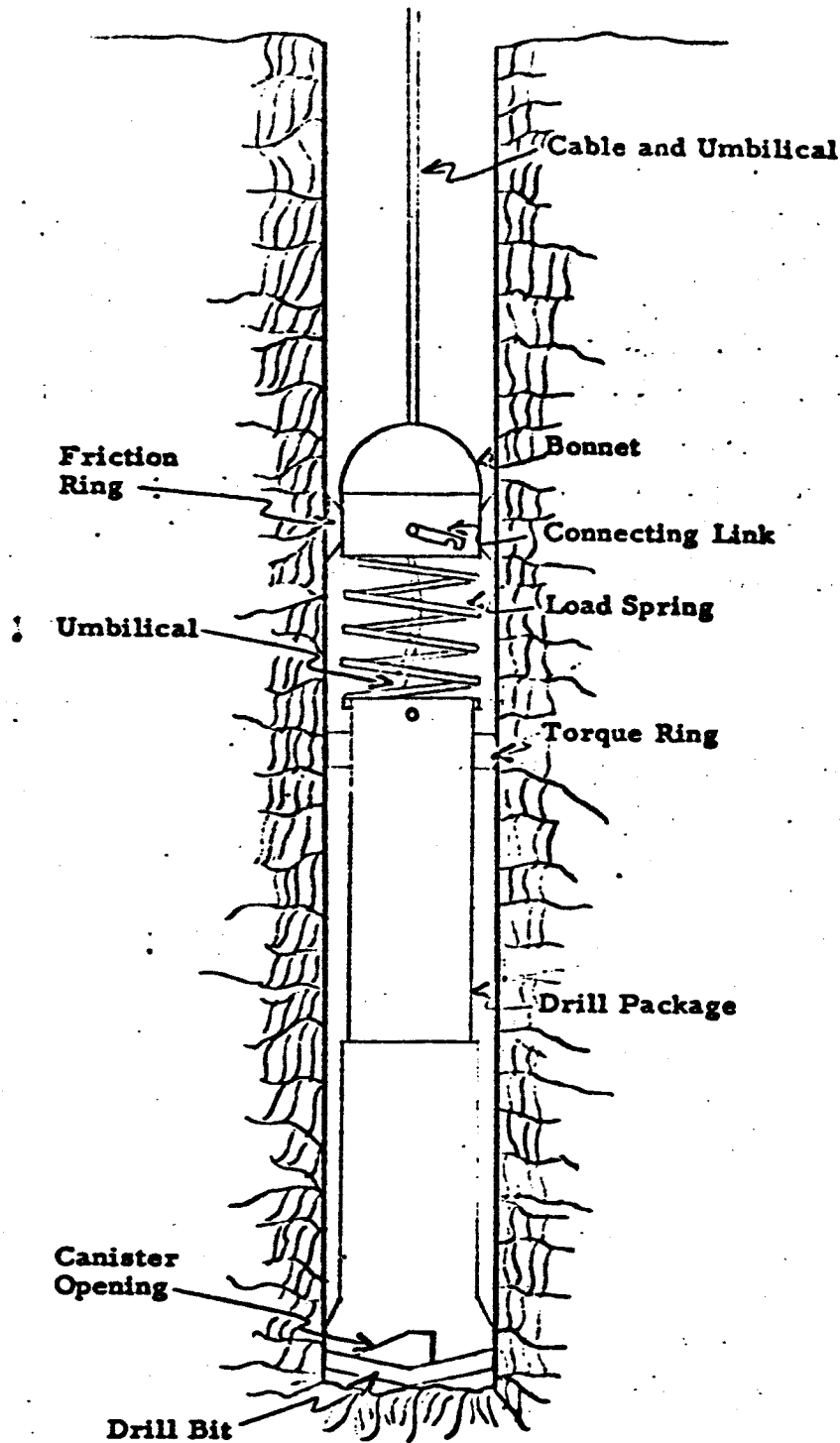


Fig. 44 BASIC CONCEPT, DOWN-THE-HOLE LUNAR DRILL

2. Rotary Drilling Systems

Because of its relative simplicity and lack of vibration, rotary drilling has some advantages over rotary-impact drilling. However, it does require a high thrust and also is generally less efficient than rotary-impact drilling. Although this type of drill is not suitable for use in the initial Surveyor system, it could be used on future systems in which a higher drill thrust is available. Its use will be influenced by the size of hole desired, and the type of rock to be encountered. Its simplicity would be a definite advantage in a roving lunar exploration vehicle. The drawings illustrating these drill systems all shown solid drill bit assemblies, however, a coring drill bit assembly, such as that described in Section III-A-3b, can also be used and for many applications would possess significant advantages.

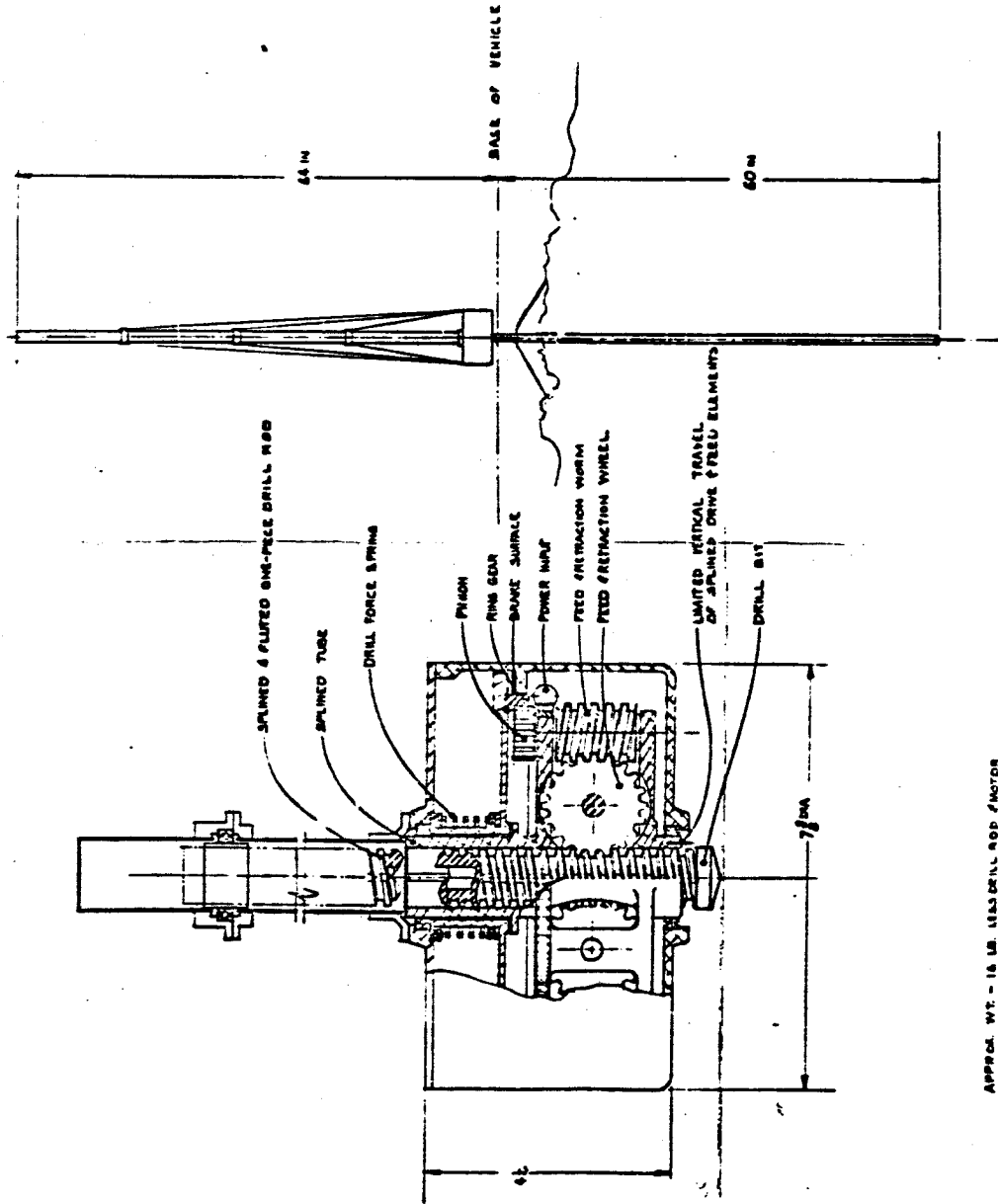
a. Rotary Drilling System - Concept No. 1

A preliminary design layout for a drill driving head is shown in Fig. 45. This drill driving head performs the functions of (a) rotating the drill bit, (b) feeding and retracting the drill rod, and (c) causing the vehicle weight to be applied to the drilling bit.

Rotation of the drill rod (see Fig. 45) is accomplished by means of a pair of vertical, shallow keyways cut into the helical flutes of the rod. These keyways engage mating keys of the surrounding splined tube. The splined tube is integral with a drive gear driven by a motor.

Drill feeding and retraction is achieved by means of a worm and worm wheel system. This worm and gear system, as shown in the figure, is mounted on a surface, integral with, and therefore rotating with, the splined tube surrounding the drill rod. The work wheel engages the helical flutes on the exterior of the drill rod to feed the drill rod into the hole when desired. The worm wheel is driven by the feed worm, as discussed below.

The feed worm rotates about its own axis only when relative motion occurs between the ring and gear and the pinion attached to the feed worm shaft. Ordinarily, during drilling, the ring gear will rotate at the same angular velocity as the splined tube. The drill loading force will be supplied by the vehicle weight acting through the drill force spring. As the drill



APPROX. WT. - 16 LB. LEAD DRILL ROD MOTOR
APPROX. VOL. - 2.75 IN³

Fig. 45

ITEM	QTY	DESCRIPTION	REMARKS
1	1	DRILL ACTUATOR - NO. 1	
2	1	DRILL ROD - 60 IN.	
3	1	DRILL BIT	
4	1	DRILL FORCE SPRING	
5	1	DRILL TUBE	
6	1	DRILL PINION	
7	1	DRILL RING GEAR	
8	1	DRILL WORM	
9	1	DRILL WORM WHEEL	
10	1	DRILL POWER INPUT	
11	1	DRILL FEED MECHANISM WORM	
12	1	DRILL FEED MECHANISM WHEEL	
13	1	DRILL LIMITED RETICAL TRAVEL OF SPLINED DRIVE FEED ELEMENTS	
14	1	DRILL DRILL BIT	

penetrates the lunar soil, the spring will extend, thereby causing the ring gear brake surface to contact the stationary brake surface in the drilling head case.

This causes the pinion to rotate. The worm is rotated, causing the wheel to advance, and the drill rod to feed until the rod action lifts the ring gear to release the brake. The mechanism automatically feeds to apply the unit, without relative motion, between the ring gear and the other rotating parts.

Retraction is accomplished by braking the ring gear through an auxiliary brake and reversing the rotation of the drive motor.

All of the drill chip removal methods, which are described in Section III-A-4 of this report, could be used with this drill system. That selected would depend on the particular application of the drill.

The driving unit, as shown in Fig. 45, employs a one-piece drill rod about 64-in. long. It therefore requires a vertical headspace of that amount. The unit weighs about 16 lb without the drill rod and motor and occupies a volume of about 275-in.³. If the drill bit assembly and the sample collector mechanism similar to that described in Section III-A-2b were used, the total unit weight would be about 38 lb.

b. Rotary Drilling System - Concept No. 2

This system is a modification of the previously described drill device, Concept No. 1, in which either the total package height may be reduced or the drilling of deeper holes is possible. This system, Fig. 46, uses a drilling head similar to that described in Fig. 45 and Section III-A-2-a. The drill rod, however, is made up in three lengths. These lengths are stowed vertically in their respective places in a turntable, or magazine, which can be indexed so that each section of drill rod is brought in line with the drilling station.

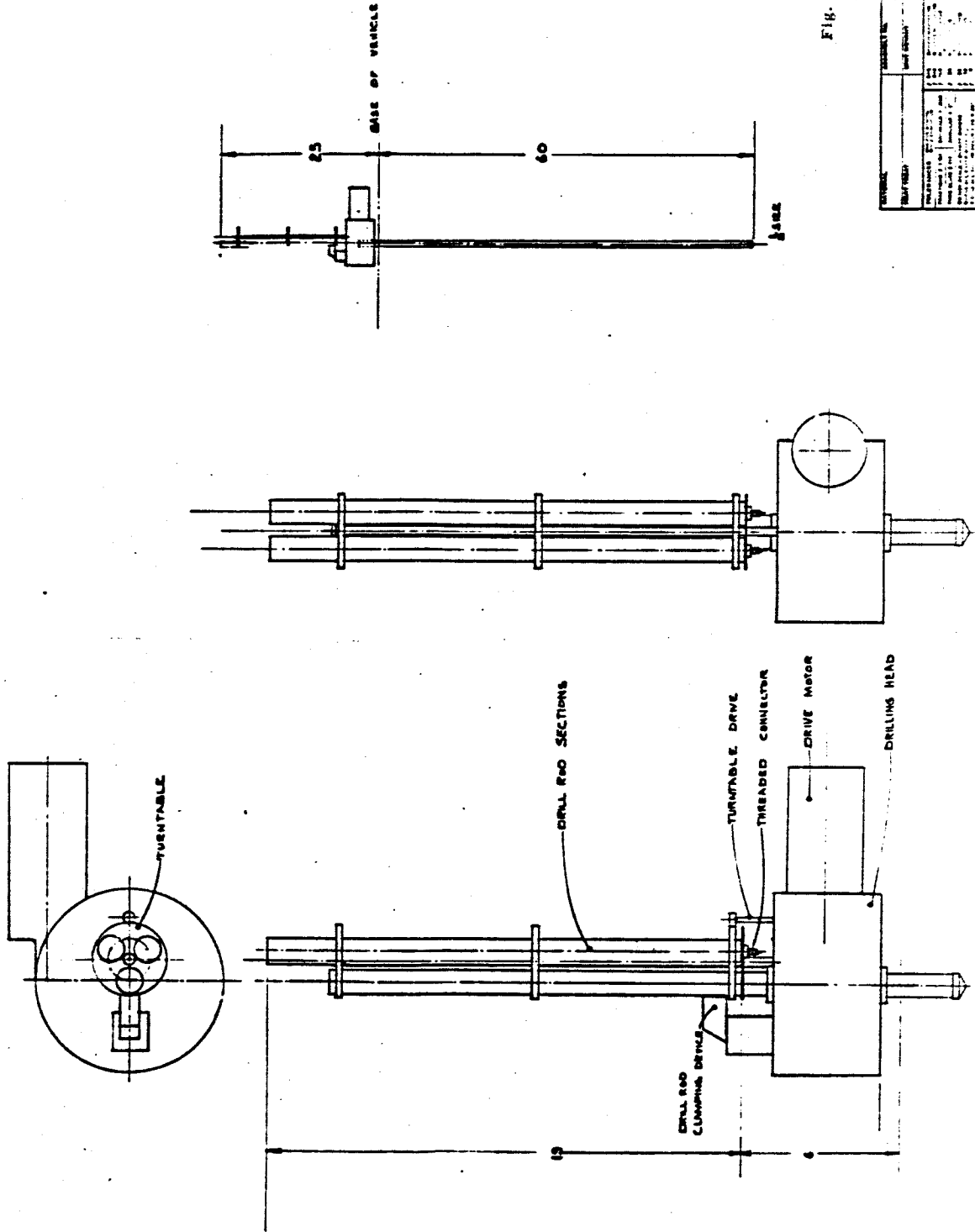


Fig. 46

REVISION		REVISION NO.		REVISION DATE		REVISION BY		REVISION FOR	
NO.	DATE	NO.	DATE	NO.	DATE	NO.	DATE	NO.	DATE
1	10/1/50	1	10/1/50	1	10/1/50	1	10/1/50	1	10/1/50
2	10/1/50	2	10/1/50	2	10/1/50	2	10/1/50	2	10/1/50
3	10/1/50	3	10/1/50	3	10/1/50	3	10/1/50	3	10/1/50
4	10/1/50	4	10/1/50	4	10/1/50	4	10/1/50	4	10/1/50
5	10/1/50	5	10/1/50	5	10/1/50	5	10/1/50	5	10/1/50
6	10/1/50	6	10/1/50	6	10/1/50	6	10/1/50	6	10/1/50
7	10/1/50	7	10/1/50	7	10/1/50	7	10/1/50	7	10/1/50
8	10/1/50	8	10/1/50	8	10/1/50	8	10/1/50	8	10/1/50
9	10/1/50	9	10/1/50	9	10/1/50	9	10/1/50	9	10/1/50
10	10/1/50	10	10/1/50	10	10/1/50	10	10/1/50	10	10/1/50

After the lunar drill proceeds to point where the first section of drill rod is fully extended into the hole, drilling is interrupted and the turntable is indexed so that the second drill rod section is positioned in the station over the hole. The second station is clamped to prevent its rotation and the drill head output direction is reversed to bring the first section of the drill shaft upward to engage the threads of the second station. When coupling is completed, the reverse rotation is stopped, and the clamps on the second station are released. The drill head rotation is then changed to the forward direction. The drill rod will now feed and the drill will now rotate. The sequence is repeated for the third drill rod section.

If it is desired to retract the drill the procedure described above is reversed. The drill rod sections are unscrewed and the turntable is indexed backwards to stow the sections.

This concept presents considerable functional flexibility and has good growth potential for drilling deeper holes. Additional stations could be added to the turntable to hold more drill rod extensions or instrumentation probes.

c. Rotary Drilling System - Concept No. 3

Another type of rotary drilling actuator is illustrated in Fig. 47. This system is functionally similar to those previously described but uses a different type of drive and feed mechanism. Intermittent drilling requirements are designed into the system, thus allowing sample delivery from any programmed depth. A non-coring carbide-tip drilling tool is shown in the schematic layout; however, the actuator will accommodate other types of drill bits.

A vertically mounted rotary motor drives a torque tube through a miter and worm gear train. The upper end of the torque tube consists of a disc having a square opening, into which a four-flat spindle is mated. As the torque tube revolves, the spindle revolves and drives the drill. Mounted on the inside diameter of the torque tube is a ball bearing, supporting a bell-shaped nut. This unit, which is the feeding and retracting mechanism, engages partial threads on the spindle and is driven through a gear-clutch train by the torque tube. The clutch is included to provide torque control.

ARMOUR RESEARCH FOUNDATION OF ILLINOIS INSTITUTE OF TECHNOLOGY

CROSS SECTION

SIDE VIEW

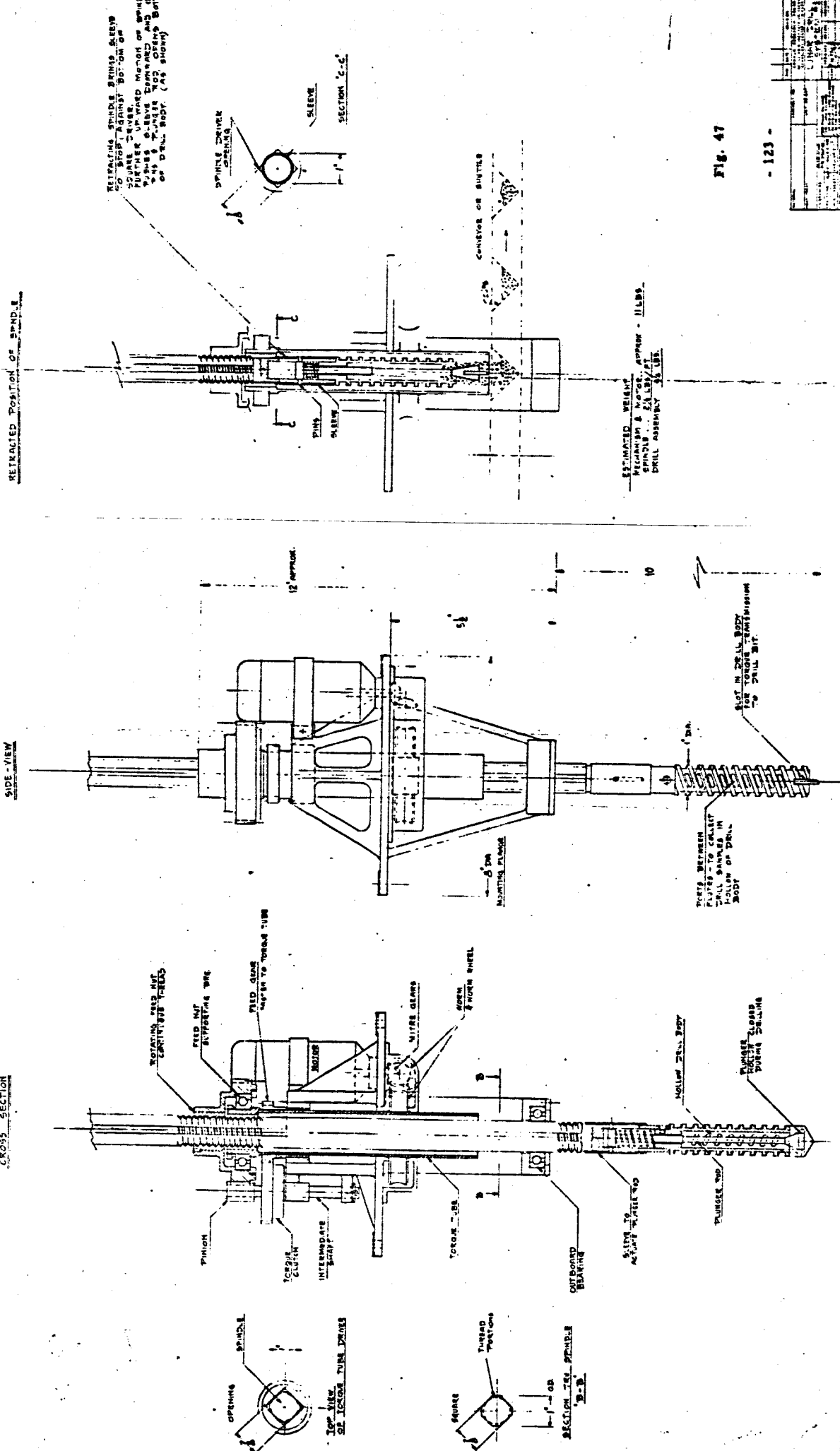


Fig. 47

The drill is rotated by the flates on the spindle, and downward feed is accomplished by the threads from the feed nut. Motor rotation is reversed to retract the drill.

The chips are collected in a canister which is described in Section III-A-3a. When the canister is filled the motor is reversed, which retracts the drill bit. The chips can then be deposited in a sample collector or conveyor system. Any of the sample collectors previously described can be used with this drill system.

The weight of this system with a 5 ft long drill spindle and a 12-station sample collector, Section III-A-1, would be about 38 lb. If a conveyor sample collector were used the weight would be slightly less.

d. Rotary Drilling System - Concept No. 4

This fourth conceptual system uses rotary milling type cutters rather than the conventional rotary drilling boring cutters. It features a telescoping packaging technique to conserve space during transportation and a pressure-stabilized structure during the drilling phase.

The major components of this system, Fig. 48, are: conveyor-type, contra-rotating, cable-mounted, cutting bits, a constant-length cable drive, three independent telescoping metal structures equipped with flexible inner pressure tubes and the necessary valving, pulleys, and pressure supply.

Operation of this system is as follows:

1. Upon landing of the spacecraft on the lunar surface the system is pressurized, which extends the side booms and tightens the drilling cable.
2. Drilling commences. Because the main boom is maintained at a constant level and the side booms bleed gas at a specified rate, a gas supply for the main boom is required. The main boom lengthens and both side booms contact during drilling. Cutting tools serve simultaneously as chip transportation containers.
3. At the end of operation, the main boom fully extended and side booms set at terminal minimum lengths.

e. Comparison of Rotary Drilling Concepts

The weights and functioning of concepts 1 and 3 are similar, and the selection of one over the other would be influenced by development problems and reliability. The advantages of a system of this type can be summarized as:

1. A one-piece drill eliminates the complexity of adding drill rod extensions.
2. The system can be pressure-sealed by static seals at all points except at the drill rod.
3. The system provides auger holes that could be used to transport the chips to the surface.
4. Automatic sensing and feeding of the drill provides maximum utility of the vehicle weight.
5. The system not sensitive to temperature extremes.

The disadvantages of this type of system are:

1. The system requires 65 in. of head space to drill a 60-in. hole.
2. Little growth possibility is allowed for deeper holes.
3. Pressure sealing will be required around the threaded shaft.
4. If drilling chips travel up the helical thread, they can damage the drive and feed mechanism.
5. The drive and feed mechanism is relatively complicated.

Concept 2 has advantages and disadvantages similar to Concepts 1 and 3. However, it requires less head space and has a moderate growth possibility. However, it is more complicated than those systems and consequently would require a more extensive development system.

The cable mounted cutter system, Concept 4, has several unique advantages, but also introduces complications common to unconventional approaches. The concept is credited with the following advantages:

1. Space-saving structure for rocket vehicle transportation.
2. Possible configuration advantages for lunar landing shock.
3. Continuous drilling and sample delivery technique from any depth of the hole.
4. Low wear rate per cutting tool.
5. Possible continuous cutting speed variation, if controlled from earth.
6. Cable-actuated boom retraction system.

The disadvantages are:

1. Pressurization requirements.
2. Catastrophic results due to accidental leakage.
3. Structural stability problems.
4. Need of at least three counterrotating cable systems to offset torsional motion tendencies.
5. Dynamic stability requirements of the travelling cable systems.
6. Large number of vacuum- and rock-particle-exposed bearing surfaces.

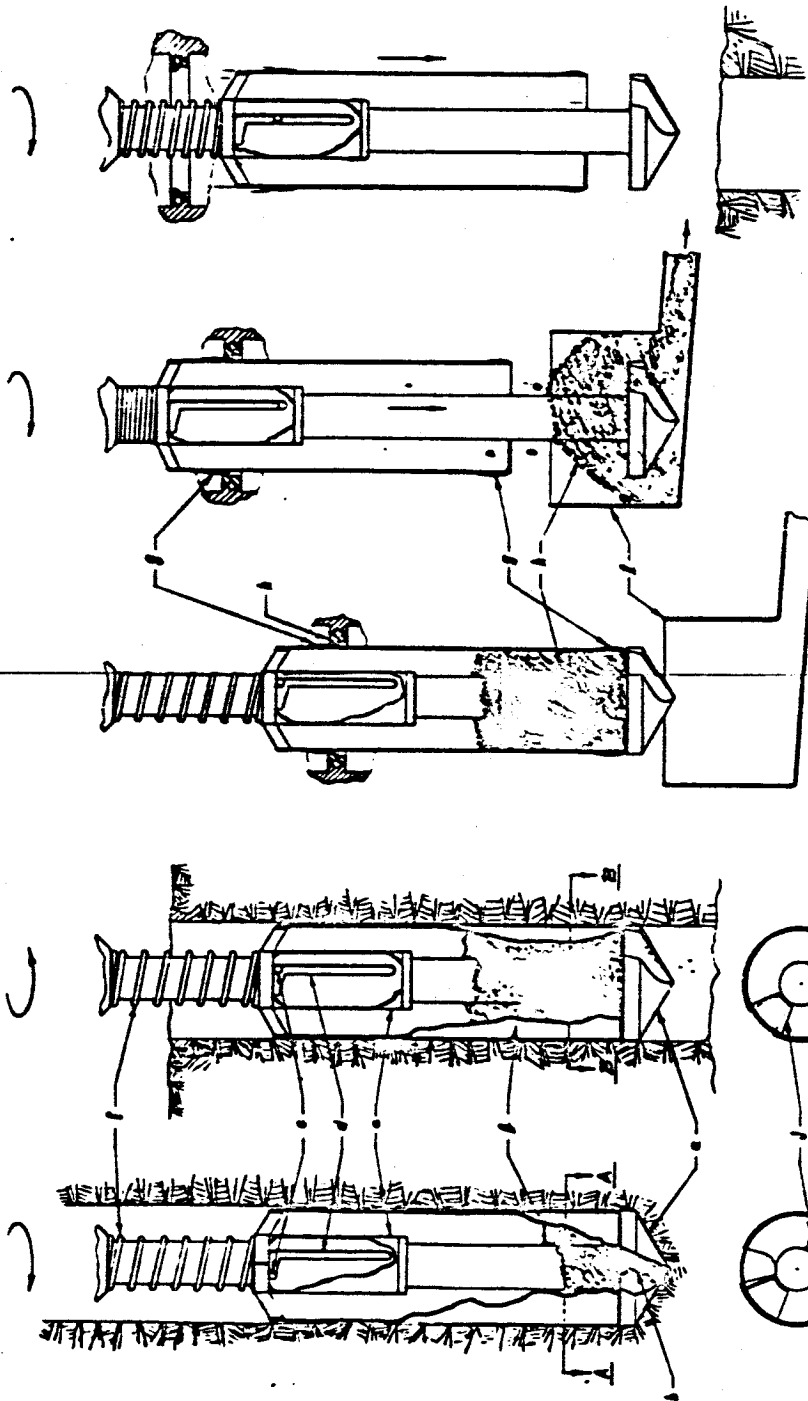
This fourth concept would not be recommended for use in initial drilling studies, however it might prove advantageous for future special-purpose drilling experiments.

3. Chip Removal

As the hole is drilled in the lunar surface, it will be necessary to clear the hole of chips, or the drilling efficiency will decrease and eventually the drill will stall. Five concepts are described for this purpose of which three collect the materials in a canister that forms a part of the drill bit assembly. In these, when the canister is filled, the drill bit is retracted and the canister is emptied on the lunar surface. In two such systems, the canisters are for use only with solid drill bits; while in the third a coring drill bit is used. The remaining two methods continuously remove chips from the hole; one of them uses a spiral ramp vibratory conveyor, and the other uses fluidized particle conveyance. These latter two methods are illustrated with solid drill bits, but are readily adapted to a coring bits. The fluidized particle conveyance chip removal system could be readily incorporated for use with diamond core drilling.

a. Chip Removal Canister

This drill chip removal system, Fig. 49, provides a relatively simple and positive way to remove the chips from the bottom of the hole. The cutting tool consists of a short drill bit with a two-flute cutter and a reduced-diameter shank. The canister, which is slightly smaller in diameter than the bit, is mounted so as to slide on the shank of the drill



Section A-A
 Section B-B
 Section C-C
 Section D-D
 Section E-E
 Section F-F
 Section G-G
 Section H-H
 Section I-I
 Section J-J
 Section K-K
 Section L-L
 Section M-M
 Section N-N
 Section O-O
 Section P-P
 Section Q-Q
 Section R-R
 Section S-S
 Section T-T
 Section U-U
 Section V-V
 Section W-W
 Section X-X
 Section Y-Y
 Section Z-Z

Source: - Donald P. Sauer
 Witness: - John A. Campbell
 Date: - November 11, 1960

Fig. 49

Section A-A	Section B-B	Section C-C	Section D-D	Section E-E	Section F-F	Section G-G	Section H-H	Section I-I	Section J-J	Section K-K	Section L-L	Section M-M	Section N-N	Section O-O	Section P-P	Section Q-Q	Section R-R	Section S-S	Section T-T	Section U-U	Section V-V	Section W-W	Section X-X	Section Y-Y	Section Z-Z
Section A-A	Section B-B	Section C-C	Section D-D	Section E-E	Section F-F	Section G-G	Section H-H	Section I-I	Section J-J	Section K-K	Section L-L	Section M-M	Section N-N	Section O-O	Section P-P	Section Q-Q	Section R-R	Section S-S	Section T-T	Section U-U	Section V-V	Section W-W	Section X-X	Section Y-Y	Section Z-Z

Section A-A

Section B-B

Section C-C

Section D-D

Section E-E

Section F-F

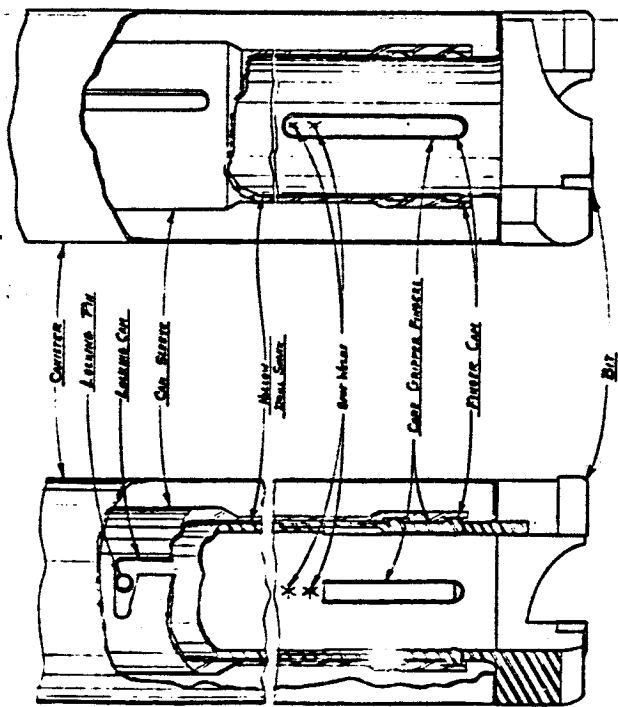


Fig. 50

ITEM NO.	DESCRIPTION	QTY	UNIT	PRICE	TOTAL
1	COUPLER	1	PC	1.00	1.00
2	LUBRICATOR PIN	1	PC	.50	.50
3	LUBRICATOR CONE	1	PC	.50	.50
4	OIL RETURN	1	PC	.50	.50
5	WATER SEAL	1	PC	.50	.50
6	GEAR MESH	1	PC	.50	.50
7	GEAR COUPLING PINION	1	PC	.50	.50
8	PINION GEAR	1	PC	.50	.50
9	BOLT	1	PC	.50	.50
10	TOTAL				7.00

When it is desired to remove the drill chips from the hole, the bit is rotated backwards. The detent springs on the canister resist the rotation until the pin reaches the end of its travel in the cam slot. At this time, the canister flaps have been rotated far enough with respect to the bit that they cover the bit flutes, and thus prevent the drill chips from dropping out through the flutes. Continued reverse rotation causes the drill to be retracted from the hole.

Retraction continues until the detent springs pass through and engage a ring detent. This is the highest point reached by the bit in its upward motion. The bit is now lowered slightly exposing the drill chips as the detent springs prevent the canister from lowering with the drill. The drill is next rotated several times while a stationary brush in the hopper brushes the chips off of the bit and into the hopper. The drill is now raised again, the hopper swung out of the way, and the drill again lowered toward the hole. When the drill is lowered far enough, the detent springs can no longer retain the canister in the upper location. The springs are forced through the ring detent, and the canister spring pushes the canister to its normal location on the bit. When the bit enters the hole and starts turning, the detent springs again drag on the sides of the hole, to rotate the canister, and in so doing, lock it vertically in place and again expose the flutes in order to collect chips.

When a given depth of drilling is accomplished, a projection on the inside of the hollow shank of the drill rubs against the outside of core and breaks it off. Then the drill is reversed to close the canister, and the fingers are cammed against the core to grip it by means of the finger cams, so that when the drill is lifted out of the hole, the core is lifted with it. When the canister is engaged by means of the detents and the drill is lowered to dump the chips, the finger cams disengage, allowing the fingers to release the core and drop it into the collector bin.

c. Canister Drill Bit

This canister-type chip removal system functions in a manner similar to that of the systems previously described. It is however mechanically different. Its application is illustrated in Fig. 47. A fluted hollow drill with a sliding cutting tool to transport the chips from the hole is proposed.

The chips enter the hollow body of the drill through elongated portholes. When retracted, the spindle passes within the torque tube so as to push the trip sleeve down against the spring, causing the bottom section of the drill body to open. Through this opening, the chips are delivered either to sampling troughs or a dumping conveyor. With downward feed, the spring brings the plunger into drilling position again and locks it in the slot, ready for the next drilling sequence.

d. Vibrating Spiral Ramp Conveyor

Removal of the chips or drillings from the hole may present a problem because of the lack of a suitable atmosphere for entrainment of the particles. The spiral ramp conveyor (Fig. No. 51) is designed to remove the chips as fast as they are produced to prevent the possibility of packing. It is an accomplished fact that particles can be moved - even uphill - by a vibrating conveyor, although the present applications of this mode of conveying materials of this type are in straight-line conveyors.

The spiral ramp conveyor is essentially as a straight-line conveyor wrapped around the inside of a tube. Vibration of the tube in a helical-torsional mode should then move particles around the curved ramp in a direction dependent upon the direction and mode of the vibration. Because different particle sizes and densities respond most efficiently to different frequencies and amplitudes of vibration, a "voice coil" capable of reproducing a range of frequencies and amplitudes is shown in the accompanying layout as the actuating mechanism.

The drill point and shank are shown surrounded by a spiral ramp on the inside of a tube as described above. Near the top of the tube, the spiral ramp ends in a discharge trough. The actuating mechanism at the tip of the tube consists of the above-mentioned voice coil, shown in conjunction with a permanent field magnet, cam rolls, and cam tracks.

In operation, the drillings will accumulate on the top of the drill bit. When a layer of ground-up materials becomes thick enough to engage the lowest point of the spiral ramp, some of them overflow onto the ramp and are conveyed upwards. When the drillings reach the top of the spiral ramp they spill out through the discharge trough to be conveyed away.

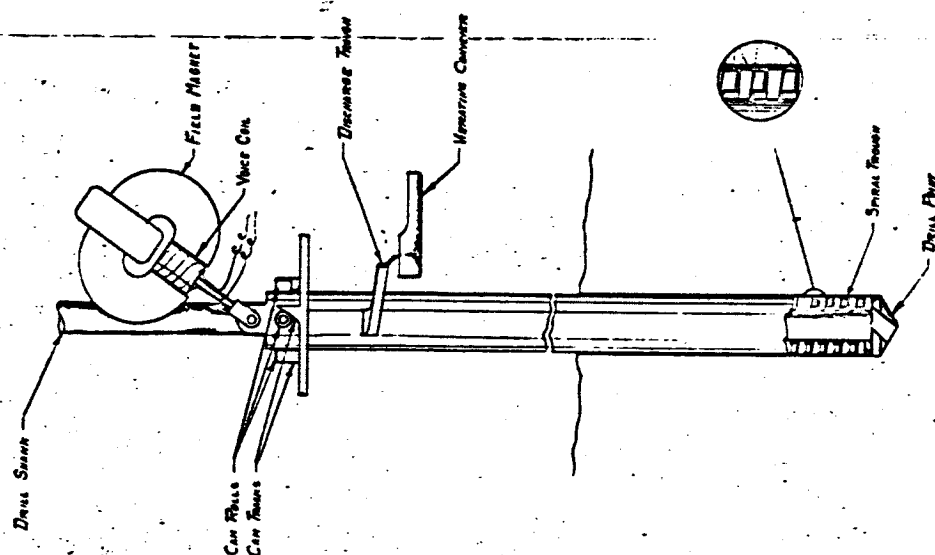


Fig. 51

- 134 -

[illegible]

e. Fluidized Particle Conveyance

A chip fluidization technique was investigated, and the system described schematically in the block diagram (Fig. 52) and in the component layout study (Fig. 53) was conceived. The system requires no in-the-hole casing and relies on the assumption that no sub-surface cavities or porous material layers will be encountered. The drill unit features a hollow straight-fluted drill, similar to the types known as a "gun drill." (Fig. 53 shows the layouts for both helical- and straight-fluted drills.) The drill could be used with solid or coring carbide drills or with diamond core drills. It is the only concept developed herein which can be practically adapted to diamond core drilling.

The distance from the actuating mechanism to the lunar surface is enclosed by a telescoping tube sealed to the lunar surface. Quick-freezing, plastic, non-diffusing materials are visualized to seal the contact surface. Gas is fed from the fluting into a cyclone separator where the particles are removed from the stream. The gas is then returned through a compressor to an accumulator and thence into the hollow drill shank. A gas make-up reservoir is provided to compensate for leakage.

Analytical efforts were concentrated on helium as the particle fluidization medium. The following assumptions were made:

1. Isothermal flow, except in the compressor where an adiabatic process was assumed.
2. Temperature = 32° F.
3. Pressure = 10 lb/in.² absolute.
4. Solid density of fluidized particles, 1.56 slugs/ft³
(= 50 lb/ft³; for comparison: dry clay density = 63 lb/ft³).

The multiparticle terminal (free-fall) velocity equation Ref. 61 is presented as a function of particle diameter in Fig. 54. A velocity of 10 ft/sec is chosen for analysis, corresponding to a particle diameter of 35×10^{-4} ft ($35 \times 10^{-4} = 1050$ microns). Experimentally determined particle size distribution (Fig. 4) indicates that this velocity would remove better than 95% of the particles.

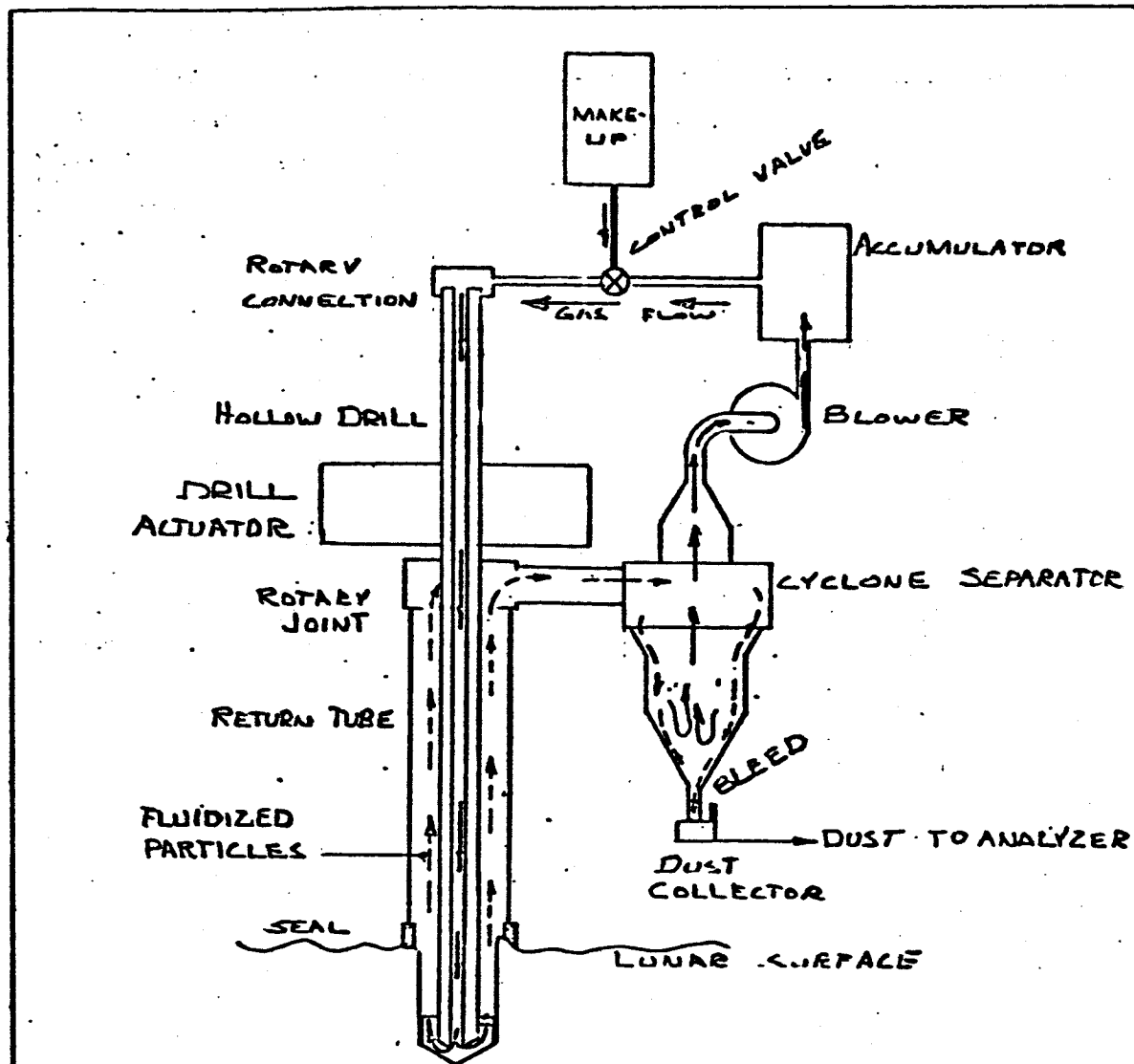
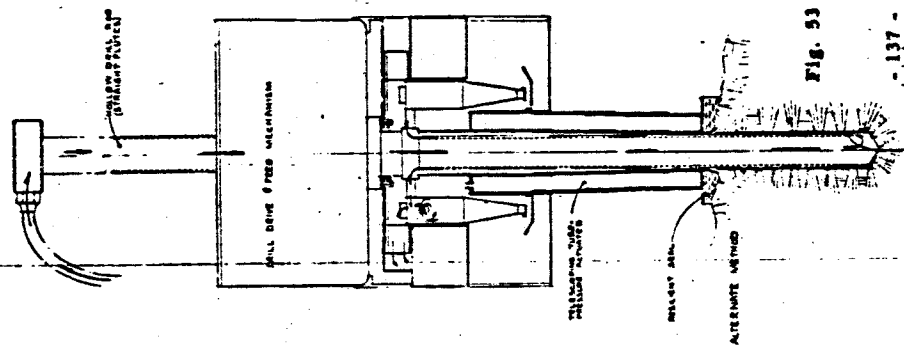


Fig. 52

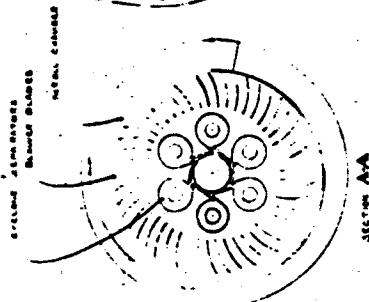
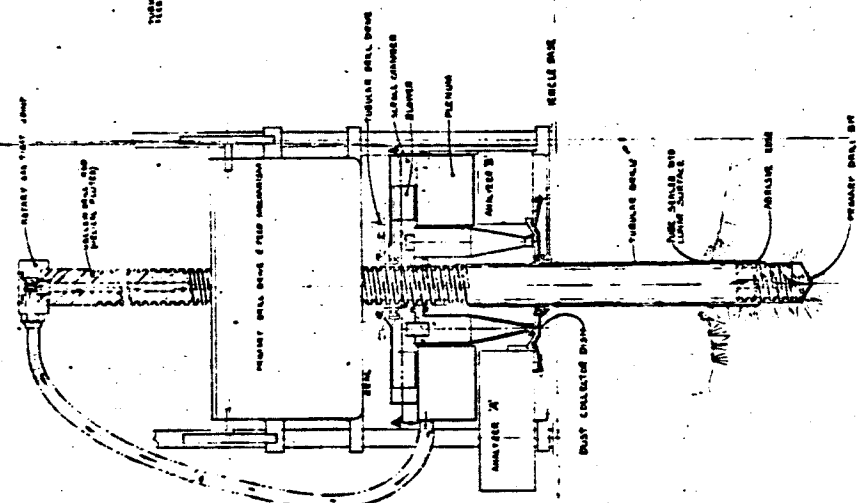
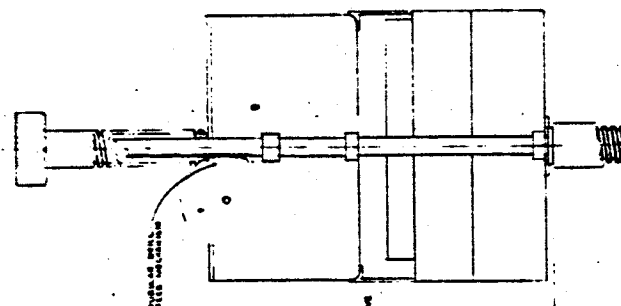
MATERIAL		ASSEMBLY No.	SYM.	DATE	REVISION	NAME
HEAT TREAT		UNIT WEIGHT	ARMOUR RESEARCH FOUNDATION OF ILLINOIS INSTITUTE OF TECHNOLOGY TECHNOLOGY CENTER CHICAGO 16, ILLINOIS			
			SCHEMATIC DIAGRAM- LUNAR DRILL FLUIDIZATION			
TOLERANCES UNLESS OTHERWISE SPECIFIED FRACTIONS $\pm \frac{1}{16}$ DECIMALS $\pm .005$ THDS CLASS 2 FIT ANGULAR $\pm 1^\circ$		500 ROUGH MACHINED 250 COARSE MACHINED 125 MEDIUM COARSE MACHINED 63 MEDIUM FINE MACHINED 32 FINE MACHINED 16 FINE GROUND 8 FINE LAPPED SCALE	DESIGNED	DRAWN	CHECKED	APPROVED
DO NOT SCALE — REPORT ERRORS BREAK ALL SHARP CORNERS CHISEL ALL TAPPED HOLES $\pm 45^\circ$ REMOVE BURRS			NAME	J.S.		
			DATE	10-10-60		
			RELEASED	PROJECT No.	DRAWING No.	
				K208		

A

ARMOUR RESEARCH FOUNDATION OF ILLINOIS INSTITUTE OF TECHNOLOGY



- 137 -



BALANCING VELOCITIES VS PARTICLE DIAMETER

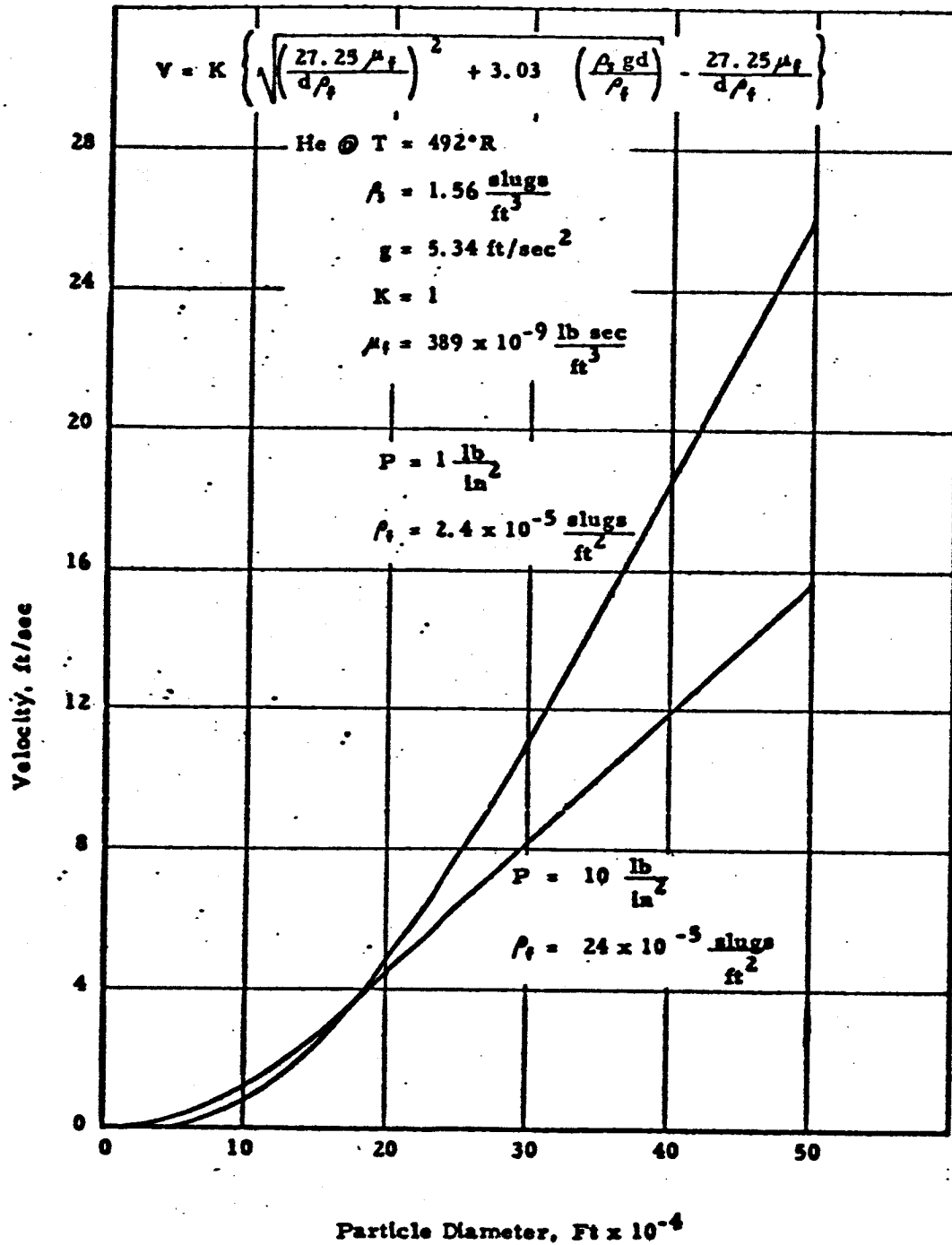


Fig. 54

Pressure drop calculations follows:

1. Pressure drop across the fluidized bed (Ref. 65):

$$p = \frac{v_f^2 \rho_{f1}}{2g} + \frac{Wv_s}{g} + \frac{2f \rho_{f1} v_f^2 L}{gD} \left(1 + \frac{f_s v_s W}{f v_f^2 \rho_{f1}} + \frac{WL}{v_s} \right) = 0.03 \frac{\text{lb}}{\text{in.}^2}$$

where:

v_f = superficial fluid velocity, 20 ft/sec

v_s = actual solid particle velocity, 10 ft/sec

ρ_{f1} = fluid lunar density, $1.28 \times 10^{-3} \text{ lb}_{\text{lunar}}/\text{ft}^3$

g = acceleration due to lunar gravity, 5.34 ft/sec^2

f = fluid friction factor, 0.1

f_s = particle-fluid friction factor, 0.1

W = solids mass velocity, $0.01 \text{ lb}_{\text{lunar}}/\text{sec-ft}^2$

L = fluidized bed height, 10 ft

D = effective pipe diameter, 0.062 ft.

2. Pressure drop across the cyclone:

$$\Delta p = \frac{1}{2} \left[\frac{\rho_{f1} v_t^2}{g n} \right] \left[\left[\frac{r_1}{r} \right]^{2n} - 1 \right] = 0.2 \frac{\text{lb}}{\text{in.}^2}$$

where:

v_t = tangential fluid velocity at r_1 , 100 ft/sec

r_1 = outer radius, $r_1 = 2r$

r = central core radius

n = a constant, 0.75.

3. Pressure drop across the hollow section of the drill (ref. 60):

$$\frac{fL}{D} = 16.1, \text{ corresponding to } \frac{P_2}{P_1} = .97$$

$$\Delta p = 0.3 \text{ lb/in.}^2$$

The compressor is required to make a small pressure drop only:

$$\Delta p_{\text{total}} \approx 0.03 + 0.2 + 0.3 = 0.5 \text{ lb/in.}^2$$

Pressure drop estimates indicate that power requirements for transportation of fluidized particles are low. In view of the results, weight and energy trade-offs were not studied.

Controlled leakage was considered, with orders of magnitude checked for the following model: Helium pressurized container, at $T = 492^\circ \text{R}$, 10-lb/in.^2 pressure and one opening, 1 mm in diameter. Critical flow equations used:

$$w_{\text{He}} = A \frac{P_o}{\sqrt{T_o}} \sqrt{\frac{k}{R} \left[\frac{2}{k+1} \right]^{\frac{k+1}{k-1}}} = 2 \times 10^{-5} \text{ lb}_{\text{earth}}/\text{sec},$$

where:

A = unsealed area, $8.75 \times 10^{-6} \text{ ft.}^2$

P_o = stagnation pressure, 10 lb/in.^2

T_o = 492°R

k = 1.67

R = gas constant, $386 \text{ ft-lb/lb-}^\circ \text{F}$

In 20 days, or 1,730,000 sec, leakage would amount to $36 \text{ lb}_{\text{earth}}$ of helium. Additional plots included for comparison and conversion of units are:

1. Hydrogen fluidization at $T = 492^\circ \text{R}$, Fig. 55
2. Hydrogen fluidization at $T = 150^\circ \text{R}$, Fig. 56
3. Feet vs microns - a conversion plot, Fig. 57

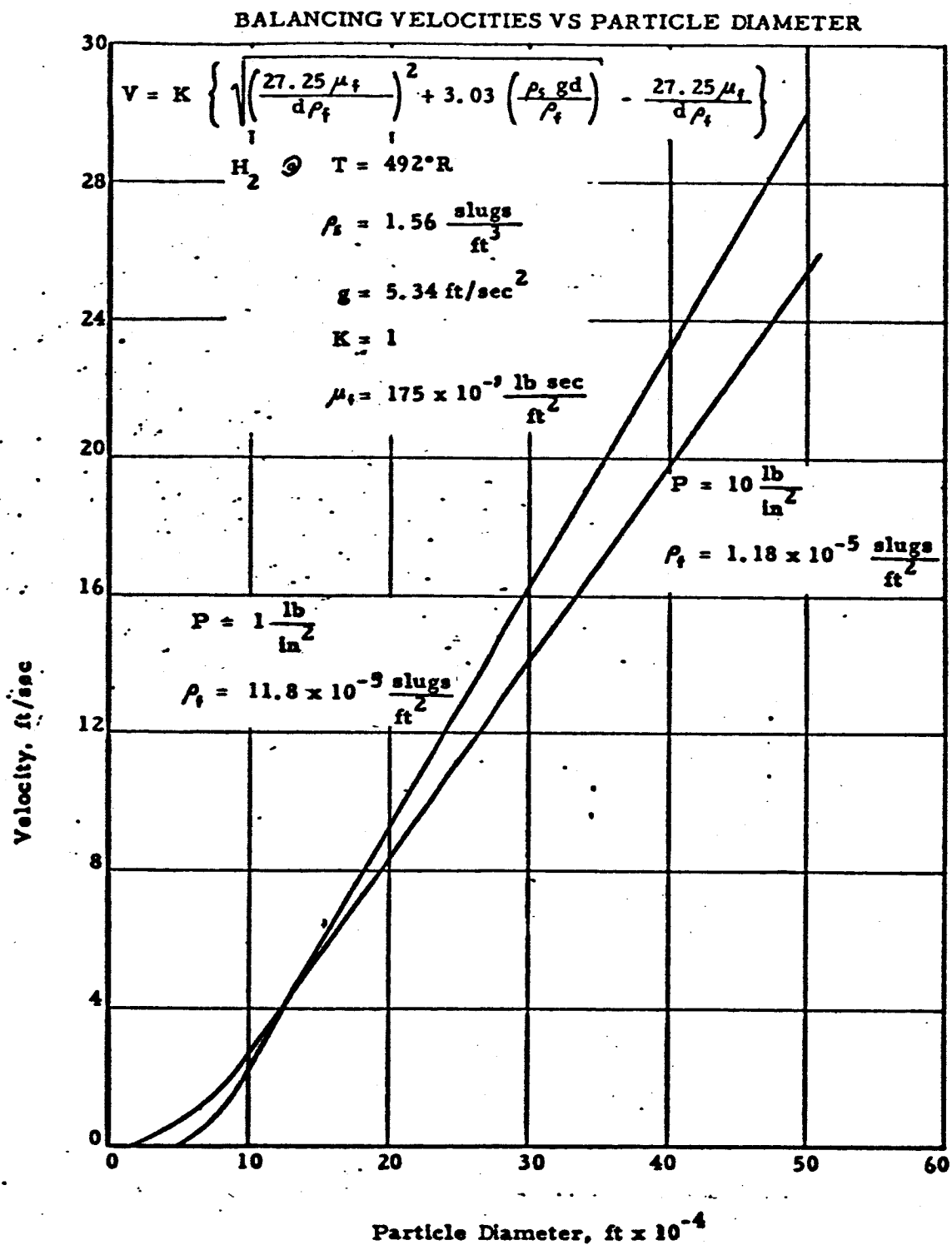


Fig. 55

BALANCING VELOCITIES VS PARTICLE DIAMETER

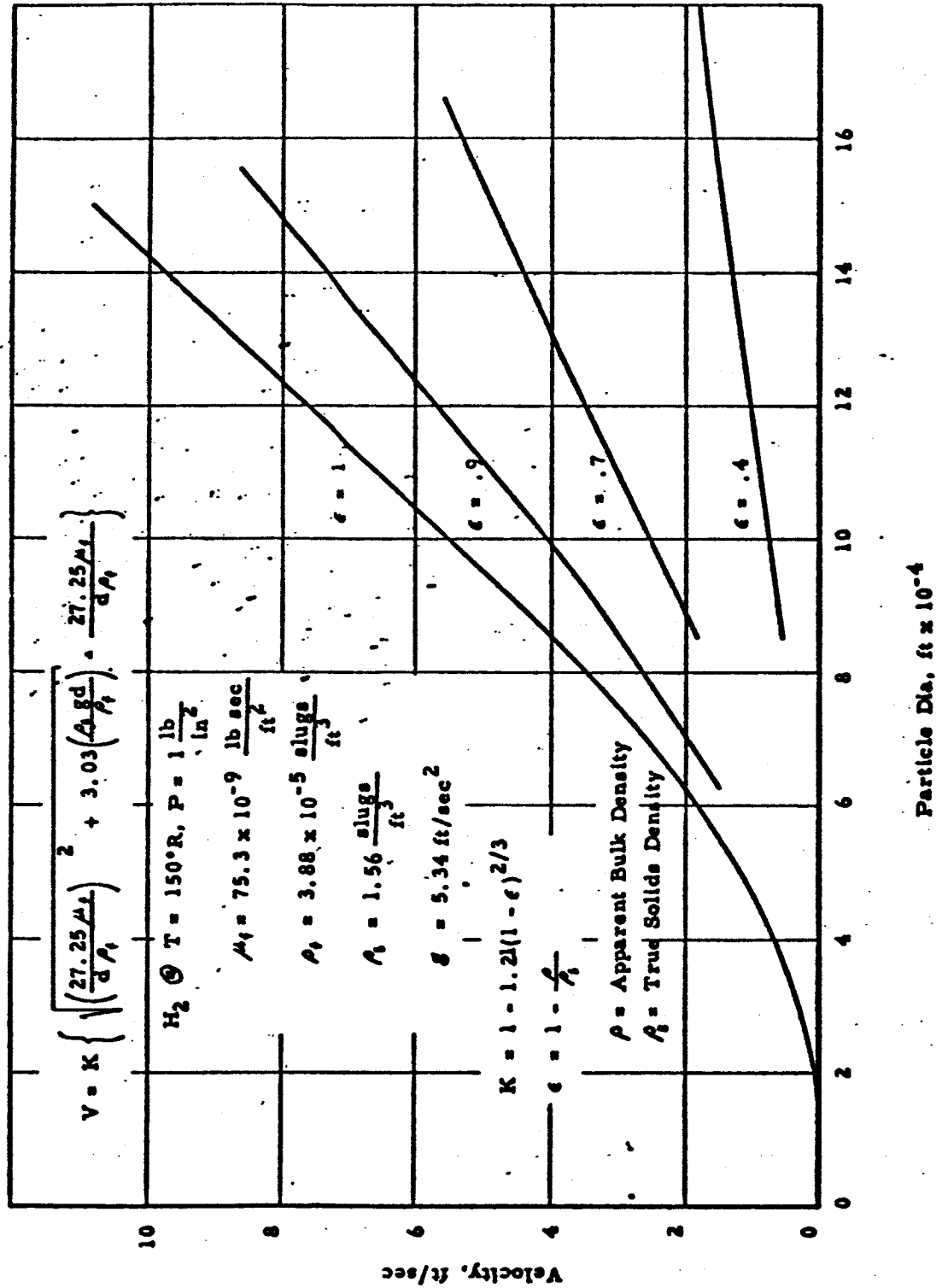


Fig. 56

FEET VS MICRONS
PLOT: 1 mc = 3.28×10^{-6} FT

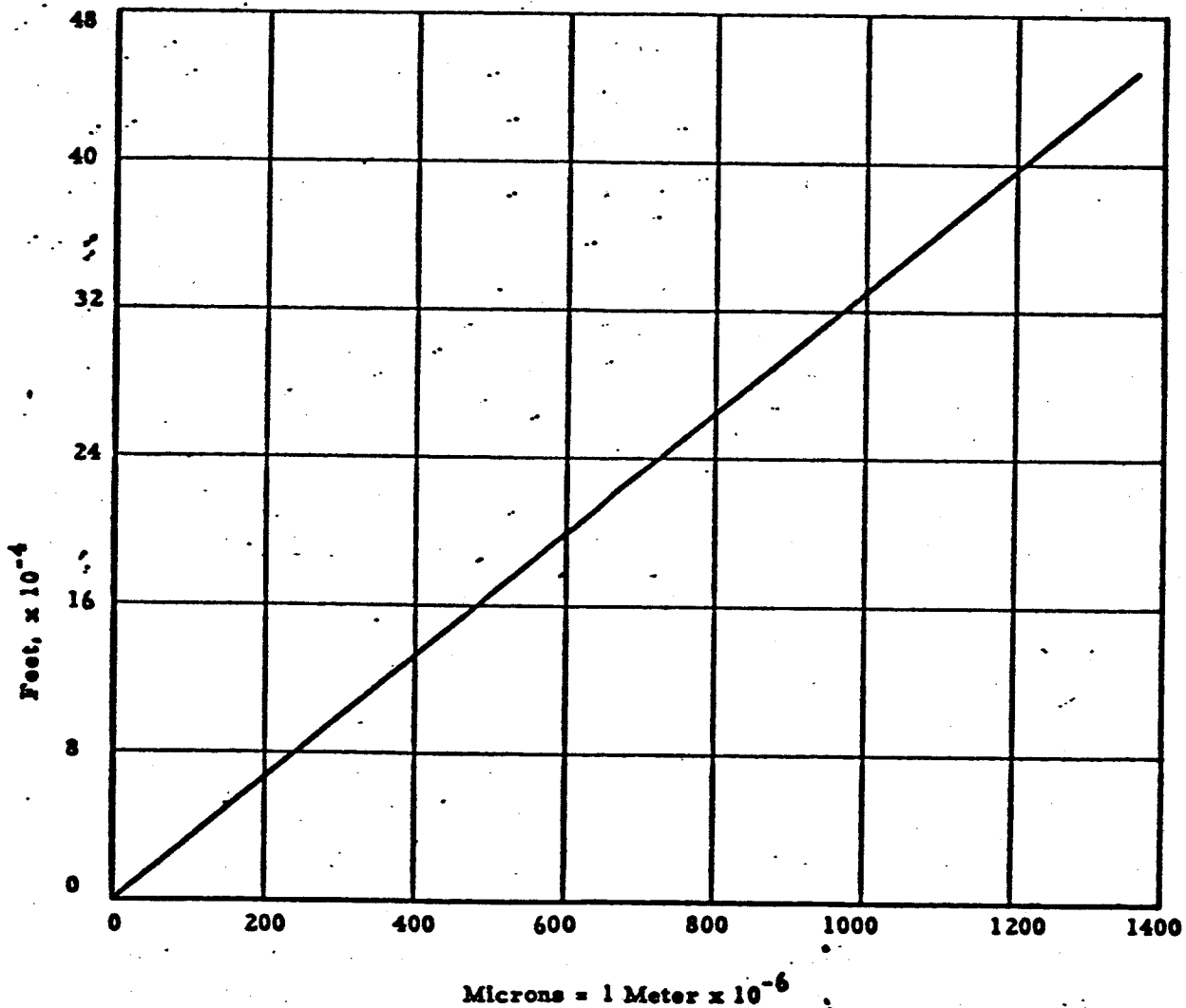


Fig. 57

4. Casing the Hole

In the event that the lunar surface is composed of a compacted or semi-compacted aggregate, dust, or other loose material, the danger of cave-in exists. A cave-in at the least would spoil the stratafication effect of the material being extracted and analyzed and at most would jam the drill and render it inoperative. The presence of a casing above the drill would prevent such mishaps.

The difficulties attendant to installing a single piece of tubing the full depth of the hole are obvious. Several lengths of tubing, to be fastened together as the hole depth progresses, present a number of problems in programming, assembling, etc. A simple system would add the casing continuously as the hole depth progresses. Such a system is presented in Fig. 58.

The casing consists of a tube, spirally formed of flat spring wire, with the wire edges formed into a channel and an interlocking ridge. The leading edge of the casing is a solid ring, pre-located in position to start the casing. The balance of the casing is stored in the cover adjacent to the axis of the hole. As the hole progresses, feed rollers rotate the stored casing. The motion separates the lead end of the stored section from the stored tube and feeds it through the guides into engagement with the vertical, or "in-the-hole," casement. Close guidance of the detached part of the casing assures proper rematch. Retraction of the casing from the hole requires only that the feed rolls be reversed.

In order to accommodate a casing as shown in Fig. 58 the drill bit must be able to be withdrawn for changing or chip removal; either the drill bit must be collapsible or the hole must be larger than the drill bit. Fig. 58 also depicts a means of enlarging the hole to accommodate a casing through which a solid drill bit can be withdrawn. The mechanism consists of a pair of reamer bits, which position themselves radially with respect to the mechanism center as a function of the direction of rotation of the system.

Specifically, the reamer bits, a, are T-shaped in cross section, and mate with and slide in slots, b, of matching cross section in the mechanism body, g. A single gear tooth, c, formed on the cutter, engages a matching

ARMOUR RESEARCH FOUNDATION OF ILLINOIS INSTITUTE OF TECHNOLOGY

Note: Drill Stem May Be Flange, Flange
 Reamer, Or Spinner, And Must
 Be 10% Or Reamer I.D.

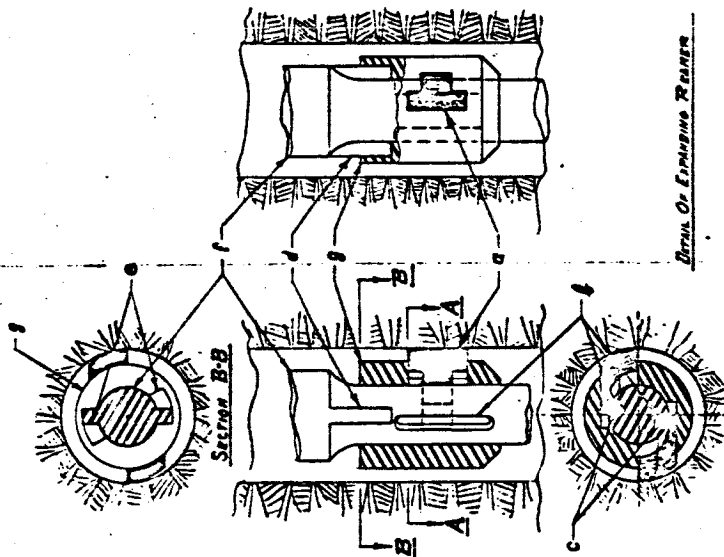
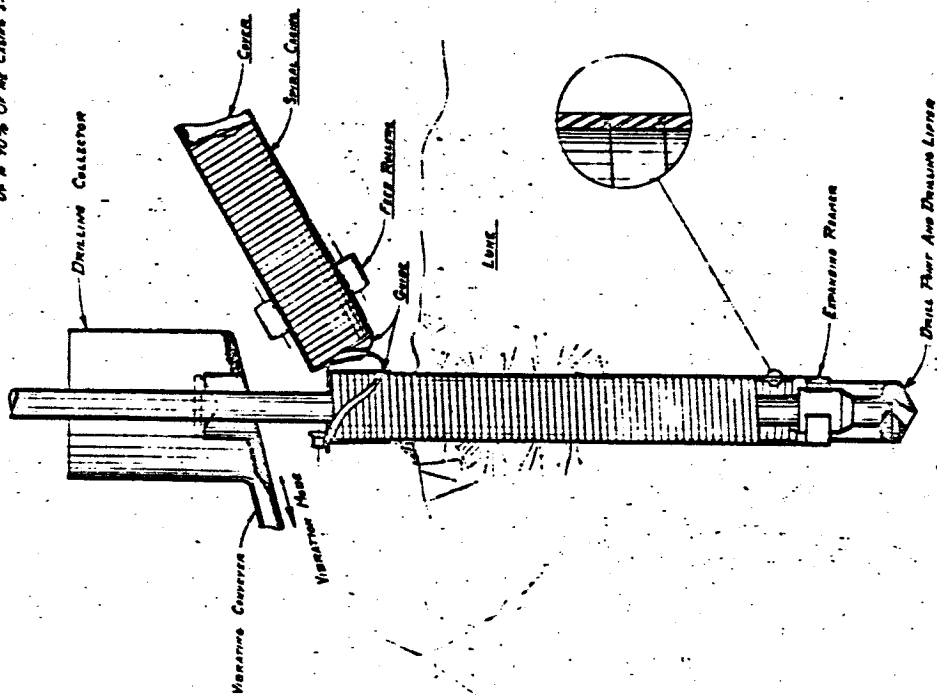


Fig. 58

- 145 -

REVISION	DATE	BY	REASON
1			ASSEMBLY PROVISION
2			REVISION
3			REVISION
4			REVISION
5			REVISION
6			REVISION
7			REVISION
8			REVISION
9			REVISION
10			REVISION
11			REVISION
12			REVISION
13			REVISION
14			REVISION
15			REVISION
16			REVISION
17			REVISION
18			REVISION
19			REVISION
20			REVISION
21			REVISION
22			REVISION
23			REVISION
24			REVISION
25			REVISION
26			REVISION
27			REVISION
28			REVISION
29			REVISION
30			REVISION
31			REVISION
32			REVISION
33			REVISION
34			REVISION
35			REVISION
36			REVISION
37			REVISION
38			REVISION
39			REVISION
40			REVISION
41			REVISION
42			REVISION
43			REVISION
44			REVISION
45			REVISION
46			REVISION
47			REVISION
48			REVISION
49			REVISION
50			REVISION
51			REVISION
52			REVISION
53			REVISION
54			REVISION
55			REVISION
56			REVISION
57			REVISION
58			REVISION
59			REVISION
60			REVISION
61			REVISION
62			REVISION
63			REVISION
64			REVISION
65			REVISION
66			REVISION
67			REVISION
68			REVISION
69			REVISION
70			REVISION
71			REVISION
72			REVISION
73			REVISION
74			REVISION
75			REVISION
76			REVISION
77			REVISION
78			REVISION
79			REVISION
80			REVISION
81			REVISION
82			REVISION
83			REVISION
84			REVISION
85			REVISION
86			REVISION
87			REVISION
88			REVISION
89			REVISION
90			REVISION
91			REVISION
92			REVISION
93			REVISION
94			REVISION
95			REVISION
96			REVISION
97			REVISION
98			REVISION
99			REVISION
100			REVISION

slot in the driving shaft. Thus, when the shaft, f, is rotating in the direction required for cutting, the reamer bits are held extended as shown in Fig. 58, and, when rotation is reversed, the reamer bits are retracted.

The reamer bits are actually driven by extensions of the shaft forming keys, d, on the driving shaft, which engages slots, e, in the reamer body. These slots are circumferentially sufficiently larger than the keys to allow enough relative radial motion between the shaft and the reamer body to extend and retract the bits.

5. Instrumentation (Rotary-Impact Drill)

Instrumentation of the drill system will be required to determine the hardness of the rock being drilled and to operate the drill. In addition a knowledge of operating conditions would be very useful, if not necessary, in a failure analysis.

The rate of drill penetration will give an indication of the hardness of the rock. ARF experiments with sandstone, Gabbro granite, and concrete confirmed that a relation existed between the characteristics of the material drilled and the rate of penetration in rotary-impact drilling. To obtain additional quantitative data, a series of experiments must be made with a wide variety of rock. It has been postulated that with some resilient types of rock or with a dull drill bit the rate of penetration alone would not be a reliable index of the rock hardness. Data supplied by an accelerometer located in the drill would provide additional data regarding rock characteristics.

Drill can be sensed by use of a spring-loaded rotary position transducer driven by a cable and drum linkage. If a multi-turn potentiometer is used, the linear travel of five feet can be converted directly into rotation without a gear reduction. If, because of environment considerations, the potentiometer-type sensor is undesirable, a single-turn rotary differential transformer with an appropriate gear reducer can be used. Since drill travel velocity will be low, this type of sensing device provides a compact and rugged instrument with adequate speed of response.

The determinations of rock hardness by sensing the axial acceleration of the drill shank can be accomplished by use of a seismically mounted sensor sensitive to the axial acceleration. A two-section pickup coil (magnetically shielded from the motor inference) is seismically attached to the drive housing. The drill shank is magnetized so as to induce voltages in the coil when relative axial displacements occur between the drill shank and coil. The two sections of the coil are so connected so as to add the induced voltages. The device may be described as a velocity-sensitive sensor. In order to obtain an acceleration signal, the output must be differentiated with respect to time. This can be done in a simple passive network, since static response is not necessary. Some d-c voltages and voltages of the shaft rotational frequency will be generated because of errors of symmetry and concentricity of the coil with respect to the shaft. Because shaft speeds are low (500 rpm), these frequencies can be electrically filtered since the impact accelerations contain relatively high-frequency components.

An open loop or command system of drill control will require knowledge of the penetration, the drill speed, and the power consumption. In an automatic system, this information would be desirable for use in any failure analysis. Power, speed, and any other operating conditions could be monitored by off-the-shelf-type equipment.

The complete instrumentation package chosen must be compatible with the data channel space available. In general, neither continuous nor simultaneous monitoring of this instrumentation is necessary.

6. Dynamic Environment

The problem of dynamic environment as applied to the lunar drill package may be considered in two parts. The first part constitutes rocket vehicle transportation and lunar landing environment: here the drill need only be structurally sound to survive the trip. The second part constitutes actual drilling operation and the resulting environment as imposed on the lunar vehicle.

Design for transportation environment would follow well established methods. The natural frequencies of the drill and the mounting structure must be such that the drill unit has a higher natural frequency than that of the primary spacecraft structure to eliminate the possibility of the drill acting as an efficient dynamic absorber for the primary structure. Special attention should be given to all long and slender structures, actuating and locking mechanisms.

Drilling operations produce vibrations which might excite lunar operational structures such as the solar panels or antennas. The strength of the source, the forcing frequency, the transmissibility of the intermediate structures must be considered. The drill unit itself must have the capacity to operate in its own environment.

Forcing frequencies would probably fall in the low range of the spectrum e. g., Skil Model 736 however produces 2200 blows per min., which is equivalent to 37 cps. The long rotating unbalanced shanks will be rotating at less than 1000 rpm (16.7 cps). Dynamic absorbers will probably be required though the in hole drill configuration will produce some damping effects.

7. Friction and Lubrication

The coefficient of friction between two metal surfaces is higher in a vacuum than at normal atmospheric pressure for both metallic and nonmetallic materials. The magnitude of this increase depends largely on the condition of the surface and on the amount of outgassing that has occurred. This increase is believed caused by the removal of surface films which allow the materials to weld at the points of contact. Successive welds and shears then gouge the surface, greatly increasing the resistance to motion.

Experiments described in ref. 66 and 68 record values of the coefficient of friction between metal surfaces generally between four and six although the value in air was less than one. In the experiments, thoroughly cleaned samples were outgassed at 600°C for 1 to 2 hr in a vacuum chamber. The samples were cooled in the chamber, and the experiments were conducted at a pressure of about 10^{-6} mm Hg. Other studies were conducted on the

vacuum coefficient of friction using merely degreased metal samples with no outgassing, ref. 67. These surfaces exposed to an immediate vacuum showed only an average of a 50% increase in the coefficient of friction over that recorded at atmospheric pressure.

During flight and the time spent on the lunar surface, the drill may be exposed to pressures of 10^{-12} to 10^{-14} mm Hg at temperatures up to 260°F.

Bearing surfaces heated by friction during operation can reach temperatures in excess of 260°F. The outgassing rate varies directly as the change in pressure and as an exponential function of the temperature, and varies inversely as the square root of the time. The total outgassing of the drill components can be calculated, however there is insufficient data available to permit correlation of the total outgassing of the material with the increase in the coefficient of friction.

In addition, the experimental data available were largely obtained at vacuums down to only about 10^{-6} mm Hg. At a residual pressures of 10^{-6} , a completely contaminated surface absorbs a monomolecular layer of gas in about 1.6 sec. Therefore, some surface films were present in all these experiments. Not until experiments can be made at pressures below 10^{-9} mm Hg will the surfaces stay clean for hours instead of for seconds or minutes. Until this data are available no accurate estimate can be made of the coefficient of friction between surfaces in the lunar atmosphere.

Very little data are available on the coefficient of friction in a vacuum between non-metallic materials. Studies reported in ref. 67 indicate a definite increase in the coefficient of friction between Kel-F blocks, but no noticeable increase between often-impregnated fiberglass. Reference 73 indicates that Teflon works well in vacuum seals around rotating shafts. However, some preliminary studies indicate that the low coefficient of friction of Teflon results from surface film. Therefore, at pressures below 10^{-6} mm Hg after exposure to 260°F temperatures, Teflon may lose its surface film and exhibit a high coefficient of friction.

The available experimental data indicate that for operation of bearings on the moon either lubrication must be provided or a semi-closed system must be used. Lubrication may be accomplished by using low vapor pressure greases or solid lubricants. Both will evaporate after a period of time. Although the grease will evaporate more rapidly, it can be self-replenishing. Solid lubricants are plated on the metal surfaces and therefore are not self-replenishing. The most common of the solid lubricants are molybdenum disulfide and tungsten disulfide. These have performed satisfactorily in some applications down to 10^{-6} mm Hg, ref. 74, 75. Proprietary studies, ref. 78, claim another type of dry lubricant to be greatly superior to molybdenum disulfide at pressures of 10^{-6} to 10^{-8} mm Hg.

A closed system will operate all bearings under pressure to avoid the loss of surface films. Since such a system could not be hermetically sealed on a lunar drill, a pressurizing supply would have to be used.

The best lubrication system based on present knowledge appears to be the use of solid lubricants in a system pressurized to about 10^{-6} mm of Hg. The leakage over such a small differential pressure would be low and could be made up either with subliming solids or a compressed-gas supply. Bearing surfaces in a lunar drill device should be lubricated and pressurized to 10^{-6} mm of Hg wherever possible. Lightly loaded guide bearings can probably be used with solid lubrication, but without pressurization.

8. Evaporation of Materials

The lunar vacuum environment will increase the rate of evaporation of materials and of surface coatings on the materials. The loss of material will change the clearances of bearings and seals, dissipate protective coatings, and eventually could effect structural integrity. In addition, since the evaporation rate depends upon the temperature, material evaporated from a hot area may condense on a cooler one. This could be particularly troublesome if metal vapors were to condense in electronic components.

Most structural metals will evaporate at very low rates and are suitable for even long-term exposure to the lunar environment, ref. 79. However, zinc, cadmium, and pure magnesium have fairly high evaporation rates and should be avoided, although in general magnesium alloys can be used.

ARMOUR RESEARCH FOUNDATION OF ILLINOIS INSTITUTE OF TECHNOLOGY

Estimates on the weight loss of metals can be made using the Langmun equations (ref. 70) and vapor pressure curves for the elements. This equation is

$$p = 17.14G (T/M)^{1/2},$$

where

- p = vapor pressure in mm Hg at T °K
- G = rate of evaporation in $\text{gm/cm}^2\text{-sec}$
- T = temperature, °K
- M = gram molecular weight.

This equation was developed from the kinetic theory of gases in order to calculate the vapor pressure of metals based on experimental data on the evaporation rate of metals at elevated temperature in a vacuum. Vapor pressure curves plotted from this equation, ref. 76 , can be used to determine the weight loss of metals under exposure to a particular temperature vacuum environment.

Organic materials will generally be more severely affected by the lunar environment, particularly the vacuum combined with high temperature. The effects may include evaporation of the material itself or mechanical degradation due to the evaporation of volatile components of the material. The percent of weight losses of some organic materials after 24-hr exposure at 300° F. at 3 to 4×10^{-5} mm Hg are shown below (ref. 71):

<u>Material</u>	<u>Weight Loss, %</u>
Kel-F	1.6 - 2.2
Phonotec	4.6 - 6.2
Polyvinyl Butral	9.1 - 41.7
Silicone Alkyd	14.2 - 36.0
Acrylic	19.1 - 43.0
Neoprene	26.4
Nitro Cellulose	47.6 - 86.2

The wide variation of the experimental results indicates the need for additional experimental work and caution in the use of these materials.

Work discussed in ref. 69 indicates that Teflon will lose less than 10% of its weight per year at temperatures as high as 700°F and vacuums of 1×10^{-6} mm Hg.

On the basis of available data both Teflon and Kel-F appear satisfactory for use in the lunar environment. For short-term exposure, some of the other materials could be used as protective coatings where some evaporation could be tolerated.

9. Fatigue Life

The fatigue life of metals in a vacuum may be considerably greater than the fatigue life in a normal atmosphere. Data from references showed that the fatigue life of 316 stainless steel was greater in a vacuum than in air by factors of 25 to 77. The increase for nickel was 9, and, for aluminum and copper, ranged from 2 to 40. A possible explanation of this phenomena are discussed in the above references, but no explanation is completely confirmed by experimental data. It is suggested, in ref. 72, that there may also be temperature-stress combinations at which the fatigue life is lower in a vacuum than in air.

The increase in fatigue life under vacuum environment is indefinite and cannot be used in a lunar drill design until more experimental data are available. Engineering materials that already have a high endurance limit may not show any improvement in a vacuum life. The stress-operating temperature condition of lunar drill components may also be such that they have a lower fatigue life in a vacuum. Therefore, in any drill design, components subject to fluctuating stresses must be experimentally tested to determine their fatigue life under the environment in which they will be expected to operate.

10. Motor Operation

The operation of direct-current electric motors in a low-pressure environment is impaired because an adequate lubricating film does not form on the commutator and the brushes tend to powder and wear away very rapidly. Alternating-current induction motors are available which will function in an atmosphere of 10^{-14} mm Hg without any pressurization of the motor case (except that required for satisfactory bearing operation). The overall system weight of a d-c electric motor driven unit will be considerable less than an a-c motor system. In this application, the primary energy source will be d-c current from either batteries or solar cells. Therefore, an a-c motor will necessitate the use of d-c to a-c inverter. Presently available aircraft-type 400-cycle 31 v with a 550-w output weigh about 27 lb and are about 45% efficient. This would add to the system not only the 27-lb weight for the inverter, but also weight for additional batteries or solar cells because of the low efficiency of the inverter. For example, if 1000 w-hr were required at the drill motor, a total of 2225 w-hr would have to be supplied to the inverter; this would require 22.5 lb of additional batteries (based on 50 w-hr/lb). this added weight of 49.5 lb makes an a-c motor drive impractical unless an inverter is necessary in the spacecraft for other purposes. Even then, the low efficiency alone will cause considerable weight penalty. The weight that could be saved when using an a-c motor on the motor pressurization system and on the weight of the motor itself is quite low compared to the added inverter and battery weight.

A d-c motor can be operated in a vacuum by pressurizing the motor case. High altitude brushes are available that will permit operation at pressure altitude of over 150,000 ft. Satisfactory brush wear and low bearing friction can be obtained by pressurizing the motor case to this altitude, which corresponds to about 3 psf.

An additional problem of operating an electric motor in a vacuum is the same as in operating a motor in a high-temperature environment: Under very low atmospheric pressures, the heat developed within the motor must be dissipated almost entirely by radiation. Therefore, the operating temperature of the motor must be considerably above the ambient. The temperatures the insulation system can withstand will limit the rating of the motor. In addition, the increased resistance of conductor materials at the higher temperatures results in a decrease in motor efficiency, hence more heat must be dissipated for a given work output. The effects of using silver as a conductor for this application should be investigated.

Another important factor is the degradation of magnetic characteristics at high motor temperatures. Magnetic materials having high Curie temperatures are required because such materials generally retain a reasonable part of their room-temperature magnetic properties at the elevated temperatures. Silicon steels used in development work on 500°C components have been found to be adequate.

High-temperature bearings and lubricants are available for use in electric motors. Gaseous and solid lubricants can be used to provide satisfactory low-friction and high-temperature operation.

If continuous motor operation is necessary, a cooling system must be incorporated to remove heat. However, this would add additional weight and complexity and is unnecessary when the motor can be operated intermittently.

11. Pressurization

From the standpoint of measurements and sampling of the lunar atmosphere, it is desirable that gas not leak from the drill assembly. However, from a practical viewpoint this is probably impossible. Outgassing and evaporation of the materials will, in themselves, yield a slight contamination. Any drilling system for minimum weight and reliability must be pressurized in some areas for motor operation and to insure acceptable bearing friction. These parts cannot be hermetically sealed and must employ dynamic seals.

A no-contamination system could be built at a great increase in weight and decrease in reliability. An example of such a system would be a hermetically sealed d-c. to a-c inverter supplying current to operate an electromagnetic hammer. Rotation and feed would be provided by an a-c induction motor. The inverter (or a vibratory power supply) would add substantial weight. A more important consideration is the doubtful behavior of bearings, even with solid lubricants, at pressures of 10^{-14} mm Hg.

The most reliable approach consists of pressurizing the interior of the various components sufficiently to insure reliable operation. Leakage can be minimized by careful seal design and the use of multiple seals.

The effect of the contamination can be reduced by either of two methods. The first is to use a gas with a mean-square molecular velocity that is close to the escape velocity on the moon of 2.4 km/sec. Such a gas will quickly dissipate from the moon. Either hydrogen or helium, with mean-square molecular velocities at 100°C of 2.15 km/sec and 1.53 km/sec respectively, would be suitable. A second solution is to use a gas such as one of the freons that would immediately be recognized as a contaminate in an analysis of the lunar atmosphere.

The second method has several advantages over the first. The heavier would be easier to seal. Also, some of the freons, such as CF_2Br_2 or CF_3Br , perform satisfactorily as lubricants at temperatures as high as 1200°F. These gases would serve as pressurizing mediums and as lubricants permitting high-temperature operation of the components.

Bearing and rotary seals will be a source of gas leakage from any pressurized components. Since these components may be pressurized to less than 3 psf and possibly as low as 1×10^{-6} mm Hg, the normal dynamic seal leakage equations cannot be used. Therefore, the following equation was derived, which can be applied to the flow of gas through a narrow annulus:

$$Q = \frac{\pi g}{8 \mu} (a^2 - b^2) \frac{dp}{dL} \left[a^2 + b^2 - \frac{(a^2 - b^2)}{\ln a/b} + \frac{4 \mu (a - b)}{\rho m} \right]$$

$$\left(\frac{2}{f} - 1 \right) \left(\frac{\pi}{2 \rho_0 g} \right)^{1/2}$$

where:

Q is the volume flow, ft^3/sec

q is $32.2 \text{ ft}/\text{sec}^2$

a is the outer radius of the annulus

b is the inner radius of the annulus

ρ is the gas viscosity in $\text{lb}/\text{ft}-\text{sec}$

p is the pressure in psf

p_m is the mean pressure

ρ is the gas density at unit pressure,

$\frac{dp}{dz}$ is the differential pressure drop over a length, dz

The derivation and solution procedure for this equation is described in Appendix E.

With the equation, the leakage through an annulus 1-in. -long and 1.000-in. inner diameter and 1.010-in. -outer diameter was calculated for H_2 and CF_3Br at an initial pressure of 0.1 mm Hg and a temperature of 460°R . If entrance losses are neglected, the leakage rate for H_2 is $6.8 \times 10^{-5} \text{ lb/hr}$ and for He is $3.2 \times 10^{-3} \text{ lb/hr}$. An annulus of such dimensions is a very poor seal, and considerable improvement could be made by using lower clearance or labyrinth seals.

12. Day Versus Night Drilling

The advantages of day drilling versus night drilling need only be considered when sufficient energy is available to complete the drilling operation without depending on energy from solar cells. If solar cells are necessary to operate the drill or to recharge batteries that operate the drill, only the lunar day can be considered as a suitable operating period. The main advantage of drilling during the lunar night is that thermal energy produced during drilling is more readily dissipated because of the sub-zero ambient temperature environment. A continuous drilling operation could be possible during the lunar night, while intermittent drilling, with pauses to cool the equipment, would be necessary during the lunar day, if supplementary cooling were not employed. If, for sampling or analysis of materials, intermittent drilling may be desired, the continuous capability of night operation would be of no advantage.

A more efficient system can be designed if the operating temperature range is fairly narrow than if the drill must operate over the entire range of -244 to $+260^{\circ}\text{F}$. For operation at the lower temperatures, it will probably be necessary to use heated bearings at the start of the drilling operation. If the pressurizing gas boiling point above -244°F , it will also have to be heated initially. Once the drill is operating, it should generate sufficient thermal energy to keep the bearings and pressurizing gas warm.

The entire day-versus-night drilling concept must be evaluated in terms of the demands imposed by the entire lunar mission. Interference with other measurements or operations may, in itself, dictate the time when drilling is carried out.

13. Heat Dissipation

The dissipation of heat produced by the operation of electrical equipment, friction, or other work, will be almost entirely by radiation. Therefore, all components which produce heat must operate at a temperature well above that of the surface to which they are radiating heat. During the lunar night heat can be dissipated by radiation relatively easily. It may even be desirable to minimize the radiative heat transfer to permit the components to operate at an efficient temperature level.

During the lunar day radiation from the moon's surface is a more serious problem than radiation directly from the sun, ref. 63. Therefore, the surface from which heat is to be rejected should be oriented parallel to the lunar surface and insulated from this surface.

IV. PRIME MOVER CLASSIFICATION STUDY

A. Survey

The objective of this study was a survey of the prime mover field and the determination of energy-power-weight relations that would find application in the lunar drill unit development.

A number of restrictive conditions were formulated, all in accordance with the lunar drill philosophy:

- a. Relatively low power converters were considered, most of them in the 1/2- to 2-hp range.
- b. Airborne machines specially designed for aircraft and missile application were examined.
- c. Only the maximum values operating efficiency were considered.
- d. Only equipment designed for continuous operation was studied, thus eliminating, a great number of high-performance, intermittent-duty-cycle (15 sec-on, 5 min-off, for instance) electric motors. Lunar drill systems considerations indicate that frequent duty cycling is undesirable. Reliability, sampling techniques, variation in drill speed during starting and stopping, and temperature control all argue against a prime-mover-dictated, short-time-interval operational cycle. Therefore, a continuous operation is arbitrarily defined as one which allows at least 5 min of component operating time.

Literature search and data requests sent out to 120 electric, pneumatic, hydraulic, auxiliary power gas generator unit manufacturers, formed the basis for this study. Tabulated data appears in Appendix C of this report.

1. Electric Motors

Nineteen a-c and d-c motors, manufactured by five companies (Eemco, Western Gear, AiResearch, Dalmotor, Hydro-Drive) were studied. The results are summarized in the weight-vs-output-power plot, Fig. 59. Two dominant parameters are speed and voltage. An increase in either or both tends to give lower specific weight (weight per horsepower) values. Generally, a-c motors feature lower specific weight than comparable d-c units. Both a-c and d-c motors operate on an average 72% efficiency value.

ELECTRIC MOTORS: WEIGHT VS. POWER

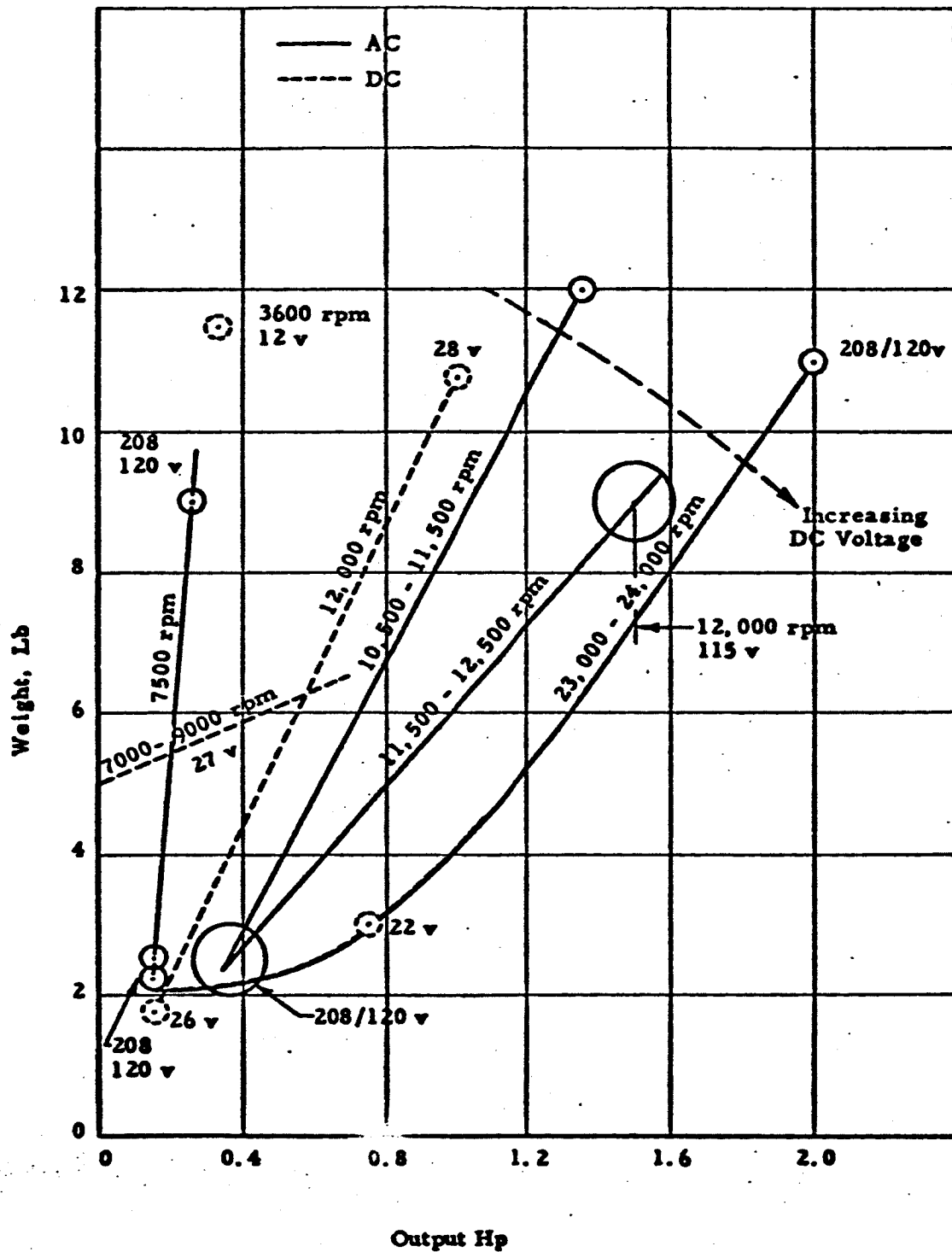


Fig. 59

ARMOUR RESEARCH FOUNDATION OF ILLINOIS INSTITUTE OF TECHNOLOGY

2. Pneumatic Motors

All pneumatic motors featured output shaft reduction gearing. The weight-horsepower analysis pertains to the testing state of the unit. Thirteen machines from Gardner-Denver, Bendix and AiResearch were analyzed (Fig. 60). Three motor types were considered: axial piston motor, which can be stalled without any subsequent damage; vane motor; nutating disc motor which is a recent development, especially aimed at higher power levels. Generally, at a constant speed air consumption increases with output horsepower. The limiting low weight-horsepower combination studied was, the 1-lb at 0.123-hp. A pneumatic motor application would involve frequent cycling requirements, the limiting factor being the capacity of compressed and recycled gas.

3. Hydraulic Motors

Hydraulic motors and pumps were assumed to be interchangeable. This is generally the case although minor modifications maybe required. Nine units manufactured by Vickers and Cornelius were included in the study. (Fig. 61).

An increase in operating pressure results in appreciable specific weight savings, while an increase in fluid flow rate tends to increase power output. Hydraulic units are applicable to relatively high power levels, (the industry does not feature anything below 1 hp). The units are efficient (average efficiencies: 90%). The lunar drill application will require short-time cycling operation.

4. Gas Generators

Little data was obtained on this topic. Data was received from Vickers, Olin Mathieson, and Walter Kidde. A literature search, conducted in periodicals and the ASTIA Library provided a knowledge of the state of the art.

PNEUMATIC MOTORS WEIGHT VS. POWER

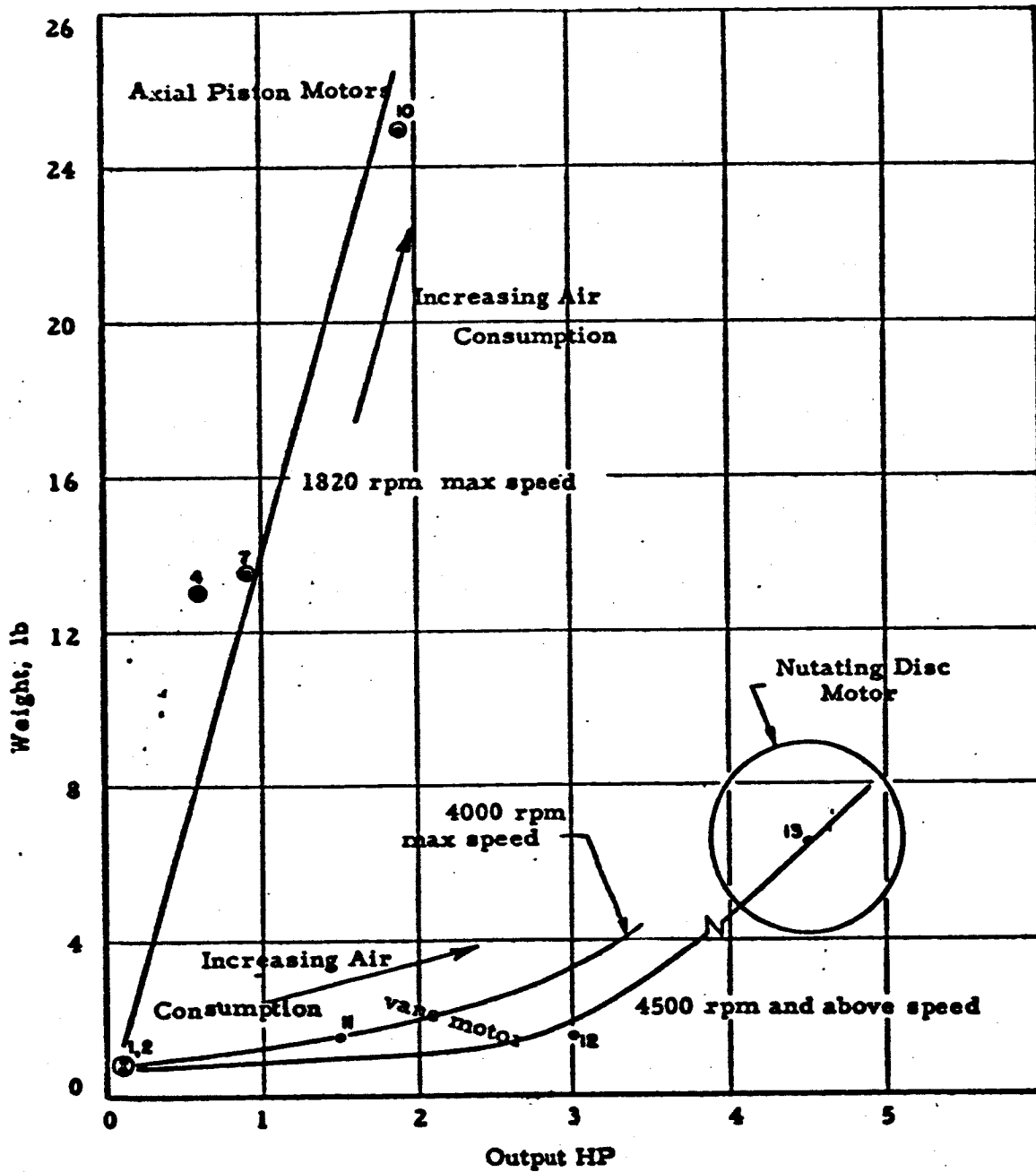


Fig. 60

HYDRAULIC MOTORS AND PUMPS

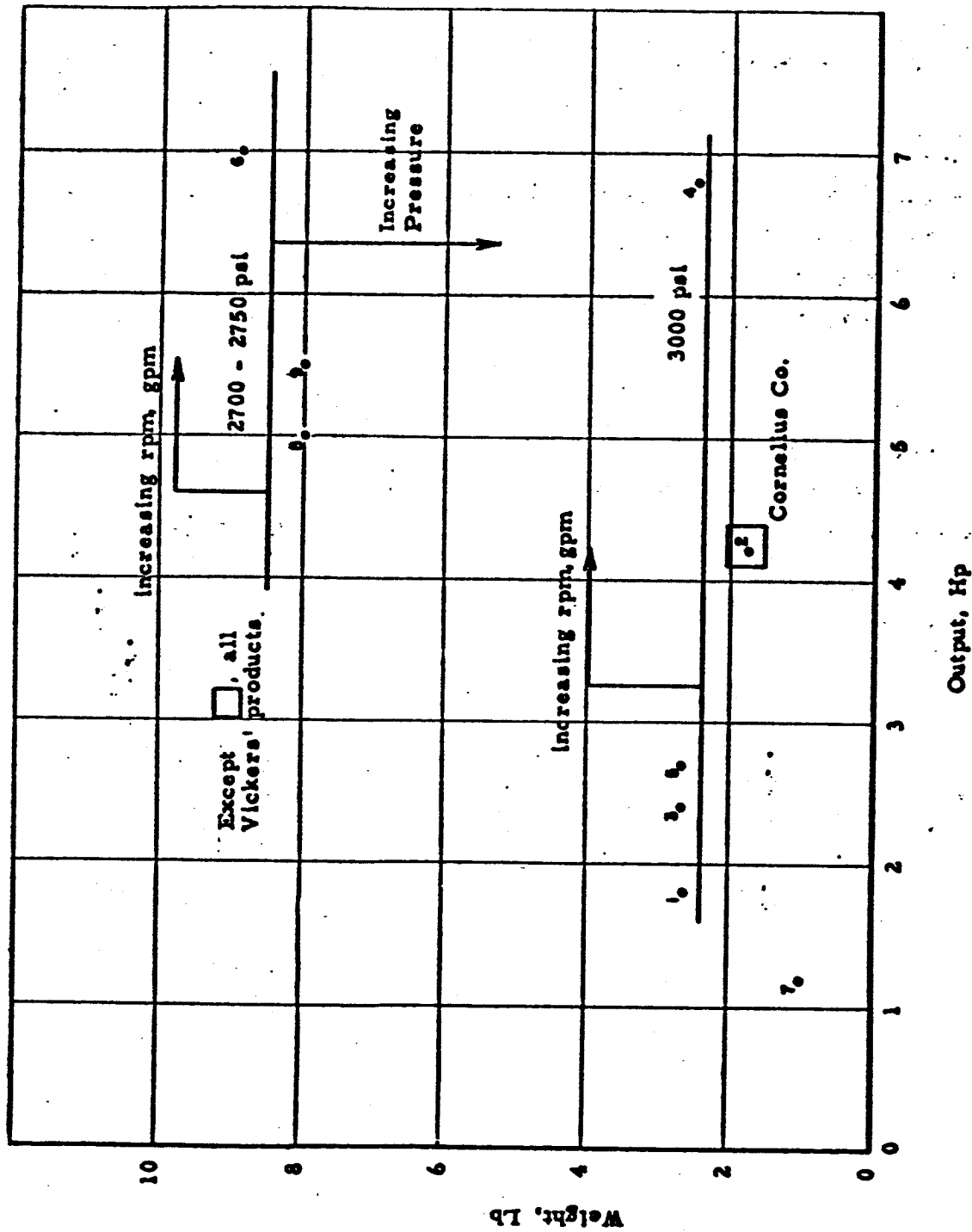


Fig. 61

Many existing solid propellant or hydrogen-oxygen systems are of very limited power and duration or remain in the early development phases. Some gas generators could be used to pressurize expended pneumatic or hydraulic systems tanks at a prohibitive weight penalty.

It may be generalized that the weight of the hardware is significant for very short operating time intervals only. With longer operating times, propellant weight is of dominant importance. Hardware weights are not yet available for system weight calculations. Several systems weights vs. duration presented below for 1 and 3 hp units consider only propellant weights.

At the 1-hp range which is of most interest to the present task Fig. 63 indicates that a hydrazine motor would deliver 1 hp-hr of energy at approximately a 15- to 25-lb weight level. At higher power levels (3 hp, Fig. 64), a minimum weight of 30 lb can be attained with a hydrogen-oxygen motor.

A positive displacement hydrogen-oxygen engine is being developed by Vickers, Inc. Preliminary weight data for a complete system (including engine, fuel, tankage, electric generator, and controls) are given in Fig. 62.

In view of the information studied, it may be concluded that as of now no economical, hot gas power system exists that is suitable for immediate lunar drill application. However, excellent possibilities are in view for future applications.

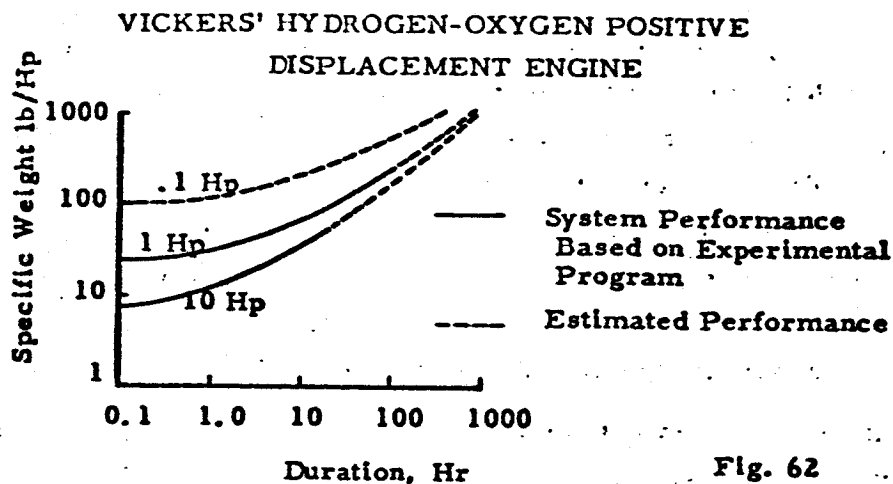


Fig. 62

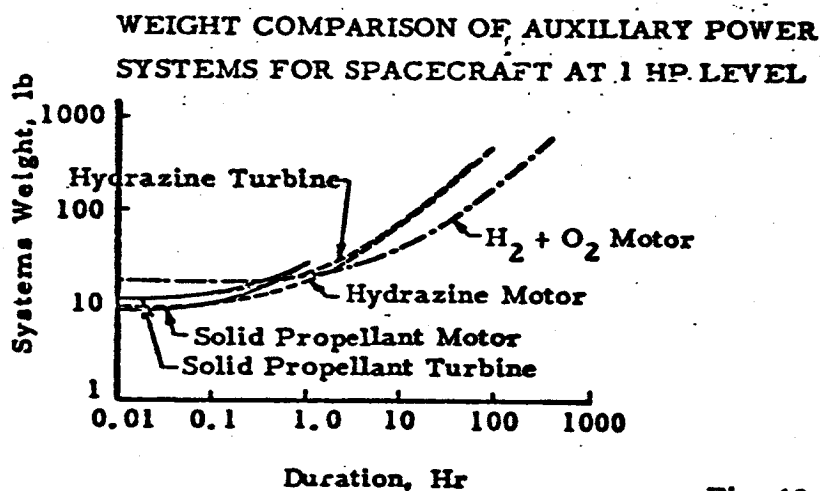


Fig. 63

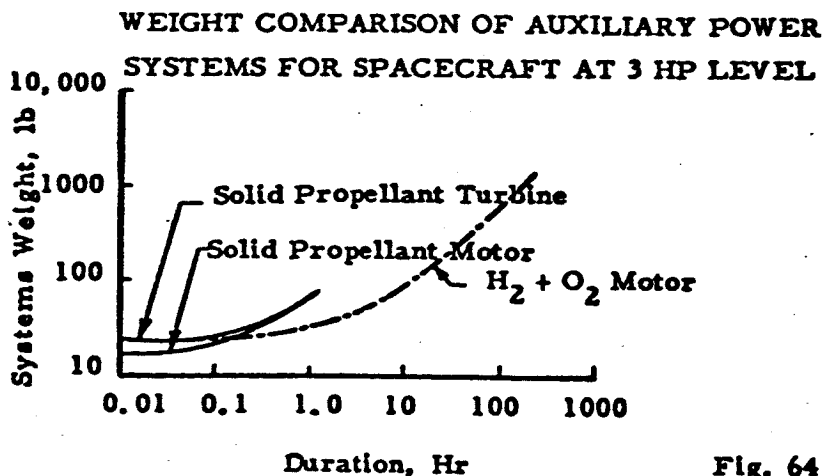


Fig. 64

B. Comparisons of Systems

A prime mover comparison chart is presented in Fig. 65. The data indicate that pneumatic axial piston type motors are comparable to electric motors, and pneumatic vane type to hydraulic motors, respectively. Data for this plot was taken directly from the individual classification plots. The results are in quantitative agreement with the summary gathered by C. K. Trotman (Ref. 45), Fig. 66, for higher power levels. Three other plots (Fig. 67, 68, 69) are included from the same article, with the hope that they may help to map out the field outside the immediate interest range..

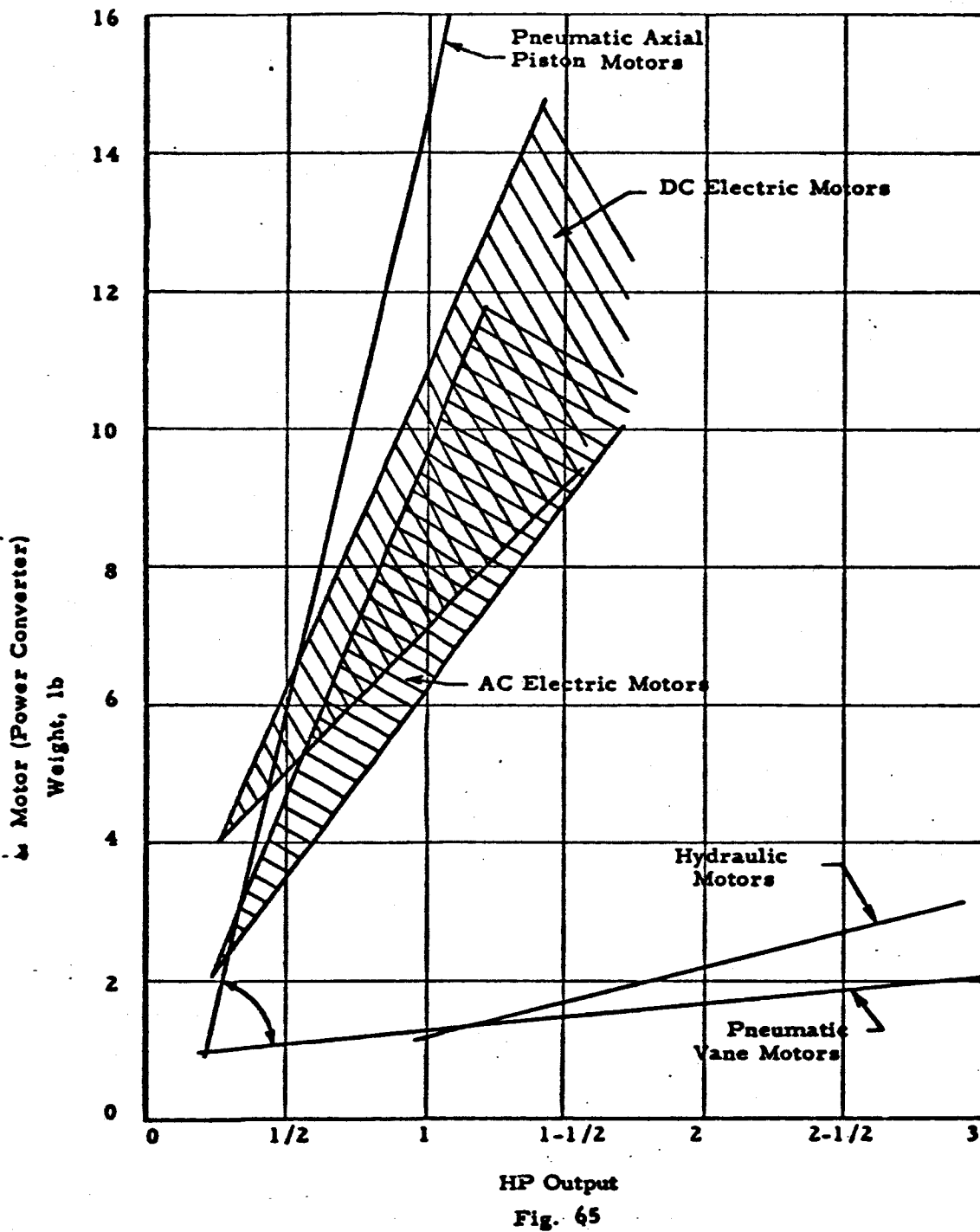
A complete picture cannot be presented, however by comparing only the motor units. Hydraulic, pneumatic power systems require motors, pumps, compressors, storage vessels - just to name a few other components. In view of the above considerations, Fig. 70 was prepared, presenting several power level weights for each type of system.

1. Electric Motor

A constant 3-lb reduction gearing weight correction was introduced in the high-speed electric motor data, and a weight penalty for the electric power source was not included. The weight requirements for a number of complete electrical systems are shown below.

1

PRIME MOVER COMPARISON: WEIGHT VS. POWER



ARMOUR RESEARCH FOUNDATION OF ILLINOIS INSTITUTE OF TECHNOLOGY

WEIGHT OF POWER CONVERTERS (MOTORS)

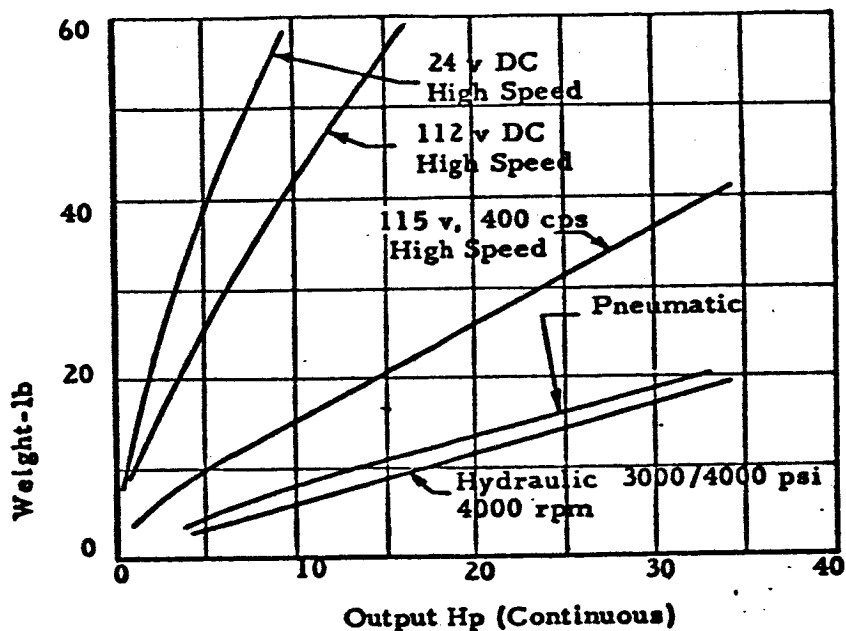


Fig. 66

WEIGHT VS POWER FOR POWER CONVERTERS (GENERATORS)

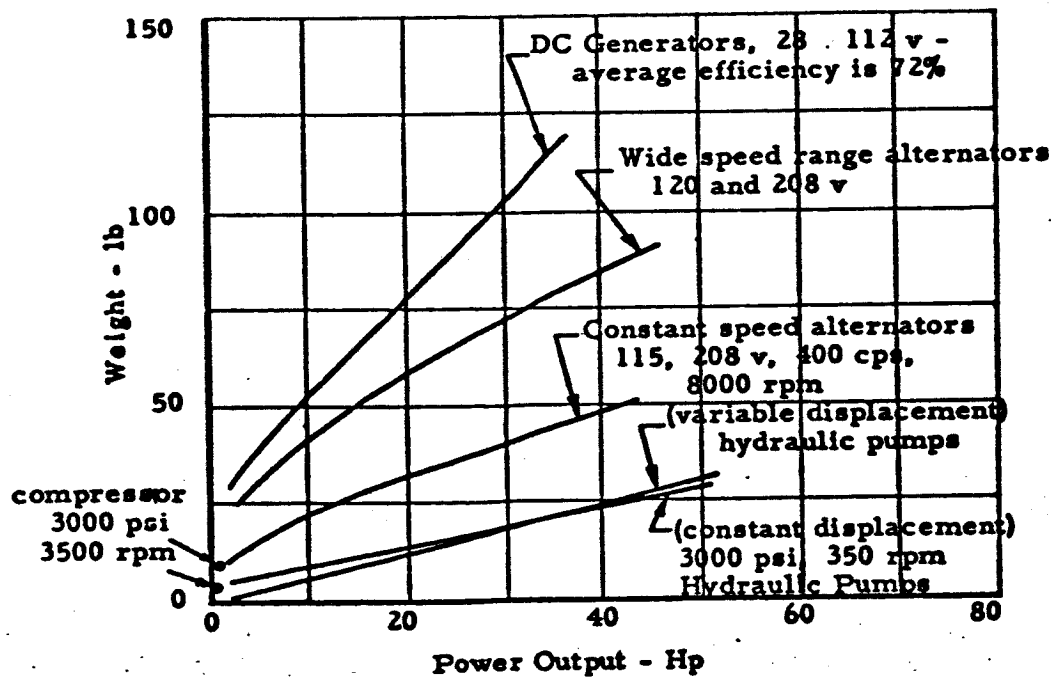


Fig. 67

HEIGHT OF STORAGE SYSTEMS

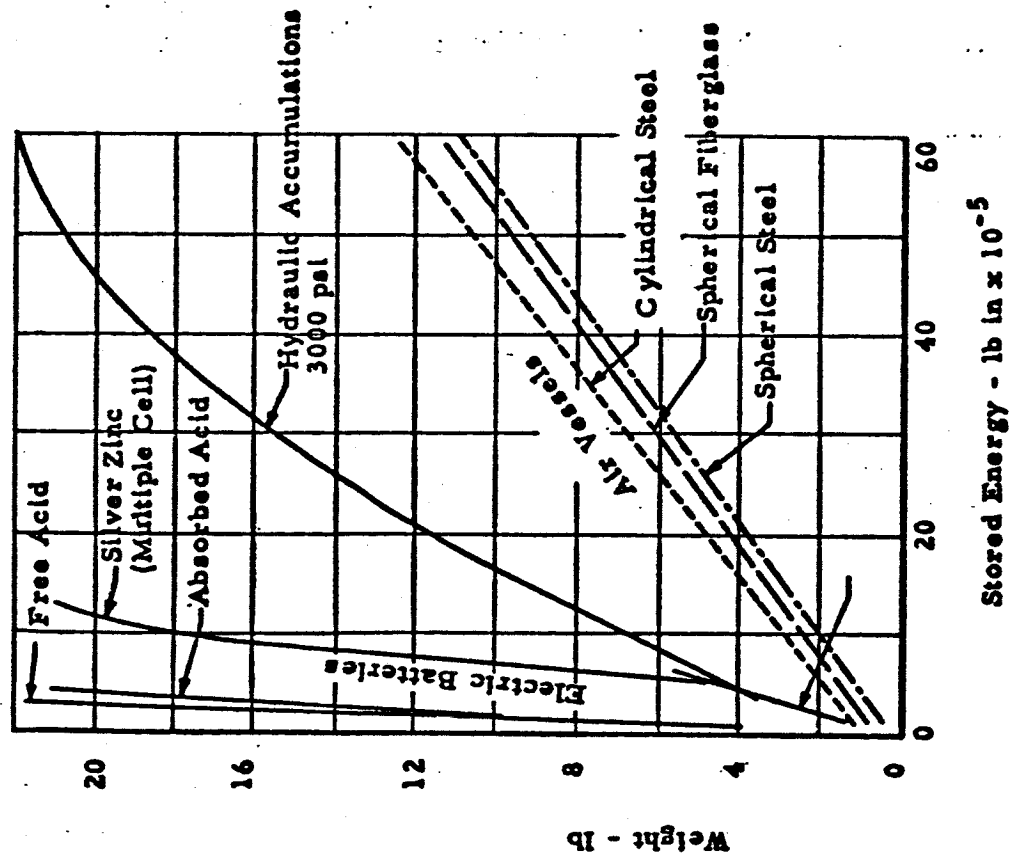


Fig. 69

WEIGHT OF ACTUATORS

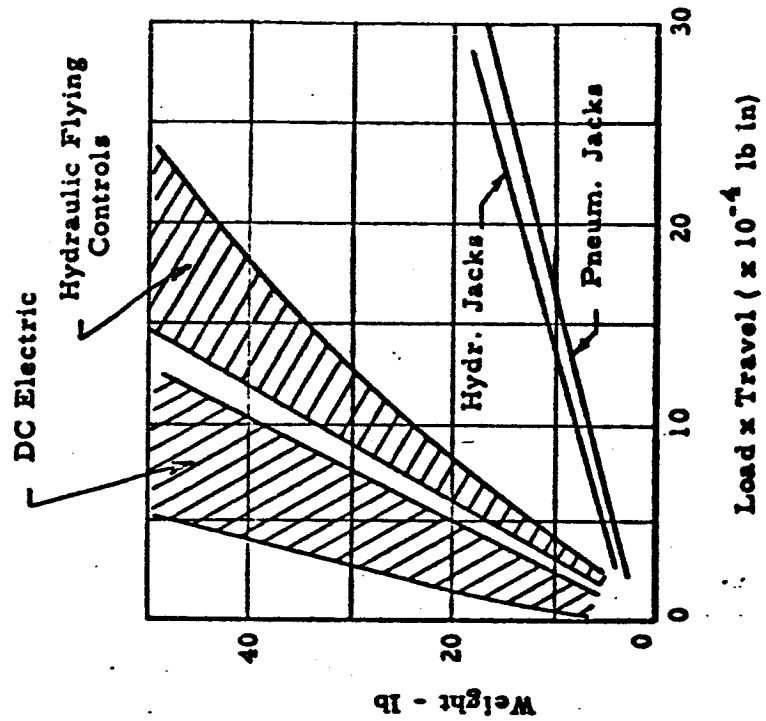
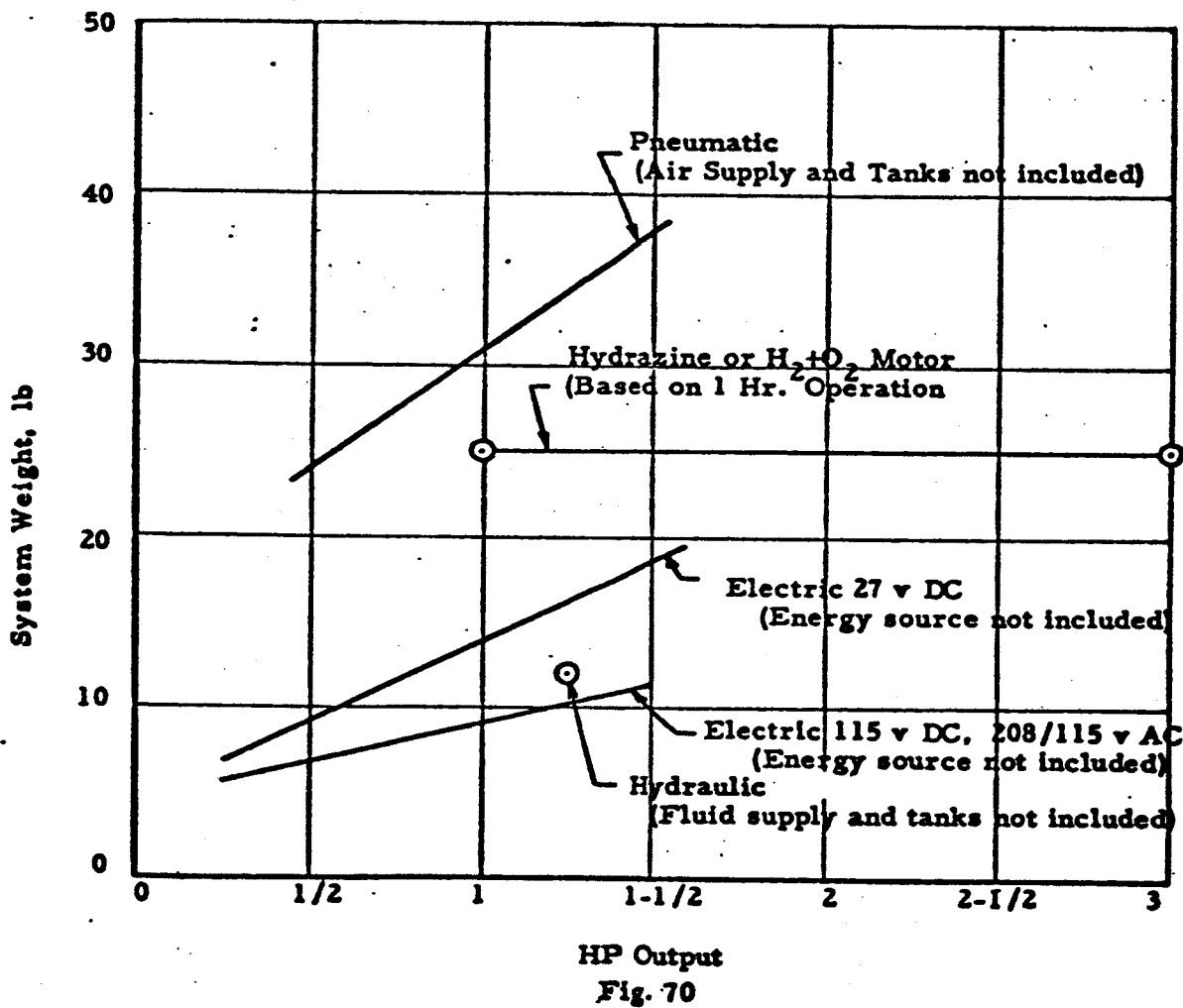


Fig. 68

PRIME MOVER SYSTEMS COMPARISON: WEIGHT VS. POWER



Power hp	Type	Speed rpm	Weight of Motor lb	Assumed Weight of Reduction Gearing lb	Total Weight lb
1/4	115/208 _v a-c	11,500	2.2	3	5.2
1/4	28-v d-c	11,700	4	3	7
1/2	115/208-v a-c	11,500	3.5	3	6.5
1/2	27-v d-c	8,000	6	3	9.0
1	115-v a-c	11,500	6	3	9
1	28-v d-c	12,000	11	3	14
1-1/2	115-v a-c	12,500	9	3	12
1-1/2	115-v d-c	12,500	9	3	12

2. Pneumatic Systems

Because the type of gas and the length of the operating cycle influences the capacity of the storage vessels, the two items were not considered in the systems analysis. The system then was visualized to be made up of the pneumatic motor, reduction gearing, compressor (equivalent in weight to the 1/2 hp pneumatic motor) and an electric motor to drive the compressor. The resulting system weight for typical pneumatic units is shown below.

Power hp	Speed rpm	Weight of Penetration Motor lb	Gearing lb	Compressor lb	Electric Motors lb	Gas Supply lb	Tanks lb	Total Weight lb
1/2	500	7	1	7	9	-	-	24
1	500	14	1	7	9	-	-	31
1-1/2	100	21	1	7	9	-	-	38

3. Hydraulic Systems

Because hydraulic systems are available only at power levels greater than 1 hp only the weight of a 1 hp system was found. Again, weights of hydraulic fluid and storage vessels were not taken into account. The system studied consisted of a hydraulic motor, a hydraulic motorpump, an electric motor, and reduction gearing. Weight calculations are shown below.

Power hp	Speed lb	Hydraulic Motor lb	Gearing lb	Motorpump lb	Electric Motor lb	Hydraulic Fluid lb	Tanks lb	Total Weight lb
1.25	800	1	1	1	9	-	-	12

4. Conclusions

The analysis indicates that an electrically powered motor is the most desirable prime mover of the types considered. From the prime mover systems point of view (Fig. 70), electric motors possess lowest weight to power ratios to about 1-hp range. At higher horsepower levels, other system considerations may be of over-riding importance. When considering only the prime mover (power converter) see Fig. 65, pneumatic vane motors give the lowest specific weight values, to power levels of about 1 hp.

V RECOMMENDATIONS FOR FUTURE RESEARCH

Before a lunar drill system can be designed with minimum weight and maximum reliability, additional research is necessary in several areas. For future geological exploration systems, further study is required.

The most important areas where data are lacking are:

1. Friction and lubrication
2. Metal fatigue
3. Seal integrity
4. Properties of carbides under lunar environment
5. Drilling and chip removal in the lunar vacuum-temperature environment
6. Optimization of the rotary impact drill shank configuration.

The first three areas cover fundamental data necessary for any mechanical system design for the lunar environment. Areas 4 and 5 will be generally applicable to drilling systems, while item 6 is only applicable to a rotary-impact drill using a long drill shank.

In future lunar explorations, the drill may have to operate over a period of one or more months. This will necessitate data on the long-term lunar environment effects, including the -244 to $+260^{\circ}\text{F}$ temperature variation. In addition, radiation exposure and meteor strikes may be important considerations. It will also be necessary to develop a lightweight, effect deep-hole drilling system.

Data obtained in these areas, especially that of friction, lubrication and metal fatigue, will be dependent on the amount of outgassing the samples undergo. Studies made at pressures higher than 10^{-9} mm Hg will not stimulate the real effect of the outgassing because gas will rapidly be reabsorbed on the sample surface. At a pressure of 10^{-6} mm Hg, a monomolecular layer of air will be absorbed on a clean surface in 1.6 sec, while at 10^{-9} mm of Hg, 23.3 min are required. For reliable data, all these experiments should be conducted at pressure of 10^{-9} mm of Hg or lower. In addition, the outgassing of the sample should simulate the most severe time-temperature condition to which the components will be exposed.

In the more distant future, geological exploration will be conducted on the other planets. To aid in preliminary payload and mission planning and to determine what additional experimental work is required, studies on this problem should be begun at the present time.

REFERENCES

1. "Proceedings of the 5th Annual Drilling (and Blasting) Symposium, University of Minnesota, 1955.
2. E. W. Inett, "Some Further Factors Effecting Percussive Drilling Performance and Their Influence on Size Distribution of Cuttings, Instn. Min. and Met. Trans., vol. 68, pt. 2.
3. "Continuous Reverse Circulation Coring Rig", California Oil World, p. 3 - 4, Sept., 1952.
4. "Some Advantages and Uses of Reverse Circulation", Drilling, p. 86 - 87, Nov., 1955.
5. "New Drilling Techniques Recovers 100% Continuous Core", Oil World, p. 111, Jan., 1960 (Stratodrilling Inc.).
6. Collected Reports, Drilling Research, Inc., vol. 1 - 6, 1949 - 1954.
7. H. L. Hartman, "Basic Studies of Percussion Drilling", Min. Eng., vol. 11, N. 1, Jan., 1959.
8. Journal of Petroleum Technology, Apr., 1960.
9. J. H. Pound, "Development of Equipment for Rotary Well Drilling (1900-1940)", M.E. 1940, p. 441.
10. Summary Report "Vibratory Drilling of Oil Wells", Battelle Mem. Inst. to Drilling Research Inc., Dec., 1957.
11. "Behavior of Materials in the Earth's Crust", 2nd Annual Symposium on Rock Mechanics Quarterly of the Colorado School of Mines, vol. 52, N. 3, July, 1957.
Part I - Basic Concepts of Materials Behavior
Part II - Deformation in Geological Mosses
Part III - Stress Instrumentation and Interference
Part IV - Support of Underground Openings.
12. E. Wells, "Penetration Speed Reference for the Drillability of Rocks", Proc. Australian Inst. of Mining and Metallurgy, 1950, N. 158 - 159, p. 453 - 64.
13. S. Kinoshita, "Studies on Drillability of Rock by Rotary Drills", Min. and Met. Ins. Japan, vol. 75, N. 852.

14. "Symposium on Rock Mechanics", Quarterly of the Colorado School of Mines, vol. 51, N. 3, July, 1956.
Part I - Rock Failure
Part II - Design and Support of Underground Openings
Part III - Mining by Block Caving
Part IV - Rock Fragmentation by Blasting.
15. W. D. Lacabanne and E. P. Pfeider, "Rotary-Percussion Blasthole Machine May Revolutionize Drilling", Mining Engineering No. 9, 850.
16. R. Simon, D. E. Cooper, and M. L. Stoneman, "The Fundamentals of Rock Drilling", presented at the spring meeting of the Eastern District of A. P. I. Division of Production, Columbus, Ohio, April 25 - 27, 1956.
17. E. W. Inett, "A Survey of Rotary-Percussive Drilling", Mine and Quarry Engineer J.L., vol. 23, N. 1, Jan., 1957, p. 2 - 7.
18. R. Simon, "Rock Drilling by Vibration", Journal of Engineering for Industry, vol. 81, series B, N. 1, Feb., 1959.
19. E. N. Kemler, "Rotary Percussion Drilling - A Patent and Literature Summary".
20. A Laboratory Study of the Two Percussive Rotary Drilling Machines, Mine and Quarry Engineering, 1960, vol. 26, June.
21. "The Effects of Weight and Speed on Penetration", World Oil 1958, vol. 146, p. 120 - 121, Jan.
22. J. R. Eckel, "Effect of Pressure on Rock Drillability," A. I. M. E. Transactions of Petroleum Technology, vol. 213, p. 1 - 6, Jan.
23. "Exploratory Drilling Practices and Costs at Western Uranium Deposits," U. S. Bu. Mines Circular 7944, 1960.
24. H. D. Outmans, "The Effect of Some Drilling Variables on the Instantaneous Rate of Penetration," Journal of Petroleum Technology, vol. 12, p. 137 - 149, June, 1960.
25. Carl Gatlin, PETROLEUM ENGINEERING DRILLING AND WELL COMPLETIONS, 341 pages, Prentice Hall Inc., Englewood Cliffs, N.J., 1960.
26. H. S. Alpan, "Factors Affecting the Speed of Penetration of Bits in Electric Rotary Drilling - Part II", TIME, London, vol. 111, p. 375 - 385.

27. J. W. Axelson, J. T. Adams, Jr., J. F. Johnson, J. N. Kong, and E. L. Piret, "Basic Laboratory Studies in the Unit Operations of Crushing," Mining Engineering, vol. 3, Trans. Dec., 1951, p. 1061 - 1069.
28. C. O. Babcock, "The Cutting Action of the Diamond Drill Bit Related to the Particle Sizes Produced, A Statistical Analysis," Master of Sci. Thesis, Univ. of Minn., 1955, 120 pages.
29. B. E. Blair, "Physical Properties of Mine Rock," U. S. Bu. of Mines Rept. of Investigations 5130, 1955, 69 pages.
30. Rolland Blake, "Cutting Action of the Diamond Drill Bit," Master of Sci. Thesis, Univ. of Minn., 1951, 127 pages.
31. C. Fairhurst, "The Design of Rotary Drilling Bits," Mine and Quarry Engineering, June, 1954, p. 271 - 275.
32. B. W. Gilbert, "Shores Scleroscope Hardness Tests made on Moh's Scale Minerals from Talc Through Quartz Inclusive," Univ. of Ill., Urbana, Ill., 1954.
33. J. M. Miller, "A Study of the Size of Diamonds in Drilling," Bulletin, School of Mines and Metallurgy, Univ. of Missouri (Technical Series), N. 81, Sept., 1952.
34. F. R. Archibald, "Analysis of the Stresses in a Cutting Edge," ASME Paper No. 53, A160.
35. N. H. Cook, I. Finnie, and M. C. Shaw, "Discontinuous Chip Formation," ASME Transactions, Feb., 1954.
36. Leonard Obert, S. L. Windes, and W. I. Duvall, "Standardized Tests for Determining the Physical Properties of Mine Rock," U. S. Bu. of Mines Rept. of Investigations 3891, 1946, 67 pages.
37. E. P. Pfeider, "Diamond Orientation in Drill Bits," AIME TP 3228A, Mining Engineer, Feb., 1952, p. 177 - 186.
38. "Orientation of Cube Diamonds in Drill Bits," Mining Engineering, Oct., 1953, p. 998 - 1003.
39. D. Watstein, "Effect of Straining Rate on the Compressive Strength and Elastic Properties of Concrete," Am. Concrete Inst., vol. 24, April, 1953, p. 729 - 744.
40. S. L. Windes, "Physical Properties of Mine Rock, Part I," U. S. Bu. of Mines Rept. of Investigations 4459, 1949, 79 pages.
41. "Physical Properties of Mine Rock, Part II," U. S. Bu. of Mines Rept. of Investigations 4727, 1950, 37 pages.

42. E. P. Pfeider and W. D. Lacabanne, "Effects of Static Loading on Impact Failure of Rocks," Bulletin Missouri School of Mining and Metallurgy, Symposium of Mining Research, 1956, Technical Series No. 94.
43. J. A. Whelan, "The Failure of Rock Under Dynamic Loading as Related to Rotary Drilling," Master of Science Thesis, University of Minnesota, 1956.
44. K. J. Trigger, "Heat Treatment of Metals," University of Illinois, p. 91 - 92.
45. C. K. Trotman, "Auxiliary Systems," Aircraft Engineering, Sept., 1960, vol. 32, N. 379.
46. T. B. Johnson, "Analysis of the Effect of Variations in Diameter and Cutting Speed on Instantaneous Stress Fluctuations in a Rotary Rock Cutting Tool," Univ. of Minn., Graduate Thesis, 1957.
47. W. B. Mather, "Rock Hardness Vs. Rock Penetrability in Making Holes," Oil and Gas Journal, Oct. 25, 1951, p. 98.
48. W. B. Mather, "Rock Hardness as a Factor in Drilling Problems," AIME Paper, New York Meeting, Feb., 1950.
49. J. B. Cheatham, Jr., "An Analytical Study of Rock Penetration by a Single Bit Tooth," Drilling and Blasting Symposium, Oct. 2 - 4, 1958.
50. J. D. Cumming, "Diamond Drill Handbook" 2nd Ed., 1956, published by J. K. Smit and Sons of Canada, Ltd.
51. E. N. Kemler, "Rotary Percussion Drilling a Patent and Literature Summary", University of Minnesota.
52. "The Effects of High Vacuum and Ultraviolet Radiation of Plastic Materials," WADD, TR 60-125, Feb., 1960.
53. O. W. Eshback, HANDBOOK OF ENGINEERING FUNDAMENTALS, published by John Wiley and Sons, 1952.
54. S. D. Stookey, "Glass Ceramics," Mechanical Engineering, Oct., 1960.
55. A. I. Brown and S. M. Marco, INTRODUCTION TO HEAT TRANSFER, published by McGraw-Hill, Inc., 1951.
56. K. J. Trigger, HEAT TREATMENT OF METALS, Campus Book Store, Inc., University of Illinois, 1954.

57. H. S. White, "Small-Oil-Free Bearings Project," Progress Report 1, Jan. 31 - March, 1955, Report No. 4074, National Bu. of Standards, Washington, D. C., AD 68849.
58. G. R. Beiley, "Effect of High and Low Temperatures on the Operational Characteristics of Ball Bearings," Consolidated Vultee Aircraft Corp., San Diego, California, Sept. 23, 1952, AD 16476.
59. J. G. Weir, "Teflon Bearing Project," (Task No. PL RE 8-1-77-51), Naval Ord. Plant, Indianapolis, Ind., 1953.
60. R. C. Binder, "Fluid Mechanics," Prentice-Hall Publ., New York, 1949.
61. N. A. Weil, "Fluidization, Transport, and Recovery of Fine Particles," unpublished paper.
62. V. L. Streeter, "Fluid Mechanics," McGraw-Hill Book Co., New York, 1951.
63. J. A. Stevenson and J. C. Grafton, "Lunar Temperature Environment," 1960 Proceedings Institute of Environmental Sciences, April, 1960, Los Angeles.
64. G. J. Danek and M. R. Achter, "A High Temperature, Vacuum, and Controlled Environment Fatigue Tester," ASTM Bulletin No. 234, Dec., 1958.
65. Zenz and Othmer, "Fluidization and Fluid Particle Systems," New York, 1960.
66. F. P. Bowden and J. E. Young, "Friction of Clean Metals and the Influence of Adsorbed Films," Proc. Royal Soc., A208, 1951, p. 311.
67. S. Hansen, "Research Program on High Vacuum Friction," AFOSR Report TR-59-97, Litton Industries of Calif., March, 1959, ASTIA No. AD 227352
68. F. P. Bowden and T. P. Hughes, "The Friction of Clean Metals and the Influence of Adsorbed Gases," Proc. Royal Soc. A 172, 1939, p. 263.

69. J. H. Atkins, R. L. Bisplenghoff, J. L. Hans, E. G. Jackson, and J. C. Simmom, Jr., "Effects of Environment on Space Materials," O. S. U. Research Foundation, Project No. 920, Nat. Res. Corp., Project No. 40-1-041, Aug., 1960.
70. G. F. Vanderschmidt and J. C. Simon, Jr., "Material Sublimation and Surface Effects in High Vacuum," First Symposium, Surface Effects on Spacecraft Materials, Ed. by F. J. Clauss, J. Wiley and Sons, 1960, p. 247.
71. Lt. G. F. Matacek, "Vacuum Volatility of Organic Coatings," First Symposium, Surface Effects on Spacecraft Materials, Ed. by F. J. Clauss, J. Wiley and Sons, 1960, p. 263.
72. M. R. Achter, "Effects of High Vacuum on Mechanical Properties," First Symposium, Surface Effects on Spacecraft Materials, Ed. by F. J. Clauss, J. Wiley and Sons, 1960, p. 286.
73. T. B. Daniel, "Surface Phenomena and Friction," First Symposium, Surface Effects on Spacecraft Materials, Ed. by F. J. Clauss, J. Wiley and Sons, 1960, p. 307.
74. V. R. Johnson and G. W. Vaughn, "Investigation of MoS₂ Lubrication in Vacuum," J. Applied Physics, vol. 27, N. 10, Oct., 1956, p. 1173-9.
75. V. R. Johnson, M. T. Laveck, and G. W. Vaughn, "Mechanism of WS₂ Lubrication in Vacuum," J. Applied Physics, vol. 28, N. 7, July, 1957, p. 821.
76. S. Dushman, "Scientific Foundation of Vacuum Techniques," J. Wiley and Sons, 1949.
77. G. P. Brown, A. D. DiNardo, G. K. Cheng, and T. K. Sherwood, "The Flow of Gases in Pipes at Low Pressures," J. Applied Physics, vol. 17, Oct., 1946, p. 802 - 813.
78. "Vacuum Bearings and Dry Film Lubricants," C. B. S. Laboratories, Technical Bulletin 463-6.
79. R. A. Happe, "Materials in Space," JPL Technical Release No. 34-143, Oct., 1960.

80. D. H. Buckley and R. L. Johnson, "Friction and Wear of Corrosion Resistant Metals Lubricated by Reactive Gases at Temperatures to 1200°F," Amer. Chem. Society, Petroleum Devices Symposium on Chemistry of Friction and Wear, Chicago, Illinois, Sept. 8-12, 1958.
81. W. H. Baier, ARF Research Proposal No. 60-941K, ARMOUR RESEARCH FOUNDATION.
82. J. H. Griffith, "Physical Properties of Typical American Rocks," Bulletin 131, Iowa Engineering Experimental Station, Iowa State College, 1937.
83. C. Fairhurst and W. D. Lacabanne, "Some Principles and Developments in Hard Rock Drilling Techniques," Proceedings of the Sixth Annual Drilling and Blasting Symposium, Univ. of Minn., 1956.
84. R. Simon, "Theory of Rock Drilling," Proceeding of the Fifth Annual Drilling Symposium, Univ. of Minn., Oct. 1955.
85. E. J. Wells, "Penetration Speed References for the Drillability of Rocks," Proceedings of Australian Institute of Mining and Metallurgy, N. S., Nos. 158 - 159, 1950.
86. L. W. Ledgerwood, Needed Now: "A Better Understanding of the Basics of Earth Boring," The Oil and Gas Journal, vol. 58, N. 19, 1960.
87. E. W. Inett, "The Rotary Percussive Drilling System," Proceedings of the Fifth Annual Drilling Symposium, Univ. of Minn., 1955.
88. J. D. Cumming, "Diamond Drill Handbook," J. K. Smith and Sons of Canada, Limited, 1956.
89. L. R. Ingersoll, O. J. Zobel, and A. C. Ingersoll, "Heat Conduction," Univ. of Wisc. Press, 1954.
90. "Research Program on High Vacuum Friction," Litton Industries of California, Beverly Hills, AFOSR Report No. TR-59-97, ASTIA AD-227352.
91. I. Kilpatrick, "Predicting Reliability of Electro-Mechanical Devices," Proceedings of the Sixth National Symposium on Reliability and Quality Control, Jan., 1960.
92. D. E. Johnston, and D. T. McRuer, "A Summary of Component Failure Rate and Weighting Function Data and Their Use in Systems Preliminary Design," Kelsey Hayes, Control Specialists Division, WADC Technical Report 57-668, ASTIA AD-142120.

93. B. G. Fish, and J. S. Barker, "Comparative Studies of Tools for Rotary Drilling in Rock," Colliery Guardian, vol. 193, N. 4977, 1956.
94. F. C. Bond and Jen-Tung Wang, "A New Theory of Comminution," Transactions AIME, vol. 187, Aug., 1950.
95. B. B. Burbank, "Measuring the Crushing Resistance of Rocks and Ores."
96. B. B. Burbank, "Measuring the Relative Abrasiveness of Rocks, Minerals and Ores."
97. Symposium on Diamond Drilling, Journal of the Chemical Metallurgical and Mining Society of South Africa, Johannesburg, Apr., 1952.
98. Diamond as Cutting Tool for Metals and Non-Metallic Materials, Harrison and Sons, Ltd., London, Feb., 1945.
99. The Diamond Tool Industry in 1951, Industrial Distributors (Sales) Ltd., London.
100. D. R. Walker and M. C. Shaw, "A Physical Explanation of the Empirical Laws of Comminution," Transactions AIME, March, 1954, Mining Engineering.
101. E. J. Wells, "Penetration Speed References for the Drillability of Rocks," Proceedings of Institute of Mining and Metallurgy, 1950.
102. A. W. Calder, Orval Robson and Robert Fletcher, "Thrust and Speed for Rotary Drilling," Mining Congress Journal.
103. K. N. Emmott, "Material Costs in Electric Rotary Drilling," Colliery Engineering, Jan., 1953.
104. R. Simon, "Drilling by Vibration," Journal of Engineering for Industry, Feb., 1959.
105. B. G. Fish and J. S. Barker, "A Laboratory Study of Rotary Drilling," Colliery Engineering, April, 1956.
106. H. Henderson and J. F. Earl, "New Drilling Technique Recovers 100 Percent Continuous Core," World Oil, Jan., 1960.
107. P. L. Moore and C. Gatlin, "How to Reduce Drilling Costs, Part IV," vol. 58, N. 21, May 23, 1960.

108. P. L. Moore and C. Gatlin, "How to Reduce Drilling Costs, Part III," The Oil and Gas Journal, vol. 58, N. 15, April 11, 1960.
109. W. D. Lacabanne and E. P. Pfeider, "Rotary Percussion Blasthole Machine May Revolutionize Drilling," Mining Engineering, Sept., 1955.
110. "Power Systems for Missiles and Spacecraft," Vickers Incorporated, Aero Hydraulics Division, Bulletin A-5239, F-1.00.
111. S. L. Sandelman and R. W. McJones, "Evaluating APU Systems for Spacecraft," Vickers Incorporated, Aero Hydraulics Division, March, 1959.
112. N. Rittenhouse and G. Hall, "Interim Report on Hydrogen-Oxygen Fuel for Auxiliary Power Systems," Walter Kidde and Company, Incorporated, May, 1959.
113. "Integrated Cryogenic Fueled Spacecraft Subsystems," Walter Kidde and Company, Incorporated, Sept., 1960.
114. "Design Drawings and Performance Charts for Aircraft Actuators and Special Motors," EEMCO, vol. 1.
115. "Design Drawings and Performance Charts for Aircraft Actuators and Special Motors," EEMCO, vol. 2.
116. "Airesearch Electric Motors," Copyright 1960 by The Garrett Corporation.
117. "Rotary Electrical and Electronic Equipment," Western Gear, Electro Products Division, Bulletin No. 5721.
118. "Motors... Actuators and Electromechanical Systems for Missile, Space Vehicle, Aircraft, Marine and Industrial Use," Electronic Specialty Co., EEMCO Division, Bulletin No. EE100.
119. Dalmotor Division, Yuba Consolidated Industries, Incorporated, Catalog.
120. American Electronics, Incorporated, Electro Mechanical Division, Catalog.
121. "Fractional Horsepower Motors," Carter Ecliptic, Carter Motor Company.
122. "Hydro-Aire Motors," Hydro-Aire Company, A Division of Crane Company.

123. "Application Engineering Data for the Aircraft Miniature Vane Pump," Vickers, Aero Hydraulics Division, E-13061-2.
124. "Miniaturized Hydraulics (Components and Packaged Systems) for Missile Applications," Vickers Incorporated, Bulletin A-5216B.
125. "Airborne Constant Displacement Piston Type Pumps 3000 psi Series," Vickers Incorporated, Bulletin A-5206-B, A-1.00.
126. "Airborne Constant Displacement Piston Type Hydraulic Motors 3000 psi Series," Vickers Incorporated, Bulletin A-5205-A, D.100.
127. "Airborne Electrically Depressurized Variable," Vickers Incorporated, Bulletin A-5202A.
128. "Yoke-Type Pressure Compensated Pumps and Their Application in Hydraulic Systems," Vickers Incorporated, Descriptive Summary SE-85.
129. "Basic Characteristics of Vickers Aircraft-Type Hydraulic Pumps and Motors," Vickers Incorporated, Data Summary SE-18D.
130. "Application Engineering Data for the 4000 psi Variable Delivery Pump," Vickers Incorporated, A-5219.
131. "5000 psi Hydraulic Pump (Axial Piston-Variable Displacement)," Vickers Incorporated, Bulletin No. A5232-A.
132. "Motorpumps Reliable, Independent Auxiliary Power Sources for Aircraft, Missiles, and Spacecraft, Bulletin No. A-5258, C-1.00.
133. "Design Principle Description of the Vickers Fixed Angle Delivery Pumps." Vickers, Inc.
134. "New Fixed Angle Variable Delivery Pumps for Aircraft and Missile Use," Vickers Incorporated, Bulletin A5233A, B1.01.
135. "Selection of Airborne Auxiliary Power Transmission Systems," Vickers Incorporated, SE 96.
136. "Balanced Vane Type Hydraulic Motors," Vickers Incorporated, Bulletin I and M-5103A.
137. "Airborne Constant Displacement Piston Type Hydraulic Motors, 3000 psi Series," Vickers Incorporated, Bulletin A-5205-A, D-1.00.
138. "High Temperature Hydraulic Pumps and Motors, Pesco Products Division, Borg-Warner Corporation, March, 1959.

139. "Hydraulic Pumps - Fluid Motors," Eastern Industries, Incorporated, Bulletin 810.
140. "Standard Hydraulic Pumps for Fluid Temperature to 400°F - Lowest Weight/ Displacement and Lowest Weight/Horsepower Ratio at Reliable Speeds, Bendix Hamilton, Bendix Aviation Corporation.
141. The Cornelius Company, Aero Division, Catalog.
142. "Adel Hydraulic Pumps," Adel Precision Products, A Division of General Metals Corporation.
143. "Air Tools Engineered to Industry," Gardner-Denver Company, Aug. 7, 1959.
144. "Air Motors," Bendix-Pacific Division, The Bendix Corporation, PB 103.
145. "Airesearch Floating Lobe Pneumatic Motors," The Garrett Corporation, Airesearch Manufacturing Division, Report No. AE-7618-R, Sept., 1960.
146. "Control Systems and Valves," The Garrett Corporation, Airesearch Manufacturing Division, June 30, 1960.
147. "High Speed Diamond Drilling in Reinforced Concrete and Masonry Materials," Felker Manufacturing Company.
148. "Steelset Diamond Impregnated Products," Fish-Schurman Corporation, Catalog DG 395.
149. "Felker Core-Lock Resettable Surface-Set Diamond Drills with Built-In Adaptors," Felker Manufacturing Company, Form FCL-1.
150. "Industrial Diamond Bits and Bit Adapters," E. J. Longyear Company, Form 415.
151. "Di-Cor Diamond Core Drills," Diamond Core and Saw, Division Portomag, Incorporated.
152. "North American-Viking Twist Drills," North American-Viking Drill Company, Catalog No. 161.
153. "Roatry Masonry Drills," Relton Corporation, Catalog No. CT-60.
154. U. S. Expansion Bolt Company, Catalog VR-488, Cat. No. GC-2/60.
155. "Carbide Tipped Red Bits," Vascoloy-Ramet Corporation, Catalog VR-488, May 11, 1959.

156. "New England Carbide-Tipped Masonry Bits," New England Carbide Tool Company, Incorporated, MBC-59.
157. "Du-Drill the Miracle Drill with the Welded Tungsten-Carbide Tip," Coffey-Cummins Manufacturing Company.
158. "Anchoring and Drilling Devices for Masonry, Arro Expansion Bolt Company, Catalog No. 71.
159. Skil Power Tools, Skil Corporation, 1960 Catalog.
160. "Stanley No. 404 Heavy Duty Impact Drill," Stanley Electric Tools, Division of the Stanley Works.
161. "Thor UE-100 Universal Electric Hammer," Thor Power Tool Company.
162. Syntron Company, Portable Power Tools, Catalog.
163. J. J. Gilvarry, "Origin and Nature of Lunar Surface Features," Nature, December 10, 1960, vol. 188..
164. R. J. Charles and P. L de Bruyn, "Energy Transfer by Impact," Mining Engineering, January, 1956.
165. C. K. Rose and S. Utter, "Cutting Action of Rotary Bits in Oil Shale," Un. S. Department of the Interior, November 1955.

APPENDIX ADIMENSIONAL ANALYSIS

APPENDIX A

DIMENSIONAL ANALYSIS

I. INTRODUCTION

To obtain data regarding the fundamental relations existing between the various quantities which affect drilling performance, a dimensional analysis of these quantities, based on the methods of Ref. 53, was carried out. Details of this analysis are presented in this appendix. Both solid and coring drills were analyzed.

II. SOLID DRILLS

A. Dimensionless Parameters

The rock and drill characteristics which are considered to influence the drilling problem are tabulated in Table A-1.

Table A-1

ROCK AND DRILL CHARACTERISTICS

Characteristic	Symbol	Unit	Dimension	Dimensional Parameters
Rock Strength	σ	lb/in. ²	(F/L ²)	σ
Rock Modulus	E	lb/in. ²	(F/L ²)	$\frac{\sigma d^2}{d^2}$
Rock Density	ρ	slugs/in. ³	(FT ² /L ⁴)	$\frac{\sigma}{d_o^2 N^2}$
Hole Diameter	d	in.	(L)	d
Hole Depth	Z	in.	(L)	d
Applied Load	F	lb	(F)	d ² σ
Drill Speed	N	rad/sec	(1/T)	N
Penetration Rate	R	in./sec	(L/T)	dN
Power Input	P	in.-lb/sec	(FL/T)	σd ³ N
Developed Torque	T	in.-lb	(FL)	σd ³

ARMOUR RESEARCH FOUNDATION OF ILLINOIS INSTITUTE OF TECHNOLOGY

The basic variables in the drilling problem are assumed to be those listed in Table A-2.

Table A-2
BASIC VARIABLES

Variable	Symbol	Dimension
Hole Diameter	d_o	(L)
Rock Strength	σ	(F/L^2)
Drill Speed	N	(1/T)

The fundamental quantities of (F), (L), and (T) can be obtained from these basic variables as:

$$(F) = \sigma d^2 \quad (A-1)$$

$$(L) = d \quad (A-2)$$

$$(T) = 1/N \quad (A-3)$$

When each of the rock and drill characteristics of Table A-1 is written in terms of Eq. A-1, A-2, A-3, the dimensional parameters of the last column of that table are obtained.

From these dimensional parameters, a number of dimensionless parameters may be derived. These parameters, obtained by multiplying each of the dimensional parameters by the appropriate basic variables, are tabulated in Table A-3.

Table A-3
DIMENSIONLESS PARAMETERS

Parameter	Value
π_1	E/σ
π_2	$\rho d^2 N^2 / \sigma$
π_3	z/d
π_4	$F/d^2 \sigma$
π_5	R/dN
π_6	$P/\sigma d^3 N$
π_7	$T/\sigma d^3$

B. Functional Relationships

Reference 53 indicates that for a system of three basic variables, three relationships of the type,

$$\pi_n = \phi_n \left[\pi_{n_1}, \pi_{n_2}, \pi_{n_3}, \dots \right] \quad (A-4)$$

may be established, where ϕ indicates a functional relation.

An examination of the experimental data indicated that relations of the type listed below, would best correlate the results obtained.

$$\frac{R}{dN} = \phi_5 \left[\frac{E}{\sigma}, \frac{\rho d^2 N^2}{\sigma}, \frac{z}{d}, \frac{F}{d^2 \sigma} \right] \quad (A-5)$$

$$\frac{P}{d^3 N} = \phi_6 \left[\frac{E}{\sigma}, \frac{\rho d^2 N^2}{\sigma}, \frac{z}{d}, \frac{F}{d^2 \sigma} \right] \quad (A-6)$$

$$\frac{T}{\sigma d^3} = \phi_7 \left[\frac{E}{\sigma} \cdot \frac{d^2 N^2}{\sigma} \cdot \frac{z}{d} \cdot \frac{F}{d^2 \sigma} \right] \quad (A-7)$$

Because power, P , is a function of drill torque, T , and drill speed, N ; if any two of the functions ϕ_5 , ϕ_6 , or ϕ_7 are found, the remaining one is determined. Therefore, ϕ_7 was not studied as such.

Reference 36 indicates that σ , E , and ρ are interrelated for most rocks. Accordingly, it is assumed that $\pi_1 = E/\sigma$ remains constant and is of no significance in the present analysis. Results of the present experimental program showed no marked dependency of power and speed on the depth at which drilling was taking place. Therefore, $\pi_3 = z/d$ was assumed to have no significance in the present analysis.

Equation A-5 and A-6 may then be written as

$$\frac{R}{dN} = \phi_5 \left[\frac{\rho d^2 N^2}{\sigma} \cdot \frac{F}{d^2 \sigma} \right] \quad (A-8)$$

$$\frac{P}{\sigma d^3 N} = \phi_6 \left[\frac{\rho d^2 N^2}{\sigma} \cdot \frac{F}{d^2 \sigma} \right] \quad (A-9)$$

These represent the equations used in the dimensional analysis. Other combinations of rock and drill characteristics may be chosen, however, these were found to correlate most closely with experimental results among those tried.

III. CORING DRILLS

A. Dimensionless Parameters

The dimensional analysis for coring drills is similar to that for solid drills. However, a number of modifications resulting from the difference in drill geometries are introduced. These are listed below.

1. The drill performance is influenced by the relative values of the inner and outer diameters of the cutting bit, d_o and d_i , respectively.
2. A new characteristic, the total length of cutting edge, l , whose units are inches, and which has the dimension (L).
3. A new dimensionless parameter was formed as shown below.

$$\pi_8 = \frac{l}{d_o - d_i}$$

where, for the present case, l is a multiple of 3/16-in., the length of the drill bit insert.

B. Functional Relationships

1. Drill C-4 in Sandstone

When these modifications are incorporated into Eq. A-8 and A-9, these equations become

$$\pi_5' = \frac{R}{(d_o - d_i)N} = \phi_5 \left[\frac{\rho(d_o^2 - d_i^2)N^2}{\sigma} \cdot \frac{F}{(d_o^2 - d_i^2)\sigma} \cdot \frac{l}{d_o - d_i} \right] \quad (A-10)$$

$$\pi_6' = \frac{P}{\sigma(d_o^3 - d_i^3)N} = \phi_6 \left[\frac{\rho(d_o^2 - d_i^2)N^2}{\sigma} \cdot \frac{F}{(d_o^2 - d_i^2)\sigma} \cdot \frac{l}{d_o - d_i} \right] \quad (A-11)$$

It should be noted that the denominator of the middle term in Eq. A-10 is $(d_o - d_i)$ instead of $\sqrt{d_o^2 - d_i^2}$ as would result from an exact replacement of the terms in Eq. A-8 and A-9. In either case, the results are the same dimensionally, however, an improved correlation with experimental data results with the choice made in Eq. A-10.

The effect of cutting bit length, introduced into the equations for the coring drills is pointed out in Appendix D.

IV. NUMERICAL DATA

The numerical data used in establishing the values of the functional relations π_5 and π_6 in the main body of the report are tabulated below.

A. Drill C-4 in Sandstone

Table A-4

DIMENSIONLESS PARAMETERS FOR DRILL C-4 IN SANDSTONE^{1/}

Load, lb	735 RPM		650 RPM		550 RPM	
	π_4	π_5	π_4	π_5	π_4	π_5
50	0.00715	0.000076	--	--	--	--
80	0.0114	0.00069	0.0114	0.00071	0.0014	0.000755
120	0.0172	0.00157	0.0172	0.00132	0.0172	0.00099
160	0.023	0.00025	0.023	0.00196	0.023	0.00116

^{1/} 1-in. drill diameter

σ for sandstone = 7,000 lb/in.²

If π_5 is plotted as a function of π_4 for each of the rpm values of Table A-4, the results are straight lines. The slope of these lines is tabulated in Table A-5.

Table A-5

SLOPE VERSUS RPM FOR π_5 VERSUS π_4 CURVES

RPM	Slope (m)
550	0.0342
650	0.104
735	0.15

B. Drill C-8 in Granite

The results of Drill C-8 performance in granite are tabulated in Table A-6.

Table A-6**PERFORMANCE OF DRILL C-8 IN GRANITE^{1/}**

Drill Dia., in.	RPM	Penetration Rate, in./sec
1	250	0.0057
	500	0.0
1.5	250	0.0048
	500	0.000834
2	250	0.00347
	500	0.002

^{1/} 160-lb drill loading

The number of tool bit inserts varied with drill diameter; this variation is shown in Table A-7.

Table A-7**NUMBER OF INSERTS VERSUS
DRILL DIAMETER, DRILL C-8**

Drill Dia., in.	Insert Length, in.	No. of Inserts	Total Cutting Length, in.
1	3/16	5	15/16
1.5	3/16	6	9/8
2	3/16	8	3/2

The values of the dimensionless parameters for Drill C-8 in granite are shown in Table A-8.

Table A-8
DIMENSIONLESS PARAMETERS FOR
DRILL C-8 IN GRANITE

Drill Dia., in.	RPM	π_5	π_4, π_2, π_8
1	250	0.00058	0.62×10^{-7}
1.5	250	0.000487	0.736×10^{-7}
	500	0.000423	2.94×10^{-7}
2	250	0.000345	0.98×10^{-7}
	500	0.0001	3.91×10^{-7}

APPENDIX B

PARAMETRIC SYSTEMS ANALYSIS DATA

APPENDIX B

PARAMETRIC SYSTEMS ANALYSIS DATA

The results of the drilling tests used in the parametric systems analysis are tabulated below.

1. C-4 Drill in Sandstone

<u>Penetration Rate, in./min</u>	<u>Power, watts</u>	<u>Load, lb</u>	<u>Speed, rpm</u>	<u>Energy, w-min/in.</u>
0.05	130	50	300	2600
0.25	200	50	400	800
0.35	230	50	500	658
0.35	250	50	550	715
0.35	270	50	650	773
0.35	270	50	735	773
2.1	300	80	500	143
2.4	300	80	550	125
2.8	330	80	650	118
3.0	370	80	735	123
3.1	530	80	900	171
2.6	640	80	1000	246
3.3	370	120	500	112
3.4	420	120	550	123
5.4	480	120	650	89
7.3	490	120	735	67
2.2	450	150	500	204
4.0	520	160	550	130
8.0	570	160	650	71.4
11.4	590	160	732	516

2. C-8, 1-in. Drill in Sandstone

<u>Penetration Rate,</u> <u>in./min</u>	<u>Power,</u> <u>watts</u>	<u>Load,</u> <u>lb</u>	<u>Speed,</u> <u>rpm</u>	<u>Energy,</u> <u>w-min/in</u>
1.0	170	50	350	170
1.9	230	50	500	121
2.3	320	50	600	139
2.8	480	50	700	171
3.1	680	50	800	219
1.8	170	80	350	94.5
2.9	210	80	500	72.4
3.6	280	80	600	77.8
4.4	370	80	700	84.1
5.1	500	80	800	98
2.0	470	160	350	235
3.3	660	160	500	200
3.5	770	160	600	220
3.0	840	160	700	280
1.3	880	160	800	676
2.4	200	120	350	83.4
3.6	250	120	500	69.5
4.4	300	120	600	68
4.9	430	120	700	88
4.9	510	120	800	104

3. C-8, 2-in. Drill in Sandstone

<u>Penetration Rate,</u> <u>in./min</u>	<u>Power,</u> <u>watts</u>	<u>Load,</u> <u>lb</u>	<u>Speed,</u> <u>rpm</u>	<u>Energy,</u> <u>w-min/in.</u>
0.4	230	50	250	575
0.4	260	50	350	650
0.45	290	50	400	645
0.45	330	50	500	735
0.7	370	50	600	530
1.0	420	50	700	420
0.55	290	80	250	528
1.5	320	80	350	213
2.4	370	80	400	154
5.25	660	80	500	126

4. C-8 Drills in Granitea. 1-in. Drill

0.41	344	160	250	840
0.0353	270	80	735	7650
0.0492	362	160	500	7350
0.0208	120	50	250	5760
0.0555	310	50	735	6500
0.148	202	50	500	1365

b. 1-1/2-in. Drill

0.286	385	160	250	1350
0.055	370	160	500	6740

c. 2-in. Drill

0.186	415	160	500	2230
0.2	400	160	250	2000

APPENDIX C

PRIME MOVER CLASSIFICATION DATA

APPENDIX C

PRIME MOVER CLASSIFICATION DATA

The characteristics of the various prime movers analyzed during the program are tabulated below.

1. Electric Motors

Model	Horse-power	Torque, in.-lb	Speed, rpm	Weight, lb	Voltage	Efficiency, %
<u>EEMCO</u>						
C-591-C	1/3	6	3,600	11.5	12 DC	65
C-721-C	3/4	6.1	7,900	6.75	27 DC	78
C-901-C	1.5	7.5	12,500	9.5	115 AC-DC	75
C-1033	3/4	1.94	24,000	2.94	22 DC	65
D-455	1.34	8	10,500	12.0	112 AC, 60 cps	75
C-1042	1/4	22	11,700	3.87	28 DC	72
C-851	1.5	7.5	12,500	8.5	115 AC-DC	75
D-993	0.65	4.4	8,800	6.2	27 DC	72
<u>Western Gear</u>						
IH35YH6	0.14	0.44	23,000	2.25	208/120, 400 cps, 3 ϕ	78
IH35YH11	0.125	1.25	7,300	2.6	208/120, 400 cps, 3 ϕ	70
IH35YH15T	1/3	3.12	11,500	2.9	200, 400 cps, 3 ϕ	75
IH38YG2	0.25	6.25	7,500	9.0	208/120, 400 cps, 3 ϕ	85
<u>AiResearch</u>						
6-14AD-2	0.15	1.26	7,500	2.3	115 AC, 400 cps, 1 ϕ	
6-14A-E-2	2.0	5.5	22,900	11.0	208/120, 400 cps, 3 ϕ	
6-14B-C-3	0.15	0.75	12,500	1.8	26 DC	

<u>Model</u>	<u>Horse- power</u>	<u>Torque, in.-lb</u>	<u>Speed, rpm</u>	<u>Weight, lb</u>	<u>Voltage</u>	<u>Efficiency, %</u>
<u>Dalmotor</u>						
SC-5	1.0	4.7	12,000	10.8	28 DC	62
SC-23	1/8	2.44	7,100	5.5	27 DC	62
<u>Hydro-Aire</u>						
A-1747	0.33		11,500	2.5	115, 400 cps, 3 ϕ	
70-187	1/4		11,500	2.2	208/120, 400 cps, 3 ϕ	

2. Air Motors

Model	Speed, rpm	Horse- power	Torque, in.-lb	Weight, lb	Inlet Pressure, psig	Consumption	Direct Drive Speed, rpm	Torque, in.-lb	Specific Weight, lb
<u>Gardner-Denver</u>									
71A-1200	9000	0.125	1.0	0.75	90	10 ft ³ free air	9,000	1.0	6.0
71A-150	2375	0.125	4.0	0.75	90	10 ft ³ free air	10,900	0.87	6.0
71A-110	475	0.125	18.0	0.875	90	10 ft ³ free air	10,000	0.85	7.0
71J-55		1.5		7.0	90	50 ft ³ free air			4.7
71J-54				11.0					7.3
71J-53									
71J-52									
71J-50									
71J-530				7.0					
71J-515									
71J-510									
71J-58									
71J-56									
70A-22	2360	0.6	23.4	13.0		21 ft ³ free air	2,360	23.4	22.0
70A-24	575		96.0						
70A-26	255		216.0						
70A-42	2150	0.9	27.6	13.5		40 ft ³ free air	4,200	27.6	15.0
70A-44	525	0.9	108.0	13.5		40 ft ³ free air		26.4	15.0
70A-62	1820	1.9	68.4	25.0		62 ft ³ free air	1,820	68.4	13.1
<u>Bendix</u>									
1011679	4000	1.5	25.2	1.5	75	25.4 ft ³ /min air			1.0
1011679	5000	3.0	37.9	1.5	125	39 ft ³ /min air			0.5
<u>AIRResearch</u>									
124044	4500	4.5	116.0	6.5	60	2.2 lb/min air			1.45

3. Hydraulic Motor-Driven Pumps

Model	Outlet Pressure, * psi	Delivery, gpm	Input, rpm	Electrical Input, hp	Weight, lb
<u>Vickers</u>					
AA-19020	3000	1.0	8400	2.4	2.65
AA-19033	3000	2.6	7600	6.8	2.5
AA-19036	3000	0.85	2430	2.7	2.65
AA-19523	2700	3.2	2050	7.0	8.9
AA-19054	1050	0.87	8000	1.2	1.0
AA-60201	2750	2.9	3750	5.0	8.0
AA-60201	2750	3.5	4500	5.5	8.0

* Maximum efficiency.

4. Hydraulic Motors

Model	Speed, * rpm	Torque, in.-lb	Output hp	Pressure, psi	Weight, lb	Delivery, in. ³ /rev
<u>Vickers</u>						
MF-3906-30	2600	44	1.8	3000	2.6	0.095
<u>Cornelius</u>						
63025-201-01	2600	115	4.2	3000	1.75	0.253

* Maximum efficiency.

APPENDIX D

CORING DRILL PERFORMANCE ANALYSIS

APPENDIX D

CORING DRILL PERFORMANCE ANALYSIS

I. INTRODUCTION

In this Appendix the results of two analytical studies of coring drill performance are summarized. The objectives of these analyses are the investigation of possible drilling functions or models which would permit the extrapolation of experimental data, and to obtain a better understanding of the drilling process itself.

II. MODEL DEVELOPMENT

A. Model Based on Load and Speed

The first approach attempted was based on the assumption that two drills of different diameter but of the same type, would have the same performance if they were both subjected to the same drill load per tooth and to the same linear cutting speed. Data for correlation purposes was available for the C-8 drill, both 1-in. dia. and 2-in. dia., in sandstone. The effective drill tooth radius for the 1-in. drill is 0.4 in. and that for the 2-in. drill, 0.9 in. The 1-in. drill has 5 cutting teeth, and the 2-in. drill, 8 cutting teeth.

The linear velocity of the mean radius of the 1-in. drill is $V_1 = 2.52N_1$, where N_1 corresponds to the rpm of the drill. The corresponding value for the 2-in. drill is $V_2 = 5.65N_2$.

For a drill loading of 50 lb and a speed of 80 rpm, the value of the tooth loading for the 1-in. drill is 10 lb, and $V_1 = 2020$. Under these conditions, a penetration rate of 3 in./min and a power consumption of 670 watts was obtained.

If the same drill loading per tooth is applied to the 2-in. drill, the corresponding drill loading is 80 lb. At the same linear velocity, the rotational speed is 356 rpm. From Fig. 26, at an 80-lb drill loading and 350

rpm, the penetration rate for the 2-in. drill was 1.5 in./min, and the power input 321 watts.

It is seen, therefore, that at identical tooth loading and mean tooth velocities, penetration rates are different for the two drills. Accordingly, it was decided that these two criteria were not basic in predicting the performance of the drills.

B. Model Based on Curve Fitting Techniques

As an alternative to the above, it was assumed that the law relating penetration rate, R , to drill diameter, D , drill load, F , and drill speed, N , was:

$$R_1 = C_1 D + C_2 F + C_3 N + C_4 D^2 + C_5 F^2 + C_6 N^2 + C_7 DF + C_8 DN + C_9 FN + C_{10} D^3 + C_{11} F^3 + \dots C_{19} FDN.$$

Data from 19 points of the C-8 drill performance map was inserted in this equation to obtain 19 simultaneous equations in the Constants C_i . The system was solved on a Univac 1105, using Crout's method. Unfortunately, the choice of points was such that the resulting equations were not independent and no solution was obtained.

A new attempt at solution using different data points should provide the proper values for the constants C_i . A similar method should provide a law relating the power input to D , F , and N .

APPENDIX E

GAS FLOW THROUGH A NARROW ANNULUS:

APPENDIX E

GAS FLOW THROUGH A NARROW ANNULUS

1. Introduction

The derivation below is based on the Poisselle equation for flow through an annulus and on the kinetic theory of gases, Ref. 62 and 77. An equation is derived for the leakage of gas through a simple seal assumed to consist of a narrow annulus of inner radius b , outer radius a , and length L . End effects or entrance and exit losses are neglected. They may be accounted for by replacing the actual length, e , by an equivalent length that produces the same effect as the seal. Because of the very low pressures involved, turbulent flow will not occur.

2. Nomenclature

- a = outer radius, ft
- b = inner radius, ft
- L = length, ft
- U_o = velocity of the fluid at the walls, ft/sec
- u = velocity of the fluid, ft/sec
- g = 32.2 ft/sec²
- μ = viscosity, lb/ft-sec
- p_m = mean pressure, lb/ft²
- λ_m = mean free molecular path, ft
- ρ_o = gas density at unit pressure, lb/ft³
- r = radius of the annules, ft.

3. Analysis

If the force tangent to the wall of the annulus and parallel to the axis of the annulus is assumed proportional to both U_o , the velocity at the wall, and A_w , the surface area of the wall, this force is

$$F = \frac{K}{g} U_o A_w . \quad (1)$$

If U_o is the same at the inner and the outer walls of the annulus, the force F is given by

$$\begin{aligned} F &= KU_o (2\pi a dl + 2\pi b dl) \\ &= 2\pi(a+b) \frac{K}{g} U_o dl. \end{aligned} \quad (2)$$

If the fluid undergoes a pressure drop of dp as it moves a distance dl , the unbalanced pressure force acting on an element of fluid of length dl and cross-sectional area A is

$$F' = -Adp. \quad (3)$$

This may be written as

$$F' = \pi(a^2 - b^2) dp. \quad (4)$$

For equilibrium,

$$F = F'.$$

Equation 4 may be set equal to Eq. 2 to obtain

$$\pi(a^2 - b^2) dp = 2\pi(a+b) \frac{K}{g} U_o dl. \quad (5)$$

Equation 5 may be solved for U_o or,

$$U_o = \frac{(a-b)}{2K} g \frac{dp}{dl}. \quad (6)$$

From Ref. 77, the ratio of the viscosity μ to K is given by

$$\frac{\mu}{K} = \left(\frac{2}{f} - 1 \right) \lambda_m, \quad (7)$$

where $(1 - f)$ is the fraction of the molecules striking the wall of the annulus that would be specularly reflected, and λ_m is the mean free path of the gas molecules at the mean pressure, p_m . From the kinetic theory of gases, Ref. 2, the mean free path may be written as

$$\lambda_m = \left(\frac{\pi}{2 \rho_o g} \right)^{1/2} \frac{\mu}{p_m} \quad (8)$$

where ρ_o is the gas density at unit pressure.

If Eq. 7 and 8 are substituted into Eq. 6, the velocity may be written as

$$U_o = \left(\frac{2}{f} - 1 \right) \left(\frac{a-b}{2 p_m} \right) \left(\frac{\pi}{2 \rho_o g} \right)^{1/2} \frac{dp}{dl} \quad (9)$$

The differential equation for laminar flow through an annulus is given by (Ref. 62)

$$\frac{dp}{dl} + \frac{1}{r} \frac{d(\tau r)}{dr} = 0 \quad (10)$$

where τ is the shear stress in the fluid at the radius r .

By substituting Newton's law of viscosity,

$$\tau = \frac{\mu}{g} \frac{du}{dy} \quad (11)$$

into Eq. 10 and integrating the result, the following equation is obtained:

$$\frac{dp}{dl} \frac{r^2}{4} - \frac{\mu}{g} U = A \ln r + B \quad (12)$$

where A and B are constants of integration.

The boundary conditions,

$$\begin{aligned} r = a & \quad u = U_o \\ r = b & \quad U = U_o \end{aligned} \quad (13)$$

are substituted into Eq. 12 and the result solved for U to obtain:

$$U = \frac{g}{4\mu} \frac{dp}{dl} \left(a^2 - r^2 + \frac{(a^2 - b^2)}{\ln b/a} \ln a/r \right) + U_o \quad (14)$$

The flow rate Q through the annulus is given by the equation,

$$Q = \int_b^a 2\pi r u dr. \quad (15)$$

When the value of U from Eq. 14 is inserted in Eq. 15 and the result is integrated, the flow rate is found to be

$$Q = \frac{\pi g}{8\mu} \frac{dp}{dl} \left[a^4 - b^4 - \frac{(a^2 - b^2)^2}{\ln a/b} + \pi(a^2 - b^2) U_o \right]. \quad (16)$$

The value of U_o from Eq. 9 may be substituted in Eq. 16 with the result

$$Q = \frac{dp}{dl} \frac{\pi g}{8\mu} (a^2 - b^2) \left[a^2 + b^2 - \frac{(a^2 - b^2)}{\ln a/b} + \frac{4(a - b)}{p_m} \mu \left(\frac{2}{f} - 1 \right) \left(\frac{\pi}{2\rho_o g} \right)^{1/2} \right] \quad (17)$$

Equation 17 can be written as

$$Q = A \frac{dp}{dl} \left(B + \frac{C}{p_m} \right), \quad (18)$$

where A , B , and C depend on the cross section of the annulus and the type and temperature of the gas under consideration.

At low pressures dp/dl is not a constant over the entire length of the annulus, and, therefore, the equation may not be integrated directly.

An approximate solution for Eq. 18 can be obtained by evaluating the term $(B + \frac{C}{p_m})$ for various values of p_m and plotting the results against p_m .

The resulting curve may be divided into three portions:

1. That part in which C/p_m is much larger than B , and B may be neglected in comparison.
2. That in which B and C/p_m are of the same orders of magnitude and both must be considered.
3. That in which B is much larger than C/p_m , and C/p_m can be neglected in comparison.

The first condition above corresponds to molecular flow. Here, the energy used is a function of the number of collisions between the molecules and the wall. The third condition represents the usual laminar flow case where the energy used is considered to be only a function of the number of collisions between molecules. The second condition is the "slip flow" region, Ref. 1, where both intermolecular collisions and collision with the wall are influencing factors. By use of a mean pressure for each flow condition and knowing the overall initial and final pressures, the initial and final pressures for each condition can be obtained from the following:

$$P_{m1} = \frac{P_{o1} + P_{f1}}{2} \quad (19)$$

$$P_{m2} = \frac{P_{o2} + P_{f2}}{2} \quad (20)$$

$$P_{m3} = \frac{P_{o3} + P_{f3}}{2} \quad (21)$$

If dp/dl is assumed constant over each condition, the relation

$$\left(\frac{dp}{dl} \right)_n = \frac{P_{on} - P_{fn}}{l_n}, \text{ where } n = 1, 2, 3 \quad (22)$$

may be written. The quantity Q at each condition may be found from Eq. 18 through 21 to be

$$Q_n = A \frac{P_{on} - P_{fn}}{l_n} \left(B + \frac{2C}{P_{on} + P_{fn}} \right) \quad (23)$$

Because $\sum l_n = L$ this may be written as $l_1 + l_2 + l_3$, while for continuity $\rho_1 Q_1 = \rho_2 Q_2 = \rho_3 Q_3 = W$. The following four equations result:

$$W = A \frac{\rho_1}{l_1} (P_{o1} - P_{f1}) \left(B + \frac{2C}{P_{o1} + P_{f1}} \right) \quad (24)$$

$$W = A \frac{2}{l_2} (P_{o_2} - P_{f_2}) \left(B + \frac{2C}{P_{o_2} + P_{f_2}} \right) \quad (25)$$

$$W = A \frac{3}{l_3} (P_{o_3} - P_{f_3}) \left(B + \frac{2C}{P_{o_3} + P_{f_3}} \right) \quad (26)$$

where $l_1 + l_2 + l_3 = L$.

These are treated as four equations with four unknowns, and by solving these equations simultaneously, the value of W , the weight flow, may be determined.

A Reproduced Copy
OF

Reproduced for NASA
by the
NASA Scientific and Technical Information Facility